



# Cenozoic tectonic evolution of the Himalayan orogen as constrained by along-strike variation of structural geometry, exhumation history, and foreland sedimentation

An Yin \*

*Department of Earth and Space Sciences and Institute of Geophysics and Planetary Physics, University of California, Los Angeles, CA 90095-1567, United States*

Received 26 August 2003; accepted 2 May 2005  
Available online 8 February 2006

## Abstract

Despite a long research history over the past 150 years, the geometry, kinematics, and dynamic evolution of the Himalayan orogen remain poorly understood. This is mainly due to continued emphasis on the two-dimensionality of the Himalayan orogenic architecture and extrapolation of geologic relationships from a few well-studied but small areas to the rest of the orogen. Confusion and misconception are also widespread in the Himalayan literature in terms of the geographic, stratigraphic, and structural divisions. To clarify these issues and to provide a new platform for those who are interested in studying the geologic development of this spectacular mountain belt, I systematically review the essential observations relevant to the along-strike variation of the Himalayan geologic framework and its role in Cenozoic Himalayan exhumation, metamorphism and foreland sedimentation. A main focus of my synthesis is to elucidate the emplacement history of the high-grade Greater Himalayan Crystalline Complex (GHC) that occupies the core of the orogen. Because the north-dipping Main Central Thrust (MCT) above and South Tibet Detachment (STD) below bound the GHC in most parts of the Himalaya, it is critical to determine the relationship between them in map and cross-section views. The exposed map pattern in the central Himalaya (i.e., Nepal) indicates that the MCT has a flat-ramp geometry. The thrust flat in the south carries a 2–15-km-thick slab of the GHC over the Lesser Himalayan Sequence (LHS) and creates a large hanging-wall fault-bend fold continuing > 100 km south of the MCT ramp zone. In the western Himalayan orogen at the longitude  $\sim 77^\circ\text{E}$ , the MCT exhibits a major lateral ramp (the Mandi ramp). West of this ramp, the MCT places the low-grade Tethyan Himalayan Sequence (THS) over the low-grade LHS, whereas east of the ramp, the MCT places the high-grade GHC over the low-grade LHS. This along-strike change in stratigraphic juxtaposition and metamorphic grade across the MCT indicates a westward decrease in its slip magnitude, possibly a result of a westward decrease in total crustal shortening along the Himalayan orogen. Everywhere exposed, the STD follows roughly the same stratigraphic horizon at the base of the THS, exhibiting a long (> 100 km) hanging-wall flat. This relationship suggests that the STD may have initiated along a preexisting lithologic contact or the subhorizontal brittle–ductile transition zone in the middle crust. Although the STD has the THS in its hanging wall everywhere in the Himalayan orogen, no THS footwall cutoffs have been identified. This has made slip estimates of the STD exceedingly

\* Tel.: +1 310 825 8752; fax: +1 310 825 2779.

E-mail address: [yin@ess.ucla.edu](mailto:yin@ess.ucla.edu).

difficult. The southernmost trace of the STD either merges with the MCT (e.g., in Zaskar) or lies within 1–2 km of the MCT frontal trace (e.g., in Bhutan), suggesting that the MCT may join the STD in their up-dip directions to the south. This geometry, largely neglected by the existing models, has important implications for the deformation, exhumation, and sedimentation history of the entire Himalayan orogen.

© 2005 Elsevier B.V. All rights reserved.

*Keywords:* Himalayan orogen; Main Central Thrust; South Tibet Detachment; passive-roof fault; active-roof fault; erosional exhumation

## 1. Introduction

“Distinguishing between myth and science is subtle, for both seek to understand the things around us. The characteristic style of mythic thinking is to place special emphasis on a selective conjecture, based typically on the initial observation or recognition of a phenomenon, which is thereafter given privileged status over alternate interpretations.”  
William. R. Dickinson

The Himalaya is a classic example of an orogenic system created by continent–continent collision (e.g., Dewey and Bird, 1970; Dewey and Burke, 1973). Its youthfulness and spectacular exposure make the orogen ideal for studying diverse geologic processes related to mountain building. Its potential as a guide to decipher the feedback processes between lithospheric deformation and atmospheric circulation has motivated intense research in recent years on the history of the Himalayan–Tibetan orogen, its role in global climate change, and its interaction with erosion (e.g., Harrison et al., 1992, 1998a; Molnar et al., 1993; Royden et al., 1997; Ramstein et al., 1997; Tapponnier et al., 2001; Beaumont et al., 2001; Yin et al., 2002). Many workers have also used the Himalayan knowledge to infer the evolution of other mountain belts: the Altai system in central Asia (Yang et al., 1992; Qu and Zhang, 1994), the Trans-Hudson orogen and Canadian Cordillera in North America (e.g., Nabelek et al., 2001; Norlander et al., 2002), the Caledonides in Greenland (e.g., McClelland and Gilotti, 2003), and the East African–Antarctic orogen in Africa and Antarctica (e.g., Jacobs and Thomas, 2004). Despite the broad interests, it has become increasingly daunting for both a beginner and an experienced Himalayan geologist to comprehend the intricate complexity of the Himalayan geology in its

entirety. This may be attributed to the following factors:

- (1) Himalayan research is long (over 150 yr, e.g., Hooker, 1854; Godwin-Austen, 1864; Mallet, 1875; La Touche, 1883; Pilgrim, 1906; Auden, 1935; Lahiri, 1941) and rich, making its literature nearly intractable. The problem is compounded by the accelerated rate of publication on more and more specialized subjects on Himalayan geology in the past two decades.
- (2) The terminology of the Himalayan geology is often confusing. Its physiographic division is commonly equated to structural and stratigraphic divisions. Names of the same stratigraphic units and structures vary from place to place across international borders or even within the same country.
- (3) There has been a proliferation of kinematic, thermal, and dynamic models for the development of the Himalayan orogen in the past two decades. Debate is intense and consensus changes rapidly. This has made it especially difficult to evaluate the validity of each model or apply them to other mountain belts.

The classic reviews of the Himalayan geology by Wadia (1953), Gansser (1964) and LeFort (1975) laid the foundation for productive geologic research in the next several decades to follow. However, their reviews are largely out of date in light of new observations. Although several recent reviews on the Himalayan geology could potentially overcome the problem, they cover only selected segments of the Himalayan orogen. For example, reviews by LeFort (1996), Hodges (2000), Johnson (2002), DeCelles et al. (2002), and Avouac (2003) emphasize the central Himalayan orogen, while syntheses by Searle et al. (1992), Thakur (1992), Steck (2003), and DiPietro and Pogue (2004) focus exclusively on the western

Himalayan orogen. Similarly, geologic summaries by Acharyya (1980), Singh and Chowdhary (1990), and Kumar (1997) only cover the geology of the eastern Himalayan orogen. The lack of an updated overview of the entire Himalayan orogen makes it difficult to assess how the Himalayan deformation has responded to the well-understood plate boundary conditions and its impact on the overall Indo-Asian collision zone and evolution of great rivers in Asia (e.g., Patriat and Achaiche, 1984; Dewey et al., 1989; Le Pichon et al., 1992; Brookfield, 1998; Hallet and Molnar, 2001; Clark et al., 2004).

The present review intends to introduce the Himalayan geology in its entirety. In order to separate observations from interpretations, I approach the synthesis in the following order. First, I define the basic terminology commonly used in Himalayan literature and discuss their pitfalls in limiting our ability to understand the complexity of the geology. Second, I provide a systematic overview of the Himalayan structural framework, metamorphic conditions, exhumation history, and foreland sedimentation. Third, prominent tectonic hypotheses and quantitative physical models for the evolution of the Himalayan orogen are outlined and their predictions are evaluated in light of the available data. Finally, the current understanding of Himalayan geology is integrated into an internally consistent tectonic model that accounts for both map and cross-section views of the Himalayan architecture and the exhumation and sedimentation histories.

## 2. Basic terminology

### 2.1. Himalayan range, Himalayan Orogen, and Himalayan tectonic system

Before embarking on an exhaustive synthesis, it is useful to have a clear distinction of the politically, geographically, structurally, and stratigraphically defined Himalaya. Geographically, the *Himalayan range* lies between its eastern and western syntaxis as represented by the Namche Barwa and Nanga Parbat peaks (Fig. 1A). The northern boundary of the Himalayan range is the east-flowing Yalu Tsangpo (Tsangpo—big river in Tibetan) and west-flowing Indus River (Fig. 1A). The southern boundary of the Himalayan range is the Main Frontal Thrust (MFT) that

marks the northern limit of the Indo-Gangetic depression (Fig. 1A). Immediately to the west of the Himalayan range are the Hindu Kush Mountains, to the east the Indo-Burma Ranges (commonly known as the Rongkang Range), and to the north the Karakorum Mountains and the Gangdese Shan (also known as the Transhimalaya in Heim and Gansser, 1939) (Fig. 1A). The southern political boundary of Tibet (i.e., Xizang in Chinese) follows approximately the crest of the Himalayan range. The difference in political and geographic divisions has led to different naming of the same structures in the Himalayan range (e.g., the North Himalayan Normal Fault versus South Tibet Detachment System; Burg et al., 1984a; Burchfiel et al., 1992).

The *Himalayan orogen* is defined by the Indus–Tsangpo suture in the north, the left-slip Chaman fault in the west, the right-slip Sagaing fault in the east, and the Main Frontal Thrust (MFT) in the south (Fig. 2A) (LeFort, 1975). Because the MFT links transpressional systems in the Indo-Burma Ranges (=Rongkang Range) in the east (e.g., Guzman-Speziale and Ni, 1996) and the Kirthar-Sulaiman thrust salients in the west (e.g., Schelling, 1999) (Fig. 2A), the Himalayan orogen defined above extends all the way from the Himalayan range to the Arabian Sea and the Bay of Bengal. I consider the Sillong Plateau bounded by the active south-dipping Dauki thrust as part of the broadly defined Himalayan orogen, because its bounding structure is linked with the transpressional system in the Indo-Burman Ranges (Fig. 2A).

The *Himalayan tectonic system* is a broader concept than the Himalayan orogen. It consists of the Himalayan orogen, the active Himalayan foreland basin (=Indo-Gangetic depression), and the Indus and Bengal Fans (Fig. 2A). All of these features were produced by the Cenozoic Indo-Asian collision.

The Indo-Gangetic depression is a broad up-side-down “U-shaped” basin in map view (Fig. 1A). Its basement dips at about 2–3° from the Peninsula Highlands of the Indian craton towards the Himalayan orogen, with the thickness of basin fill increasing progressively to about 4–5 km against the Himalayan front (Hayden, 1913; Rao, 1973; Lyon-Caen and Molnar, 1985; Raiverman, 2000). The northern boundary of the depression is sharply defined, whereas the southern boundary is diffuse and highly irregular. The southern boundary is referred to as the hinge zone in this paper, which separates the Himalayan foreland basin in

the north from the Peninsula Highlands of the Indian craton in the south. Burbank (1992) notes that the east-flowing Ganges drainage system is currently flowing about 200 km away from the Himalayan mountain front directly against the hinge zone defined here (Fig. 1A). He attributes this pattern to erosion-dominated Himalayan development in Plio-Pleistocene times, which caused isostatic uplift of both the Himalayan range and southward progradation of large alluvial fans and pushed the river far away from the mountain front. Based on successive southward onlapping unconformities in the depression, Lyon-Caen and Molnar (1985) suggest that a hinge line ~200 km from the Himalayan thrust front has migrated steadily southward at a rate of ~15 mm/yr (also see Avouac, 2003). Raiverman (2000) later questions the model and argues instead that the hinge zone may have migrated episodically both to the north and south during the Cenozoic development of the Himalayan orogen.

## 2.2. Himalayan divisions

In the Himalayan literature, the politically, geographically, structurally, and stratigraphically defined Himalaya is often assumed to be interchangeable (e.g., LeFort, 1975, 1996). This tradition can be traced back at least to the classic work of Heim and Gansser (1939), who based on their experience in the Kumaun region of NW India (Fig. 2A), divided the Himalaya into four east-trending geographic belts that correspond exactly to four geologic domains. These geographic and geologic zones are assumed continuous along the entire Himalayan orogen (Gansser, 1964; LeFort, 1975) and include:

- (1) sub-Himalaya (Tertiary strata);
- (2) Lower Himalaya (nonfossiliferous low-grade metamorphic rocks; it is also known as the Lesser Himalaya, see LeFort, 1975);
- (3) Higher Himalaya (crystalline complex consisting of gneisses and aplitic granites; it is also known as the Greater Himalaya, see LeFort, 1975); and
- (4) Tethyan Himalaya (marine, fossiliferous strata).

Heim and Gansser's (1939) division implies the following interchangeable relationships:

- (1) structurally defined MBT footwall=lithologically defined sub-Himalaya=topographically defined sub-Himalaya;

- (2) structurally defined MBT hanging wall=lithologically defined Lower Himalaya=topographically defined Lower Himalaya;
- (3) structurally defined MCT hanging wall=lithologically defined Higher Himalaya=topographically defined Higher Himalaya;
- (4) structurally defined STD hanging wall=lithologically defined Tethyan Himalaya=topographically defined Tethyan Himalaya north of the Himalayan crest.

These relationships are broadly valid in the central Himalaya in Nepal and the Kumaun region of easternmost NW India. However, the definition precludes the possibility that individual lithologic units may extend across major thrusts, such as the MCT and MBT, outside the type locality where these divisions were derived. The inability in the past decades to recognize this limitation has led to circular reasoning in locating major Himalayan structures and the lack of appreciation of along-strike variation of the Himalayan architecture (e.g., Argles et al., 2003; also see discussion on this issue by DiPietro and Pogue, 2004).

The division of Heim and Gansser (1939) is in fact contradictory to many geologic observations. For example, the high-grade Higher Himalayan Crystallines of Heim and Gansser (1939) are exposed in all three geographical zones they defined: the Tethyan Himalaya, Higher Himalaya, and Lower Himalaya (e.g., Stöcklin, 1980; Schärer et al., 1986; Frank et al., 1995; Fuchs and Linner, 1995; de Sigoyer et al., 2000, 2004; Lee et al., 2000; Murphy et al., 2002) (Fig. 2). Conversely, the Tethyan and Higher Himalayan lithologic units of Heim and Gansser (1939) are also present in the geographically defined Lower and Higher Himalaya (e.g., Stöcklin, 1980; Gansser, 1983). Furthermore, the Tethyan Himalayan Sequence of Heim and Gansser (1939) is exposed in both the MCT hanging wall and footwall in northern Pakistan (e.g., Pogue et al., 1992, 1999). Attempts to avoid the above confusion were made at local scales, for example in Nepal (Upreti, 1999) and in northern Pakistan (DiPietro and Pogue, 2004), but there has been no systematic effort in doing so for the entire Himalaya.

### 2.2.1. Geographic division

In order to decouple the Heim-Gansser Himalayan divisions from one another, the following geographic

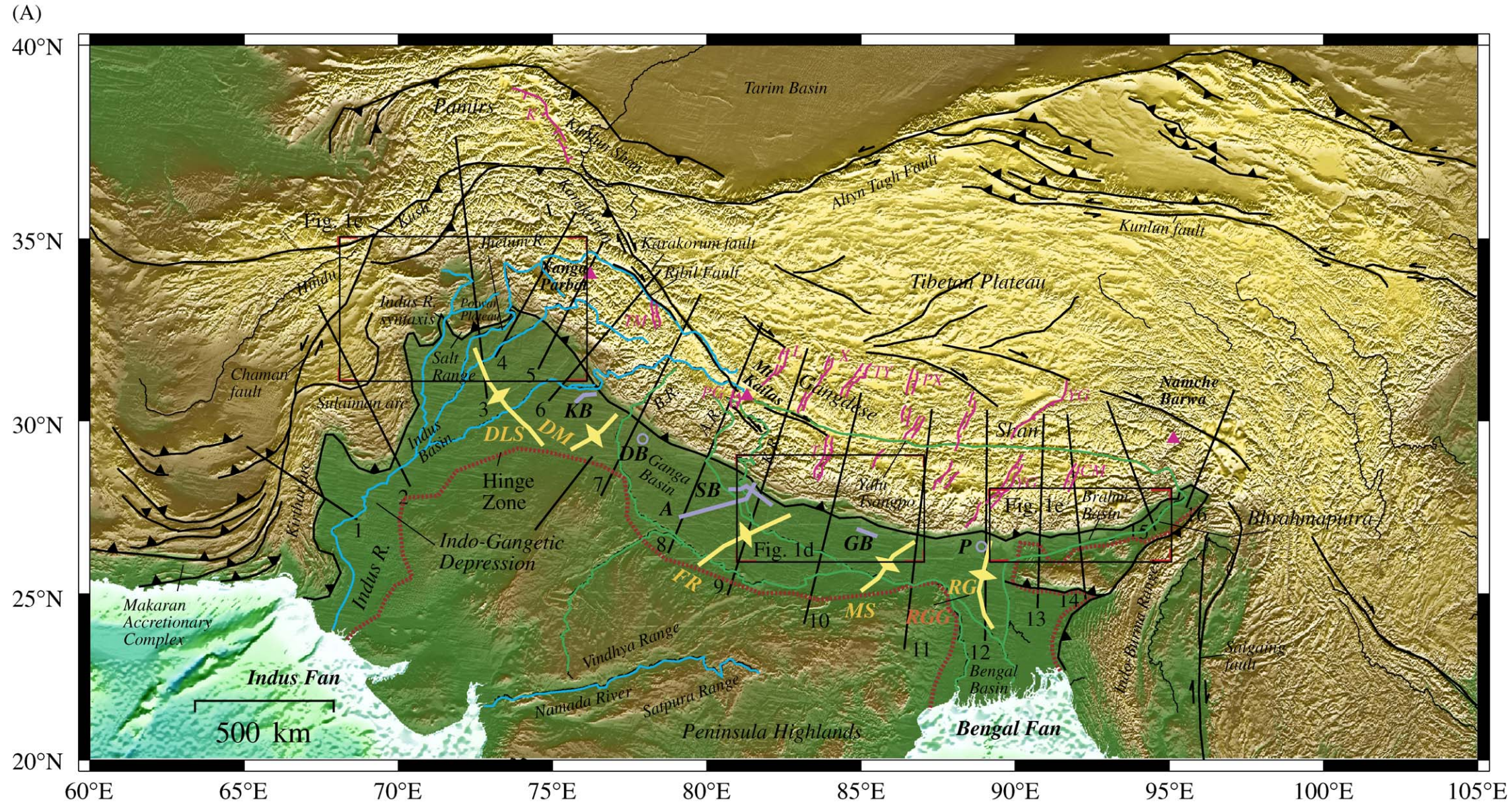


Fig. 1. (A) Topographic map of the Himalayan orogen. Regions outlined by yellow lines are basement ridges beneath the Indo-Gangetic depression after Rao (1973) and Raiverman (2000). DLS, Delhi–Lahore–Sargodha basement high; DM, Delhi–Muzaffarnagar ridge; FR, Faizabad ridge; MS, Manghyr–Saharsa ridge; RGR, Rajmahal–Garò Gap ridge; RGG, Rajmahal–Garò Gap. Rivers: B.R., Bhagirathi River; A.R., Alaknanda River; K.R., Kali River. Rifts: K, Kongur Shan extensional system; TM, Tso Morari rift; PG, Pulan–Gurla Mandhata extensional system; T, Thakkhola graben; L, Longge rift; X, Xiakangjian rift; TY, Tangra Yum Co rift; YG, Yadong–Guru rift; CM, Coma rift. Line A is the location of stratigraphic sections of the Indo-Gangetic depression shown in Fig. 3. Locations of stratigraphic sections based on drill hole data: KB, Kanga sub-basin, DB, Dehradun sub-basin, SB, Sarda sub-basin, GB, Ganak Basin, P, Purnea. The stratigraphic sections from Raiverman (2000) are shown in Fig. 3. (A) Stratigraphic sections beneath the Indo-Gangetic plains from Burbank (1992). (B) Topographic profiles across the Himalayan orogen using data from GTOPO 30. Each profile is an average of data from a 4-km wide swath using a 400 m running bin. (C) Close up view of topographic expression of western Himalayan orogen. The region is characterized by the presence of large basins with low aspect (i.e., width versus length) ratios. See panel (A) for location. (D) Close up view of topographic expression of central Himalayan orogen. The region is characterized by the presence of large basins with large aspect (i.e., width versus length) ratios. See panel (A) for location. (E) Close up view of topographic expression of eastern Himalayan orogen. Note that no prominent intermontane basins are present in this region. See panel (A) for location.

(B)

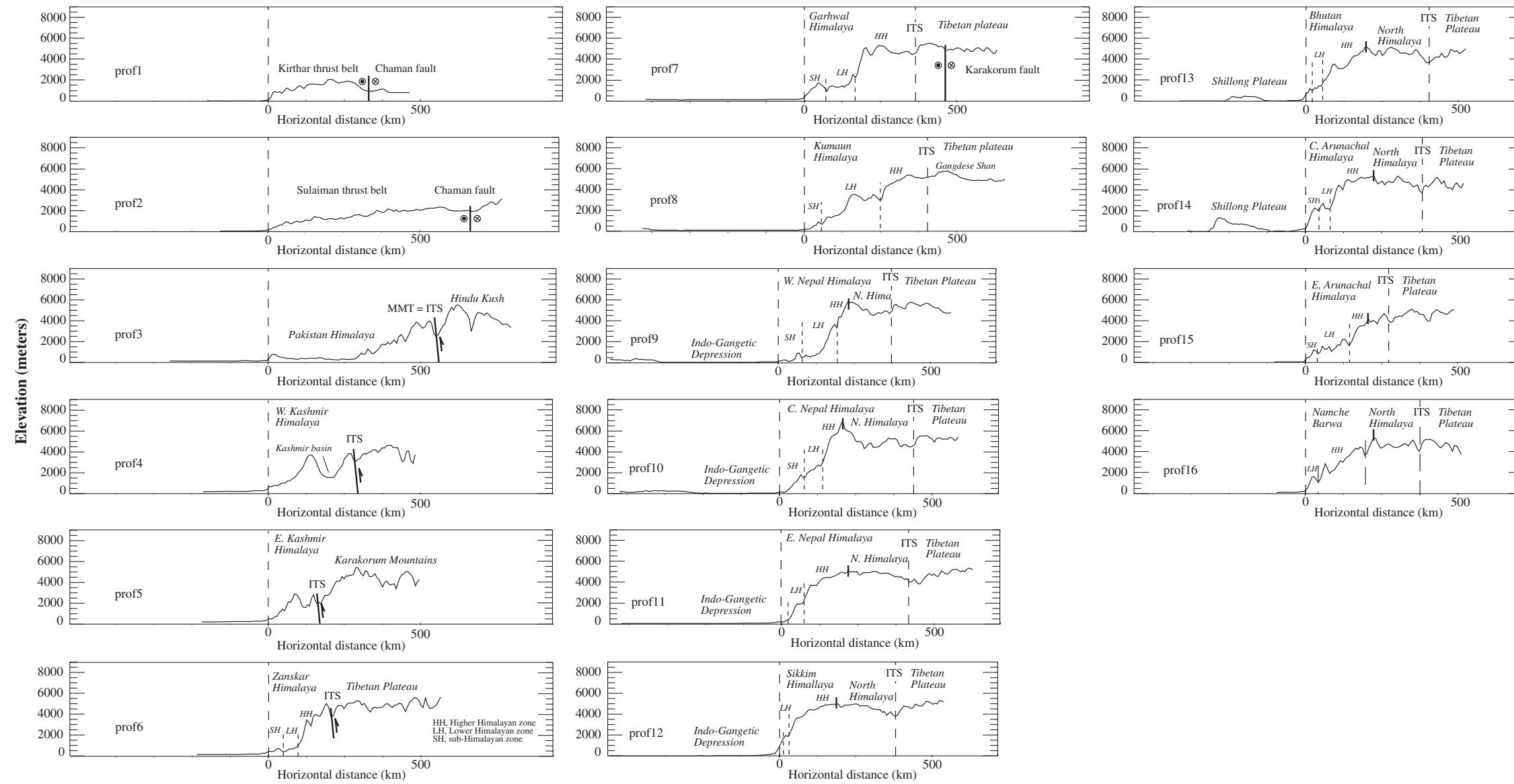


Fig. 1 (continued).

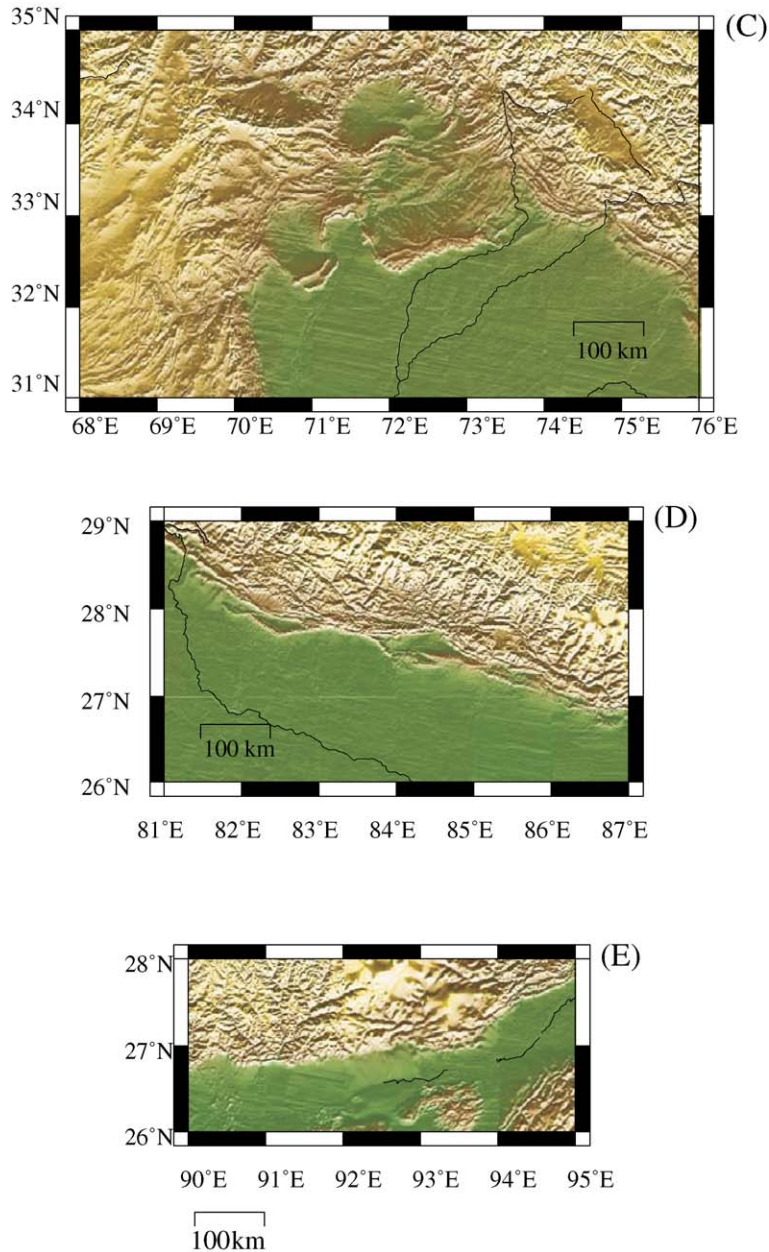


Fig. 1 (continued).

definitions of the Himalayan orogen are adopted. In the north–south direction, the Himalayan orogen may be divided into the *North Himalaya* and *South Himalaya* partitioned by its high crest line (Table 1). The North Himalaya is approximately equivalent to the geographically defined *Tethyan Himalaya* of Heim

and Gansser (1939) or the *Tibetan Himalaya* of LeFort (1975). Following the tradition of Heim and Gansser (1939) and Gansser (1964), the South Himalaya is divided into *Higher*, *Lower*, and *sub-Himalaya* from north to south (Table 1). I define the southern boundary of the Higher Himalaya at the base of the

Table 1  
Geographical, stratigraphic, and structural division of the Himalayan range and Himalayan orogen

Geographical/Topographic Division in this Paper		Litho- and Chrono-stratigraphy	Structural Division
<i>Map View:</i>	Tibetan Plateau	1. <i>Siwalik Group</i> : Neogene fine- to coarse-grained continental strata (~20–2 Ma).	1. STD hanging wall
	—— Indus River/Yalu Tsangpo ——		-----STD-----
	North Himalaya	2. <i>Lesser Himalayan Sequence (LHS)</i> : Metasedimentary and metavolcanic strata, augen gneiss (1870–800 Ma).	2. MCT hanging wall
	—— <i>Himalayan Crest</i> ——		-----MCT-----
	Higher Himalaya <i>Base of northernmost steep slope</i>		3. <i>Greater Himalayan Crystalline Complex (GHC)</i> : High-grade metamorphic rocks (800–480 Ma).
Lower Himalaya <i>Lowest intermontane valley</i>	4. <i>Tethyan Himalayan Sequence (THS)</i> : Late Precambrian to Eocene (~650–40 Ma) sedimentary sequence locally interlayered with volcanic flows. a. Late Prot.-D: pre-rift b. C-J1: syn-rift c. J2-K: passive-margin d. Paleocene-Eocene: syn-collision	-----MBT-----	
Sub-Himalaya		4. MFT hanging wall	
<i>Vertical Division:</i>	Upper Himalaya (> 3500 m)	5. North Indian Sequence (NIS): Phanerozoic cover sequence above LHS (520–20 Ma).	-----MFT-----
	Middle Himalaya (1500–3500 m)		5. MFT footwall
	Basal Himalaya (50–1500 m)		
<i>Along-strike Division:</i>	Western Himalayan orogen (west of 81°E, including Salt Range, Kashmir, Zaskar, Spiti, Himachal Pradesh, Garhwal, and Kumaun)		
	Central Himalayan orogen (81°E–89°E, including Nepal, Sikkim, and south-central Tibet)		
	Eastern Himalayan orogen (east of 89°E, including Bhutan, Arunachal Pradesh, and southeast Tibet)		

northernmost steepest slope of the southern Himalayan range, whereas the boundary between the Lower Himalaya and sub-Himalaya lies along the axis of the lowest intermontane valley parallel to the range (Table 1) (Fig. 1B). Although these boundaries are relatively easy to define on individual topographic profiles (Fig. 1B), in map view they can be discontinuous. This problem is particularly striking for the boundary between the Lower and sub-Himalaya, because most range-parallel intermontane valleys are discontinuous in the Pakistan and NW India Himalaya, become narrower in Nepal, and disappear completely east of Sikkim (Fig. 1C–E).

Elevation of some parts of the Lower Himalaya is in fact higher than some lower parts of the Higher Himalaya (Duncan et al., 2003) (Fig. 1B). To avoid confusion over the traditionally defined Higher, Lower, and sub-Himalaya, I suggest that the Himalayan range may be divided vertically into the *Basal* (<1500 m), *Middle* (1500–3500 m), and *Upper Himalaya* (>3500 m) (Table 1). Following this definition, the Upper Himalaya is mostly absent in northern

Pakistan south of the Indus–Tsangpo suture (=Main Mantle Thrust) as noted by DiPietro and Pogue (2004) (Fig. 1B).

Along strike, the Himalayan orogen may be divided into the *western* (66°–81°), *central* (81°–89°), and *eastern* (89°–98°) segments (Table 1). The western Himalayan orogen covers the following regions that commonly appear in the literature: Salt Range in northern Pakistan, Kashmir (also known as the Jammu–Kashmir State of NW India), Zaskar, Spiti, Chamba, Himachal Pradesh, Lahul, Garhwal, and Kumaun (also spelled as Kumaon) (Fig. 2A). The central Himalayan orogen occupies Nepal, Sikkim, and south-central Tibet, whereas the eastern Himalayan orogen includes Bhutan, Arunachal Pradesh of NE India, and southeastern Tibet (Fig. 2A).

A systematic along-strike change in the Himalayan topography is best expressed by the geometrical variation of the modern intermontane basins in the South Himalaya. For example, intermontane basins with north–south widths >80–100 km are present in northern Pakistan (e.g., Jalalabad and Peshawar

basins) and Kashmir (Kashmir basin) (Figs. 2A and 1C). However, intermontane basins become more elongated and narrower (<30–40 km in the north–south width) in the central Himalayan orogen (Fig. 1D) and are completely absent in the eastern Himalaya (Fig. 1E). As discussed in Section 7.6, this variation may be a direct result of an eastward increase in the total crustal shortening along the Himalayan orogen (also see Yin et al., submitted for publication).

### 2.2.2. Stratigraphic division

Stratigraphically, the major lithologic units in the Himalayan orogen consist of the Neogene *Siwalik Group*, the Proterozoic *Lesser Himalayan Sequence* (LHS), the Proterozoic–Ordovician *Greater Himalayan Crystalline Complex* (GHC), and the Proterozoic to Eocene *Tethyan Himalayan Sequence* (THS) (Table 1) (e.g., LeFort, 1996). Among these units, the definition and lateral correlation of the Greater Himalayan Crystalline Complex are most problematic. Heim and Gansser (1939) originally define the unit as high-grade metamorphic rocks structurally below the fossiliferous Tethyan Himalayan Sequence. This definition was followed by LeFort (1975) who replaced the GHC by the term “Tibetan slab” and designate it as “highly metamorphic and tectonized basement of the Paleozoic and Mesozoic Tethyan sediments” (p. 4, LeFort, 1975). Because the basal parts of the THS in northern Nepal and south-central Tibet also exhibit up to amphibolite facies metamorphism (e.g., Schenider and Masch, 1993), the Heim and Gansser (1939) definition is untenable. In this paper, I regard both the Greater Himalayan Crystalline Complex and Tethyan Himalayan Sequence as chronostratigraphic units regardless of their metamorphic grades. This definition has been implicitly or explicitly adopted by many workers (e.g., DeCelles et al., 2000; Steck, 2003; DiPietro and Pogue, 2004). Another problem in the Himalayan stratigraphic division is the use of lithostratigraphy as the basis for defining chronostratigraphic units.

### 2.2.3. Structural division

The major tectonostratigraphic units in the Himalayan orogen are defined as the *MFT hanging wall*, *MBT hanging wall*, *MCT hanging wall*, and *STD hanging wall* (Table 1). Unlike Gansser (1964) and LeFort

(1975), the structural units defined here do not have unique correlations with individual lithologic units (e.g., DiPietro and Pogue, 2004). That is, identifying and differentiating Himalayan lithologic units alone are not sufficient to determine the location of major Himalayan thrusts (cf. Ahmad et al., 2000), because the faults may cut up and down sections laterally and in their transport directions across major lithological boundaries.

### 2.2.4. Temporal division

The history of the Himalayan evolution has been generally divided into two stages: the Eohimalayan event that occurred during the middle Eocene to Oligocene (45–25 Ma) and the Neohimalayan event that occurred since the early Miocene (e.g., LeFort, 1996; Hodges, 2000). This division was originated from the recognition that several phases of metamorphism occurred during the development of the Himalayan orogen, with the older phases typically induced by crustal thickening and expressed by prograde metamorphism and later phases by unroofing and retrograde metamorphism (e.g., LeFort, 1975; Brunel and Kienast, 1986; Hodges and Silverber, 1988; Searle et al., 1999a). The essence of this division is the implicitly assumed synchronicity of similar deformation and metamorphic styles occurring along the entire length of the Himalayan orogen. As shown by DiPietro and Pogue (2004), application of this interpretation to the evolution of the western Himalayan orogen is problematic, where the typical “Neohimalayan” event associated with unroofing and retrograde metamorphism is completely absent. Because of its limited application to the evolution of the whole Himalaya, one should treat the above temporal division as a hypothesis rather than an accepted fact.

## 2.3. Major Himalayan lithologic units

### 2.3.1. Tethyan Himalayan Sequence (THS) (1840 Ma–40 Ma; Paleoproterozoic to Eocene)

The Tethyan Himalayan Sequence consists of Proterozoic to Eocene siliciclastic and carbonate sedimentary rocks interbedded with Paleozoic and Mesozoic volcanic rocks (Baud et al., 1984; Garzanti et al., 1986, 1987; Gaetani and Garzanti, 1991; Garzanti, 1993, 1999; Brookfield, 1993; Steck et al., 1993; Critelli and Garzanti, 1994; Liu and Einsele,

Table 2  
Selected stratigraphic sections of the Tethyan Himalayan Sequence

SE Zanskar	Northern Nepal	South-central Tibet
Chulung La FM. (Eocene ?) (siltstone, 100 m)	Muding FM. (E. Cret.) (marlstone, > 40m)	Zongshan FM (L. Cret.) (limestone, marl, sandstone, 270 m)
Spanboth FM. (L. Cret.-Pa.) (calcarenite, 120-140 m),	“glaucconitic horizon” (E. Cret.) (arenite, 25 m)	Jiubao FM. (L. Cret.) (limestone, sandstone, 90-180 m)
Kangi La FM. (L. Cret. ?) (siltstone, shale, sandstone, 400-600 m)	Daong FM. (E. Cret.) (shale and sandstone, 400 m)	Lengqingre FM. (L. Cret.) (shale, marl, 210-230 m)
Chikkim FM. (L. Cret. ?) (limestone, 90-100 m)	Kagbeni FM. (E. Cret.) (volcaniclastics, coal, 130 m)	Chaqiela FM. (E. Cret.) (shale, limestone, 160-180 m)
Giurnal Sandstone (L. Cret.-Pa./Eo.) (sandstone, 200-300 m)	Dangardzong Quartzarenite (L. Cret.) (sandstone, shale, 45 m)	Dongshan FM. (E. Cret.) (black shale, 500-800 m)
Spiti Shale (L. Jurassic-E. Cret.) (shale, 30 to >150 m)	Spiti Shale (L. Jr.) (black shale, 150 m)	Xiumo FM. (L. Jr.) (limestone, sandstone, 1800 m)
Laptal FM. (no information)	Dangar FM. (M. Jr.) (marlstone, 10 m)	Menbu FM. (L. Jr.) (shale, >500 m)
Kioto Limestone (E. Jurassic) (dolostone, 400 m)	Ferruginous Oolite FM. (M. Jr.) (ironstone, arenite, 7 m)	Lalongla FM. (M. Jr.) (limestone, quartzarenite, 740 m)
Quartzite Series/Alaror FM. (E. Triassic) (sandstone, quartzarenite, 120 m)	Laptal FM. (M. Jr.) (marl, arenite, 100-120 m)	Niehnieh Hsionla FM. (M. Jr.) (oolitic limestone, sandstone, 780 m)
Zozar FM. (L. Triassic) (limestone, 20 m)	Kioto Limestone (E.-M. Jr.) (carbonate, 250-300 m)	Pupuga FM. (E. Jr.) (siltstone, shale, sandstone, 880 m)
Hans FM. (M. Triassic) (marls, limestone, 410 m)	Zhamure Sandstone (L. Tr.-E. Jr. ?) (arenite, sandstone, 30 m)	Zhamure FM. (L. Tr.) (shale, sandstone, 140 m)
Tamba Kurkur FM. (E.-M. Triassic) (limestone, shale, 40-100 m)	Yak Kharka FM. (L. Tr. ?) (siltstone, limestone, arenite, 150 m)	Derirong/Qulonggongba/Yazhi FM. (L. Tr., sandstone) (shale, limestone, 1000 m)
Kuling FM. (L. Permian) (quartz arenite, 30-55 m)	Tarpa FM. (M. Tr.) (siltstone, sandstone, 400-500 m)	Kangshare FM. (L. Tr.) (limestone, shale, 99 m)
Panjal Traps (Permian) (volcanics and volcaniclastics, 2500 m)	Mukut FM. (E. Tr.) (marl, marly limestone, 200-270 m)	Qudenggongba FM. (M. Tr.) (carbonate, shale, 200-400 m)
Ganmachidam FM. (Carb.- E. Permian) (sandstone, siltstone, shale; no thickness estimates)	Tamba-Kurkur FM. (E. Tr.) (pelagic limestone, 23-50 m)	Tulong FM. (E. Tr.) (limestone, shale, 100-300 m)
Po FM. (Carboniferous) (sandstone, limestone, 80-100 m)	Nar-Tsum Spilites (E. Permian) (spilitized tholeiitic basalt, 0-85 m)	Baga FM. (L. Permian) (domestone, marl, 10 m)
Lipak FM. (E. Carb.) (marly limestone, 50-70 m)	Puchenpra FM. (E. Permian) (sandstone, arenite, 100-150 m)	Shengmi FM. (E. Permian) (shale, limestone, sandstone, 400 m)
Muth Quartzite (Devonian) (massive white quartzite, > 200 m)	Atali Quartzarenite (L. Carb.) (sandstone, 100 m)	Jiling FM. (L. Carb.) (Quartzarenite, diamicctite, 700 m)
Thaple FM. (Ordov.-Silu.) (conglomerate, > 300 m)	Braga FM. (L. Carb. ?) (shale, sandstone, diamicctite, 120 m)	Naxing FM. (E. - M. Carb.) (shale, marl, sandstone, 60 m)
----- <i>unconformity</i>	Bangba FM. (L. Carb.) (sandstone, shale, diamicctite, 90 m)	Poqu Group (M.-L. Dev.) (shale, quartzarenite, 320 m)
Karsha FM. (M.-L. Camb.) (dolostone and slate, ~200 m)	Col Noir Shale (L. Carb.) (shale, sandstone, 160 m)	Liangquan FM. (E. Dev.) (arenite, limestone)
Phe FM. (late Protero.-Camb.?) (shale, sandstone, ~ 1500 m)	“Syringothyris beds” (L. Carb.) (arenite, shale, sandstone, 65 m)	Pulu Group (M. - L. Silurian) (quartz arenite, limestone, 50 m)
	Marsyandi FM. (E. Carb.) (shale, sandstone, arenite, 400 m)	Shiqipo FM. (E. Silurian) (shale, sandstone, limestone, 90 m)
	Ice Late/Tilcho Lake FM. (E. Carb.) (carbonate, 320 m)	Hongshantou FM. (L. Ordo.) (shale, sandstone, 70 m)
	Tilicho Pass FM. (L. Dev.) (quartzarenite, carbonate)	Jiacun Group (E. - M. Ordo.) (carbonate, 820 m)
	Muth FM. (M. - L. Dev.) (carbonate, quartzarenite, mudstone)	Ruqiecun Group (Cambrian ?) (marble, banded limestone, 240 m)
	Dark Band FM. (E. Silurian-Early Dev.) (pelite, limestone, marl)	
	North Face Quartzite/Gyaru FM. (L. Ordo.) (quartzite, mudstone)	
	Dhaulagiri Limestone/Nilgiri FM. (M. Ordo.) (strongly recrystallized carbonate)	
	Annapurna Yellow FM. (Cambrian ?) (Bt+Ms calc schist, psammite)	
	Sanctuary FM. (Cambrian ?) (BT+Ms schist, sandstone)	

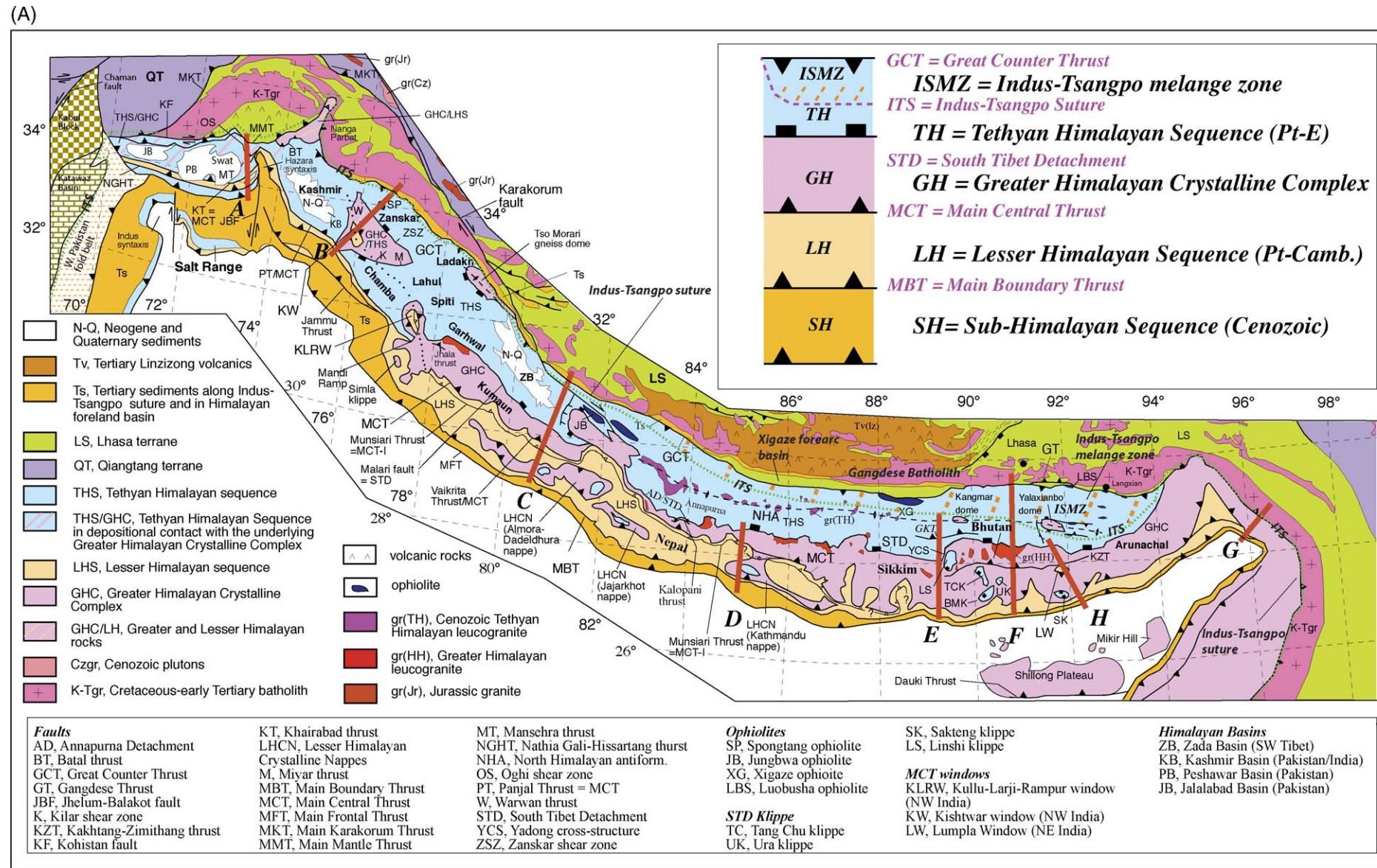


Fig. 2. (A) Regional geologic map of the Himalayan orogen. Main sources are from Liu (1988), Frank et al. (1995), Fuchs and Linner (1995); Yin and Harrison (2000), Ding et al. (2001), DiPietro and Pogue (2004) and my own observations and interpretations. All map symbols are defined below the map. (B) Geologic cross-section of the Hazara region of northern Pakistan. Geology portrayed on the cross-section is mostly based on Greco and Spencer (1993), Pogue et al. (1999), DiPietro et al. (1999), Treloar et al. (2003), and DiPietro and Pogue (2004). Major lithologic units: Ts, Tertiary sediments; THS, Tethyan Himalayan Sequence; LHS, Lesser Himalayan Sequence; THS/GHC, unmetamorphosed (with respect to Cenozoic deformation) Tethyan and Greater Himalayan Sequences; GHC, Greater Himalayan Crystalline Complex. MBT, Main Boundary Thrust; MMT, Main Mantle Thrust; MCT, Main Mantle Thrust. (C). Geologic cross-section across the Chamba–Zaskar Himalaya. See Fig. 7 for detailed geology and sources of references. DV, Dras volcanic complex; GCT, Great Counter thrust; JT, Jammu thrust; MZBT, Main Zaskar backthrust; PJB, Panjal basalt; SP, Spongtang ophiolite; STD, South Tibet Detachment; ZSZ, Zaskar shear zone. (D). Geologic cross-section across southwest Tibet and western Nepal modified from DeCelles et al. (2001) and Murphy and Yin (2003). LHCN, Lesser Himalayan Crystalline Nappe; SKT, South Kailas thrust; GCT, Great Counter thrust. (E). Geologic map across the Kathmandu nappe of south-central Nepal modified from Johnson et al. (2001) with additional information from Arita (1983). gr(Or), Ordovician granite; gr(Pt), Paleo- to Meso-Proterozoic plutons. (F). Geologic cross-section of easternmost Nepal and south-central Tibet, slightly modified from Hauck et al. (1998). MHT, Main Himalayan Thrust. (G) Geologic cross-section across southeast Tibet and Bhutan. Geology is based on Yin et al. (1994, 1999), Gansser (1983), and Grujic et al. (2002). See Fig. 10 for symbols of major units and structures. GKT, Gyrong–Kangmar thrust. (F). Geologic cross-section of the Lohit Valley. Geology is based on Gururajan and Choudhuri (2003).

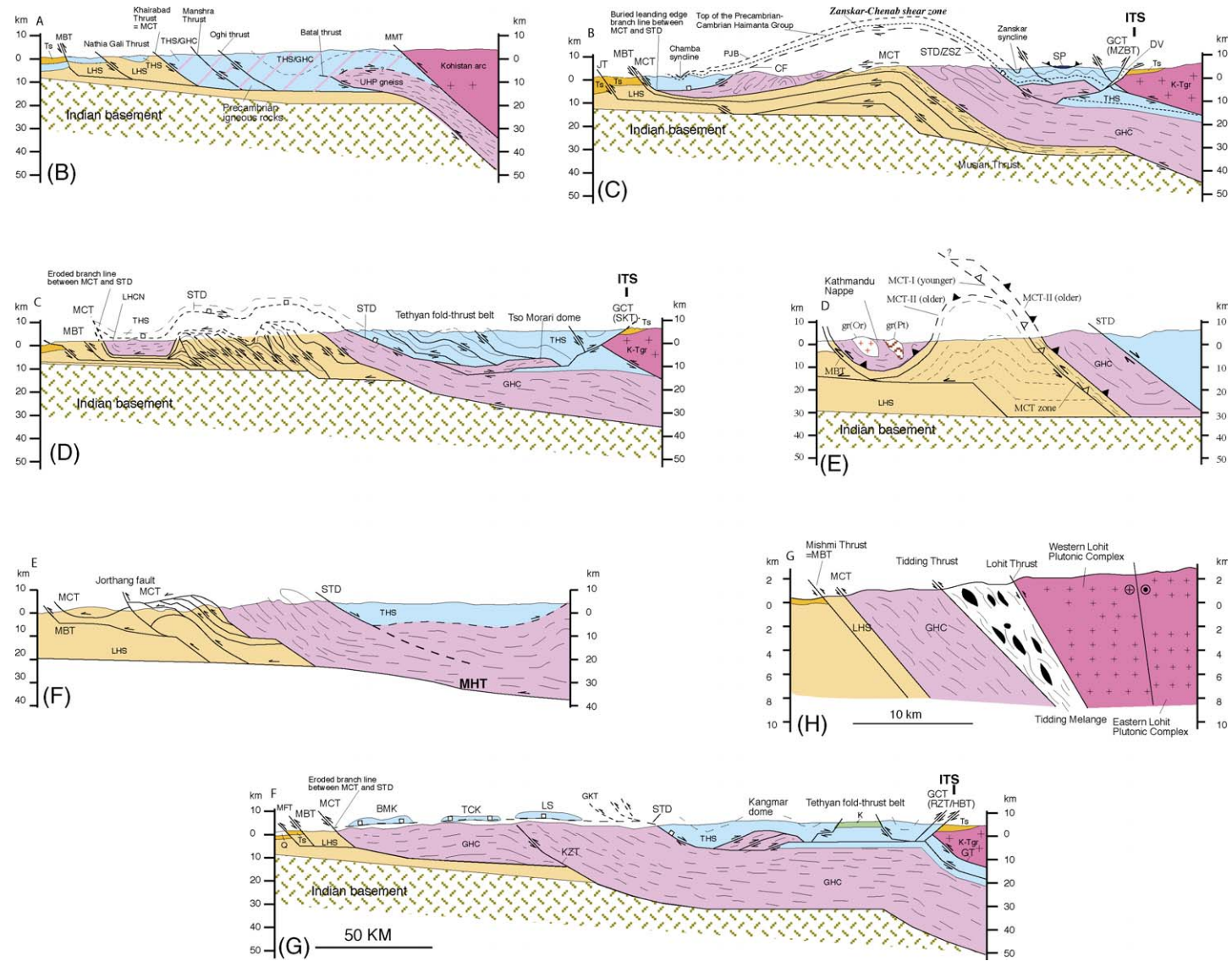
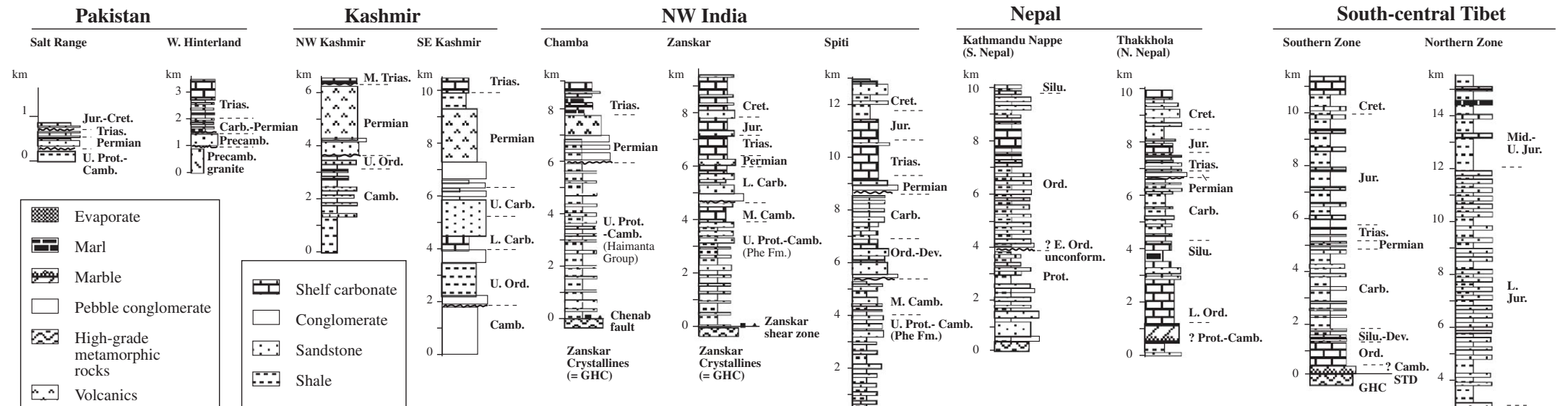
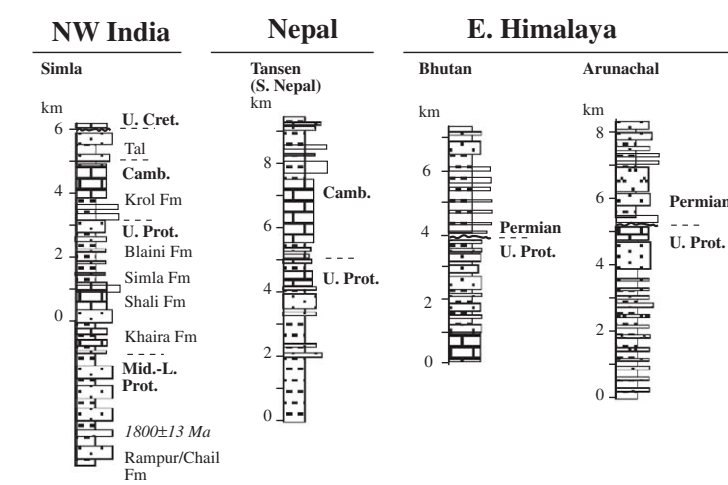


Fig. 2 (continued).

### TETHYAN HIMALAYAN SEQUENCE



### LESSER HIMALAYAN SEQUENCE



### CENOZOIC STRATA BELOW INDO-GANGETIC PLAINS

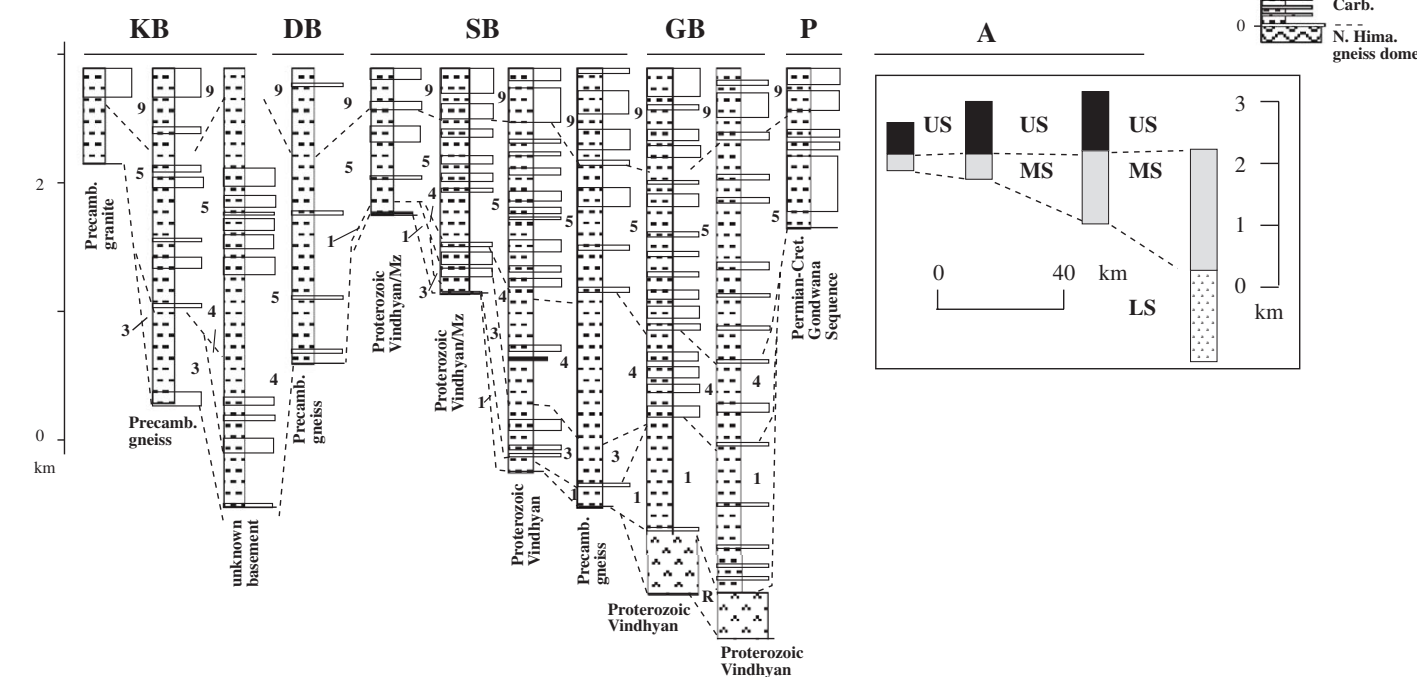


Fig. 3. Selected stratigraphic sections of Tethyan Himalayan, Lesser Himalayan, and Cenozoic sequences. Salt Range section is from Gee (1989), Western Hinterland of northern Pakistan from Pogue et al. (1999), south-central Tibet from Liu and Einsele (1994), and the rest is modified from Brookfield (1993). Cenozoic sections of the Indo-Gangetic depression are modified from Burbank (1992) (section (A) shown in Fig. 1A) and Raiverman (2000) (sections KB, DB, SB, GB, and P). Note that the age of Proterozoic strata in Arunachal was considered as Mesoproterozoic by Brookfield (1993) but here is changed to Upper Proterozoic based newly available detrital zircon ages from the region (Yin et al., submitted for publication). Also, the age of metabasalt in the Rampur Formation is from Miller et al. (2001). Stratigraphic sections of the Indo-Gangetic depression based on drill hole data: KB, Kanga sub-basin; DB, Dehradun sub-basin; SB, Sarda sub-basin; GB, Ganak Basin; and P, Purnea. The stratigraphic sections from Raiverman (2000) and their locations are shown in Fig. 1A. Numbers in the Cenozoic sections of the Indo-Gangetic depression are (1) late Paleocene to middle Eocene; (2) late Eocene to early Oligocene (this section is complete missing); (3) late Oligocene to early Miocene; (4) early Miocene to middle Miocene; (5) late Miocene; (6) late Miocene to early Pleistocene; (7) middle Pleistocene; (8) late Pleistocene; (9) late Pleistocene to Holocene; and R, Late Cretaceous Rajmahal trap basalt. In section (A), US, Pliocene–Holocene Upper Siwalik Group (=7, 8 and 9); MS, late Miocene–Pliocene Middle Siwalik Group (=5 and 6); LS, middle Miocene Lower Siwalik Group (4).

Table 3  
Hanging-wall and footwall stratigraphic cutoffs along the Main Central Thrust System from west to east

		74°E	75°E	77°E	78°E	82°E	86° E 90° E	92° E	94° E			
		N Pakistan	W Pakistan	Kashmir/Chamba	Kishtwar Window	Kullu Window	E. Garhwal/W. Nepal	Central Nepal	Kathmandu Nappe	Bhutan	W. Arunachal	E. Arunachal
Hanging Wall Units and Faults	Ordovician		Misri Banda Quartzite						Paleozoic Tethyan strata (Phuchauki Group)			
	Cambrian		Ambar FM									
Proterozoic		Kaghan Group Quartzite, schist, gneiss, marble, pegmatite, and granite	Tanawal FM Quartzite, schist, marble	Salooni FM (early Paleozoic)	Greater Himalayan Crystallines Kyanite-sillimanite ± staurolite gneiss and schist, orthogneiss, and leucogranites	Greater Himalayan Crystallines Kyanite-sillimanite ± staurolite gneiss and schist, orthogneiss, and leucogranites	Greater Himalayan Crystallines = Vaikrita Group Kyanite-sillimanite ± staurolite gneiss and schist, migmatite, orthogneiss, leucogranites	Greater Himalayan Crystallines = Tibetan Slab Kyanite-sillimanite ± staurolite gneiss and schist, migmatite, orthogneiss, leucogranites	unconformity	Greater Himalayan Crystallines = Thimphu Group Kyanite-sillimanite ± staurolite gneiss and schist, migmatite, orthogneiss, tourmaline granite, and pegmatite	Greater Himalayan Crystallines = Se La Group Kyanite-sillimanite ± staurolite gneiss and schist, migmatite, orthogneiss, tourmaline granite, and pegmatite	GHC = Mishmi Crystallines Garnet-staurolite-kyanite schist, marbles, mylonitic augen gneiss
		Sharda Group gneiss, marbles, granite, migmatites, and amphibolites	Manki FM. Phyllite, quartzite, marble, argillite	Chamba FM. Phyllite, slate, limestone					U. Bhimpheedi Group Marku FM Kulikhani FM Chisapani FM			
Footwall Units and Faults		MCT	KPT=MCT	PT=MCT	MCT	MCT	VT=MCT	MCTII=upper MCT	L. Bhimpheedi Group Kalitar FM Bhainsedobhan FM Raduwa FM	High-grade gneiss, schist, leucogranites	MCT	MCT
			Hazara FM. Slate, argillite, greywacke, and minor limestone	Shali Group Phyllite, slate, limestone	Lower Crystalline Nappe Bajaura FM: mylonitic augengneiss, carbonate	Munsiari Thrust Sheet schist, orthogneiss, metabasic sills	Almora Group Metapelite, gneiss, and quartzite	Upper Midland Sedimentary Zone (mylonitic gneiss, augen gneiss, schist)	Mahabharat Thrust (=upper MCT)	Daling-Shumar Group (Late Precambrian, phyllite, shale, slate, quartzite)	Dirang FM Garnet-muscovite-biotite schist, phyllite, quartzite, and marble.	Lesser Himalaya Sequence Phyllite, metavolcanic rocks
Fault Names		BF = Batal Fault	OSZ=Oghi shear zone MT=Mansehra Thrust KPT = Khairabad-Panjal thrust NGHF = Nathia Gali-Hissartang fault	PT = Panjal Thrust		MST = Musiari Thrust	AT = Almora Thrust DT = Dadel dhura Thrust VT = Vaikrita Thrust RT = Ramgarhi Thrust			KT = Kakhtang Thrust		
	References	Chaudhry and Ghazanfar, 1990	Calkin et al., 1975 Greco et al., 1989 Pogue et al., 1999	Thakur 1998 Frank et al., 1995	Frank et al., 1995	Frank et al., 1995; Wiesmayr and Grasmann, 2002	Srivastava and Mitra, 1994 Valdiya, 1980	Arita, 1983	Johnson et al., 2001; Upreti and LeFort, 1999; Stocklin, 1980	Gansser, 1983 Grujic et al., 2002	Kumar, 1997	Gururajan and Chouduri, 2003

1994, 1999) (Table 2) (Fig. 3). The THS can be divided into four subsequences:

- (1) Proterozoic to Devonian *pre-rift sequence* characterized by laterally persistent lithologic units deposited in an epicratonal setting;
- (2) Carboniferous–Lower Jurassic *rift and post-rift sequence* that show dramatic northward changes in thickness and lithofacies;
- (3) Jurassic–Cretaceous *passive continental margin sequence*; and
- (4) uppermost Cretaceous–Eocene *syn-collision sequence* (Liu and Einsele, 1994; Garzanti, 1999) (Table 2).

Liu and Einsele (1994) interpret the start of the syn-rift sequence at the beginning of the Permian while Garzanti (1999) places this boundary at the earliest Carboniferous. Garzanti's (1999) suggestion is based on his study in north-central Nepal, which shows that the thickness of the Carboniferous strata varies from being completely absent to over 700 m thick over a distance of ~40–50 km (Fig. 4). In Lahul of NW India (Fig. 2A), Vannay and Steck (1995) show that Ordovician–Carboniferous strata are absent in the overturned north-verging Tandri syncline (Fig. 7). They also show that the missing Paleozoic strata reappear about 15 km to the north in the THS and attribute it to late Paleozoic rifting. The Carboniferous–Jurassic rifting event in the North Himalaya is commonly related to separation of the Lhasa terrane from northern India and the eventual opening of Neo-Tethys (e.g., Burg et al., 1983; Sengör, 1984; Brookfield, 1993; LeFort, 1996; also see Ricou, 1994 and Sengör and Natal'in, 1996 for systematic paleogeographic reconstructions of Neo-Tethys). The stratigraphic boundary between the passive margin sequence and the overlying syn-collision strata of the THS is poorly defined. This is because the age for the onset of Indo-Asian collision is not well constrained, with estimates ranging from ~65 Ma to ~43 Ma (Patriat and Achahe, 1984; Rowley, 1996; Yin and Harrison, 2000; Najman et al., 2001, 2002, 2003; Zhu et al., 2005; Ding et al., 2005). The issue is complicated by possible latest Cretaceous or even Eocene collision of an oceanic arc with India prior to the final collision between India and Asia (e.g., Reuber, 1986; Corfield et al., 1999, 2001;

Ziabrev et al., 2004; cf., Rowley, 1996; Yin and Harrison, 2000).

In the northwestern Indian Himalaya, the pre-rift sequence can be further divided into the Proterozoic–Middle Cambrian Haimanta Group and a Lower Ordovician–Devonian shelf sequence. The two units are separated by a regional unconformity with the lower unit extensively intruded by 550–470 Ma granites (e.g., Baud et al., 1984; Brookfield, 1993; Frank et al., 1995; Miller et al., 2000). The lower age bound of the Haimanta Group is poorly known and is considered by most to be Neoproterozoic in age (Frank et al., 1995; see also Draganits, 2000 for detailed review of this problem). However, Miller et al. (2001) using Rb–Sr dating of a mylonitic orthogneiss unit (the Baragaon gneiss) show that the basement of the THS has an age of ~1840 Ma in the Kullu–Larji–Rampur window (Fig. 2A). Note that most Indian geologists regard the Baragaon gneiss as part of the LHS (e.g., Pandey and Viridi, 2003). The age of the Baragaon gneiss is similar to that of the Ulleri gneiss in Nepal, which is considered to be part of the LHS and is located within the Ramgarh thrust sheet (e.g., DeCelles et al., 2001). This lateral variation of assigning the potentially same lithologic units to thrust sheets both above the MCT (i.e., the Baragaon gneiss in NW India) and below the MCT (i.e., the Ulleri gneiss in Nepal) implies that the MCT cuts up-section laterally to the west and the Heim and Gansser (1939) tectonostratigraphic division is unworkable in the Himalaya.

A Proterozoic sequence below an Ordovician unconformity in the THS has been inferred in southern Nepal within the Kathmandu Nappe and possibly in Bhutan (Stöcklin, 1980; Bhargava, 1995) (Fig. 2A). This unconformity appears absent in northern Nepal and south-central Tibet where the basal THS has experienced greenschist to amphibolite facies metamorphism (e.g., Liu and Einsele, 1994; Schenider and Masch, 1993; Garzanti et al., 1994; Garzanti, 1999) (Fig. 3). In both areas, Ordovician strata appear to lie conformably on top of metamorphosed carbonate and sandstone that have been assigned Cambrian and Proterozoic ages without any fossil evidence or radiometric age constraints (e.g., Colchen et al., 1986; Upreti, 1999). The apparent absence of the Ordovician unconformity in northern Nepal and south-central Tibet may be due to either

intense Cenozoic deformation and metamorphism (Brookfield, 1993; Garzanti et al., 1994; Searle and Godin, 2003) or a change in lithofacies from coarse conglomerates in NW India to finer clastic deposits in northern Nepal (Gehrels et al., 2003).

The lithostratigraphy of the THS changes both along and perpendicular to the Himalayan orogen. Brookfield (1993) notes that sedimentation of the THS in the Indian Himalaya is markedly different east and west of the Nanga Parbat syntaxis prior to the onset of the Indo-Asian collision. He attributes this to two rifting events: one in the Jurassic along the western margin of India and one in the Permian along the northern margin of India. Recently, DiPietro and Pogue (2004) trace major Himalayan stratigraphic units (i.e., GHC, THS, and LHS) continuously across the Nanga Parbat syntaxis based on the presence of distinctive igneous and metamorphic units and show that the GHC, THS, and LHS all belong to the same stratigraphic sequence deposited on the northern margin of India.

The THS has also been divided into the northern (= outer) and southern (= inner) zones (Brookfield, 1993; Liu and Einsele, 1994). The thickness and lithofacies of the Proterozoic to Carboniferous strata are similar in that both zones were deposited in a shelf setting, but their Mesozoic strata differ dramatically. The northern THS zone consists of a thick slope sequence, whereas the southern THS zone is dominated by shelf and shelf-edge sequences (Fig. 3) (also see detailed comparison of the two zones by Liu and Einsele, 1994). It is interesting to note that Cambrian to Devonian strata in south-central Tibet are missing in the northern zone but exist in the southern zone. This could either result from Carboniferous rifting or Cenozoic development of the North Himalayan gneiss domes, as the latter form the basement of the Carboniferous strata in the northern THS zone (e.g., Liu, 1988; Lee et al., 2000).

### 2.3.2. Greater Himalayan Crystalline Complex (GHC) (?1800–480 Ma; Paleoproterozoic to Ordovician)

Although the GHC consists generally of high-grade rocks, they become indistinguishable in northern Pakistan from the THS, where it appears as low-grade to unmetamorphosed sedimentary strata interlayered with ~500 Ma granites (e.g., Pogue et

al., 1999). The high-grade GHC rocks generally form a continuous belt along the east-trending axis of the Himalayan range, but they also occur as isolated patches surrounded by low-grade Tethyan Himalayan strata such as in the Zaskar and Tso Morari regions of NW India, along the North Himalayan Antiform (NHA), and in the Nanga Parbat massif of northern Pakistan (Fig. 2A) (Honegger et al., 1982; Steck et al., 1998; DiPietro and Pogue, 2004).

In Nepal, the GHC is bounded by the MCT below and the STD above (Table 3). Its age is estimated to be Neoproterozoic to Ordovician (Parrish and Hodges, 1996; DeCelles et al., 2000). The metamorphic grade in the GHC first increases upward in its lower part and then decreases from the middle to the upper part towards the STD (e.g., Hubbard, 1989; LeFort, 1996). In Himachal Pradesh along the Sutlej River in NW India, inverted metamorphism appears to span the whole GHC from MCT zone to the STD (Vannay and Grase-mann, 1998). Deformed and undeformed early to middle Miocene leucogranites are widespread in the GHC, but they are mostly concentrated in the very top part of the GHC (e.g., Gansser, 1964, 1983; LeFort, 1975, 1996; Scaillet et al., 1990, 1995; Guillot et al., 1993, 1995; Parrish and Hodges, 1996; Searle et al., 1997, 1999a,b; Murphy and Harrison, 1999; Dèzes et al., 1999; Grujic et al., 2002).

In Zaskar of NW India, low-grade THS surrounds the GHC. The Carboniferous and Triassic strata of the THS are also metamorphosed to amphibolite facies (Honegger et al., 1982) and lie together with the GHC below the north-dipping Zaskar shear zone (e.g., Herren, 1987). This observation suggests that the metamorphic grade alone cannot be used as the sole criterion to differentiate the THS from GHC.

The lack of a high-grade equivalent of the GHC in northern Pakistan to that observed in the central Himalaya has been long noted (e.g., Yeats and Lawrence, 1984). Whittington et al. (1999), DiPietro and Isachsen (2001), and Zeitler et al. (2001) demonstrate the presence of high-grade Lesser Himalayan rocks within and adjacent to the Nanga Parbat syntaxis (Fig. 2A). These rocks have experienced ductile deformation, intrusion, and metamorphism at ~500, 1850, and 2174 Ma, respectively (DiPietro and Isachsen, 2001; Zeitler et al., 2001). The intrusive age of ~1850 Ma correlates with the ~1800 Ma Uleri gneiss of the LHS

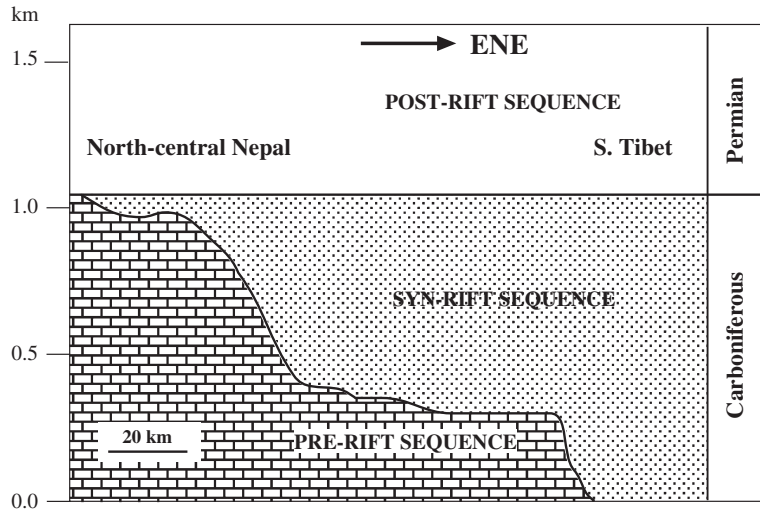


Fig. 4. Schematic diagram showing variation of syn-rift Carboniferous deposits in north-central Nepal, simplified from Garzanti (1999).

in Nepal (e.g., DeCelles et al., 2001) and Baragaon gneiss in the Kullu–Larji–Rampur window of NW India (Miller et al., 2000).

### 2.3.3. Lesser Himalayan Sequence (LHS) (1870–520 Ma; Proterozoic–Cambrian)

The stratigraphic division of the Lower or Lesser Himalayan Sequence by Heim and Gansser (1939) and LeFort (1975) only includes the nonfossiliferous low-grade metasedimentary rocks (Table 4). These strata are overlain by Permian to Cretaceous strata which are often referred to as the *Gondwana Sequence* (Gansser, 1964) (Fig. 3). In contrast to the THS, no Ordovician to Carboniferous strata are present above the LHS along the whole Himalayan orogen east of the Nanga Parbat syntaxis (Fig. 3). In light of radiometric ages of interlayered gneisses, detrital zircons, and metavolcanic rocks (Trevidi et al., 1984; Miller et al., 2000; DeCelles et al., 2000; Singh et al., 2002; Yin et al., submitted for publication), the LHS has an age range of 1870–850 Ma. Its main lithology includes metasedimentary rocks, metavolcanic rocks, and augen gneiss (e.g., Frank et al., 1995; DeCelles et al., 1998a; Upreti, 1999). Upper Proterozoic strata are in conformable contact with overlying Cambrian strata in NW India and possibly in Nepal (Valdiya, 1980; Brunel et al., 1984, 1985). But in Pakistan, Mesoproterozoic strata

of the LHS are overlain by either Cambrian or Carboniferous sequences of the THS (DiPietro and Pogue, 2004) (Fig. 5).

### 2.3.4. North Indian Sequence (NIS) (Proterozoic and Phanerozoic)

From the above descriptions, the GHC, LHS, and THS overlap in ages despite drastically different lithology and metamorphic grade. The latter could result from long-distance tectonic transport along Cenozoic thrusts. Thus, it would be useful to have a consistent chronostratigraphic division of all the Himalayan units. Following Brookfield's (1993) idea, I refer to the whole Precambrian and Phanerozoic sedimentary sequence in the Himalayan region as the *North Indian Sequence*. Their possible three-dimensional distribution is schematically shown in Fig. 5. It is within this complex three-dimensional stratigraphic framework that the main Himalayan units such as the THS, LHS, and GHS were sampled.

### 2.3.5. Cenozoic Sequence in the MFT and MBT Hanging Walls

This sequence consists of the Neogene Siwalik strata in the MBT footwall and Paleogene–early Miocene strata in both the MBT hanging wall and footwall (Fig. 2) (Table 5) (e.g., Schelling and Arita, 1991; Burbank et al., 1996; DeCelles et al., 1998a,b). The Tertiary strata

Table 4  
Lesser Himalayan Sequence

		76°E	Western Himalaya		80°E
		Western Syntaxis			
N. Pakistan		Kishtwar, Chamba, and Kullu Region			
		Outer Lesser Himalaya	Inner Lesser Himalaya		
Cambrian	Abottabad Group Carbonaceous and argillaceous turbidite, cherty stramatolitic dolostone	Permian Units: Panjal Trap, basalt, andesite, conglomerate, shale, and arenite.			
U. Proter.	Tanawal Fm. arenaceous beds with argillite and carbonates	Dogra-Simla Slates (Proterozoic) carbonate, evaporite, schist, phyllite	Shali Group (Proterozoic) stramatolite-bearing carbonates		
	Misri Banda Quartzite		Khaira Group (Proterozoic) carbonate, slate, quartzite		
Camb. (?)	Ambar Fm. unfossiliferous dolomite		Garsa Fm. (Proterozoic) Phyllite		
	Tanawal Fm. quartzite, argillite, quartz mica schist, schistose quartzite	Rampur Group (= Chail Fm. = Berinag Fm.) (Early to Mesoproterozoic) quartzite, phyllite, basic metavolcanic rocks (U-Pb zircon age of 1800±13 Ma), diabases, meta-rhyodacite (U-Pb zircon age of 1816±16Ma).			
M. - L. Proterozoic	Shekhei Fm. quartzite, limestone	Frank et al. (1995), Miller et al. (2001)			
	Utch Fm. limestone, slate, argillite				
	Shahkot Fm. limestone, argillite				
L. Proterozoic	Manki Fm. argillite, slate, phyllite, siltstone				
	Karora and Gandaf Fms. marble, carbonaceous phyllite, graphitic schist, intruded by 1.84 Ga orthogneiss and overlying an orthogneiss of 2.17 Ga				
	▲ Khairabad Thrust ▲				
Cambrian	Tarnawai Fm. siltstone, mudstone, shale				
	Kakul Fm. sandstone, shale, carbonate				
	Tanakki Conglomerate				
	unconformity				
L. Proterozoic	Hazara Fm. sandstone, shale, graywacke, algal limestone				
		Garhwal Himalaya			
		Outer Lesser Himalaya		Inner Lesser Himalaya	
Almora Group	Gumalikheth FM. (kyanite-bearing schist and gneiss) Champawat Granodiorite Saryu FM. (augen gneiss, schist, metapelite)	Almora Thrust ▲		Munsiari FM. ▲ Munsiari Thrust ▲	
Ramgarh Group	Debguru Porphyroid (mylonitic gneiss and schist, quartzite, metagranite, and slate) Nathuakhan FM. (schist, quartzite, amphibolite)	▲ Ramgarh Thrust ▲		Barkot and Bhatwari units ▲ Barkot-Bhatwari Thrusts ▲	
Sirmur Group	Subathu FM. (L. Paleocene-M. Eocene) (shale, sandstone, limestone) Singtali/Bansi FM. (L. Cret.-Paleocene) (limestone, sandstone)				
Mussoorie Group	Tal FM. (Cambrian) (shale, chert, limestone) Krol FM. (Precambrian) (limestone, shale, and sandstone) Infra-Krol (Precambrian) (limestone) Blaini FM. (Precambrian) (siltstone, conglomerate, shale)				
Jamsar Group	Nagtha FM. (Precambrian) (quartzite) Chandpur FM. (Precambrian) (shale, limestone, sandstone) Mandhali FM. (phyllite and marble)	▲ Krol Thrust=MBT ▲		▲ Berinag Thrust ▲	
	Subathu FM. (L. Eocene)				
Tejam Group		Mandhali FM. (phyllite and marble) Deoban FM. (Precambrian) (limestone, shale, sandstone)			
Damitha Group	Rautgara FM. (Precambrian) (greywacke, siltstone, shale) Chakrata FM. (Precambrian) (turbidites)	Rautgara FM. Chakrata FM.			
		Valdiya (1980), Srivastava and Mitra (1994)			

Greco and Spencer (1993)  
Pogue et al. (1999),  
DiPietro et al. (1999)



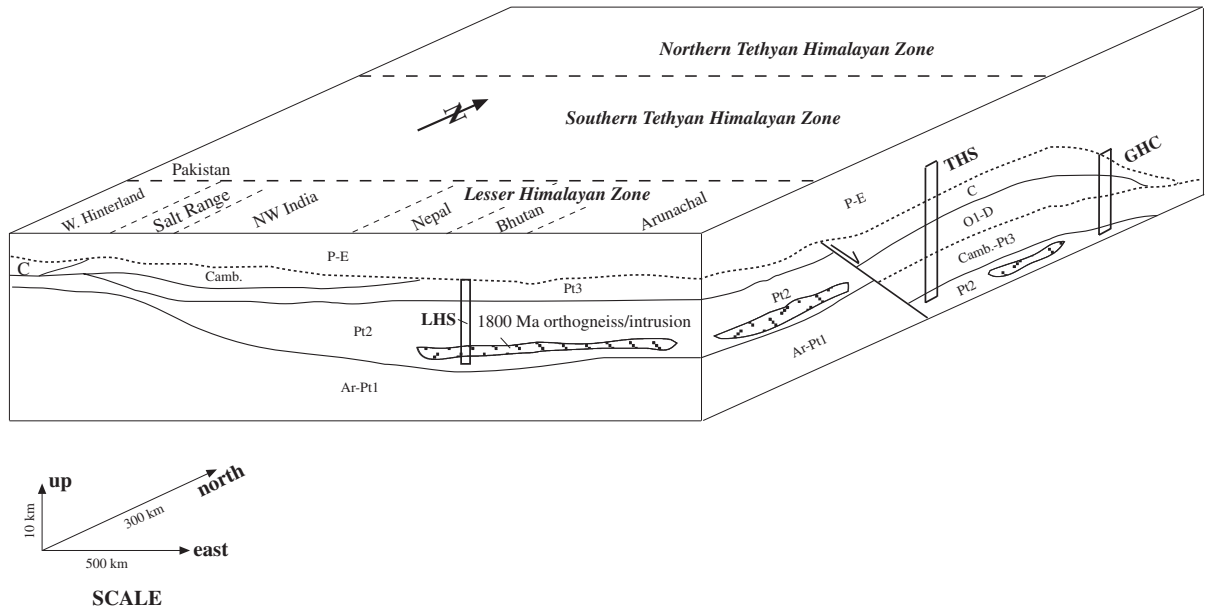


Fig. 5. Schematic block diagram showing the hypothesized original position of the Lesser, Tethyan, and Greater Himalayan sections prior to Cenozoic Indo-Asian collision. Ar-Pt1, Achaean and early Proterozoic rocks; Pt2, Mesoproterozoic strata; Camb.-Pt3, Cambrian and Late Proterozoic strata; O1-D, Ordovician and Devonian strata; C, Carboniferous syn-rift strata; P-E, Permian and Eocene strata.

Indian craton. The basin has been divided into four sub-basins: the Indus Basin covering the drainage area of the Indus River, the Ganga Basin covering the drainage area of the Ganges River, the Brahmaputra Basin covering the drainage area of the Brahmaputra River, and the Bengal Basin covering the joined Brahmaputra–Ganges River south of the Rajmahal–Garó gap (Fig. 1A). The basement of the active Himalayan foreland basin is irregular, with several subsurface ridges extending from the Peninsula Highlands northwards to the Himalayan front. These structural highs generally trend at high angles to the Himalayan range (Fig. 1A) and have structural relief locally exceeding 2 km in an east–west direction parallel to the Himalayan thrust front (Raiverman, 2000) (Fig. 3). The most prominent subsurface structural high is the Delhi–Muzaffarnagar ridge that forms the drainage divide between the Indus and Ganges Rivers (Fig. 1A). The basement highs beneath the Indo-Gangetic depression are being subducted beneath the Himalayan range along the MFT; they may have controlled the map pattern of the major Himalayan thrusts and the along-strike

variation and concentration of seismicity below the Himalayan range (Johnson, 1994; Pandey et al., 1999; Avouac, 2003).

Basement ridges beneath the Indo-Gangetic depression are either Precambrian in age (e.g., Rao, 1973) or have been developed in the Cenozoic (Duroy et al., 1989; Raiverman, 2000); the latter interpretation is based on the observations that the ridges control Cenozoic sedimentation and are locally associated with seismicity. The structural highs such as the Sargodha ridge immediately south of the Salt Range in Pakistan have been interpreted as segments of a flexural bulge (= forebulge) of the underthrusting Indian lithosphere (Yeats and Lawrence, 1984; Duroy et al., 1989). Although a forebulge may have been locally produced by bending of the Indian lithosphere beneath the westernmost and south-central Indo-Gangetic depression as indicated by gravity data (Duroy et al., 1989; Mishra et al., 2004), its topographic expression may be much smaller than the basement ridges (500–1000 m of relief) trending at high angles to the Himalayan orogen. Basin fills in the Indo-Gangetic depression are dominantly Neogene sediments of the Siwalik Group and

rest unconformably on top of Paleocene to lower Eocene strata, Precambrian granitic rocks of the Indian craton, Proterozoic shallow marine sequences of the Vindhyan Group, and Permian strata of the Gondwana sequence (Raiverman, 2000) (Fig. 3).

#### 2.4. Major Himalayan structures

In the following, I define the terminology and general geographic distribution of major Himalayan structures. The kinematic nature of these structures will be discussed at length in later sections of the article.

##### 2.4.1. South Tibet Detachment (STD)

The South Tibet Detachment is best defined in south-central Tibet where it juxtaposes unmetamorphosed or low-grade THS over high-grade GHC (Burg et al., 1984a; Burchfiel et al., 1992). Whether the same relationship persists along the entire Himalayan orogen is not clear, particularly at its western and eastern ends (e.g., Ding et al., 2001; Argles and Edwards, 2002; DiPietro and Pogue, 2004).

##### 2.4.2. Main Central Thrust (MCT)

The concept of the MCT comes from Heim and Gansser (1939). Based on observations made along the Kali and Alaknanda Rivers in the Garhwal and Kumaun regions of NW India, they show that the fault is broadly folded and juxtaposes high-grade gneisses and schists over either steeply dipping limestone (near Dharchula,  $29^{\circ}50'46''\text{N}/80^{\circ}25'45''$ ; Fig. 2A) or subhorizontal quartzite (near Berinag above 70 km west-southwest of Dharchula; Fig. 2A). The efforts of extending this major Himalayan structure along strike from NW India have led to its variable definitions.

- (1) As in Heim and Gansser (1939), the fault may be identified as a lithologic contact separating the LHS below from the GHC above.
- (2) The fault may be identified by an abrupt change in metamorphic grade (LeFort, 1975; Pêcher, 1989).
- (3) The fault may be defined as the top surface or the basal surface of a broad shear zone several kilometers thick across the uppermost part of

the LHS and the lowermost part of the GHC (Arita, 1983; Pêcher, 1989; Searle et al., 2003).

For an ideal situation, the three criteria should all be met (LeFort, 1996), but this has rarely been the case.

The problem of applying the above criteria to locate the MCT in the Himalaya may be attributed to the following factors. First, the exact lithologic composition and stratigraphy of the MCT hanging wall and footwall are not completely understood. Although stratigraphic juxtaposition relationships across the MCT are well defined in some places, they may not apply to others because the MCT hanging-wall and footwall lithology and stratigraphy vary along strike; a footwall rock at one location may become a hanging-wall rock at the other. Enforcing the same stratigraphic juxtaposition across the MCT along the entire Himalaya has not only created confusion but may have disguised the true spatial variation of the Himalayan geology. Second, metamorphic grades are often continuous across the MCT shear zone, making the assignment of a specific metamorphic isograd as the location of the MCT subjective. Heim and Gansser (1939) were well aware of this problem when they worked along the Alaknanda River, where they found that the metamorphic grade is continuous across the broad MCT shear zone. Third, due to heating and post-deformation static grain growth, structural fabrics related to shearing along the MCT may have been erased completely. This would make the definition of the MCT solely based on strain magnitude unattainable. Fourth, the MCT shear zone across the LHS and GHC is a result of finite strain deformation. That is, not all shear surfaces in the shear zone were active all at once, as indicated by the work of Harrison et al. (1997a). Therefore, the location of the MCT surface accommodating major convergence may vary with time within the broad shear zone. With this complex factor in mind, one needs to specify the timing of a structure when naming the MCT in the field.

##### 2.4.3. Main Boundary Thrust (MBT)

The MBT is defined as the thrust placing the LHS over Tertiary sedimentary strata (Heim and Gansser, 1939). This definition is not without problems because whether the LHS is juxtaposed against Tertiary strata depends on the exposure level of the fault. For example, the Jammu thrust in the western Himalaya is



considered to be a footwall structure of the MBT (Fig. 2A). However, it locally places LHS over Tertiary strata (e.g., Fuchs and Linner, 1995; DiPietro and Pogue, 2004). In addition, Cenozoic strata are also present in the MBT hanging wall in places such as in the Pakistan Himalaya foreland (DiPietro and Pogue, 2004). Consequently, the MBT defined by Heim and Gansser (1939) in one place may not be the same fault in another place. It is important to remember this point when reconstructing along-strike variation of the Himalayan history.

#### 2.4.4. Main Frontal Thrust (MFT)

This fault is regarded as the thrust contact between the Neogene Siwalik strata above and Quaternary deposits of the Indo-Genetic depression below (e.g., Gansser, 1964, 1983; Yeats and Lillie, 1991; Lavé and Avouac, 2000; Kumar et al., 2001). The fault is commonly expressed as a zone of folds and blind thrusts (Nakata, 1989; Yeats and Lillie, 1991).

#### 2.4.5. Main Himalayan Thrust (MHT)

This concept was first proposed by Schelling and Arita (1991) in their structural reconstruction of the eastern Nepal Himalaya. They suggest that major Himalayan thrusts (MFT, MBT, and MCT) in eastern Nepal of the South Himalaya may sole into a low-angle fault that they termed the *Main Detachment Fault* (MDF). This concept was later expanded to the North Himalaya based on observations from the INDEPTH seismic reflection profiles (Zhao et al., 1993; Nelson et al., 1996).

### 3. Structural geology of the Himalayan orogen

The major tectonic elements in the Himalayan orogen from north to south include:

- (1) the south-dipping *Great Counter Thrust* (GCT) immediately south of the Indus–Tsangpo suture zone (also known as Renbu–Zedong thrust or Himalayan Backthrust in southern Tibet; Heim and Gansser, 1939; Ratschbacher et al., 1994; Yin et al., 1994, 1999);
- (2) the *North Himalayan Antiform* (NHA) (Hauck et al., 1998), also known as the Tethyan or North/Tethyan Himalayan gneiss domes com-

monly associated with Miocene leucogranites (Burg et al., 1984b; Burg and Chen, 1984; Schärer et al., 1986; Debon et al., 1986; LeFort et al., 1987; Maluski et al., 1988; Chen et al., 1990; Lee et al., 2000);

- (3) the *Tethyan Himalayan fold and thrust belt* (THFTB) in the North Himalaya (Heim and Gansser, 1939; Gansser, 1964; Burg et al., 1984b; Ratschbacher et al., 1992, 1994; Corfield and Seale, 2000; Wiesmayr and Grase-mann, 2002; Murphy and Yin, 2003);
- (4) the *South Tibet Detachment System* (STDS), also known as the North Himalayan Normal Fault (Burg et al., 1984a; Searle, 1986; Herren, 1987; Pécher, 1991; Burchfiel et al., 1992);
- (5) *South Tibet fault system* (STFS) (Hurtado et al., 2001; Hodges et al., 2001);
- (6) the *Main Central Thrust* (MCT) (Gansser, 1964; LeFort, 1975; Acharyya, 1980; Arita, 1983; Brun et al., 1985; Brunel, 1986; Pécher, 1989);
- (7) the *Lesser Himalayan Thrust Zone* (LHZ) (Valdiya, 1978, 1979, 1980, 1981, 1988; Schelling and Arita, 1991; Schelling, 1992; Srivastava and Mitra, 1994; DeCelles et al., 1998a, 2001, 2002; Johnson, 2002);
- (8) the *Lesser Himalayan Crystalline Nappes* (LHCN), which are either segments of the MCT hanging wall (Gansser, 1964; Stöcklin, 1980; Johnson et al., 2001) or thrust sheets carried by imbricates in the MCT footwall (see Upreti and LeFort, 1999 for a review and references therein);
- (9) the *Main Boundary Thrust* (MBT) (Gansser, 1964; Meigs et al., 1995; Powers et al., 1998; DeCelles et al., 2001);
- (10) the *Main Frontal Thrust* (MFT) (Gansser, 1964; Yeats and Lillie, 1991; Schelling and Arita, 1991; Lavé and Avouac, 2000); and
- (11) *north-trending Neogene rifts* (Figs. 1A and 2A).

Note that the South Tibet Detachment System and the South Tibet fault system are two different concepts: the former refers to an early Miocene low-angle detachment system whose development has contributed to the Miocene construction of the Himalayan architecture whereas the latter refers to an Pleistocene–Quaternary north-dipping high- and low-angle normal

Table 6

Along-strike variation (from west to east) of timing, magnitude, structural style, and metamorphic conditions across the Himalayan orogen

Tectonic Zones	Western Himalaya (< 81°E)	Central Himalaya (81–89°E)	Eastern Himalaya (> 89°E)
<i>Great Counter Thrust</i>	<b>Age:</b> *active between 20 and 13 Ma <sup>1</sup> , but terminates prior to 9 Ma <sup>2</sup> . <b>Magnitude of slip:</b> >38 km <sup>2</sup>	<b>Age:</b> Active at ~ 18 Ma <sup>1</sup> , but initiation and termination ages are unknown. <b>Magnitude of slip:</b> unknown	<b>Age:</b> active between 19–9 Ma in Langxian <sup>1</sup> and 25–10 Ma in Zedong, respectively, in SW Tibet <sup>14</sup> . <b>Magnitude of slip:</b> > 12 km slip across thrust ramp <sup>2</sup>
<i>Eclogite terranes along the northern edge of Indian continent</i>	<b>Peak metamorphism:</b> <i>T/P</i> =670–725°C/24–30 kbars (N. Pakistan) <sup>5,30</sup> , >750°C/39 kbars (NW India) <sup>8</sup> <b>Age of UHP metamorphism:</b> 46–47 Ma (N. Pakistan) <sup>6,7</sup> , 55 Ma (NW India) <sup>9</sup> <b>Age of exhumation to middle crust:</b> 46–40 Ma (N. Pakistan) <sup>8,9</sup> , 47 Ma in the middle crust and by 30 Ma in the upper crust (NW India) <sup>10</sup> <b>Structural setting:</b> Normal fault above and thrust below for N. Pakistan <sup>8</sup> , but poorly defined in NW India due to later phases of deformation <sup>11,12,13</sup> .	<b>Peak metamorphism:</b> <i>T/P</i> =750°C/7–10 kbars (Everest-Makalu region) <sup>31</sup> <b>Age of metamorphism:</b> > 24 Ma <sup>31</sup> <b>Age of exhumation to middle crust:</b> unknown <b>Structural setting:</b> in the top part of the MCT zone between an orthogenesis unit below and the GHC above <sup>31</sup>	No eclogite has been recognized in eastern Himalaya.
<i>North Himalayan Antiform (= North Himalayan Gneiss Domes)</i>	<b>Tso Moriri dome:</b> <i>Main deformation phases:</i> D1 = SW-verging ductile folding, D2 = NW-verging back-folding, D3 = brittle normal faulting along northern edge <sup>11,12,13</sup> <i>Age of deformation:</i> poorly unconstrained.	<b>Kangmar dome:</b> <i>Main deformation phases:</i> D1 = upright and S-verging isoclinal folding, D2 = formation of mylonitic foliation <sup>32,73,74</sup> . <i>Age of deformation:</i> 15–11 Ma <sup>32</sup> .	<b>Yalaxangbo dome:</b> <i>Main phase of deformation:</i> top-NW shear, possibly related to STD <sup>52</sup> . <i>Age of deformation:</i> unknown <sup>52</sup> .
<i>Tethyan Himalayan Fold-Thrust Belt</i>	<b>Age:</b> 56–46 Ma <sup>15</sup> <b>**Shortening:</b> 30% <sup>15</sup> –62% <sup>16</sup> <b>Style:</b> Thin-skinned thrusting with detachment at a depth of ~ 10 km <sup>15</sup> .	<b>Age:</b> ~50 Ma <sup>33</sup> <b>Shortening:</b> 110–140 km <sup>33,34</sup> <b>Style:</b> Thin-skinned thrusting <sup>33,34</sup> .	<b>Age:</b> unknown. <b>Shortening:</b> unknown <b>Style:</b> Triassic flysch strata are isoclinally folded; bedding has been completely transposed by axial cleavage <sup>1</sup> .
<i>South Tibet Detachment</i>	<b>Age:</b> active 21–19 Ma in Zaskar <sup>17,18</sup> and 23–21 Ma in Garhwal <sup>19</sup> <b>Slip:</b> 35 km <sup>17</sup> , > 25 km <sup>20</sup> ; probably the upper bounds.	<b>Age:</b> active 23–13 Ma <sup>35,36,37,38,39</sup> <b>Slip:</b> > 34 km <sup>38</sup>	<b>Age:</b> active after 12 Ma, the age of pluton cut by STD <sup>53</sup> , active at 22–13 Ma <sup>54,55</sup> . <b>Slip:</b> > 100 km (?), see text for discussion.
<i>Greater Himalayan Crystallines</i>	<b>Peak P-T:</b> M1 = 9.5–10.5 kbars/550–680°C <sup>18,57,58</sup> (~35–25 Ma in Zaskar <sup>69</sup> , 40 Ma in Garhwal <sup>70</sup> ); M2 = 4.5–7 kbars/650–770°C C (22–16 Ma) <sup>18,57,58</sup> .	<b>Peak P-T:</b> M1 = 6–10 kbars/600–700°C <sup>31, 62-68</sup> (35–32 Ma <sup>71,72</sup> ) M2 = 5–8 kbars/600–750°C <sup>31, 62-68</sup> .	<b>Peak P-T:</b> M2 = 10–13 kbars, 750–800°C <sup>53,65,76</sup>
<i>Main Central Thrust</i>	<b>Age:</b> active 21–19 Ma <sup>18</sup> in Zaskar, 21–14 Ma and 5.9 Ma in Garhwal Himalaya <sup>25,26</sup> <b>Slip:</b> > 85–95 km <sup>21,22,23</sup>	<b>Age:</b> active 23–20 Ma <sup>35,36,38,40,41</sup> , reactivated at 5–3 Ma <sup>42,43,44</sup> <b>Slip:</b> > 100 km <sup>45</sup> , 175 km <sup>46</sup>	<b>Age:</b> active 18–13 Ma <sup>55</sup> <b>Slip:</b> > 75 km based on Kuru Chu-Manas River reentrant <sup>56</sup> .
<i>Inverted Metamorphic Zone</i>	Inverted P and T in Zaskar <sup>57,58</sup> ; inverted T but no change in P in but in westernmost Garhwal <sup>59,60</sup>	Inverted P and T <sup>60,62</sup> ,	Inverted T but no measurable inverted P <sup>55</sup>
<i>Lesser Himalayan Crystalline Nappes</i>	<b>Age of emplacement:</b> unknown for the Almora and Shimla nappes.	<b>Age of emplacement:</b> motion terminates by 14 Ma, active 22–14 Ma <sup>48,51</sup> (Kathmandu Nappe).	Not yet recognized
<i>Lesser Himalayan Fold-Thrust Belt</i>	<b>Age:</b> Inferred M. to L. Eocene (~49–34 Ma) <sup>24</sup> <b>Shortening:</b> 161 km <sup>24</sup>	<b>Age:</b> Ar-hb age of 41±6.7 Ma (?) <sup>47</sup> , southern belt terminated prior to 14 Ma (Ar cooling ages) <sup>48</sup> . <b>Shortening:</b> 287 km <sup>49</sup>	<b>Age:</b> 22–<14 Ma <sup>55</sup> . <b>Shortening:</b> unknown.
<i>Main Boundary Thrust</i>	<b>Age:</b> initiated > 11 Ma in western NW India <sup>27</sup> , also inferred to be older than M. Paleocene (> 58 Ma) <sup>24</sup> <b>Slip:</b> >100 km <sup>28,29</sup>	<b>Age:</b> < 5 Ma <sup>49</sup> or at 10–12 Ma <sup>50</sup> as inferred from sedimentation in Siwalik Group <b>Slip:</b> > 100 km <sup>75</sup> .	<b>Age:</b> < 5 Ma inferred from sediments in Siwalik Group <sup>49</sup> , or at 10–12 Ma <sup>50</sup> <b>Slip:</b> unknown

faults along the crest and the northern slope of the Himalayan range (Burchfiel et al., 1992; Hodges et al., 2001).

Below I describe the major Himalayan structures in the following order:

- (1) structural geometry and relationship with major lithologic units;
- (2) magnitude of deformation; and
- (3) age of initiation and duration of deformation (Table 6).

The magnitude of deformation across individual faults or thrust belts is measured either by total fault slip or strain. The description below focuses only on the east-striking segment of the Himalayan orogen and will not treat the transpressional systems along the eastern and western shoulders of the Indian sub-continent. This is because our present knowledge on these regions is too limited to warrant an informative discussion. Although most structures are discussed separately within individual segments of the Himalayan orogen, I make exceptions for the Great Counter Thrust and North Himalayan Antiform to emphasize their lateral continuity along the entire orogen.

### 3.1. Central Himalaya

The geology of the central Himalaya is best illustrated in Nepal and politically defined south-central

Tibet of China between longitudes 81°E and 89°E (Fig. 2A).

#### 3.1.1. Main Central Thrust

In Nepal the Main Central Thrust is expressed as a 2- to 10-km-thick shear zone (LeFort, 1975; Arita, 1983; Brun et al., 1985; Brunel, 1986; Hubbard, 1989; Macfarlane, 1992). The location of the Main Central Thrust *fault* in this region has been variably defined. Some workers place it at the top of the shear zone immediately above the Proterozoic LS (e.g., LeFort, 1975, 1996; Pêcher, 1989; Ahmad et al., 2000), while others locate the fault at the base of or within the MCT shear zone in the LHS (e.g., Arita, 1983; Searle et al., 2003). Arita (1983) recognizes an abrupt change in lithology and metamorphic grade in the MCT shear zone below the MCT fault of LeFort (1975) and Pêcher (1989). He termed this fault the MCT-I (or lower MCT) and the MCT of LeFort (1975) as the MCT-II (or upper MCT; also see Paudel and Arita, 2002 for an updated view of this definition) (Table 3).

The MCT zone in Nepal exhibits a flat-ramp geometry (Lyon-Caen and Molnar, 1985; Schelling and Arita, 1991; Schelling, 1992; DeCelles et al., 2001). The ramp region is commonly referred to as the root zone, above which the foliation of the GHC dips 30–60° to the north (Fig. 2D). Intense micro-seismicity and low electrical conductivity are also associated with the ramp, suggesting possible stress concentration and the presence of fluids along the fault ramp (e.g., Lemmonier et al., 1999; Pandey et

---

Notes to Table 6:

References for Table 6:

<sup>1</sup>Yin et al. (1999), <sup>2</sup>Murphy et al. (2002), <sup>3</sup>Ratschbacher et al. (1994), <sup>4</sup>Quidelleur et al. (1997), <sup>5</sup>O'Brien et al. (2001), <sup>6</sup>Smith et al. (1994), <sup>7</sup>Foster et al. (2002), <sup>8</sup>Mukherjee et al. (2003), <sup>9</sup>Tonarini et al. (1993), <sup>10</sup>de Sigoyer et al. (2000), <sup>11,12</sup>Steck et al. (1993, 1998), <sup>13</sup>Guillot et al. (1997), <sup>14</sup>Harrison et al. (2000), <sup>15</sup>Wiesmayr and Grasemann (2002), <sup>16</sup>Corfield and Seale (2000), <sup>17</sup>Dèzes et al. (1999), <sup>18</sup>Walker et al. (1999), <sup>19</sup>Searle et al. (1999a), <sup>20</sup>Herren (1987), <sup>21</sup>Fuchs (1975), <sup>22</sup>Frank et al. (1995), <sup>23</sup>Vannay and Grasemann (2001), <sup>24</sup>Srivastava and Mitra (1994), <sup>25</sup>Metcalfe (1993), <sup>26</sup>Catlos et al. (2002a), <sup>27</sup>Meigs et al. (1995), <sup>28</sup>Treloar et al. (1991), <sup>29</sup>Burbank et al. (1996), <sup>30</sup>Lombardo et al. (2000), <sup>31</sup>Lombardo and Rolfo (2000), <sup>32</sup>Lee et al. (2000), <sup>33</sup>Ratschbacher et al. (1994), <sup>34</sup>Murphy and Yin (2003), <sup>35</sup>Hodges et al. (1992), <sup>36</sup>Hodges et al. (1996), <sup>37</sup>Murphy and Harrison (1999), <sup>38</sup>Godin et al. (2001), <sup>39</sup>Searle et al. (2003), <sup>40</sup>Hubbard and Harrison (1989), <sup>41</sup>Coleman (1998), <sup>42</sup>Harrison et al. (1997b), <sup>43,44</sup>Catlos et al. (2001, 2002b), <sup>45</sup>Brunel (1986), <sup>46</sup>Schelling and Arita (1991), <sup>47</sup>Macfarlane (1993), <sup>48</sup>Arita et al. (1997), <sup>49</sup>DeCelles et al. (2001), <sup>50</sup>Huyghe et al. (2001), <sup>51</sup>Johnson et al. (2001), <sup>52</sup>Zhang and Guo (submitted for publication), <sup>53</sup>Edwards and Harrison (1997), <sup>54</sup>Grujic et al. (2002), <sup>55</sup>Daniel et al. (2003), <sup>56</sup>Gansser (1983), <sup>57</sup>Searle et al. (1999b), <sup>58</sup>Stephenson et al. (2000), <sup>59</sup>Vannay and Grasemann (1998), <sup>60</sup>Vannay et al. (1999), <sup>61</sup>Hubbard (1989), <sup>62</sup>LeFort (1996), <sup>63</sup>Davidson et al. (1997), <sup>64</sup>Brunel and Kienast (1986), <sup>65</sup>Pêcher and Le Fort (1986), <sup>66</sup>Hubbard et al. (1991), <sup>67</sup>Hodges et al. (1994), <sup>68</sup>Vannay and Hodges (1996), <sup>69</sup>Vance and Harris (1999), <sup>70</sup>Prince et al. (1999), <sup>71</sup>Godin et al. (1999a,b), <sup>72</sup>Simpson et al. (2000), <sup>73</sup>Burg et al. (1984b), <sup>74</sup>Chen et al. (1990), <sup>75</sup>Molnar (1988), <sup>76</sup>Neogi et al. (1998).

<sup>a</sup> When a fault is indicated to have been active in a specific time window, say 20–13 Ma, it means that its age of initiation and termination is unconstrained.

<sup>b</sup> Because no complete traverse is made across the entire Tethyan thrust belt in the region, the total amount of shortening across the belt is not known.

al., 1999; Avouac, 2003). The thrust flat of the MCT zone in the south carries a synformal thrust sheet composed of the GHC. The MCT thrust sheet above the flat is commonly referred to as the Lesser Himalayan Crystalline Nappes (LHCN) (e.g., Stöcklin, 1980; Upreti and LeFort, 1999). Folding of the LHCN may have been caused by either fault-bend folding over a north-dipping ramp along the MBT (Lyon-Caen and Molnar, 1985) or over a south-dipping thrust ramp cutting across the Indian basement in the middle crust (Burg et al., 1987). Folding of the MCT and the LHCN has also been related to duplex development in the MCT footwall (e.g., Schelling and Arita, 1991; DeCelles et al., 1998a, 2001, 2002; Robinson et al., 2003). Regardless of the deformation mechanism, folding of the MCT has produced several prominent half windows and klippen in Nepal (Schelling and Arita, 1991), NW India (Valdiya, 1980), Sikkim, and Bhutan (Gansser, 1983). Correlating the MCT root zone with the southern limit of the MCT flat suggests that the fault slipped for >100–140 km in Nepal (e.g., Brunel, 1986; Schelling and Arita, 1991) (Table 6).

The origin of the steeply dipping MCT root zone is not well understood. In the reconstruction of Schelling and Arita (1991), the MCT root zone is considered to be an original ramp cutting upsection in its southward transport direction. However, Robinson et al. (2003) recently suggest that the steeply dipping MCT root zone is not a ramp but a flat-against-flat thrust; its present steep-dipping geometry may have resulted from duplex development in the MCT footwall. This interpretation is based on their observation in western Nepal that hanging wall and footwall foliations are parallel to the MCT. The main problem of using geometrical relationship between foliation and the MCT to determine the original MCT geometry is that the foliation adjacent to the MCT is not primary geologic features such as sedimentary layers but secondary structures that were developed during motion along the MCT. One test of whether the MCT root zone is a primary ramp (Schelling and Arita, 1991) or a rotated flat (Robinson et al., 2003) is to determine whether the MCT preserves stratigraphic cutoffs in its hanging wall or footwall. Because footwall strata across the MCT root zone are not exposed, it remains difficult to differentiate the two hypotheses in Nepal.

### 3.1.2. Age of the MCT

The MCT root zone has a protracted history. It was active at about 20–23 Ma along its upper bounding fault (the MCT of LeFort, 1975 or MCT-II of Arita, 1983). This was deduced from  $^{40}\text{Ar}/^{39}\text{Ar}$  hornblende ages from amphibolite-grade rocks and U–Pb zircon ages of a leucogranite that cuts the MCT zone (Hubbard and Harrison, 1989; Hodges et al., 1992, 1996; Parrish and Hodges, 1996; Coleman, 1998; Godin et al., 2001). The  $^{40}\text{Ar}/^{39}\text{Ar}$  hornblende ages suggest that amphibolite-grade metamorphism associated with motion on the MCT occurred at 23–20 Ma (Table 6).

The age of deformation in the MCT root zone becomes progressively younger southward, from ~20 Ma at the top to about 5–3 Ma at the base of the MCT shear zone as indicated by Th–Pb ages of monazite inclusions in syn-kinematic garnets (Harrison et al., 1997a, 1998b; Catlos et al., 2001, 2002a,b) and  $^{40}\text{Ar}/^{39}\text{Ar}$  muscovite ages (Macfarlane, 1993). The younger 5–3 Ma cooling and metamorphic ages in the MCT root zone (Wadia, 1931) are in strong contrast to the older muscovite cooling ages of 22–14 Ma in the Kathmandu Nappe along the thrust flat portion of the MCT (Copeland et al., 1996; Arita et al., 1997). The age progression within the MCT zone and the age difference between the internal (northern) and external (southern) segments of the MCT zone could be a result of discontinuous downward migration of simple-shear deformation (Harrison et al., 1998b), southward propagation of discrete thrusts in a duplex system (Robinson et al., 2003), or out-of-sequence thrusting (Rai et al., 1998; Johnson et al., 2001). The MCT root zone was locally reactivated by down-to-the-NE brittle normal faults (Takagi et al., 2003; also Vannay et al., 2004). The extent, magnitude, and tectonic significance of this younger phase of extensional deformation along the MCT zone remain unclear and needs further study.

The age of motion along the southern part of the MCT in the geographically defined Lower Himalaya is best constrained in the Kathmandu area of south-central Nepal. Johnson and Rogers (1997) and Johnson et al. (2001) showed that the basal thrust zone of the Kathmandu Nappe was active between 22 and 17 Ma based on U–Pb ages of deformed pegmatites and Rb–Sr cooling ages of muscovite and biotite. Arita et al. (1997) also investigate the emplacement history of the Kathmandu Nappe by dating muscovites from the

MCT hanging wall and footwall. Their results suggest that the MCT shear zone was cooled below 350 °C between 21 and 14 Ma and that the southernmost portion of the MCT shear zone ceased motion since 14 Ma. A muscovite cooling age of ~21 Ma was obtained from the northern segment of the Dadeldhura thrust sheet in far western Nepal, which is equivalent to the Kathmandu Nappe in south-central Nepal (DeCelles et al., 2001). The age of the MCT below the Kathmandu nappe was also determined by U-Th ion-microprobe dating of monazite inclusions in syn-kinematic garnets in the MCT zone by Catlos (2000). The five samples she dated yield monazite ages ranging semi-continuously from 13 to 41 Ma, indicating a protracted history of motion on the MCT between 41 and 13 Ma. Noticeably lacking for the MCT zone in the Kathmandu area are the younger monazite ages of 8–3 Ma that are prevalent in the MCT ramp zone further to the north (Harrison et al., 1997a; Catlos, 2000; Catlos et al., 2001). This observation again supports the interpretation that the MCT ramp zone was reactivated in the late Miocene and Pliocene between 8 and 3 Ma, leaving its frontal fault segment to the south stranded due to inactivation since 13–14 Ma (Harrison et al., 1997a).

### 3.1.3. MCT Slip

Construction of balanced cross-sections in far eastern Nepal suggests that the MCT may have accommodated about 140–210 km of displacement (Schelling and Arita, 1991; Schelling, 1992). A greater amount of slip (~500 km) was inferred from far western Nepal (DeCelles et al., 2001).

### 3.1.4. Inverted metamorphism

The most well-known geologic feature associated with the MCT zone throughout the Himalayan orogen is the inverted metamorphism. It is characterized by upward-increasing metamorphic grade across the upper part of the LHS and the MCT zone and extends into the lower part of the MCT hanging wall (e.g., Heim and Gansser, 1939; LeFort, 1975; Pêcher, 1989; Hubbard, 1989; Macfarlane, 1995; Vannay and Gramann, 1998; Harrison et al., 1999). Above the region of maximum pressures and temperatures at the top of the inverted metamorphic zone, metamorphic grade generally decreases upward toward the STD with a normal lithostatic pressure gradient in

the central Himalaya (e.g., Vannay and Hodges, 1996; Hodges et al., 1996; Searle et al., 2003). As described below, isograds are highly condensed vertically in the western Himalaya (Zanskar; Honegger et al., 1982) and the North Himalayan gneiss domes (e.g., Lee et al., 2000). This difference indicates inhomogeneous strain distribution in the GHC. The effect of inverted metamorphism across the MCT zone is locally expressed by a systematic change in deformation mechanism, from high-temperature dynamic recrystallization of both feldspar and quartz at the top of the MCT zone to brittle deformation of feldspars and crystal-plastic deformation of quartz at the base of the MCT zone (Srivastava and Mitra, 1996).

### 3.1.5. Lesser Himalayan Crystalline Nappes

The Kathmandu Nappe is the most studied structure in the LHCN system in the central Himalaya. It lies in the geographically defined Lower Himalayan zone of Gansser (1964) or the Lesser Himalayan zone of LeFort (1975). It is bounded below by the Mahabharat thrust that most likely represents the southern extension of the MCT (Table 3) (Stöcklin, 1980; Johnson et al., 2001). As mentioned above, this segment of the MCT was active probably between 41 and 13 Ma (Catlos, 2000). One interesting aspect of the Kathmandu Nappe is the presence of 3- to 4-km-thick, lower Paleozoic Tethyan Himalayan strata (i.e., the Phulchauki Group of Stöcklin, 1980; also see Upreti and LeFort, 1999 for an updated review) (Tables 3 and 7). These fossiliferous strata rest unconformably on top of the Proterozoic Bhimphedi Group, a 10-km-thick section of high- to low-grade metamorphic rocks consisting of garnet-kyanite schist and gneiss, augen gneiss, quartzite, marble, metabasite, and early Miocene pegmatites (Stöcklin, 1980; Johnson et al., 2001) (Table 7). Cambro-Ordovician granites intrude both the lower Phulchauki Group and underlying Bhimphedi Group (Schärer et al., 1984; Debon et al., 1986; Gehrels et al., 2003). These granites have been correlated with the Cambro-Ordovician orthogneiss in the upper GHC in northern Nepal (Upreti and LeFort, 1999). The metamorphic grade in the Bhimphedi Group decreases upward, as expressed by changes from kyanite-bearing gneiss progressively to garnet schist, biotite schist, and finally phyllite and slate at the top (Stöcklin, 1980; Johnson et al., 2001).

Table 7  
 Hanging-wall stratigraphy of the STD and its laterally correlative sections from west to east in the Himalaya

Age	W. Pakistan	Nanga Parbat	Zaskar Window (N)	Zaskar Window (S)	Kullu Window (N)	Kullu Window (S)	Annapurna	Mt. Everest	Kathmandu Nappe	SE Tibet/Bhutan (N)	SE Tibet/Bhutan (S)
Mz arcs	Kohistan Arc ??MMT	Ladakh Arc ??MMT					Annapurna FM	Ordovician limestone	Phulchauki Group (= Lower Paleoz. Tethyan Strata)	Ordovician limestone	
Ordovician	Indian crust	Indian crust						GHC			
Cambrian				unconformity							Cambrian Tethyan Strata
Proterozoic											
L. Himalayan			Phe Formation	Haimanta Group	Phe Formation	Salkhala FM		L. Bhimphe Group	Marku FM Kulikhani FM Chisapani FM Group Kalitar FM Bhainselobhan FM Raduwa FM		Chekha FM
Greater Himalayan			Zaskar Shear Zone	Chenab Fault	STD	Kumharsain Shear Zone		L. Bhimphe Group	unconformity Thrust (= MCT)		
Source	Treloar et al. (2003)	Argles and Edwards (2002)	Herren (1987), Thakur (1998)	Thakur (1998)	Wyss et al. (1999)	Yin et al. (2003)	Godin et al. (1999a)	Burchfiel et al. (1992)	Inferred from Stocklin (1980) and Johnson et al. (2001)	Burchfiel et al. (1992)	Grujic et al. (2002)

The contrast in metamorphic grade between the lower Paleozoic sedimentary sequence above and the high-grade metamorphic rocks of the Proterozoic Bhimphe Group in the Kathmandu Nappe is striking. At the base of the nappe, peak metamorphism occurred under  $P-T$  conditions of  $T=500-600^\circ \pm 50^\circ\text{C}$  and  $P=8-11 \pm 1.5$  kbar in the early Miocene, whereas at the top of the nappe the strata are essentially unmetamorphosed (Johnson et al., 2001) (Table 6). The great contrast in metamorphic grade led Johnson et al. (2001) to speculate the presence of a STD-like structure within the Kathmandu Nappe. Because the contact between the Paleozoic Phulchauki and Proterozoic Bhimphe Groups is an unconformity (Stöcklin, 1980; Gehrels et al., 2003), the possible STD equivalent structure in the Kathmandu Nappe probably lies below this contact. A potential candidate for the location of the STD is the contact between the Proterozoic Chisapani Formation above and the Proterozoic Kalitar Formation below (Table 7). The Kalitar, Bhainselobhan, and Raduwa Formations consist of kyanite schist and gneiss, augen gneiss, amphibolite, and pegmatite. They are similar in lithology to the GHC as noted by Stöcklin (1980). The lithology of the upper Bhimphe Group is similar to the Haimanta Group in northwestern India of the western Himalaya and the Chekha Formation in Bhutan of the eastern Himalaya, respectively; both lie above the STD but below the Cambro-Ordovician unconformity (Thakur, 1998; Grujic et al., 2002).

3.1.6. South Tibet Detachment (STD)

The South Tibet Detachment juxtaposing the THS above and the GHC below is best defined in the central Himalaya of Nepal and south-central Tibet (Burg et al., 1984a; Burchfiel et al., 1992; Hodges et al., 1992; Brown and Nazarchuk, 1993; Lombardo et al., 1993; Hodges et al., 1996; Searle, 1999; Godin et al., 1999a,b, 2001; Searle and Godin, 2003). The STD fault zone in these areas is a few kilometers thick and consists of several subparallel faults or ductile shear zones with a complex and alternating history of top-north and top-south motion (Hodges et al., 1996; Carosi et al., 1998, 1999; Searle et al., 2003). In the northeastern Annapurna area, the Annapurna Detachment as the western extension of the STD from south-central Tibet lies below the Cambrian (?) Annapurna Yellow Formation and pre-

serves a zone of superposed top-north and top-south shear fabrics (Godin et al., 1999b). Within the broadly defined STD shear zone the top-north Deorali detachment was active and coeval with the MCT at 22.5 Ma, the top-south Modi Khola shear zone was active at 22.5–18.5 Ma, and finally the top-north Machhupuchare detachment was active after 18.5 Ma (Hodges et al., 1996). Godin et al. (2001) show that: (1) the Annapurna Detachment is cut by a ~22.5-Ma undeformed dike dated by the U–Pb zircon method and (2) the upper part of the GHC exhibits progressive upward younging of  $^{40}\text{Ar}/^{39}\text{Ar}$  muscovite ages from 15 to 12 Ma. These age data suggest that the motion on the Annapurna Detachment ceased by ~22.5 Ma and the deeply buried rocks above and below were progressively exhumed to middle crustal levels at 15–12 Ma. As discussed below, alternation of shear sense on the STD and its equivalent structures is a general phenomenon in the western and eastern Himalayan orogen as well.

Orogen-parallel motion on the STD is also documented in the Nepal Himalaya (Coleman, 1996). However, the limited spatial extent of this type of structures in the central Himalaya suggests that it is probably a local feature created by relative motion between the deforming STD hanging wall and footwall. Complex kinematics across a fault juxtaposing deforming rocks is well known; this type of faults is generally referred to as stretching faults (Means, 1990). I speculate that the STD is such a structure accommodating both discrete slip on the fault and coeval deformation in its hanging wall and footwall. Thus, local orogen-parallel strike-slip motion on low-angle STD shear zone may have no regional significance.

Low-grade or unmetamorphosed basal Tethyan Himalayan strata are generally placed over the GHC across the STD (e.g., LeFort, 1996). However, locally higher-grade rocks of the THS are also juxtaposed over lower-grade rocks of the GHC across the STD (Schenider and Masch, 1993). Everywhere mapped in Nepal and south-central Tibet, the STD places the Cambrian (?) or Ordovician strata directly above the fault, a relationship persistent for at least 500 km along strike and for more than 34 km in the fault transport direction (Burchfiel et al., 1992). Although some low-angle top-north faults are present at higher structural levels, the main STD fault always lies at the base of the THS in Nepal (e.g., Searle and Godin,

2003). This implies that the exposed part of the STD is mostly a hanging-wall flat. The possibility that the STD may also be present in the Kathmandu Nappe below the Cambro-Ordovician unconformity (Table 7) would further require that the STD flat extend for >100 km southward in its up-dip direction from its northernmost exposure.

Ductile motion on the STD is constrained between 23 and 18 Ma (e.g., Hodges et al., 1992, 1996) (Table 6). A strand of the STD system in NW Nepal is locally intruded by leucogranite dike of 18 Ma (Coleman, 1998; see also interpretation by Searle and Godin, 2003). Dating the age of STD footwall leucogranites suggests that the fault was active during and after 19–17 Ma in Rongbuk Valley directly north of Mt. Everest (Murphy and Harrison, 1999). The  $^{40}\text{Ar}/^{39}\text{Ar}$  cooling ages of muscovite from the Annapurna region of NW Nepal indicate that motion along the STD may be as young as 15–13 Ma (Godin et al., 2001). Some workers even suggest that the STD in Nepal remained active in the Quaternary mainly based on extrapolation of outcrop patterns (Hurtado et al., 2001), a notion challenged by Searle et al. (2003) citing the lack of seismicity and geomorphologic expression of the STD in the Himalaya.

In south-central Tibet, the magnitude of slip along the STD is inferred to be >34 km (Burchfiel et al., 1992), based on the distance between the southernmost STD klippe carrying Ordovician strata in the STD hanging wall and the northernmost STD exposure. This method of slip estimate requires the STD to have both hanging-wall and footwall cutoffs across the Ordovician strata. However, the matching STD footwall cutoff has not yet been identified anywhere in the central Himalaya. The absence of the STD footwall cutoff may be explained by erosion in Nepal. However, this interpretation is quite unlikely considering together the geologic relationships observed in the western and eastern Himalaya as discussed below. That is, the STD most likely is a structure following preexisting lithologic contact and is a flat-over-flat fault contact without significant repetition and omission of stratigraphic sections.

### 3.1.7. Tethyan Himalayan fold and thrust belt

The Tethyan Himalayan fold and thrust belt in the central Himalaya was examined by Heim and Gansser (1939), Gansser (1964), Burg and Chen (1984),

Ratschbacher et al. (1994), Hauck et al. (1998), and Murphy and Yin (2003). This thrust belt initiated in the Eocene (~50 Ma), remained active at ~17 Ma, and ceased motion at about 11–9 Ma (Ratschbacher et al., 1994; Harrison et al., 2000). The contractional belt has accommodated at least 110–140 km of north–south shortening (Ratschbacher et al., 1994; Murphy and Yin, 2003). After adding shortening in the Lesser Himalayan thrust belt and along the MCT (DeCelles et al., 2001, 2002; Schelling and Arita, 1991; Schelling, 1992), the total amount of crustal shortening across the central Himalaya is at least 750 km in western Nepal and southwest Tibet (Murphy and Yin, 2003) and greater than 326 km in easternmost Nepal and south-central Tibet (Hauck et al., 1998) (Table 6).

### 3.1.8. Lesser Himalayan thrust belt

The Lesser Himalayan thrust belt between the MCT and MBT has experienced multiple phases of contraction (e.g., Schelling and Arita, 1991). A complete understanding of its development is hindered by the generally poor exposure of the thrust belt in the central Himalaya and a complex interaction between the nonfossiliferous LHS and Cenozoic thrusts.

The relationship between the MCT zone and Lesser Himalayan thrust belt has been intensely examined in Nepal. Schelling and Arita (1991), Schelling (1992), DeCelles et al. (1998a,b, 2001), and Robinson et al. (2003) consider the MCT as the roof fault of a large thrust duplex. Mapping by DeCelles et al. (2001) in far western Nepal shows that the Dadeldhura (= southern extension of the MCT) and Ramgarh thrusts locally cut down section southward in their transport direction (see foldout 1a of DeCelles et al., 2001). The truncated footwall strata involve the lower Miocene Dumri Formation, suggesting that the terminal motion on the MCT and the parallel low-angle faults such as the Ramgarh thrust postdates Dumri deposition. Although motion on the MCT outlasted Dumri deposition, the above crosscutting relationship does not preclude initiation of the MCT to be coeval or even earlier than Dumri deposition.

The truncational relationship between the MCT and its underlying strata is indicative of out-of-sequence thrusting (e.g., Boyer and Elliott, 1982; Morley, 1988). It implies that contraction had already

occurred in the Lesser Himalayan thrust belt before the MCT and Rangarh thrust sheets reached to the thrust belt. Because the MCT flat in southern Nepal is itself cut by younger footwall thrusts (Schelling and Arita, 1991; Schelling, 1992; Paudel and Arita, 2002), we can infer at least three phases of deformation in the Lesser Himalayan thrust belt:

- (1) pre-MCT thrusting;
- (2) emplacement of the MCT and truncation of its footwall structures; and
- (3) younger thrusts developed initially in a duplex below the MCT as the roof fault but they later cut across the MCT (Fig. 6).

The age of deformation for the Lesser Himalayan thrust belt below the MCT zone is not well constrained. A muscovite age of 35 Ma was obtained by Catlos et al. (2001) in the uppermost part of the LHS below the MCT zone. Macfarlane (1993) analyzes a hornblende from the Lesser Himalayan Sequence using the  $^{40}\text{Ar}/^{39}\text{Ar}$  method and shows a complex release spectrum with a minimum age of  $41 \pm 6.7$  Ma. This Eocene–Oligocene cooling event may have been related to an early phase of Cenozoic thrusting in the Lesser Himalayan thrust belt. Because the emplacement of the Kathmandu Nappe along the MCT may have ceased motion after ~14 Ma (Arita et al., 1997; Catlos, 2000; Johnson et al., 2001), the duplex system below the MCT should also have become inactive since that time due to lack of exhumation-related cooling. The age of initiation for the Lesser Himalayan thrust belt has also been inferred from a marked increase in the total detrital input at ca. 10–8 Ma in the Siwalik Group (Huyghe et al., 2001), but this increase in detrital flux could alternatively be a result of climate change.

### 3.1.9. Main Boundary Thrust

The age of the MBT in the central Himalaya is considered to be either older than 11 Ma as inferred from changes in subsidence rates (Meigs et al., 1995) or <5 Ma based on the influx of coarse clastic sediments to the Himalayan foreland basin from the MBT hanging wall (DeCelles et al., 1998b) (Table 6). The total magnitude of slip across the fault is not well constrained due to the lack of correlative stratigraphic units across the fault. Some workers have speculated

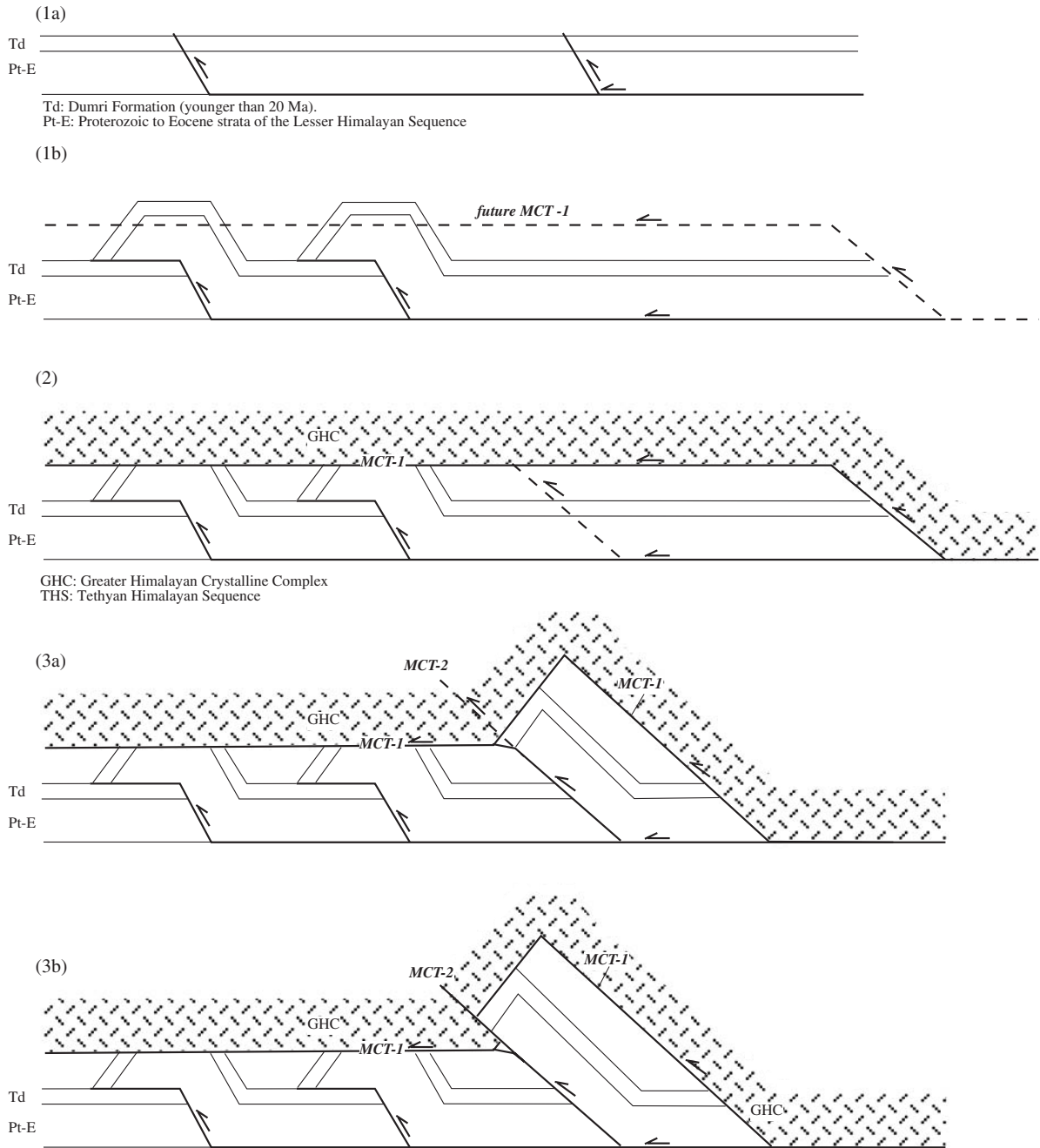


Fig. 6. Possible sequence of faulting in the Lesser Himalaya zone in Nepal. (1) Development of imbricate thrusts. (2) MCT was developed as an out-of-sequence thrust and truncates the older imbricate thrusts in its footwall. (3) A new imbricate thrust was developed in the MCT footwall to form a duplex. Its further development cuts across the MCT. Pt-E, Proterozoic to Eocene strata; Td, Tertiary (early Miocene) Dumri Formation.

the fault to have slipped >100 km without clear geologic evidence (Molnar, 1988; Powell and Conaghan, 1973a).

### 3.1.10. Main Frontal Thrust

The MFT in Nepal places Siwalik sediments over Quaternary Gangetic plain deposits (e.g., Nakata, 1989). Folds in the hanging wall were developed by flexural-slip mechanism and their shapes and developmental history have been used to determine the slip rate along the MFT (Lavé and Avouac, 2000). Using balanced cross-sections and age determination of folded terraces, Lavé and Avouac (2000) obtain a Holocene slip rate of  $21 \pm 1.5$  mm/yr on the MFT. This rate is broadly compatible with the GPS results across the Nepal Himalaya with rates of  $18 \pm 2$  mm/yr and  $15 \pm 5$  mm/yr (Larson et al., 1999; Jouanne et al., 1999) and is similar to the long-term rate of southward advancing Himalayan front deduced by overlapping unconformity beneath the Indo-Gangetic depression in the Neogene (Lyon-Caen and Molnar, 1985). This is the main reason that Avouac (2003) considers the Himalayan orogen has been in steady state.

### 3.1.11. Neogene north-trending rifts

Several north-trending Neogene rifts are present in the central Himalaya and southern Tibet (Fig. 1A) (Armijo et al., 1986, 1989; Taylor et al., 2003). Among these rifts, the Xiakangjian and Tangra Yum Co rifts extend from the central Lhasa terrane across the Indus–Tsangpo suture to the Himalayan range. In contrast, the Thakkhola graben in the Himalaya terminates northward at the easternmost branch of the right-slip Karakorum fault system (e.g., Hodges, 2000; also see foldout 1 of Taylor et al., 2003). The Thakkhola graben is believed to be active at ~14 Ma based on the age of an extensional vein parallel to the rift (Coleman and Hodges, 1995). However, its initiation age has been refined to between 10 and 11 Ma based on magnetostratigraphy of the oldest basin fill in the graben (Garzzone et al., 2000, 2003). Near the southern termination of the graben, the rift-bounding fault (i.e., the Dangardzong fault) offsets the basal

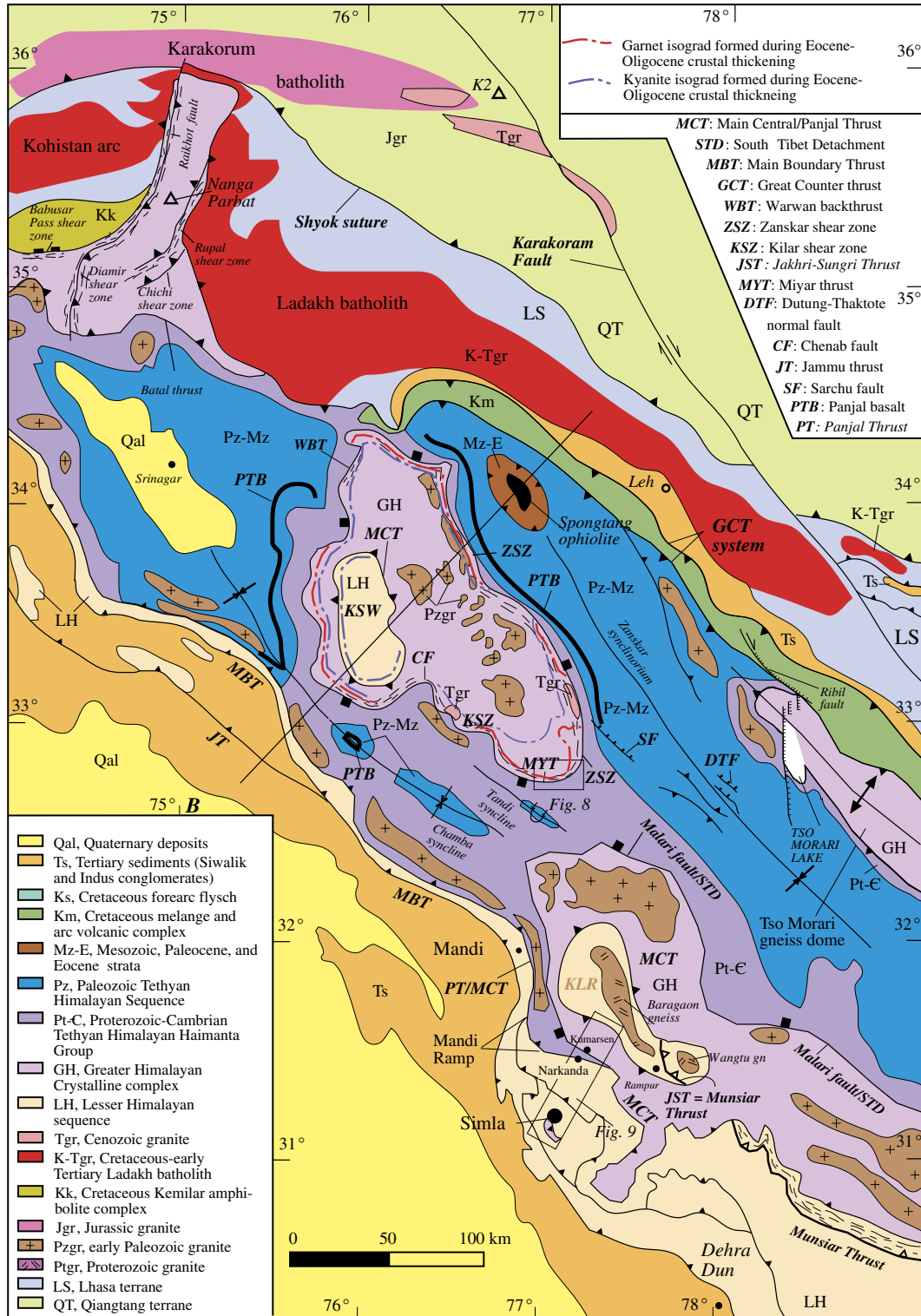
fault of the STD system (i.e., the Annapurna detachment), but the fault itself appears to terminate at a younger strand of the STD (= the Dhumpu detachment) that is younger than ca. 17.2 ka (Hurtado et al., 2001). Note that the direct structural relationship between the rift-bounding faults of the Thakkhola graben and possible young strands of the STD is not observed in the field. Instead, their possible cross-cutting relationship was extrapolated from limited bedrock exposure (Hurtado et al., 2001). Thus, whether the STD is active and synchronous with active east–west extension remains an open question and requires further research.

## 3.2. Western Himalaya

### 3.2.1. Main Central Thrust zone

The geology of the Kumaun and Garhwal Himalaya (77°E–81°E) in northwestern India can be correlated with that in the western Nepal Himalaya (Valdiya, 1980, 1988, 1989; Hodges and Silverber, 1988; Pêcher, 1991; Metcalfe, 1993; Srivastava and Mitra, 1994; Sorkhabi et al., 1997, 1999) (Figs. 2A and 7). In this region, the MCT of Heim and Gansser (1939) in its root zone is named as the Munsiri thrust and a thrust at a higher structural position as the Vaikrita thrust by Valdiya (1980) (Table 3). The definition of the Vaikrita thrust is similar to the MCT of LeFort (1975) and the Munsiri thrust is similar to the MCT-I of Arita (1983) in Nepal (Table 3). Southward, the Munsiri thrust forms a long thrust flat that extends far south (>80 km) into the geographically defined Lower Himalaya and splits in its up-dip direction into two fault splays: the Ramgarh thrust below and the Almora thrust above (Valdiya, 1980) (Table 3). Both the Ramgarh and Almora thrusts are folded into a broad synform, producing several thrust klippen in the Lower Himalaya (Fig. 2A). The Ramgarh thrust extends to western Nepal and keeps the same name, whereas the Almora thrust becomes the Dadeldhura thrust in Nepal (DeCelles et al., 1998a, 2001). Crystalline rocks immediately above the Ramgarh thrust may have originated

Fig. 7. Geologic map of the Zaskar region, compiled from mainly from Herren (1987), Pognante et al. (1990), Spring and Crespo-Blanc (1992), Searle et al. (1992), Frank et al. (1995), Fuchs and Linner (1995), Steck et al. (1998), Thakur (1998), Dèzes (1999), Dèzes et al. (1999), Wyss et al. (1999), Corfield and Seale (2000), Stephenson et al. (2001), Zeitler et al. (2001), and Walker et al. (2001). KSW, Kishtwar window; KRLW, Kullu–Larji–Rampur window. Cross-section (B) is shown in Fig. 2.



from the LHS (Valdiya, 1980), whereas the Almora crystalline thrust sheet has been correlated with the GHC (Heim and Gansser, 1939).

The Munsiri thrust can be traced northwestward from the India–Nepal border to the Kullu–Larji–Rampur window south of Lahul and Spiti, where the thrust merges with the MCT (= Vaikrita thrust; Vannay and Grasemann, 2001) (Table 3) (Figs. 2A and 7). The Munsiri thrust (= the Jakhri–Sungri thrust in Fig. 7) reappears in the Kullu–Larji–Rampur window below the MCT (Fig. 7) (Wiesmayr and Grasemann, 2002), but it is not clear how it extends farther to the northwest towards the Zaskar region.

The Wangtu orthogneiss is traditionally treated as part of the GHC above the Kullu–Larji–Rampur MCT window (e.g., Chatterji and Swami Nath, 1977; Sharma, 1977; Singh and Jain, 1995). However, recent studies by Vannay and Grasemann (1998) have lumped this unit with the LHS. The contact between the Wangtu gneiss and the Rampur Group of the LHS is the Jakhri–Sungri thrust in the Kullu–Larji–Rampur window (Pandy and Viridi, 2003), which is considered to be the Munsiri thrust by Vannay and Grasemann (2001).

From the footwall cutoff relationship, one can infer that the MCT cuts upsection southward from the Kullu–Larji–Rampur window to Simla (also spelled as Shimla). Below the MCT window in the north, the MCT lies above the Rampur Formation of the LHS, whereas in the south near Simla, the MCT thrusts over the younger Simla Slate (e.g., Thakur and Rawat, 1992; Miller et al., 2001). Because both units dip dominantly to the north, they may be juxtaposed by a north-dipping thrust in the MCT footwall (Fig. 7).

The Zaskar Himalaya lies west of Lahul (~75°–77°E) and exposes the Kishtwar window of the MCT (Fuchs, 1975; Herren, 1987; Patel et al., 1993; Fuchs and Linner, 1995; Stephenson et al., 2001) (Figs. 2A and 7). A zone of metasedimentary rocks (slate, micaschist, and limestone) and augen gneiss bounded by mylonitic shear zones above is present below the MCT in the window. This section is termed the Lower Crystalline Nappe and was correlated to the Munsiri thrust sheet in the Kullu–Larji–Rampur window (e.g., Frank et al., 1995 and references therein; Wiesmayr and Grasemann, 2002) (Table 3). DiPietro and Pogue (2004)

refer to the Lower Crystalline Nappe as the MCT schuppenzone. Although lithologically correlative, the timing of deformation for the Munsiri thrust sheet and the Lower Crystalline Nappe is quite different. The Munsiri thrust in the Garhwal Himalaya was active between 6 and 2 Ma (Catlos et al., 2002a,b, 2004), while the lower part of the MCT zone including the Lower Crystalline Nappe apparently ceased deformation at or before 16 Ma (Stephenson et al., 2001).

### 3.2.2. MCT lateral ramp and western extension

A major change in the MCT hanging-wall cutoff occurs between Simla and Mandi (Fig. 7). West of Mandi, the MCT places the low-grade to unmetamorphosed Haimanta Group of the THS over the low-grade to unmetamorphosed Proterozoic LHS, whereas east of Mandi, the high-grade GHC thrusts over the low-grade to unmetamorphosed LHS (Thakur and Rawat, 1992; Frank et al., 1995; Fuchs and Linner, 1995; Pogue et al., 1999) (Table 3). This relationship suggests that the MCT cuts upsection laterally from Mandi westwards correlating with the Panjal thrust and forming a hanging wall ramp (e.g., Fuchs and Linner, 1995) (Fig. 2) (Table 3). Alternatively, the GHC may form a southward-tapering wedge between the THS above and the LHS below; the Panjal thrust simply represents the original flat-over-flat relationship between the THS and LHS before the GHC had been squeezed between the two units.

The Panjal fault can be traced continuously south of the Nanga Parbat syntaxis and around the Hazara syntaxis (Greco et al., 1989; Thakur and Rawat, 1992; DiPietro and Pogue, 2004). Immediately west of the syntaxis, the MCT splits into three fault branches: the Oghi shear zone, the Mansehra thrust, and the Khairabad thrust from north to south (Calkin et al., 1975; Coward et al., 1988; Searle et al., 1989; Greco et al., 1989; Pogue et al., 1992, 1999) (Fig. 2A). The Oghi shear zone may be correlated with the Batal thrust of Chaudhry and Ghanfar (1990) in Kaghan Valley immediately west of the Nanga Parbat metamorphic massif. Because the age of deformation and metamorphism in the hanging wall of the Batal thrust occurred in the Eocene (e.g., Treloar et al., 2003 and references therein), it is likely that the Batal thrust and therefore the Oghi shear zone are Eocene structures, which are too old

to be correlative with the Miocene Main Central Thrust extending from the Zaskar–Chamba area in the east (DiPietro and Pogue, 2004). Pogue et al. (1999) note that the Proterozoic metasedimentary units can be correlated across the Oghi and Mansehra shear zones and both faults appear to die out westward west of the Nanga Parbat syntaxis, indicating small magnitudes of slip along these faults. These observations lead them to suggest that the Khairabad fault is the main strand of the MCT west of the Hazara syntaxis, an interpretation supported by the similar stratigraphic juxtaposition across the Panjal thrust east of the Hazara syntaxis (i.e., low-grade metasedimentary rocks over low-grade metasedimentary rocks; see Table 3).

### 3.2.3. MCT slip

The minimum slip of ~95 km along the MCT is determined by the distance between the Simla klippe and the northern limit of the Kullu–Larji–Rampur window (Vannay and Grasmann, 2001). Similarly, a minimum slip of 90 km along the MCT is determined by the distance between the southernmost trace of the MCT in Chamba and the northern limit of the Kishtwar window in Zaskar (Frank et al., 1995) (Fig. 7) (Table 6).

### 3.2.4. Age of the MCT

The age of the MCT in the Garhwal Himalaya is constrained to be 22–14 Ma by K–Ar cooling ages of muscovite in the GHC (Metcalf, 1993). Within the MCT zone below the Vaikrita thrust (=MCT), thrusting was active between 6 and 2 Ma as determined by Th–Pb ion-microprobe dating of monazites (Catlos et al., 2002a). This age is broadly consistent with the youngest K–Ar muscovite cooling ages (5.7–5.9 Ma) from the same localities (Metcalf, 1993) (Table 6).

The age of the MCT around the Kishtwar window was constrained to be active between 22 and 16 Ma (J.D. Walker et al., 1999; Searle et al., 1999a; Stephenson et al., 2001). In contrast to the 7–3 Ma young ages of the MCT obtained from Nepal and Garhwal Himalaya (Harrison et al., 1997a; Catlos et al., 2001; 2002a,b), there is no evidence of late Miocene–Pliocene reactivation of the MCT zone in the Zaskar Himalaya, because the youngest  $^{40}\text{Ar}/^{39}\text{Ar}$  muscovite ages reported in the region is about 16 Ma (Stephenson et al., 2001).

The upper age bound for motion along the MCT in the Zaskar region may be constrained by the timing of doming and warping of the MCT that lead to the exposure of the Kishtwar window. Folding of the MCT in the Kishtwar region appears to have started since ~6 Ma and lasted until after 2 Ma, as constrained by zircon and apatite fission track ages (Kumar et al., 1995). This age range overlaps with the age of thrust motion along the Munsiri thrust in the Garhwal Himalaya (Catlos et al., 2002a,b). Thus, folding of the MCT in Zaskar could have been induced by same compressional event that reactivates the lower MCT zone such as the Munsiri thrust. Specifically, it is possible that the Munsiri thrust lies below the Kishtwar window as a blind fault.

### 3.2.5. South Tibet Detachment and other major extensional faults

The South Tibet Detachment can be traced continuously from western Nepal to NW India (Valdiya, 1989; Pêcher, 1991; Burchfiel et al., 1992). In the Garhwal Himalaya, the STD is locally known as the Malari fault or the Trans-Himadri fault (Valdiya, 1980, 1989) (Table 7) (Fig. 2). Pêcher and Scaillet (1989) show that the stretching lineation in the GHC of the Garhwal Himalaya changes systematically from being nearly perpendicular to the Himalayan range at the base to being subparallel to the range at the top of the GHC. Pêcher (1991) suggests that the STD has a significant right-slip component of fault motion possibly related to eastward extrusion of the Tibetan plateau during the Indo-Asian collision. As discussed above, the STD may be a stretching fault accommodating coeval deformation in its wall rocks. Thus, local strike-slip kinematics on the fault may simply indicate inhomogeneous strain in its hanging wall and footwall rather than regional strike-slip component along the fault.

Metcalf (1993) considered the north-dipping Jhala fault (Fig. 2A) in the upper reach of the Bhagirathi River of the Garhwal Himalaya to be a segment of the South Tibet Detachment. The fault juxtaposes similar garnet-biotite schist above and below. K–Ar muscovite ages show essentially the same cooling ages (~21 Ma) across the fault (Metcalf, 1993), suggesting that the fault cannot be a significant tectonic feature since the early Miocene. Sorkhabi et al. (1999) observed the

Jhala fault to be a north-directed brittle thrust zone, which was active after 15 Ma as constrained by apatite fission track cooling ages. The earlier mapping by Pêcher and Scaillet (1989) and Pêcher (1991) also shows that the Jhala fault is a thrust. My own observation across the Jhala fault zone of Metcalfe (1993) in 2003 confirms Sorkhabi et al.'s (1999) conclusion that Jhala fault is a north-directed brittle thrust zone superposed on a zone of dominantly north-verging ductile folds in garnet-biotite gneiss and schist. In light of these observations, the STD is likely located farther north and at a higher structural level than the Jhala thrust of Pêcher and Scaillet (1989) and the Jhala “normal” fault of Metcalfe (1993) as indicated by Valdiya (1989) as the Malari fault (Fig. 2A).

In the Zaskar region, the STD equivalent is the Zaskar shear zone (Searle, 1986; Herren, 1987). Although both are prominent structures juxtaposing the basal section of the Tethyan Himalayan strata over the high-grade GHC, the Malari fault/STD in southern Spiti and the Zaskar shear zone to the west do not link with one another (Wyss et al., 1999; Dèzes et al., 1999; Robyr et al., 2002) (Figs. 2 and 7). The two faults are separated by a NE-trending, 50-km wide strip of the THS in Lahul (Vannay and Steck, 1995; Fuchs and Linner, 1995; Fig. 7), where several late stage normal faults have been mapped. The existence of the normal faults is mainly inferred from younger-over-older relationships without considering the possible effects of Cenozoic out-of-sequence thrusting and strike-slip faulting. For example, the north-dipping Sarchu fault (Fig. 7) juxtaposes Ordovician–Triassic strata over Cambrian–Ordovician strata (Spring and Crespo-Blanc, 1992), whereas the Dutung–Thaktote fault (Fig. 7) juxtaposes either Jurassic over Triassic strata or younger Triassic units over older Triassic units (Steck et al., 1998). Limited stratigraphic throws suggest that these faults only have 1–3 km of slip at most, insufficient to transfer extension on the STD in Garhwal to the Zaskar shear zone, because the latter may have moved >30 km at its apparent eastern termination (Dèzes et al., 1999).

### 3.2.6. Folding of the Zaskar shear zone over the Kishtwar window

Although it has been portrayed in many regional tectonic maps that the STD and GHC extend continuously along the axis of the Himalayan orogen from

the eastern syntaxis to the western syntaxis (e.g., Gansser, 1964; Windley, 1983; Sorkhabi and Macfarlane, 1999; Searle et al., 1999a,b, 2003; Hodges, 2000), geologic investigations of the western Himalaya in the past three decades have shown that the GHC in the Garhwal Himalaya is separated from the high-grade metamorphic rocks in Zaskar by the THS in Lahul (Fig. 7) (Powell and Conaghan, 1973a; Vannay and Steck, 1995; Fuchs and Linner, 1995). The THS strip consists of the Upper Proterozoic–Middle Cambrian Haimanta Group and its equivalent the Phe Formation (Srikantia, 1977, 1981), both of which are intruded extensively by 550–470 Ma granites (Frank et al., 1995; Miller et al., 2001). In Zaskar, the Phe Formation is overlain conformably by the Middle Cambrian Karsha Formation (Hughes and Jell, 1999). This unit in turn lies unconformably below the conglomeratic Lower Ordovician Thaple Formation (Baud et al., 1984) (Table 2). In the Chamba region to the south, Permian strata lie directly over the Haimanta Group in the cores of the Chamba and Tandi synclines without Ordovician to Carboniferous strata that are present to the north in Spiti and Zaskar (Vannay and Steck, 1995; Frank et al., 1995). The disappearance of Ordovician to Carboniferous strata of the THS in the Chamba and Lahul regions has been related to upper Paleozoic rifting during the opening of the Neo-Tethys ocean; the Chamba region represents a rift shoulder whereas the Spiti and Zaskar regions represent a rift zone (Vannay and Steck, 1995).

The above relationship raises the question of why the Malari fault/STD and the Zaskar shear zone terminate so abruptly at their western and eastern end, respectively, towards Lahul (Fig. 7). To address this question, we need to examine the relationship between MCT and STD and how the THS is distributed in the western Himalaya. Although it has been long known that the MCT is folded in the Himalayan orogen (Heim and Gansser, 1939) and its motion was synchronous with the STD (e.g., Burchfiel and Royden, 1985; Hodges et al., 1992), there has been no inference that the low-angle STD could also have been folded in geometrical concordance with the MCT. Folding of the MCT in the western Himalaya is best expressed by the formation of the Kishtwar and Kullu–Larji–Rampur windows. Naturally, these two areas would be ideal places to

examine whether the low-angle STD is folded over the MCT because the GHC is surrounded by the THS in the areas (Fig. 7).

In the Zaskar Himalaya, the high-grade Zaskar crystallines are bounded in the north by the north-dipping, top-northeast Zaskar shear zone (Searle, 1986; Herren, 1987; Dèzes et al., 1999; Walker et al., 2001) (Fig. 7). The Zaskar crystallines consist most of the GHC but also have minor THS protolith that has been metamorphosed to the amphibolite grade (Honegger et al., 1982). Directly above the Zaskar shear zone is the Proterozoic to Lower Cambrian Phe Formation, equivalent to the Haimanta Group south of the Zaskar crystallines in Chamba (Garzanti et al., 1986; Hughes and Droser, 1992; Frank et al., 1995; Thakur, 1998) (Table 7) (Fig. 3). Patel et al. (1993) show that early motion on the Zaskar shear zone was dominated by top-SW shear, which also occurred throughout the underlying GHC and overlying THS. This event was later superposed by top-NE sense of shear. They also point out the lack of extensional basins in the hanging wall of the Zaskar shear zone and attribute it to distributed shear rather than discrete extensional detachment faulting. Patel et al. (1993) disagree with Herren's (1987) interpretation that the Zaskar shear zone truncates the footwall isograds. Instead, they believe that the isograds are continuous laterally and parallel to the shear zone but only condensed vertically by post-metamorphism deformation.

In the east and south, the high-grade crystalline rocks in the Zaskar region are bounded by a south-dipping, top-northeast shear zone that has been locally mapped as the Miyar thrust (Pognante et al., 1990), Kilar shear zone (Stephenson et al., 2001), Warwan backthrust (Searle et al., 1999b; Walker et al., 2001), and Chenab normal fault (Thakur, 1998), respectively. Collectively they are referred to as the Chenab normal fault zone (Thakur, 1998) (Fig. 7). This south-dipping fault expressed by a thick ductile shear zone up to several kilometers juxtaposes the lower members of the Haimanta Group in the hanging wall over the high-grade GHC in the footwall (Frank et al., 1995). Despite the fact that these faults put lower-grade rocks over higher-grade rocks, they have been consistently interpreted as top-north thrusts (e.g., Pognante et al., 1990; Searle et al., 1999b).

The top part of the south-dipping Miyar thrust zone also contains top-south shear fabrics (J.D. Walker et

al., 1999). This is interpreted as a result of reactivation of late top-south shear along the south-dipping Khanjar normal shear zone (Steck et al., 1999). Similarly, Thakur (1998) also notices that a segment of the Chenab fault west of the Kilar shear zone preserves top-south S-C mylonitic fabric. These observations suggest that the broadly defined Chenab fault zone has a complex kinematic history, with an early phase of top-north motion followed by top-south motion (also see Robyr et al., 2002).

The critical link between the Zaskar shear zone in the north and the Chenab normal fault zone in the south was established by Dèzes (1999). His mapping along the Gianbul valley at the eastern termination of the Zaskar shear zone shows that the shear zone together with the footwall kyanite, staurolite, and garnet isograds are warped together with the overlying Zaskar shear zone around an east-trending fold axis (see Fig. 5.8 on pp. 71 in Dèzes, 1999) (Fig. 8). The doubly plunging antiform defines the broad Gianbul gneiss dome in the GHC that is bounded by the Zaskar shear zone in the north and east and the Miyar thrust of Pognante et al. (1990) in the south (pp. 53, Dèzes, 1999). Based on this relationship, Dèzes (1999) suggests that the north-dipping Zaskar shear zone is folded over the Zaskar crystallines (= GHC) and links with the south-dipping Miyar thrust (Fig. 8). Dèzes's (1999) mapping also shows that the ductile Zaskar shear zone is cut by a late high-angle normal fault with a relatively small amount of throw (~2–3 km). This late normal fault could be a branch of the late Miocene–Quaternary northwest-trending extensional system in the western Himalayan orogen, because it shares a similar strike to the major rifts such as the northwest-trending Tso Morari normal fault system (Fig. 7).

The western margin of the Zaskar GHC window is bounded by the Warwan backthrust. This fault was mapped within <2 km from the western termination of the Zaskar shear zone, both placing the Haimanta Group over the high-grade GHC (Fig. 7) (Searle et al., 1999b; Walker et al., 2001). Because the Warwan fault truncates late Oligocene–early Miocene metamorphic isograds in the footwall, it is interpreted to be a separate structure postdating the Zaskar shear zone (Searle et al., 1992, 1999b). However, the same isograds cut by the Warwan thrust are also truncated by the Zaskar

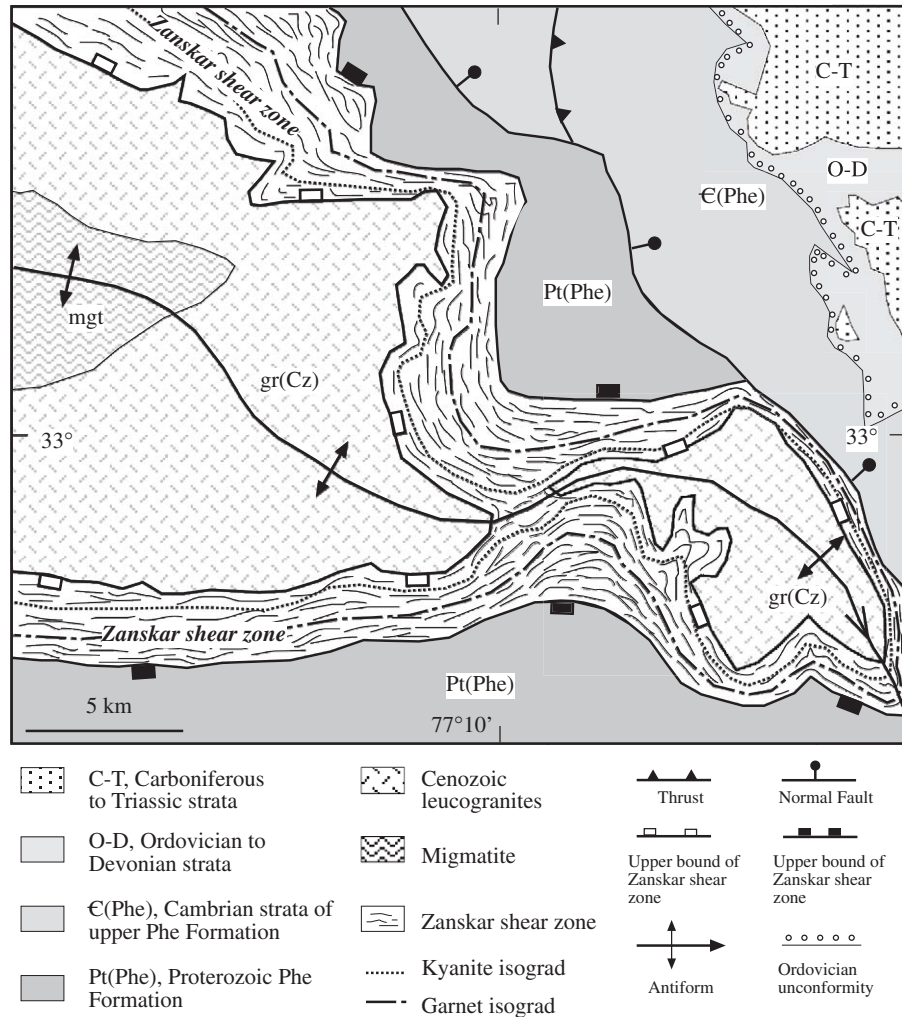


Fig. 8. Geologic map of the eastern termination of the Zanskar shear zone, simplified from Dèzes (1999).

shear zone (Herren, 1987; Dèzes et al., 1999; Walker et al., 2001) (Fig. 7). The above observations permit the Zanskar shear to be coeval with and link directly to the Warwan thrust. The similar stratigraphic positions along which the two faults lie, the abrupt fault terminations at their western ends, and the close proximity of the two major faults all suggest that the Warwan fault and the Zanskar shear zone are parts of the same folded low-angle fault. This single-fault interpretation implies that the connected Zanskar shear zone, Warwan Thrust, and Chenab normal fault zone completely encircles the Zanskar crystallines as first suggested by Thakur

(1992, 1998). I refer to this united fault zone as the Zanskar–Chenab shear zone (Fig. 2C).

The single-fault interpretation is consistent with the fact that the Permian–Triassic Panjal Trap basalt is exposed on all sides of the Zanskar crystalline window (Fig. 7) (Papritz and Rey, 1989; Frank et al., 1995). Additionally, a united domal Zanskar–Chenab fault zone is consistent with the warped pattern of metamorphic isograds in the GHC and the folding pattern of the MCT (Honegger et al., 1982; Searle and Rex, 1989; Stäubli, 1989; Kündig, 1989; Pognante et al., 1990; Dèzes et al., 1999; Searle et al., 1999b; C.B. Walker et

al., 2001; Robyr et al., 2002) (Fig. 7). Correlating the Zaskar shear zone with the Chenab fault requires that:

- (1) the MCT and Zaskar shear zone be concordantly folded;
- (2) the Zaskar shear zone and the Malari fault/STD be a blind fault east and west of the Zaskar crystallines window; and
- (3) the Zaskar shear zone/STD and MCT merge southward to form a leading edge branch line (e.g., Boyer and Elliott, 1982), bounding a thin (<10 km) but long (>70 km) north–south direction slice of the GHC in between (Figs. 2C and 7).

The composite nature of the Zaskar and Chenab shear zones with both top-north and top-south shear fabrics is similar to the observations made in the Annapurna and Mt. Everest areas of the central Himalaya, where top-north and top-south shear zones are located next to one another or superposed over one another (Hodges et al., 1996; Godin et al., 1999a; Searle, 1999). The stratigraphic positions of the hanging-wall cutoff require that the Zaskar–Chenab fault cut down section slightly to the south (Table 7). This relationship may have resulted from an early phase of deformation that had tilted the THS before the initiation of the Zaskar shear zone. In other words, the Zaskar shear zone is an out-of-sequence fault.

The revival of the isoclinal folding model of Heim and Gansser (1939) in the past two decades (e.g., Searle and Rex, 1989) is mainly based on the observation that the traces of metamorphic isograds in the MCT hanging wall are enclosed in map view as observed in Zaskar. However, the isograd pattern could also be produced by broad warping the Zaskar crystallines without overturning the originally subhorizontal isograds. So far, there have been no focused studies to document the dip angle and dip direction of major metamorphic isograds above and below the MCT. However, the detailed geologic mapping of Dèzes (1999) at the eastern end of the Zaskar shear zone appears to suggest that the isograd surfaces are warped and dip in the same direction of their bounding low-angle shear zones. This mapping would support upward warping rather than isoclinal folding of originally subhorizontal isograds. Clearly, more research needs to be devoted on this subject.

### 3.2.7. Folding of the STD over the Kullu–Larji–Rampur window

Directly north of the Kullu–Larji–Rampur window, the contact between the Phe Formation and the GHC was mapped as the western extension of the STD/Malari fault from Garhwal (Wyss et al., 1999; also see Valdiya, 1989). In this area, the STD is a 2- to 5-km-thick shear zone that has experienced four phases of deformation:

- (1) south-verging folding;
- (2) top-north shear;
- (3) south-verging folding; and
- (4) north-verging folding (Jain et al., 1999; Steck et al., 1999; Wyss et al., 1999; Wyss, 2000).

The exact location of the STD west of Spiti has not been mapped (see Fig. 1 of Vannay and Grasemann, 2001).

The GHC around the Kullu–Larji–Rampur window is surrounded by the Haimanta Group on the north, west and south sides, forming an east-facing half window (Fig. 7). If the STD follows the Haimanta/GHC contact, as seen for the Zaskar shear zone around the Kishtwar window, the STD must also be folded over the Kullu–Larji–Rampur window. That is, the east-trending STD turns south and joins the MCT between Mandi and Simla (Fig. 7). This interpretation is slightly different from that of Thakur (1998) who terminates the STD farther to the north at the northwestern corner of the Kullu–Larji–Rampur window. To test whether the STD is present south of the Kullu–Larji–Rampur window, Yin et al. (2003) carried out a field investigation along a traverse between Narkanda in the south and Sutlej River in the north (Figs. 7 and 9). The contact between the Haimanta Group above and the GHC below is a low-angle brittle fault juxtaposing highly folded phyllite of the THS Haimanta Group over a mylonitized orthogneiss unit of the GHC at Kumharsain (also spelled as Kumarsen) (Fig. 9). The gneiss unit is part of the Baragaon gneiss that has been dated by Bhanot et al. (1978) and Miller et al. (2001) as ~1830–1840 Ma. Drag folds in the fault zone indicate top-south motion. The mylonitic shear zone directly below the fault records a complex deformational history. Its upper part (>200 m thick) is marked by top-south S-C fabric. The

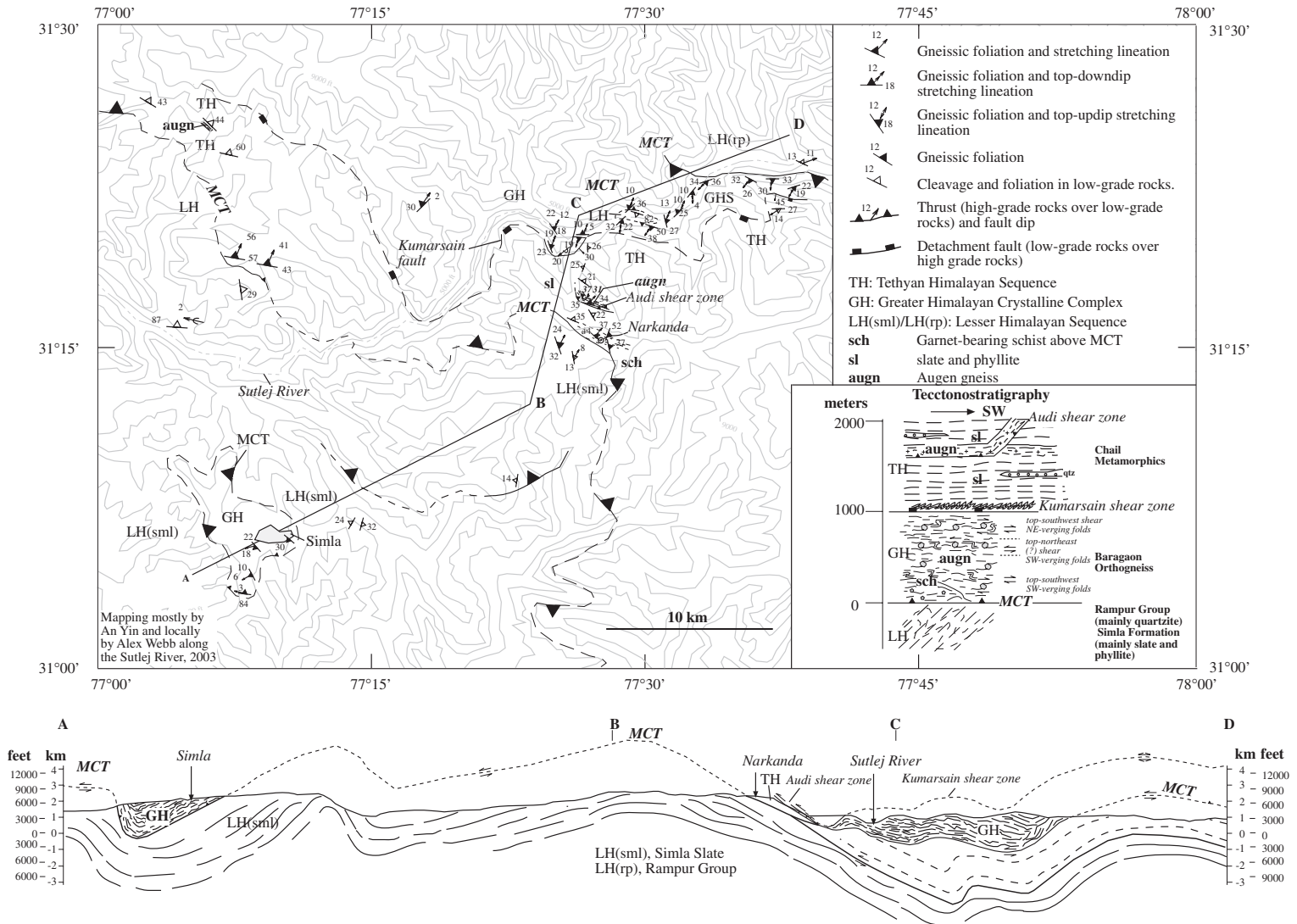


Fig. 9. Geologic map of the Kumharsain shear zone.

upper part (>50 m thick) exhibits dominantly top-south fabrics, but locally preserves relicts of top-north shear fabrics that are in turn deformed by south-verging folds. The lowermost part (>100 m) of the shear zone contains top-south S-C fabric that is deformed by later north-verging kink folds. The stratigraphic juxtaposition and cross-cutting relationships are quite similar to those observed along the STD north of the Kullu–Larji–Rampur window, where top-south shear is also preserved in the STD zone (Wyss et al., 1999). Thus, the Kumharsain shear zone and the STD zone of Wyss et al. (1999), both placing the Haimanta/Phe strata over the high-grade GHC on the north and south sides of the Kullu–Larji–Rampur window, may be correlative and are parts of the same folded low-angle fault (Fig. 7).

### 3.2.8. Age of the STD

In the Garhwal Himalaya  $^{40}\text{Ar}/^{39}\text{Ar}$  and K–Ar cooling ages and the age of a cross-cutting leucogranite suggest the STD to have been active between 23 and 21 Ma (Searle et al., 1999b). To the west in Zaskar, motion on the Zaskar shear zone was active between 22 and 19 Ma (Dèzes et al., 1999; J.D. Walker et al., 1999; Robyr et al., 2002). Apatite fission track ages obtained from the footwall of the Zaskar shear zone suggest that it ceased motion by 11–9 Ma (Kumar et al., 1995) (Table 6). There are no constraints on the initiation age of the STD in the Western Himalaya.

### 3.2.9. Slip on STD

The minimum slip across the central segment of the Zaskar shear zone was estimated by Herren (1987) to be >25 km based on the assumption that vertical condensation of the footwall metamorphic field gradient is solely caused by simple-shear deformation. Again, assuming simple-shear deformation, Dèzes et al. (1999) estimate  $35 \pm 9$  km of slip on the Zaskar shear zone at its eastern end. As pointed out by Grujic et al. (1996) and many others (e.g., Grasmann et al., 1999; Vannay and Grasmann, 2001; Searle et al., 2003; Law et al., 2004), general shear combining both simple and pure shear strain may be more characteristic of deformation in the STD shear zone. This implies that vertical condensation of metamorphic isograds near the STD could be caused

mainly by pure-shear deformation (i.e., vertical flattening) without significant simple-shear translation along the shear zone. Consideration of pure-shear contribution would make the slip estimates of Herren (1987) and Dèzes et al. (1999) only as the upper bounds.

### 3.2.10. Cutoffs across the Zaskar shear zone

In all tectonic reconstructions of the Zaskar shear zone, the fault is assumed to cut up section to the south (e.g., Gapais et al., 1992; Dèzes et al., 1999; C.B. Walker et al., 2001). The cutoff structure or breakaway fault implied by this interpretation must dip north and truncate the Tethyan Himalaya strata in its footwall. However, existing map relationships in the Zaskar–Chamba region present no candidates for such a structure (Fig. 7). One possible solution is that the Miyar thrust is younger than the Zaskar shear zone and its northward motion has buried the breakaway structure in its footwall (Fig. 10a). However, this interpretation would require the Miyar thrust to have a substantial northward displacement and extend laterally to the east into the Tethyan Himalayan strata with significant stratigraphic offset. The continuity of the Haimanta strata around the eastern rim of the Zaskar crystalline window (Frank et al., 1995) and the folded nature of the Zaskar shear zone at its eastern termination (Dèzes, 1999) (Fig. 8) do not favor this possibility. Alternatively, the MCT is younger than the Zaskar shear zone and cuts off the breakaway system of the Zaskar shear zone (Fig. 10b). This scenario is also unlikely, because this would require the STD together with the THS to be present in the footwall of the MCT, which has not been observed. Thus, the simplest solution to this problem is that the Zaskar shear zone is folded and forms a large window placing the THS above and the high-grade Zaskar crystallines below (Fig. 7).

### 3.2.11. Nanga Parbat syntaxis

The Nanga Parbat syntaxis (also known as the Nanga Parbat–Haramosh Massif) forms a tectonic window exposing high-grade metamorphic rocks of foliated tonalitic biotite gneiss, meta-pelite, and marble (e.g., Zeitler et al., 2001). The metamorphic massif is bounded in the north, east and west by

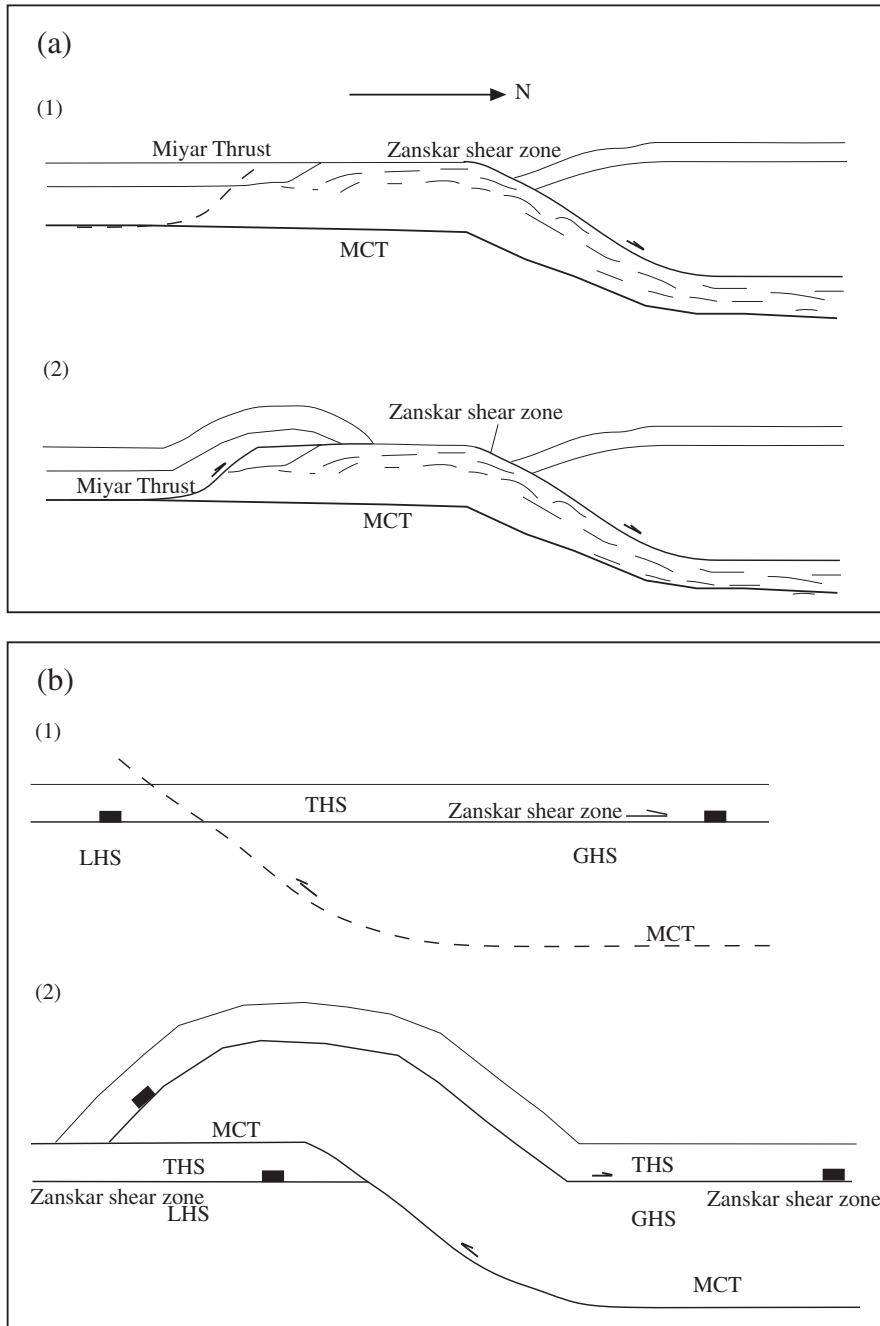


Fig. 10. Possible relationship between the Warwan backthrust and the Zanskar shear zone. (a) The Warwan thrust postdates the Zanskar shear zone and overrides the footwall cutoff of the Tethyan Himalayan strata. (b) The MCT cuts and offsets the united Chenab–Zanskar shear zone.

the warped Main Mantle Thrust (MMT), which is the western extension of the Indus–Tsangpo suture zone. The western and eastern margins of the Nanga

Parbat massif are marked by late Cenozoic north-striking ductile and brittle shear zones, together forming a large pop-up structure (Seeber and

Pêcher, 1998; Schneider et al., 1999a; Butler et al., 2000) (Fig. 7). The southern boundary of the Nanga Parbat massif is not well defined and appears to be bounded by a north-dipping thrust (i.e., the Diamir shear zone of Zeitler et al., 2001 or the Batal thrust of DiPietro and Pogue, 2004). U–Pb zircon dating indicates that the metamorphic rocks have protolith ages of ~2600 Ma, ~1850 Ma, and ~500 Ma and the massif experienced both Proterozoic and Cenozoic ductile deformation and high-grade metamorphism (Zeitler et al., 1989; Zeitler and Chamberlain, 1991; Schneider et al., 1999a,b,c, 2001; Treloar et al., 2000). Although the high-grade metamorphic rocks of the Nanga Parbat massif were traditionally considered part of the GHC (e.g., Fuchs and Linner, 1995), Nd–Sm and Sr isotopic analyses and U–Pb zircon dating has led some workers to interpret the Nanga Parbat massif as a high-grade expression of the LHS (Whittington et al., 1999; Zeitler et al., 2001; Argles et al., 2003).

The Zaskar shear zone terminates at the north-western corner of the Zaskar crystallines window (Searle et al., 1992) (Fig. 7). Farther to the west, before reaching to the Nanga Parbat metamorphic massif, the THS is continuous across the Kashmir Himalaya without exposing the high-grade GHC (Wadia, 1931, 1934; Fuchs and Linner, 1995; Argles and Edwards, 2002; DiPietro and Pogue, 2004). Several workers consider that the STD reappears in the Nanga Parbat massif or farther to the west along the MMT (Treloar and Rex, 1990; Hubbard et al., 1995; Burg et al., 1996; Argles and Edwards, 2002; Treloar et al., 2003). Because the Zaskar shear zone/STD is not present in Kashmir, this fault could either die out beneath the Kashmir basin (DiPietro and Pogue, 2004) or becomes a blind structure that re-emerges in the syntaxis (Argles and Edwards, 2002). The latter interpretation requires that the STD form a tectonic window in the Nanga Parbat massif because the metamorphic terrane is completely surrounded by the low-grade THS in the south and Cretaceous–lower Tertiary arc rocks in the north, east, and west (Figs. 2A and 7) (DiPietro and Pogue, 2004). This interpretation in turn would require that the frontal trace of the STD be exposed south of the Nanga Parbat massif, a prediction not supported by known field relationships in the region (Fig. 2A; also see Fig. 1 of DiPietro and Pogue, 2004).

The north-dipping Kohistan fault (= MMT) juxtaposes the Kohistan arc over the northern Indian margin and has been interpreted as a normal fault by Treloar et al. (2000). In contrast, DiPietro et al. (2000) and DiPietro and Pogue (2004) show that the fault was mainly a thrust active between the early Eocene and early Miocene. They also note that the juxtaposition relationship across the Kohistan fault is similar to the Gangdese thrust of Yin et al. (1994) in south Tibet. This relationship is in turn similar to the Lohit thrust east of the Namche Barwa syntaxis where the thrust places Cretaceous–early Tertiary arc rocks over Indian continental affinity (Gururajan and Choudhuri, 2003).

### 3.2.12. Tethyan Himalayan fold and thrust belt

The amount of shortening across the Himalayan fold and thrust belt in Pakistan is estimated to be 58–62% in the Zaskar region north of the Kishtwar window (Corfield and Seale, 2000; Wiesmayr and Grasemann, 2002), but only about 30% in the Spiti region north of the Kullu–Larji–Rampur window (Wiesmayr and Grasemann, 2002). The age of the Tethyan Himalayan thrust belt is determined to be 45–56 Ma by  $^{40}\text{Ar}/^{39}\text{Ar}$  dating of illites grown along cleavage domains (Wiesmayr and Grasemann, 2002) (Table 6). An interesting conclusion reached by Wiesmayr and Grasemann (2002) and Neumayer et al. (2004) is that the decollement of the Tethyan Himalayan thrust belt (i.e., the Sangla Detachment) can be projected onto the STD, implying that the latter may have been reactivated from an older thrust decollement. In Pakistan, Coward and Butler (1985) show that the amount of shortening between the MBT (Murree thrust) and the Nathia Gali thrust on the southeast side of the Hazara syntaxis (Fig. 2A and B) is about 150 km. Recent work by DiPietro and Pogue (2004) suggests that the total amount of shortening across the entire Himalayan orogen west of the Nanga Parbat and the Hazara syntaxes is on the order of ~200 km.

### 3.2.13. Lesser Himalayan thrust belt

Nowhere in the Himalaya is the research on the Lesser Himalayan thrust belt more influential than that from the Garhwal and Kumaun regions of NW India. Expanding on the classic stratigraphic work of Auden (1934, 1937) and structural work of Heim and

Gansser (1939), Valdiya (1978, 1979) was perhaps the first geologist to systematically analyze the complex interplay between stratigraphy of the LHS and thrust kinematics in the Lower Himalaya of NW India. His classic treatise (Valdiya, 1980) has laid the foundation for our current understanding of the Lower Himalayan geology (Table 4) and subsequent constructions of balanced cross-sections in the Kumaun and Nepal Himalaya (Srivastava and Mitra, 1994; DeCelles et al., 2001). Valdiya (1980) recognizes several younger-over-older faults in the Lesser Himalayan thrust belt, which he interprets as out-of-sequence thrusts. This structural complexity was not considered in otherwise an excellent structural reconstruction of the Kumaun Himalaya by Srivastava and Mitra (1994). Assuming only forward thrust propagation, Srivastava and Mitra (1994) obtain a total crustal shortening of ~161 km across the Lesser Himalayan thrust belt. Adding the displacement along the MCT, they further suggest that a total shortening of 687–754 km has occurred between the Himalayan foreland and the Indus–Tsangpo suture.

Because the width of the Lesser Himalayan thrust belt between the MCT and the MBT is only a few kilometers west of Mandi (Fig. 7), its detailed structural style and the magnitude of shortening are not very well constrained south of the Kishtwar window. However, the presence of a MCT klippe in Simla ~90 km south of the Kullu–Larji–Rampur window suggests that the Lesser Himalayan structures and stratigraphic units are mostly underthrust below the MCT south of the Kishtwar window. It is possible that the MCT is the roof fault of the Lesser Himalayan duplex system beneath the Kishtwar window as envisioned by Gapais et al. (1992).

### 3.2.14. MBT, MFT, and sub-Himalayan thrust belt

In northwestern India, the width of the sub-Himalayan belt between the MBT and MFT varies from 30 to 80 km, due to the presence of large reentrants of the MBT (Figs. 2A and 7) (Johnson, 1994; Fuchs and Linner, 1995; Powers et al., 1998). Based on the map pattern of the MBT and its duration of activity, Treloar et al. (1991), Meigs et al. (1995), and Burbank et al. (1996) suggest the MBT to have a slip magnitude of >100 km.

The Cenozoic foreland basin strata are highly deformed by thrusting and folding, making correlation of

Tertiary stratigraphic sections difficult from one thrust panel to the other (e.g., White et al., 2001). The total amount of shortening across the sub-Himalayan belt in NW India is ~23 km (Powers et al., 1998).

The MFT is well exposed in the western Himalaya due to a drier climate than the central and eastern Himalayan orogen (e.g., Thakur, 2004). The fault has an average slip rate of ~8–10 mm/yr over the past 1500 years (Kumar et al., 2001). Although with large uncertainties ( $\pm 3$ –7 mm/yr), it appears that the slip rate across the MFT in the western Himalaya is significantly lower than that in the central Himalaya of Nepal, which is ~21 mm/yr as determined by Lavé and Avouac (2000).

### 3.2.15. Neogene north-trending rifts

Two prominent NNW-trending rifts are present in the western Himalaya: the Pulan rift in SW Tibet (Fig. 1A) and the Tso Morari rift in NW India (Fig. 7), both are restricted to the Himalayan orogen. These rifts strike at an angle of about 30–40° from the N45°W trend of the western Himalayan orogen. The Pulan (also spelled as Purang) rift of Ratschbacher et al. (1994) is part of the Gurla Mandhata detachment system of Murphy et al. (2002). The Pulan–Gurla Mandhata extensional system is linked with the right-slip Karakorum fault and has accommodated ~35–60 km of east–west extension (Murphy et al., 2002). This extensional system was already in operation between 9 Ma and 6 Ma and remained active since (Murphy et al., 2002).

In comparison to the Pulan–Gurla Mandhata extensional system, we know relatively little about the age of motion and the magnitude of extension along faults bounding the Tso Morari rift. Existing geologic maps indicate that the NNW-trending Tso Morari rift system terminates at a northeast-dipping high-angle fault (the Ribil normal fault) along the Indus–Tsangpo suture zone (Fig. 7) (also see geologic maps of Steck et al., 1998 and Steck, 2003). Steck et al. (1998) interpret the Ribil fault as a normal fault. However, this interpretation would create kinematic incompatibility for normal faulting across both the Tso Morari rift and Ribil fault. As an alternative, I suggest that the Ribil fault is a branch of the right-slip Karakorum fault system and has served as a linking strike-slip structure to terminate east–west extension across the Tso Morari extensional system (Fig. 7).

### 3.3. Eastern Himalaya

Major Himalayan lithologic units can be traced continuously from the central Himalaya to the eastern Himalaya (Acharyya and Ray, 1977; Acharyya, 1980, 1994; Gansser, 1983; Burchfiel et al., 1992; Edwards et al., 1996, 1999; Edwards and Harrison,

1997; Wu et al., 1998; Grujic et al., 2002). An interesting aspect of the eastern Himalayan orogen is the preservation of several large STD klippen on top of the GHC (Gansser, 1983; Grujic et al., 2002) (Fig. 11). The southernmost trace of these klippen is located only ~1.5 km north of the trace of the MCT (Gansser, 1983) (Fig. 11).

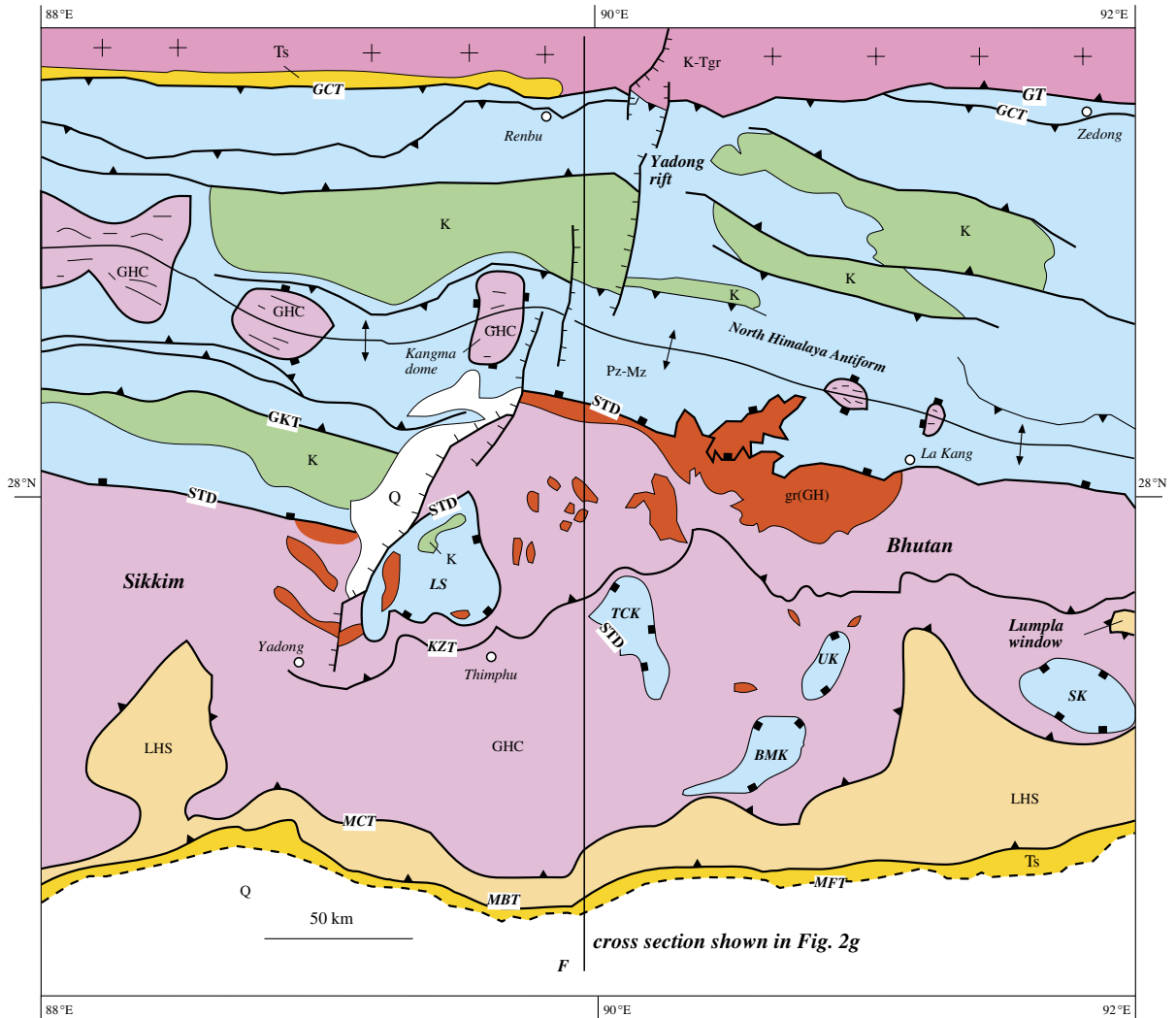
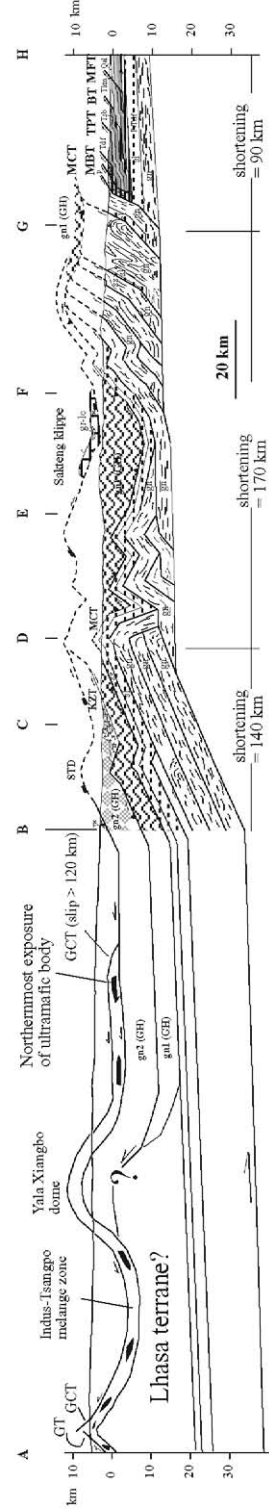
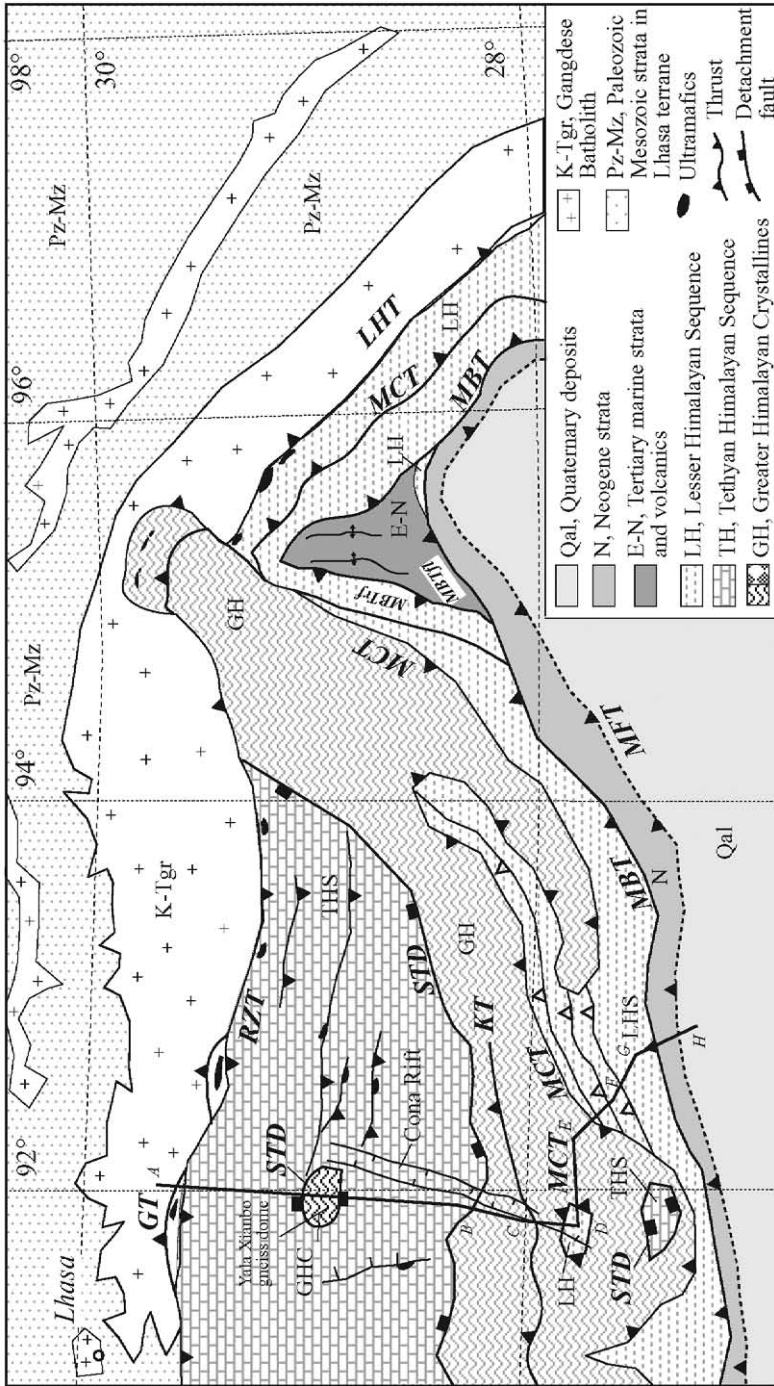


Fig. 11. Geologic map of southeastern Tibet and Bhutan. Sources from Gansser (1983), Liu (1988), Burchfiel et al. (1992), Yin et al. (1994, 1999), Edwards et al. (1996, 1999), Wu et al. (1998), and Grujic et al. (2002). GT, Gangdese thrust; GCT, Greater Counter thrust; GKT, Gyirong–Kangmar thrust; STD, South Tibet Detachment; MCT, Main Central Thrust; MBT, Main Boundary Thrust; BMK, Black Mountain klippe; TC, Tang Chu klippe; UK, Ura klippe; SK, Sakteng klippe; KZT, Kakhtang–Zimithang thrust; LS, Linshi klippe; gr(GH), Miocene leucogranites; GHC, GHC; K, Cretaceous strata; Pz-Mz, Paleozoic–Mesozoic Tethyan Himalayan Sequence; LHS, Lesser Himalayan Sequence. Ts, Tertiary Siwalik Group. Q, Quaternary deposits. Note that both the Black Mountains and Sakteng klippen are mapped within less than 1.5 km from the trace of the MCT. Geologic cross-section (F) is shown in Fig. 2.



1. LH + foreland shortening in the MCT footwall = ~ 400 km
  2. MCT > 130 km
  3. Zimithang thrust > 50 km
- Total shortening > 580 km

### 3.3.1. Main Central Thrust

The MCT can be traced from far eastern Nepal, through Sikkim, Bhutan, Indian State of Arunachal, and finally to the eastern Himalayan syntaxis (Gansser, 1964, 1983; Mohan et al., 1989; Singh and Chowdhary, 1990; Kumar, 1997; Ding et al., 2001; Gururajan and Choudhuri, 2003) (Figs. 2 and 8). In Sikkim, the MCT forms large reentrants and exposes the LHS in a series of south-facing half windows (Acharyya and Ray, 1977; Acharyya, 1980) (Fig. 2A). In Bhutan, the MCT is a broad shear zone extending several hundreds of meters downward into the LHS (Table 4) and >10 km upward into the GHC (Gansser, 1983). In contrast, the MCT is a sharp contact in Arunachal farther to the east, placing kyanite and garnet schist over phyllite, quartzarenite, and metavolcanic rocks and is broadly folded (Singh and Chowdhary, 1990; Yin et al., submitted for publication) (Fig. 12). On both sides of the eastern syntaxis, the MCT juxtaposes staurolite-kyanite schist and gneiss of the GHC over quartzite, phyllite, carbonate, and metavolcanics of the LHS (Singh and Chowdhary, 1990; Gururajan and Choudhuri, 2003). This is in contrast to the MCT in the western Himalayan syntaxis where the fault juxtaposes low-grade Proterozoic phyllite of the THS over low-grade to essentially unmetamorphosed Proterozoic–Cambrian strata of the LHS (Pogue et al., 1999) (Table 3). This difference suggests that the MCT hanging wall in the eastern Himalayan syntaxis has been exhumed much more deeply than that in the western Himalaya.

Grujic et al. (1996) show that in Bhutan a top-south shear fabric with a significant pure-shear component exists across the entire GHC. The top-south shear fabric was later overprinted by top-north shear in the top part of the GHC immediately below the STD (Grujic et al., 2002). The GHC consisting of metasediments and extensive Miocene leucogranite intrusions experienced rapid decompression from a lower crustal condition (~11–13 kbar) to a middle

crustal condition (~5 kbar) under high temperatures (Swapp and Hollister, 1991; Davidson et al., 1997) (Table 6). Petrologic analysis indicates that the peak pressure remains constant across the MCT zone at about 11–13 kbar while the peak temperature decreases across the shear zone, from ~660 °C at the base to 780 °C at the top of the shear zone (Daniel et al., 2003). This observation indicates that the isograds cannot be overturned by isoclinal folds because pressure profile is not inverted. Similar observations were also made across the MCT zone in the Kullu–Larji–Rampur window area by Vannay et al. (1999) and Vannay and Grasemann (2001) and were used as evidence to support the general shear model. But this observation is also consistent with the hot-iron model of LeFort (1975).

### 3.3.2. Slip on MCT

Using the thrust reentrants in Sikkim and Bhutan (Gansser, 1983; Grujic et al., 2002) (Fig. 11), the MCT has a minimum slip of 75 km. In Arunachal, Yin et al. (submitted for publication) show that slip on the MCT may exceed 195 km.

### 3.3.3. Age of MCT

In Sikkim, petrological analysis has established that rocks ~1 km above the MCT experienced an early phase of prograde metamorphism under a pressure condition of 10–12 kbar followed by decompression to reach a condition of 8 kbar and 750 °C (Harris et al., 2004). Sm–Nd growth ages of garnet cores and rims indicate pre-decompression garnet growth at  $23 \pm 3$  Ma and near-peak temperatures at  $16 \pm 2$  Ma (Harris et al., 2004). These ages suggest that the MCT was active at ~23 Ma during prograde metamorphism.

The MCT in Bhutan cuts 16-Ma-old leucogranite, whereas the north-dipping Kakhtang thrust in the MCT hanging wall cuts a leucogranite of 14–15 Ma (Grujic et al., 2002). Based on this age relationship, Grujic et al. (2002) infer that the Kakhtang thrust is

Fig. 12. Tectonic map of the eastern Himalaya. Imbricate thrusts in Lesser Himalaya based on Yin et al. (submitted for publication), STD klippe from Grujic et al. (2002), eastern syntaxis geology from Ding et al. (2001), and the MCT trace from Singh and Chowdhary, 1990. Geology of southeast Tibet from Yin and Harrison (2000). Cross-section is modified from Yin et al. (submitted for publication). Symbols in the geologic cross-sections represent the following: gn and gn (LH), Lesser Himalayan orthogneiss; gn1 (GH), gneiss unit in the lower part of the MCT hanging wall; gn2 (GH), gneiss unit dominantly orthogneiss in the upper part of the MCT hanging wall; TH, Tethyan Himalayan strata; sl, ss, and sl (LH), shale and quartzarenite units in Lesser Himalayan Sequence; P, Permian strata; Tsb, Tkm, and Tdf are Tertiary units; Qal, Quaternary deposits; STD, South Tibet Detachment fault; ZT, Zimithang thrust; MCT, Main Central Thrust; MBT, Main Boundary Thrust; TPT, Tipi thrust; BT, Bhalukpung thrust MFT, Main Frontal Thrust.

younger than the STD and its motion reactivated the MCT. However, the lack of direct crosscutting relationship between the Kakhtang thrust and the STD casts considerable doubts on this interpretation. In fact, it is possible that the Kakhtang thrust was coeval with or even older than motion on the STD.

U–Pb dating of monazite and xenotime indicates that the MCT in Bhutan was already active at 22 Ma and continued its motion during and after ~14 Ma (Daniel et al., 2003). Similar Th–Pb monazite ages between 22 and 14 Ma were also obtained for the MCT zone in Sikkim (Catlos et al., 2002b). In the Arunachal Himalaya, Yin et al. (submitted for publication) show that the MCT was active at and after ~10 Ma based on ion-microprobe dating of monazite inclusions in garnets from the MCT zone.

#### 3.3.4. South Tibet Detachment

The STD directly east of the Yadong Cross Structure at the longitude of 89°–90°E in southeastern Tibet juxtaposes Ordovician and Carboniferous strata over the GHC (Burchfiel et al., 1992) (Fig. 2A). In Bhutan, the STD lies below the Upper Proterozoic Chekha Formation (Grujic et al., 2002) (Table 7), which is composed of garnet-staurolite schist at its base and phyllite at the top with a rapid upward decrease in metamorphic grade. The Chekha Formation is overlain by latest Proterozoic–Cambrian strata (Bhargava, 1995); their ages were determined by trace fossils and trilobites (Bhargava, 1995; Hughes et al., 2002). The different stratigraphic positions for the STD in southern Tibet (Ordovician strata over GHC, Burchfiel et al., 1992) and in southern Bhutan (late Proterozoic strata over GHC) indicate that the STD slightly cuts down section southward. This observation is at odds with the typical geometry of an extensional detachment fault but can be explained by superposing a younger extensional event over an older contractional event, such as the case documented in southeastern Tibet along the STD (Burchfiel et al., 1992).

The STD has been traced to the western limb of the Namche Barwa syntaxis where the fault changes its east–west strike along the Bhutan–China and India–China border to a north–south strike and dips to the west (Wang et al., 2001; Ding et al., 2001). The change in the STD strike may result from warping of the eastern syntaxis. On the east side of

the syntaxis, geologic investigation along the Lohit Valley across the eastern limb of the Namche Barwa syntaxis indicates the absence of both the STD and THS (Gururajan and Choudhuri, 2003). Along the Lohit Valley, the GHC is bounded by the MCT below and the Lohit thrust above. The Lohit thrust juxtaposes the GHC directly below the Indus–Tsangpo suture and Cretaceous–Tertiary plutons equivalent to the Gangdese batholith in southern Tibet (Gururajan and Choudhuri, 2003). The above observation reinforces the notion that the eastern Himalaya is more deeply exhumed than that in the western Himalaya.

#### 3.3.5. Slip on STD

The presence of large STD klippen in Bhutan is similar to the Mt. Everest region (Burchfiel et al., 1992). However, a key difference in Bhutan is that the STD klippen extend >100 km southward towards the trace of the MCT from its northernmost exposure. Using a similar argument made by Burchfiel et al. (1992), one would conclude that the STD has a minimum slip of >100 km in Bhutan. However, this method of slip estimate requires that the STD cut upsection southward and that the hanging-wall cutoff can be matched by a footwall cutoff. Projecting the STD klippen onto a north–south cross-section suggests that the STD is approximately a hanging-wall flat extending for ~100 km in its transport direction (Figs. 2G and 11). Given the proximity of the STD and MCT traces (<1.5 km), there is simply not enough space for the existence of a footwall ramp that could match a possible hanging-wall cutoff across the THS, which is about 7–15 km thick in southern Tibet (Brookfield, 1993; Liu and Einsele, 1994) (Fig. 3). This problem prevents us from making accurate estimates of slip on the STD.

#### 3.3.6. Age of STD

The age of the STD along the Tibet–Bhutan border is determined to be active after 12 Ma (Edwards and Harrison, 1997). As the STD in the area is also cut by the Yadong rift that initiated at ~8 Ma (Harrison et al., 1995) (Fig. 11), the fault must have ceased motion before this time. Wu et al. (1998) also report a U–Pb monazite age of ~12 Ma from a sheared granite below the STD that constrain the STD to have been active after this time.

### 3.3.7. Tethyan Himalayan fold and thrust belt

The Tethyan Himalayan fold and thrust belt in the eastern Himalaya is drastically different from that in the central and western Himalaya in that (1) the contractional structures are dominated by isoclinal folds and slaty cleavage (Yin et al., 1994, 1999) and (2) widespread ultramafic bodies are present in thrust zones (Pan et al., 2004) (Fig. 2A). Isoclinal folds in the northern belt dominate and have transposed the original bedding of mostly Triassic flysch strata into regional slaty cleavage (Yin et al., 1999). In the south, contractional structures are dominated by tight folds and brittle thrusts involving Jurassic and Cretaceous strata (Liu, 1988; Xizang BGMR, 1993; Pan et al., 2004). Although small ultramafic blocks could be parts of an ophiolite complex that was obducted onto the northern Indian margin during or prior to the Indo-Asian collision (e.g., the Spongtang ophiolite in the Ladakh Himalaya, see Reuber, 1986), their occurrence along thrust zones suggests that they were structurally below the GCT and have been brought up later by thrusting. This interpretation would imply that the GCT has moved >120 km over the Indus–Tsangpo accretionary complex in the eastern Himalaya (Fig. 12).

### 3.3.8. Lesser Himalayan thrust belt

This belt is located in southern Bhutan and the Arunachal region of NE India (Fig. 2A). Over the past decades, major efforts have been devoted to delineating lithostratigraphic units of the region (Thakur and Jain, 1974; Jain et al., 1974; Verma and Tandon, 1976; Singh and Chowdhary, 1990; Acharyya, 1994; Kumar, 1997). However, timing, magnitude of deformation and the kinematic evolution of the Cenozoic thrust systems in the region are quite poorly constrained. Recent studies in the Arunachal Himalaya by Yin et al. (submitted for publication) show that the MCT and its footwall structures have accommodated >585 km of crustal shortening (Fig. 12). This estimate is greater than shortening of ~240–500 km accommodated by the equivalent structures in Nepal (Schelling and Arita, 1991; DeCelles et al., 2001). When considering that the GCT may have slipped >120 km, the total amount of shortening across the eastern Himalayan orogen is >700 km.

### 3.3.9. MBT and MFT

The most striking relationship in the eastern Himalaya is that the traces of the MCT, MBT, and MFT are much closer together than those in the central and western Himalaya (Fig. 2A). The cause of this field relationship is not clear, but could be a reflection of an eastward increase in the total magnitude of shortening along the Himalayan strike. The MBT in Sikkim and Arunachal is folded together with the overlying MCT (Acharyya and Ray, 1977; Acharyya, 1980). This is in contrast to the MBT in Nepal and NW India that has been shown to have a simple planar or flat-ramp geometry (Schelling and Arita, 1991; Fuchs and Linner, 1995; DeCelles et al., 2001). Folding of both the MCT and MBT in the eastern Himalaya indicates a major change in structural style and may have resulted from duplex development between the MBT above and the MFT below. This would imply that the amount of shortening in the MBT footwall is greater in the eastern Himalaya than in the central Himalaya. Little is known about the development of the Main Frontal Thrust in the eastern Himalaya.

### 3.3.10. Neogene north-trending rifts

Several Neogene north-trending rifts are present in the eastern Himalaya (Fig. 1A). These rifts are nearly perpendicular to the trend of the eastern Himalayan orogen in the west but at an angle of about 60–70° in the east towards the eastern Himalayan syntaxis. The best-studied rift in the eastern Himalaya is the Yadong rift north of Sikkim. This rift is the southernmost extension of the 400-km long Yadong–Guru rift extending from the Himalayan orogen to the interior of the Tibetan plateau (Armijo et al., 1986, 1989; Burchfiel et al., 1991). The central segment of the rift system initiated at ~8 Ma as constrained by  $^{40}\text{Ar}/^{39}\text{Ar}$  thermochronology and has accommodated >20 km of east–west extension (Harrison et al., 1995). The southern extension of the Cona rift cuts the MCT (Yin et al., submitted for publication) (Fig. 12).

## 3.4. Great Counter Thrust and North Himalayan Antiform

### 3.4.1. Great counter thrust (GCT)

Heim and Gansser (1939) first recognized and named the south-dipping Great Counter Thrust



### 3.4.2. North Himalayan antiform (NHA)

The NHA is a prominent east-trending structural high associated with gneiss domes lying between the Great Counter Thrust in the north and the STD in the south (Hauck et al., 1998). The antiform was mainly developed in the middle Miocene (e.g., Maluski et al., 1988; Lee et al., 2000) and its deformation has been superposed on the older Eocene–Oligocene Tethyan Himalayan fold belt (Fig. 2A). In contrast to the Cordilleran-type extensional metamorphic core complexes (e.g., Spencer, 1984; Lister and Davis, 1989; Wernicke, 1992; Friedmann and Burbank, 1995), the North Himalayan gneiss domes are lacking hanging wall extensional faults, supradetachment basins, and breakaway systems (i.e., footwall cutoffs) (see discussion by Yin, 2004).

Among gneiss domes, the Kangmar, Tso Morari and Gurla Mandhata metamorphic complexes have been studied the most (Figs. 2 and 7). These gneiss terranes expose Indian continental rocks and are in fault contact with the overlying THS (e.g., Steck et al., 1998). The Kangmar dome records peak metamorphic conditions of  $P=6–9$  kbar and  $T=500–650$  °C (Burg et al., 1984a, 1987; Chen et al., 1990; Lee et al., 2000). The isograds in the domes are vertically condensed, suggesting large-magnitude pure-shear extension (Lee et al., 2000). The Kangmar gneiss dome is capped either by a top-north detachment or a ductile shear zone with coeval top-north and top-south shear on the north and south limbs of the dome (Chen et al., 1990; Lee et al., 2000). Carboniferous and Permian strata in turn drape over the shear zone and the gneiss (Burg et al., 1984b, 1987; Chen et al., 1990; Lee et al., 2000). It is not clear whether the upper Proterozoic to Devonian strata, which are commonly exposed in the southern THS zone immediately above the STD (e.g., Liu and Einsele, 1994), are cut out by an extensional fault capping the gneiss dome or were never deposited.

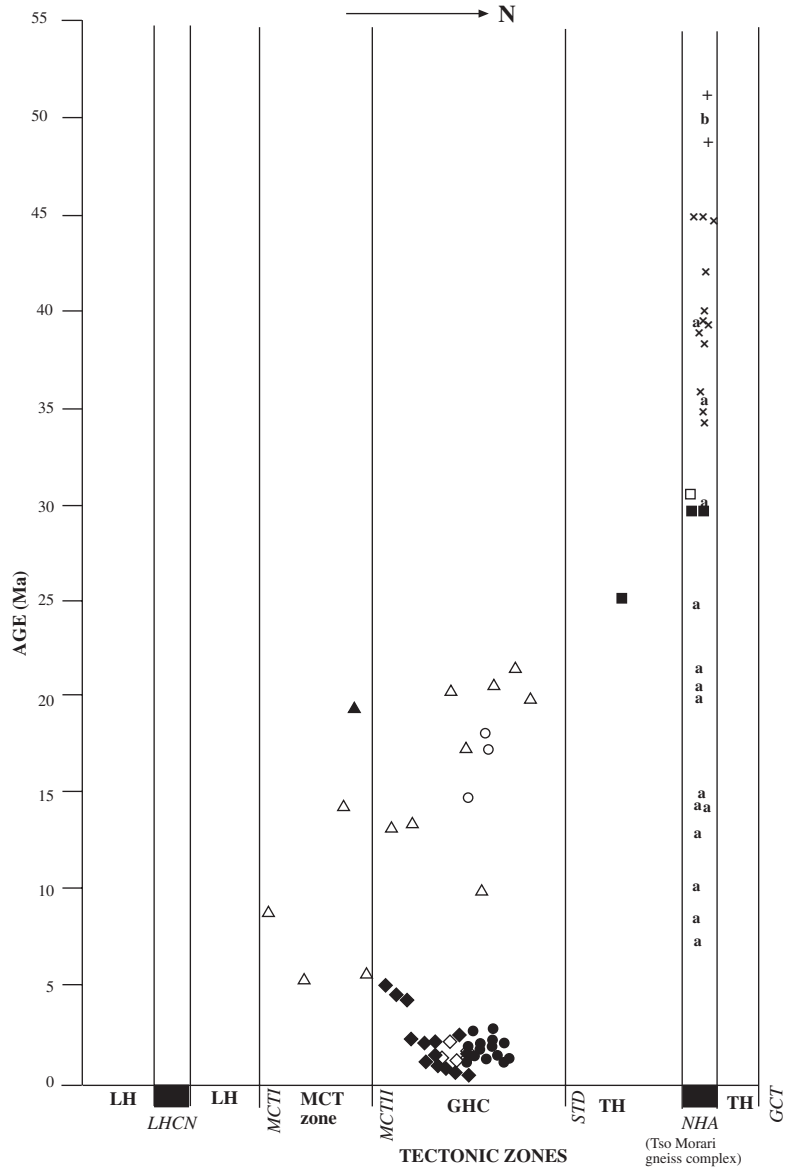
The Tso Morari gneiss complex in NW India (Figs. 2 and 7) experienced Eocene UHP metamorphism and exhumation, but contractional deformation at greenschist-facies conditions lasted until early Miocene time (de Sigoyer et al., 2000). The northern margin of the Tso Morari gneiss terrane has been affected by extensional faulting since the late Miocene (Steck et al., 1998; Schlup et al., 2003), but the structural setting and kinematic history of the Tso Morari UHP gneiss terrane remain poorly understood.

In the Gurla Mandhata area of southwest Tibet (Fig. 2), metamorphic rocks below the top-west Gurla Mandhata detachment fault and the underlying ductile shear zone contain deformed and undeformed Miocene leucogranites with Th–Pb monazite ages clustered at 24–17 Ma and 11–7 Ma (Murphy et al., 2002). Th–Pb dating of monazite inclusions in garnets suggests that prograde metamorphism due to crustal thickening occurred between 16 and 10 Ma prior to motion along the Gurla Mandhata detachment fault (Murphy et al., 2002). These monazite ages in conjunction with muscovite cooling ages of 10–6 Ma indicate that detachment faulting and east–west extension in southwest Tibet did not begin until after ~10 Ma (Murphy et al., 2002). The middle Miocene crustal thickening event between 16 and 10 Ma in the Gurla Mandhata region is broadly coeval with inferred thrusting below the Kangmar dome (Lee et al., 2000), supporting a regional extent of the NHA over a distance of >700 km along strike (Hauck et al., 1998).

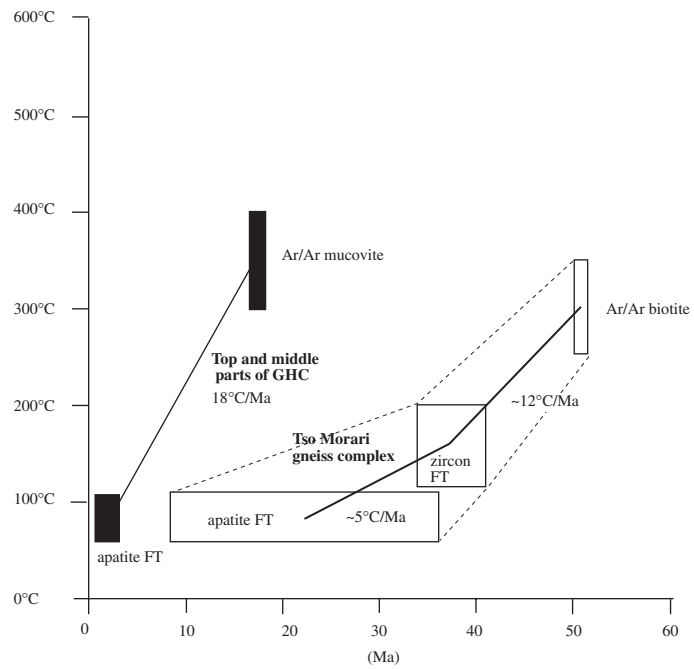
## 4. Exhumation and foreland sedimentation in the Himalayan Tectonic System

A complete understanding of the evolution of the Himalayan orogen requires the knowledge of its exhumation history and exhumation mechanisms (that is, whether the Himalayan rocks were removed vertically by erosion, faulting, or a combination of both). This information may be obtained from (1) the cooling history of the mountain range ( $T-t$  paths) as determined by  $^{40}\text{Ar}/^{39}\text{Ar}$  and fission track thermochronometry, (2) the timing and conditions of metamorphism ( $P-T-t$  paths) as determined by a combination of geochronology and thermobarometry, and (3) sedimentary history of the Himalayan foreland basin. The presence of excess argon in GHC biotite has been notorious (e.g., Maluski et al., 1988; Macfarlane, 1993; Stüwe and Foster, 2001). This is indicated by the biotite commonly having  $^{40}\text{Ar}/^{39}\text{Ar}$  ages older than muscovite from the same samples despite the fact that biotite has a lower closure temperature (McDougall and Harrison, 1999). In the following synthesis  $^{40}\text{Ar}/^{39}\text{Ar}$  biotite ages older than muscovite ages from the same samples or from nearby locations are excluded.

### Cooling History of the Garhwal Himalaya and Ladakh Region



- ●  $^{40}\text{Ar}/^{39}\text{Ar}$  muscovite age (open) and apatite fission-track age (solid) from Sorkhabi et al. (1997, 1999)
- △ K-Ar muscovite age from Metcalfe (1993)
- ▲  $^{40}\text{Ar}/^{39}\text{Ar}$  hornblende age from Metcalfe (1993)
- □  $^{40}\text{Ar}/^{39}\text{Ar}$  biotite (solid) and muscovite (open) ages dating greenschist-facies metamorphism from de Sigoyer et al. (2000)
- b  $^{40}\text{Ar}/^{39}\text{Ar}$  biotite age from Schlup et al. (2003)
- +  $^{40}\text{Ar}/^{39}\text{Ar}$  phengite age from de Sigoyer et al. (2000) and Schlup et al. (2003)
- x Zircon fission track age from Schlup et al. (2003)
- a Apatite fission track age from Schlup et al. (2003)
- ◆ ◇ Apatite and zircon fission track age from Jain et al. (2000)



#### 4.1. Western Himalaya

##### 4.1.1. Exhumation of the Northern region

In the northern region of the western Himalayan, orogen, eclogite-bearing UHP gneisses have been discovered in upper Kaghan valley of northern Pakistan and the Tso Morari area of NW India (Pognante and Spencer, 1991; Guillot et al., 1997; Fontan et al., 2000; Lombardo et al., 2000; de Sigoyer et al., 2000; O'Brien et al., 2001; Kohn and Parkinson, 2002; Mukherjee et al., 2003; Treloar et al., 2003). These rocks typically occur below the north-dipping Main Mantle Thrust/Indus–Tsangpo suture (Steck et al., 1998; de Sigoyer et al., 2000), with the protolith belonging to Indian Precambrian basement in Tso Morari (Kohn and Parkinson, 2002) and Indian basement cover sequence in northern Pakistan (e.g., Treloar et al., 2003; DiPietro and Pogue, 2004).

The UHP terrane in the upper Kaghan valley is juxtaposed by the north-dipping Batal thrust in the south over low-grade metamorphic rocks (Fig. 2A). In the north the UHP terrane of northern Pakistan is bounded by the Main Mantle Thrust (= the Indus–Tsangpo suture) that may have experienced Miocene top-north normal slip (Treloar et al., 2003; cf. DiPietro and Pogue, 2004). Lombardo and Rolfo (2000) note that eclogites in the Pakistan Himalaya record peak metamorphic temperatures of 580–600 °C and pressures >23–24 kbar, followed by isothermal decompression to epidote-amphibolite conditions. The peak UHP metamorphism in northern Pakistan (i.e., the upper Kaghan valley) occurred at ~47–46 Ma (Smith et al., 1994; Foster et al., 2002), while exhumation of UHP rocks to greenschist-facies conditions was accomplished rapidly between 46 and 40 Ma (Tonarini et al., 1993; Treloar et al., 2003). Assuming that the greenschist-facies metamorphism occurred at a pressure condition of ~4 kbar, an average crustal density of 2.85 g/cm<sup>3</sup>, and the duration of exhumation of the UHP rocks between 1 and 6 m.y., the exhumation rate for the Kaghan valley UHP terrane is about 40 ± 30 mm/yr (Table 8). The exhumation rate after 40–46 Ma must be exceedingly slow in the Kaghan valley area, averaging about 0.33 ± 0.2 mm/yr.

In the Tso Morari area of NW India, the UHP metamorphism is dated at ~55 Ma and exhumation of the eclogite to the middle crust was finished by ~47 Ma (de Sigoyer et al., 2000; also see Leech et al., 2005) (Fig. 13). By ~28–30 Ma, the northwestern part of the Tso Morari eclogite terrane reached the upper crust based on <sup>40</sup>Ar/<sup>39</sup>Ar muscovite and biotite ages that record greenschist-facies metamorphism (de Sigoyer et al., 2000). However, in the central part of the Tso Morari gneiss terrane eclogite blocks and their host metamorphic rocks of the Indian continental basement were exhumed rapidly to upper crust by 44–38 Ma, as indicated by zircon and apatite fission track ages (Schlup et al., 2003). <sup>40</sup>Ar/<sup>39</sup>Ar phengite and biotite ages of 54–51 Ma from the Tso Morari gneiss terrane suggest that eclogite and its host gneiss had cooled below 400–300 °C by the early Eocene (de Sigoyer et al., 2000; Schlup et al., 2003). Assuming a constant geothermal gradient of 30 °C/km, a depth of >75 km for UHP metamorphism because of the presence of coesite in the Tso Morari gneiss terrane (Kohn and Parkinson, 2002; Mukherjee et al., 2003), a duration of 1–4 m.y. for UHP rocks to exhume from its maximum depth to middle crust, the vertical exhumation rate is about 40 ± 20 mm/yr (Table 8). Combining the <sup>40</sup>Ar/<sup>39</sup>Ar biotite age data with the zircon and apatite fission track age data further suggests that the Tso Morari terrane between 54–51 Ma and 44–38 Ma was exhumed at a rate of ~1.1 ± 0.4 mm/yr (Table 8). The average erosion rate after 44–38 Ma over the Tso Morari region is very low as most of the rocks already passed the closure temperatures of 120 to 65 °C for zircon and apatite in the fission track thermochronometry. This would yield a cooling rate of 1.4–3.2 °C/m.y. and an exhumation rate of 0.05–0.11 mm/yr. Because the Tso Morari terrane was exposed to the surface at 44–38 Ma, the region could have been a significant source of high-grade metamorphic minerals for the Himalayan foreland basin. We will return to this point when we discuss Himalayan foreland sedimentation.

The exhumation mechanism for the Kaghan valley and Tso Morari UHP rocks remains unclear. Although normal faulting along the Indus–Tsangpo suture zone

Fig. 13. Cooling history of the Garhwal and Ladakh Himalaya. LH, Lesser Himalayan zone; LHCN, Lesser Himalayan Crystalline Nappe; MCTI, the lower MCT fault; MCTII, the upper MCT fault; GHC, Greater Himalayan Crystalline Complex; STD, South Tibet Detachment; TH, Tethyan Himalayan zone; NHA, North Himalayan Antiform; GCT, Great Counter Thrust.

may be the cause for its rapid rise, the geologic evidence for this process remains sparse (Treloar et al., 2003; cf., DiPietro and Pogue, 2004). Although erosion could be an important alternative mechanism for exhuming the Himalayan UHP rocks, as has been documented elsewhere such as the Dabie Shan UHP terrane of east-central China (e.g., Nie et al., 1994), the highly localized nature of the UHP terrane appears to favor normal faulting as the main mechanism of its exhumation.

#### 4.1.2. Exhumation of the Greater Himalayan Crystallines

Three main phases of metamorphism in the GHC have been documented by many Himalayan studies (e.g., Brunel and Kienast, 1986; Searle et al., 1989; Hodges and Silverber, 1988) (Table 6). The early phase, commonly termed the Eohimalayan event, records prograde metamorphism and is considered to have occurred in the middle Eocene to Oligocene (45–25 Ma) under  $P$ – $T$  conditions of 8–11 kbar and 600–700 °C (Searle et al., 1992; Hodges et al., 1994; Vannay and Hodges, 1996; Godin et al., 1999a; Simpson et al., 2000; Foster et al., 2000). In contrast, the second phase, commonly termed the Neohimalayan event, records retrograde metamorphism and occurred mainly in the early and middle Miocene (22–14 Ma) under  $P$ – $T$  conditions of 6–8 kbar and 500–750 °C (e.g., Searle et al., 1992; J.D. Walker et al., 1999; Hodges, 2000; Godin et al., 2001). The second phase of metamorphism has been commonly associated with early Miocene development of the MCT and STD (LeFort, 1996; Hodges, 2000). However, one should keep in mind that the initiation ages of the MCT and STD remain unknown. In addition, reactivation of the MCT zone during 7–2 Ma associated with both tectonic burial (prograde metamorphism) and rapid erosion (retrograde metamorphism) cannot be tied with the simple temporal scheme outlined above (Harrison et al., 1997a; Catlos et al., 2001).

In the western syntaxis along the eastern margin of the Nanga Parbat metamorphic massif, U–Pb dating of monazites and Sm–Nd garnet-whole rock isochrons indicate that the region had experienced prograde metamorphism between 46 and 36 Ma (Foster et al., 2000, 2002). The region has a long Cenozoic exhumation history starting before 40 Ma (Cerveny et al., 1988, 1989a,b; also see recent

summary by Zeitler et al., 2001). The  $^{40}\text{Ar}/^{39}\text{Ar}$  biotite ages decrease systematically from >40 Ma around the margin to 5–0 Ma in the core of the syntaxis, indicating differential exhumation, heat advection, or a combination of both during the development of the Nanga Parbat syntaxis (Zeitler et al., 2001). That is, the average cooling rate in the core of the syntaxis is 100–300 °C/m.y., while the rate along the margin is <10 °C/m.y. Assuming 350 °C as the closure temperature of biotite, duration of exhumation between 1 and 5 m.y., and a constant thermal gradient of 30 °C/km, the exhumation rate in the core of the syntaxis is  $7.0 \pm 4.5$  mm/yr (Table 8). Although the western Himalayan syntaxis may have experienced rapid exhumation in its core since latest Miocene time as implied by cooling rates of up to 300 °C/m.y. (Zeitler, 1985; Treloar et al., 1989; Smith et al., 1992; George et al., 1995; Winslow et al., 1995, 1996; Schneider et al., 1999a), the average cooling rates in the early and middle Miocene are much slower, at a rate of ~20 °C/m.y. (Zeitler et al., 1989; Treloar et al., 2000). This translates to an exhumation rate of 0.67 mm/yr assuming a constant geothermal gradient of 30 °C/km (Table 8). If we use the  $^{40}\text{Ar}/^{39}\text{Ar}$  biotite cooling ages 50–40 Ma around the edge of the Nanga Parbat syntaxis as a proxy for its early cooling and erosional history, we obtain an exhumation rate of  $0.30 \pm 0.20$  mm/yr around the rim of the western Himalayan syntaxis.

Farther to the east in Zaskar from the western Himalayan syntaxis, the early phase of prograde metamorphism was determined to range from 30 Ma to 25 Ma by a combination of  $^{40}\text{Ar}/^{39}\text{Ar}$  thermochronology (Searle et al., 1992) and Sm–Nd dating of garnets (Vance and Harris, 1999). In the Garhwal Himalaya, the top portion of the GHC immediately above the Jhala thrust experienced prograde metamorphism between 44 and 36 Ma, whereas within the MCT zone and at the base of the GHC prograde metamorphism occurred between 44 and 25 Ma as determined by U–Pb dating of monazite inclusions in garnets (Foster et al., 2000).

The GHC and MCT zone in the Garhwal Himalaya cooled below 350 °C between 21 and 5 Ma, with muscovite K–Ar cooling ages becoming younger from the top part of the GHC to the base of the MCT zone (Metcalf, 1993) (Fig. 13). When considering the

apatite fission track cooling ages (Sorkhabi et al., 1996, 1999; Jain et al., 2000), the cooling rate in the middle and upper parts of the GHC in the Garhwal Himalaya is  $\sim 18 \pm 4$  °C/m.y. (Fig. 13), which implies a denudation rate of  $\sim 0.67 \pm 0.13$  mm/yr assuming a constant thermal gradient of 30 °/km during 21–5 Ma (Table 8). This is probably an upper bound for the estimated exhumation rate because coeval erosion would increase the thermal gradient (e.g., Harrison et al., 1998b). The apatite and zircon fission track data also suggest that the middle part of the GHC in Garhwal did not reach the surface until after 3–1 Ma (Fig. 13).

The Oligocene–Pliocene exhumation history (29–4 Ma) of the Zaskar region is recorded by  $^{40}\text{Ar}/^{39}\text{Ar}$  and fission track cooling ages (Fig. 14). The top and base of the GHC cooled at a rate of  $\sim 16 \pm 4$  °C/m.y. For a geothermal gradient of 30 °C/km, these cooling rates translate to denudation rates of  $0.53 \pm 0.13$  mm/yr. From the apatite fission track data (Kumar et al., 1995) (Fig. 14), the top of the GHC immediately below the Zaskar shear zone did not reach near-surface levels until 9–4 Ma. The fission track data from the Zaskar region also suggest that:

- (1) its cooling rate increases from  $\sim 16 \pm 4$  °C/m.y. to  $\sim 32 \pm 2$  °C/m.y. during 2–4 Ma;
- (2) the Zaskar shear zone was inactive at and after  $\sim 9$  Ma; and
- (3) folding of the MCT did not start until after 6 Ma as indicated by the spatial distribution of the younger cooling ages of 6 to 2 Ma towards the center of the Kishtwar window (Fig. 14).

The higher cooling rate implies a higher exhumation rate of  $1.10 \pm 0.06$  mm/yr. No data are available in the Zaskar region for constraining exhumation rates prior to 30 Ma.

#### 4.1.3. Exhumation of the Tethyan Himalayan Sequence

Zircon and apatite fission track cooling ages were obtained by Lal et al. (1999) from the early Paleozoic Mandi granite that intrudes the Proterozoic–Middle Cambrian Haimanta Group in the basal THS (Fig. 7) (e.g., Jager et al., 1971; Mehta, 1977; Miller et al., 2001). This granite is located immediately above the MCT and records a cooling

rate of  $10 \pm 3$  °C/m.y. between 11–8 Ma and 5–2 Ma (Fig. 14). This cooling rate is considerably lower than the average cooling rate of the GHC in the Zaskar and Garhwal Himalaya to the north and east. It translates to an exhumation rate of  $3.3 \pm 0.1$  mm/yr assuming a constant geothermal gradient at 30 °C/km between 11 and 2 Ma.

#### 4.1.4. Sedimentation in Himalayan foreland basin

A key question in Himalayan tectonics is when the GHC was first exposed at the surface and started shedding high-grade metamorphic clasts into the foreland basin. Systematic investigation of Cenozoic Himalayan foreland basin strata has been hampered by poor age control on Neogene Himalayan non-marine deposits (e.g., Burbank et al., 1996; Najman et al., 1997; DeCelles et al., 1998a,b; Raiverman, 2000). An exceptional case can be made in the Pakistan Himalaya where foreland basin strata contain abundant vertebrate fossils and well-dated tuff beds (e.g., Burbank et al., 1996).

In NW India, Cenozoic Himalayan strata consist of the upper Paleocene–middle Eocene Subathu Formation of marine sedimentary rocks overlain unconformably by non-marine deposits of the Dagshai Formation and the Lower Dharmasala Group. These units are located in separate thrust sheets in the MBT footwall (Najman et al., 1993, 1997; Powers et al., 1998; White et al., 2002) (Table 5). The Lower Dharmasala Group was considered to be either of early Miocene age based on the presence of microflora fossils (Dogra et al., 1985) or of Oligocene–early Miocene age based on fish fossils (Tiwari et al., 1991).  $^{40}\text{Ar}/^{39}\text{Ar}$  ages of detrital muscovite from the Dagshai Formation and the base of the Lower Dharmasala Group suggest deposition younger than  $\sim 22$  Ma (Najman et al., 1997; White et al., 2002). Overlying the Dagshai Formation and the Lower Dharmasala Group are the Kasauli Formation and the Upper Dharmasala Group.  $^{40}\text{Ar}/^{39}\text{Ar}$  ages of detrital muscovite indicate that the Kasauli Formation is younger than  $\sim 22$  Ma while the base of the Upper Dharmasala Group is younger than 16 Ma (Najman et al., 1997; White et al., 2002). The upper part of the Upper Dharmasala Group contains late Miocene rodents of the Middle Siwalik affinity (Tiwari et al., 1991), while its detrital muscovite  $^{40}\text{Ar}/^{39}\text{Ar}$  ages suggests deposition younger than  $\sim 26$ –22 Ma (White et al., 2002). White et al. (2001) propose that the

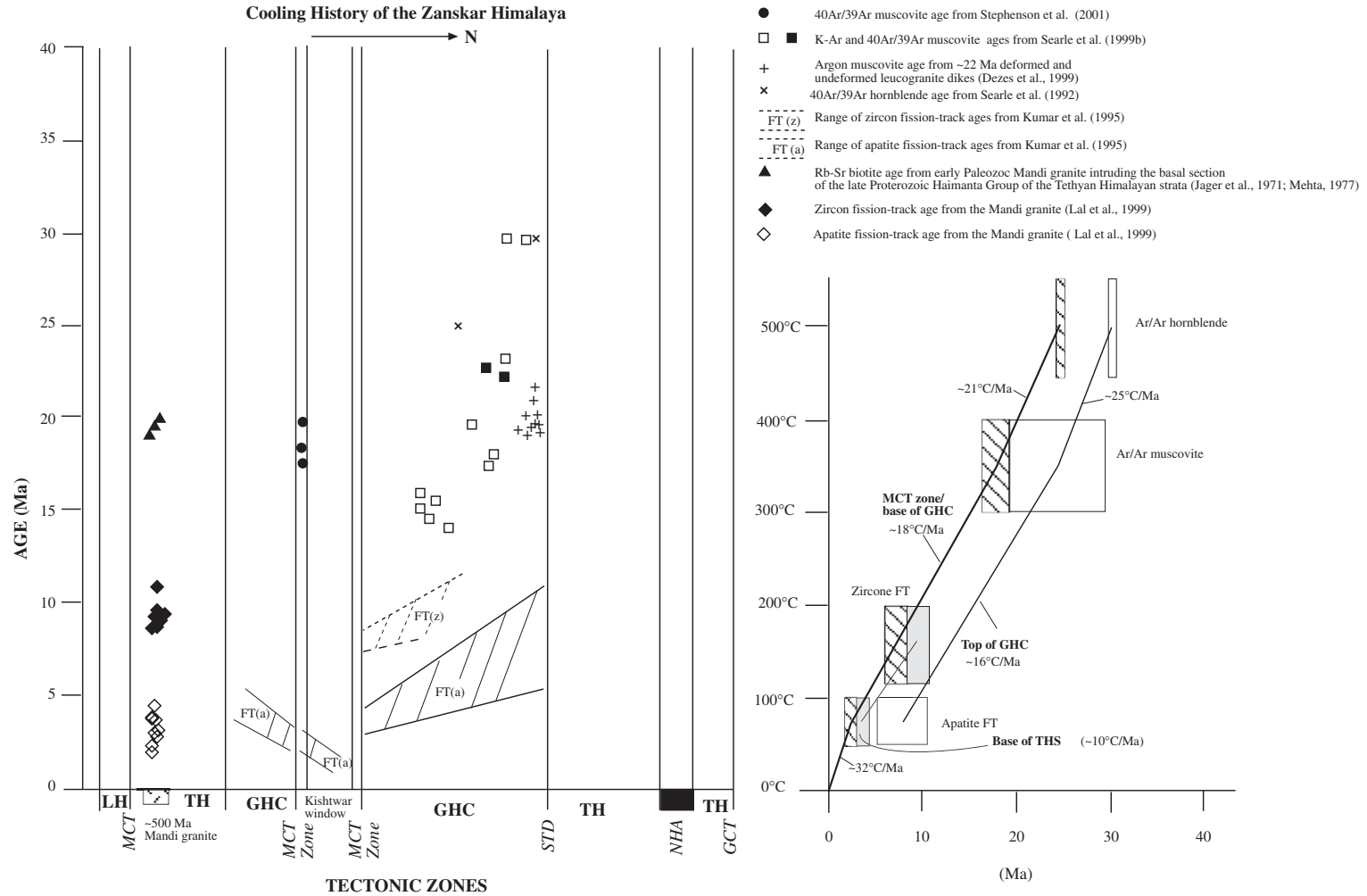


Fig. 14. Cooling history of the Zaskar Himalaya. LH, Lesser Himalayan zone; LHCN, Lesser Himalayan Crystalline Nappe; MCTI, the lower MCT fault; MCTII, the upper MCT fault; GHC, Greater Himalayan Crystalline Complex; STD, South Tibet Detachment; TH, Tethyan Himalayan zone; NHA, North Himalayan Antiform; GCT, Great Counter Thrust.

Dharmasala Group was deposited between 20 and 12 Ma based on correlation to a magnetostratigraphic section. Their correlation implies a lag time between the muscovite cooling ages and depositional ages at the base (~20 Ma) and top (~17 Ma) of the Lower Dharmasala Group to be 1 and 3 m.y. Assuming 350 °C for the closure temperature of muscovite (McDougall and Harrison, 1999), this interpreted age of the Lower Dharmasala Group would require cooling rates of 175 °C/m.y. and 116 °C/m.y. for muscovite at their source areas between 20 and 17 Ma. These exceedingly high cooling rates are not observed anywhere in the western Himalaya during this time interval, during which the average cooling rates of the GHC are only 18 °C/m.y. to 5 °C/m.y. (Figs. 13 and 14). This discrepancy indicates that the age assignment of the Lower Dharmasala Group by White et al. (2001) may be too old, and the age of its base may be younger by least 5 m.y.

The age of the Lower Siwalik Group in northwestern India is poorly constrained due to the lack of diagnostic fossils and its distinctively different lithology from the better dated Lower Siwalik Group in northern Pakistan (Burbank et al., 1996; Raiverman, 2000). Nevertheless, the age of the entire Siwalik Group is interpreted to be between 12 and <1 Ma in the northwestern Indian foreland basin based on magnetostratigraphic correlations (e.g., Meigs et al., 1995; Sangode et al., 1996; Brozovic and Burbank, 2000).

Najman and Garzanti (2000) suggest that GHC clasts first appeared in the Himalayan foreland basin occurred during the deposition of the Dagshai Formation at the end of the Oligocene. By correlating Nd and Sr isotopic compositions of sediments from the Subathu, Dagshai, and Kasauli Formations with the typical isotopic compositions of the GHC, LHS, and THS, Najman et al. (2000) interpret the GHC to have been exposed since 25 Ma or even as early as 40 Ma in the western Himalayan orogen. White et al. (2001, 2002) also noted that sparse garnet and staurolite first appeared in the lower part of the Lower Dharmasala Group, but the kyanite and sillimanite did not appear until deposition of the Middle and Upper Siwalik that are probably younger than 11 Ma.

White et al. (2001) determine U–Th–Pb ages of single monazite grains, which range from 1300–400 Ma and 37–28 Ma from the Dharmasala and Lower Siwalik strata in NW India. They obtained a monazite age of 37 Ma for the basal part of the Dharmasala

Group and ages of 27–28 Ma in the upper part of the Dharmasala Group. Based on these ages, they suggest that the young monazite grains were derived from the GHC and were deposited in the Himalayan foreland basin starting at ~20 Ma.

White et al. (2002) also obtained  $^{40}\text{Ar}/^{39}\text{Ar}$  ages of detrital muscovite from the Dharmasala Group. Their Cenozoic ages range from ~50 to 20 Ma. White et al. (2002) interpret that young detrital micas in the Miocene Dharmasala Group were derived from the GHC. A significant component of the detrital mica ages are in the range of 50–30 Ma from the Dharmasala Group (Fig. 5 of White et al., 2002). This age range is noticeably absent in the Zaskar and Garhwal GHC of the western Himalaya (Figs. 13 and 14), but is abundant in the Tso Morari UHP gneiss terrane along the northern Indian margin (de Sigoyer et al., 2000). Because the Tso Morari gneiss terrane is dominated by 22–5 Ma apatite fission track cooling ages (Fig. 13), the majority of high-grade GHC metamorphic rocks in the MCT hanging wall did not reach the surface until after 22–5 Ma, which overlaps the period of Dharmasala deposition. Thus, it is possible that the Tso Morari gneiss complex was a significant or the only source of high-grade metamorphic clasts transported to the early Miocene foreland basin of NW India and the GHC in the MCT hanging wall was not exposed prior to 9 Ma.

#### 4.1.5. Indus fan

The Indus River drains the westernmost Himalayan orogen and Mesozoic magmatic arcs and in the Karakoram Mountains, Kohistan, and southwestern Tibet north of the Indus–Tsangpo suture, transporting sediment to the Indus Fan (Clift et al., 2001). The Indus Fan occupies an area of about  $1.1 \times 10^6$  km<sup>2</sup>, with maximum thickness of ~9 km (Clift et al., 2001). Qayyum et al. (1996) divided the development of the Indus River system into two stages. In the first stage during the Eocene, the river transports sediments from the Himalayan orogen and high mountains north of the Indus–Tsangpo suture to a large basin located in the southern part of the Sulaiman arc (Qayyum et al., 1996). In the second stage, the modern Indus system and the construction of the Indus Fan were established after the beginning of the Miocene. Clift et al. (2001) dispute this notion and suggest instead that the Indus River and Indus Fan

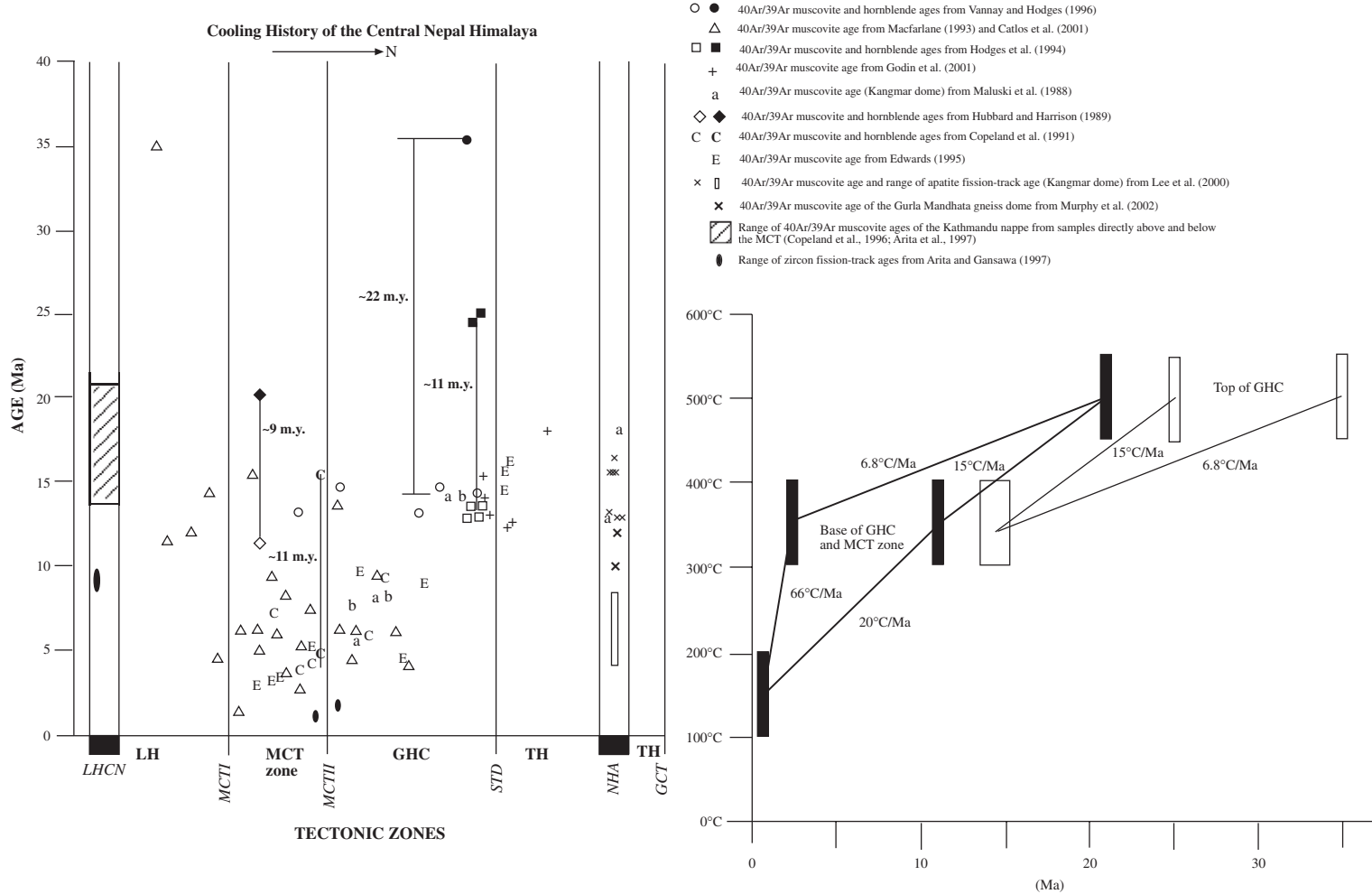


Fig. 15. Cooling history of the central Nepal Himalaya. LH, Lesser Himalayan zone; LHCN, Lesser Himalayan Crystalline Nappe; MCTI, the lower MCT fault; MCTII, the upper MCT fault; GHC, Greater Himalayan Crystalline Complex; STD, South Tibet Detachment; TH, Tethyan Himalayan zone; NHA, North Himalayan Antiform; GCT, Great Counter Thrust.

have developed since the middle Eocene, with a significant amount of Paleogene sediments accreted to the Makran accretionary complex during subduction of the Arabian Sea beneath Asia (Fig. 1A). Clift et al. (2001, 2002a) also show that Indus Fan deposits display weak isotopic signature of the major Himalayan units but strong input from the Mesozoic arcs in the Karakoram Mountains (Clift et al., 2002a). Synthesis of existing seismic reflection data indicates that rapid sediment accumulation in the Indus Fan occurred in two pulses: one in the middle Miocene and another in the Pleistocene (Clift et al., 2002b). Clift et al. (2002b) relate the middle Miocene event to rapid uplift and exhumation of the Karakoram Mountains. Correlating the Himalayan sources using Nd and Pb isotopic analysis of submarine sediments in the Indus Fan, Clift et al. (2001) propose that the Paleogene Indus sediments were dominated by the LHS, while the Neogene sediments were dominated by exhumation of both the GHC and LHS. The modern Indus River sands are dominantly (~80%) derived from bedrocks (i.e., Karakoram and Lhasa terranes) located north of the Indus–Tsangpo suture zone (Garzanti et al., 2005).

## 4.2. Central Himalayan

### 4.2.1. Exhumation of the Greater Himalayan Crystallines

The cooling history of the GHC in the Nepal Himalaya is summarized in Fig. 15. From  $^{40}\text{Ar}/^{39}\text{Ar}$  hornblende ages, we can infer that the exposed top part of the GHC was situated near its closure temperature of ~500 °C (McDougall and Harrison, 1999) between 35 and 25 Ma (Vannay and Hodges, 1996; Hodges et al., 1994), whereas the base of the GHC and the MCT zone were at this temperature between 21 and 4 Ma (Hubbard and Harrison, 1989; Copeland et al., 1991) (Fig. 15). Similarly, based on  $^{40}\text{Ar}/^{39}\text{Ar}$  muscovite ages and a closure temperature at about 350 °C (McDougall and Harrison, 1999), we may interpret that the top of the GHC in Nepal cooled to a temperature of ~350 °C at ~14–16 Ma whereas its base and the MCT zone cooled below this temperature between 12 and 3 Ma (Maluski et al., 1988; Hubbard and Harrison, 1989; Macfarlane, 1993; Hodges et al., 1994; Edwards, 1995; Vannay and Hodges, 1996; Catlos et al., 2001; Godin et al., 2001) (Fig. 15).

The cooling rate at the top of the GHC is ~7 °C/Ma between 35 and 13 Ma (Vannay and Hodges, 1996) and is doubled at ~15 °C/m.y. between 25 and 14 Ma (Hodges et al., 1994) (Fig. 15). The cooling rate at the base of the GHC is between 7° and 15 °C/m.y. from 20 to 5 Ma. Assuming a constant geothermal gradient of 30 °C/km, these cooling rates imply an exhumation rate of  $0.38 \pm 0.13$  mm/yr.

The similar cooling rates and progressively younger cooling ages from the top to the base of the GHC imply that the GHC was translated along the MCT as a coherent slab. Although this observation supports the structural models treating the GHC as a coherent thrust sheet as advocated by Lyon-Caen and Molnar (1985) and Schelling and Arita (1991), it does not preclude significant internal deformation of the GHC during its downward transport (i.e., on its prograde path caused by tectonic burial due to underthrusting). In fact, the widespread isoclinal folds and multiple phases of ductile deformation within the GHC (e.g., LeFort, 1975) may have occurred during the prograde and down-going path of the GHC transport.

The exhumation rate of the MCT zone is ~3–5 mm/yr since about 7–4 Ma, because rocks buried at a depth of ~21 km determined by thermobarometry have been brought up to the surface since that time (Harrison et al., 1997a; Catlos et al., 2001). This inference is consistent with young hornblende age of ~4.44 Ma from the MCT zone in Nepal (Copeland et al., 1991) and rapid cooling rates up to ~65 °C/m.y. between 5 and 2 Ma as indicated by the combination of zircon fission track ages of 1.2–2.3 Ma and muscovite cooling ages of 5–2 Ma in the MCT zone (Macfarlane, 1993; Arita and Ganzawa, 1997) (Fig. 15). More recently, Burbank et al. (2003) show that the erosion rate of the GHC in the Annapurna area of Nepal in the past 1 m.y. exceeds 2–5 mm/yr based on apatite fission track ages.

The cooling history of the Kathmandu Nappe in the Lower Himalaya is constrained by  $^{40}\text{Ar}/^{39}\text{Ar}$  muscovite ages of 21–13 Ma (Copeland et al., 1996; Arita et al., 1997) and zircon fission track ages of 8.4–9.6 Ma (Arita and Ganzawa, 1997). Johnson et al. (2001) noted the lack of mica ages younger than 14 Ma in the Kathmandu Nappe and suggest that the nappe as part of the MCT thrust sheet was kinematically decoupled from its root zone at or prior to this time. In other words, the root zone of the MCT remained active after 14 Ma

but the frontal MCT had stopped motion since that time.

From existing  $^{40}\text{Ar}/^{39}\text{Ar}$  muscovite ages, the top of the GHC was still at a depth of >10 km between 15 and 13 Ma based on the muscovite cooling ages and an assumed constant thermal gradient of 30 °C/km (Hodges et al., 1994; Vannay and Hodges, 1996; Godin et al., 2001) (Fig. 15). This implies that the GHC could not be exposed at surface prior to 15–13 Ma. This is an important constraint on the age and potential source areas of the Himalayan foreland basin and has important implications for the timing of the STD as we discuss the subject later in the article.

#### 4.2.2. Exhumation of the Lesser Himalayan thrust belt

Catlos et al. (2001) determine muscovite ages in the upper part of the LHS in central Nepal with ages mostly in the range of 15 Ma to 4 Ma. However, they also obtain a muscovite age of ~35 Ma. The 15–4 Ma mica cooling ages were most likely related to the emplacement history of the GHC along the MCT, whereas the older muscovite age could be a result of early thrusting in the Lower Himalaya prior to MCT activity. It is interesting to note that a hornblende from the Lesser Himalaya Sequence in Nepal with a total  $^{40}\text{Ar}/^{39}\text{Ar}$  gas age of  $141 \pm 4$  Ma was disturbed by a younger cooling event of  $41 \pm 7$  Ma as observed by Macfarlane (1993). This age may also reflect localized older Eocene deformation and metamorphism in the Lesser Himalayan thrust belt in the Nepal Himalaya.

#### 4.2.3. Exhumation of the North Himalaya Antiform

The gneiss domes in the North Himalayan Antiform north of Nepal were exhumed to the middle crust between 20 and 10 Ma, as indicated by  $^{40}\text{Ar}/^{39}\text{Ar}$  muscovite cooling ages (Maluski et al., 1988; Lee et al., 2000; Murphy et al., 2002). At 8–4 Ma, the high-grade metamorphic rocks under  $P$ – $T$  conditions of 625 °C and 8.6 kbar from the North Himalayan gneiss domes were exhumed to a near-surface level as indicated by the apatite fission track ages (Lee et al., 2000) (Fig. 15). When combining the above  $P$ – $T$ – $t$  data, one can infer that the exhumation rate in the Kangmar dome is  $8.5 \pm 6.5$  mm/yr assuming crustal density is 2.85 g/cm<sup>3</sup>. This rate is significantly higher than the average rate of exhumation for the GHC in the Miocene (Table 8).

#### 4.2.4. Foreland basin sedimentation in the western Himalaya

The Cenozoic strata of the central Himalayan foreland basin in Nepal consist of the uppermost Cretaceous–lower Paleocene fluvial and marine Amile Formation overlain unconformably by the Eocene marine Bhainskati Formation; the latter lies unconformably below the non-marine deposits of the lower Miocene Dumri Formation (e.g., Upreti, 1996, 1999) (Table 5). The age of the Amile and Bhainskati Formations are mainly constrained by the presence of marine fossils. The Dumri Formation is considered to be temporally equivalent to the lower Miocene Dagshai Formation in NW India (DeCelles et al., 1998a) and is younger than 17–20 Ma as constrained by the detrital muscovite ages (DeCelles et al., 2001, 2004). The mid-Miocene to Pliocene Siwalik Group in Nepal was considered to be younger than the Dumri Formation (e.g., Appel et al., 1991; Harrison et al., 1993; Ojha et al., 2000), although the two units are not in direct contact (DeCelles et al., 1998a). Specifically, the Dumri rocks are located in the hanging wall whereas the Siwalik rocks are in the footwall of the MBT.

The exposed Paleogene–lower Miocene strata in Nepal are located entirely in the MBT hanging wall. This is in contrast to strata of the same age in northwestern India where they only occur in the MBT footwall (Najman et al., 1993; Powers et al., 1998; Raiverman, 2000) and in northern Pakistan where they are exposed both in the MBT hanging wall and footwall (Yeats and Hussain, 1987; Burbank et al., 1996; Pogue et al., 1999). Cenozoic  $^{40}\text{Ar}/^{39}\text{Ar}$  ages of detrital muscovite from the middle Siwalik Group ranges from 20 to 10 Ma. It is not clear whether deposition of the Dumri Formation and the lower Siwalik Group overlaps temporally (DeCelles et al., 1998a).

DeCelles et al. (1998a,b, 2001) investigated the unroofing history of the central Himalaya by examining the U–Pb ages of detrital zircon and  $^{40}\text{Ar}/^{39}\text{Ar}$  ages of detrital muscovite of Cenozoic strata. They also studied sandstone composition and temporal variations in the first appearance of high-grade metamorphic index minerals. DeCelles et al. (1998a) show that Cambro-Ordovician zircons of ~500 Ma are present in the Eocene Bhainskati and

Miocene Dumri Formations. They consider the zircon population to have been derived from the THS in the Eocene and from the GHC in the Miocene. The post-20–17 Ma Dumri Formation in western Nepal is dominated by monocrystalline quartz with small amounts of plagioclase and lithic fragments of phyllite (DeCelles et al., 1998a; Sakai et al., 1999). DeCelles et al. (1998a) attributed to initial unroofing of the high-grade GHC associated with motion along the STD. This interpretation would imply that the GHC was already exposed at surface by early Miocene time.

Because early Miocene leucogranites tend to be concentrated along the STD in the NW Indian Himalaya and south-central Tibet (e.g., LeFort, 1996; Searle et al., 1999b; Murphy and Harrison, 1999), unroofing of the uppermost part of the GHC could potentially have transported early Miocene zircons to the foreland basin in far western Nepal. However, early Miocene zircons have not been documented there which implies that the plagioclase in the Dumri Formation may have derived from the Cambro-Ordovician granites from the basal part of the THS rather than from the GHC. This interpretation is consistent with the observation that high-grade metamorphic minerals indicative of the GHC source did not appear in the central Himalayan foreland basin until after ~11 Ma or even later during the deposition of the uppermost Lower Siwalik Group (DeCelles et al., 1998b). Considering the fact that the top part of the GHC in central Nepal was still at a depth of >10 km between 15 and 13 Ma as indicated by  $^{40}\text{Ar}/^{39}\text{Ar}$  muscovite ages from the Annapurna region (Godin et al., 2001), it is possible that the GHC did not reach the surface until after ~11 Ma. That is, only the middle or upper parts of the late Miocene–Pliocene Siwalik Group contain the unroofing records of the GHC. This inference is in drastic contrast to the long held view that the GHC had already been exposed at the surface to 17 Ma (e.g., France-Lanord et al., 1993).

#### 4.3. Eastern Himalaya

Below we discuss the exhumation history of the Eastern Himalaya. Because there is no information on the cooling history of the THS and

LHS in the region, our description will only focus on the GHC.

##### 4.3.1. Exhumation of the Greater Himalayan Crystallines

Thermochronologic data are very sparse in the eastern Himalaya. In south-central Bhutan, Stüwe and Foster (2001) suggest that the basal GHC cooled below ~350 °C between 14 and 11 Ma and through 110–60 °C at about 3 Ma based on  $^{40}\text{Ar}/^{39}\text{Ar}$  muscovite ages and apatite fission track thermochronology (Fig. 16). This yields an average cooling rate of  $29 \pm 4$  °C/Ma, which may be translated to an exhumation rate of  $0.97 \pm 0.13$  mm/yr assuming a constant geothermal gradient of 30 °C/km.

In Sikkim, Harris et al. (2004) use garnet zoning profiles to establish early garnet growth in the GHC at a pressure condition of 10–12 kbar and subsequent decompression causing the rock to partially melt at  $P=8$  kbar and  $T=750$  °C. Sm–Nd dating of garnet growth indicates that pre-decompression garnet growth occurred at  $23 \pm 3$  Ma and near-peak temperatures were achieved at  $16 \pm 2$  Ma (Harris et al., 2004). Their data provide an exhumation rate of  $2 \pm 1$  mm/yr.

The metamorphic massif in the core of the eastern Himalayan syntaxis cooled below 500 °C from 18 to 8 Ma, as indicated by  $^{40}\text{Ar}/^{39}\text{Ar}$  hornblende ages (Ding et al., 2001). This implies a cooling rate of 28–63 °C/m.y. for the core of the eastern Himalayan syntaxis since 18–8 Ma. This may be translated to an exhumation rate of 0.93–2.1 mm/yr assuming a constant geothermal gradient of 30 °C/km.

Despite the young  $^{40}\text{Ar}/^{39}\text{Ar}$  hornblende ages, K–Ar biotite and hornblende ages from the broader region of the eastern Himalayan syntaxis range from 1.5 Ma to 47 Ma and from 31 Ma to 57 Ma, with older ages along flanks of the syntaxis and younger ages towards the center (Zhang et al., 1992) (Fig. 16). If we use the older K–Ar hornblende ages at the flanks of the syntaxis as a proxy for early erosional rates and assume that the K–Ar closure temperature for hornblende is 500 °C, we obtain an exhumation rate of  $0.42 \pm 0.13$  mm/yr using a constant geothermal gradient of 30 °C/km over 57–31 Ma. This pattern of cooling ages for hornblende and biotite indicates that the eastern

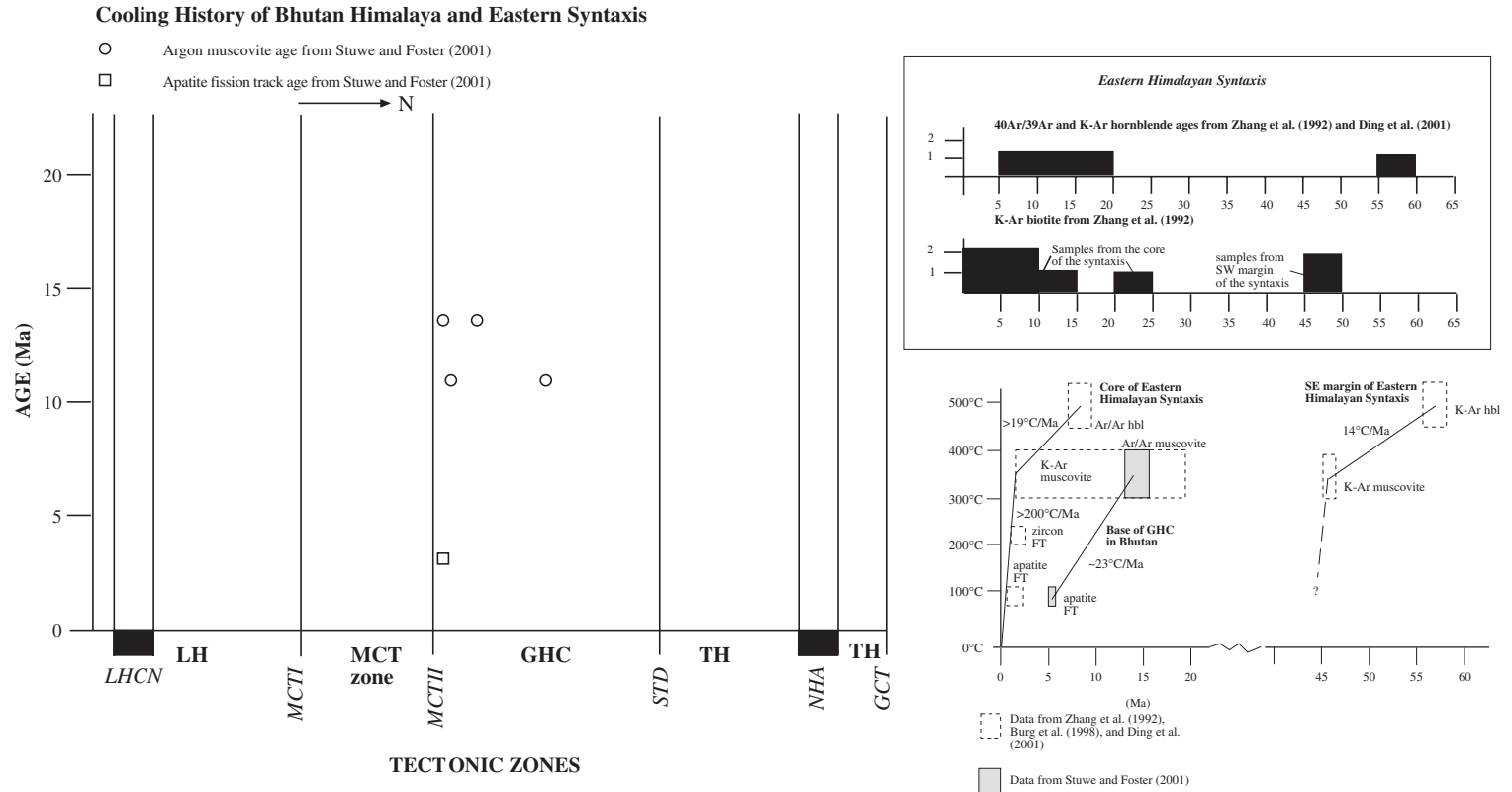


Fig. 16. Cooling history of the Bhutan Himalaya and eastern Himalayan syntaxis. LH, Lesser Himalayan zone; LHCN, Lesser Himalayan Crystalline Nappe; MCTI, the lower MCT fault; MCTII, the upper MCT fault; GHC, Greater Himalayan Crystalline Complex; STD, South Tibet Detachment; TH, Tethyan Himalayan zone; NHA, North Himalayan Antiform; GCT, Great Counter Thrust.

Himalayan syntaxis has been a long-standing topographic feature since the Eocene.

#### 4.3.2. Foreland basin and Bengal Fan

The Siwalik Group in the footwall of the MBT is the only Cenozoic unit exposed in the Bhutan Himalaya (e.g., Gansser, 1983; Bhargava, 1995) (Table 5). In Arunachal, Paleocene–Eocene marine strata are locally overlain unconformably by Miocene non-marine deposits (Table 5) (Kumar, 1997). This relationship is similar to that observed throughout the western and eastern Himalaya, supporting the speculation of DeCelles et al. (1998a) that this unconformity is a regional feature related to the evolution of the entire Himalaya.

South of the Shillong plateau where the Ganges and Brahmaputra Rivers meet, a continuous section of Eocene–Pleistocene strata is present in the Bengal Basin (Johnson and Alam, 1991; Rahman and Faupl, 2003; Alam et al., 2003). This basin is the western extension of the submarine Bengal Fan developed on a transitional continental margin (Alam et al., 2003). Together, they have received sediments from the Himalaya, southern Tibet, Indo-Burma Ranges, Shillong plateau, and the Indian craton (Curry and Moore, 1971; Ingersoll and Suczek, 1979; Copeland and Harrison, 1990; Curry, 1991; Amano and Taira, 1992; France-Lanord et al., 1993; Galy et al., 1996; Uddin and Lundberg, 1998a,b; Curry et al., 2003; Alam et al., 2003).

Using  $^{40}\text{Ar}/^{39}\text{Ar}$  thermochronology, Copeland and Harrison (1990) show that detrital K-feldspar and muscovite samples from Ocean Drilling Program (ODP) Leg 116 cores record a rapid early Miocene cooling event in the source area. Amano and Taira (1992) examine the temporal variation of heavy and light minerals from early Miocene–Quaternary samples from ODP Leg 116 and conclude that sediments of 17–15 Ma were derived from the LHS and THS. Only after 15 Ma did the Bengal Fan start receiving metamorphic minerals they interpret to have derived from a GHC-like source. They also show that the minerals from the GHC-like source decrease markedly at 7.5–6.5 Ma. Note that the GHC-like high-grade minerals could have derived from the Indian craton as discussed below (see Uddin and Lundberg, 1998a). Afterwards the Indian craton and GHC-like source are both contributors of sediments to the fan. Based

on the Nd and Sr isotopic compositions, France-Lanord et al. (1993) suggest that the Bengal Fan sediments were mostly derived from the GHC before 17 Ma, implying that the GHC was exposed to the surface before this time. Both the Indo-Gangetic foreland and the Bengal Fan experienced a decline in sediment-accumulation rates at 8 Ma, which is explained by monsoonal intensification accompanied by a decrease in mechanical weathering in the Himalaya (Burbank et al., 1993).

Because of the available deep drill hole data are only from the distal part of the Bengal Fan, the exact impact of Himalayan development on fan formation remains poorly known. This difficulty has been significantly overcome by sedimentological studies of Eocene–Oligocene strata in parts of the Bengal Basin south of the Shillong plateau that are much closer to potential source areas of the Himalayan range (Alam et al., 2003). Uddin and Lundberg (1998a) show that monocrystalline quartz grains derived from stable Indian craton are dominant in Paleogene sedimentary rocks while lower Miocene strata are rich in feldspar grains, argillite, and very low-grade metamorphic lithic fragments, possibly related to initial uplift and denudation of the Himalaya. The low- and medium-grade metamorphic lithic fragments did not appear in the Bengal basin until after late Miocene time (Uddin and Lundberg, 1998a). Uddin and Lundberg (1998b) also show that the Eocene–Oligocene strata of the Bengal Basin contain only 0.2% of stable heavy minerals (tourmaline, garnet, rutile, and zircon) while Miocene strata contain 0.5–2% diverse heavy minerals (tourmaline, kyanite, zircon, calcic amphibole, rutile, chlorite, staurolite, epidote, sillimanite, and clinopyroxene, and sparse chromite). They suggest that the former were derived from chemically weathered Indian craton and the latter from the physically weathered Himalayan orogen.

Uddin and Lundberg (1998a,b) note that the lack of evidence for orogenic activity from the Eocene–Oligocene strata in the Bengal basin contrasts sharply to the observations made in the western Himalaya where Eocene strata contain detritus derived from the Himalayan orogen and the Indus–Tsangpo suture zone (e.g., Najman et al., 1993; Critelli and Garzanti, 1994; Critelli and Ingersoll, 1994; Garzanti et al., 1996; Najman and Garzanti, 2000). Uddin and Lundberg

(1998a,b) attribute this difference to diachronous collision between India and Asia starting in the west and progressing to the east (e.g., [Patriat and Achache, 1984](#); [Dewey et al., 1989](#)). However, this explanation is not completely satisfactory because by Oligocene time the Indo-Asian collision along the eastern Indus–Tsangpo suture zone had already been completed (e.g., [Rowley, 1996](#); [LeFort, 1996](#); [Yin and Harrison, 2000](#); [Ding et al., 2003](#); [Zhu et al., 2005](#)). Furthermore, crustal shortening was already active during the Eocene–Oligocene in the Tethyan Himalayan thrust belt in southeastern Tibet (e.g., [Ratschbacher et al., 1994](#); [Yin et al., 1994, 1999](#); [Harrison et al., 2000](#)). As discussed below, it is possible that Himalayan sediments were not transported to the Bengal Fan until after the beginning of the Miocene, because the Rajmahal–Garó Gap may have remained closed before this time, blocking the Himalayan rivers from entering the Bay of Bengal in the Paleogene.

A recent synthesis of the Bengal Basin by [Alam et al. \(2003\)](#) shows multiple detrital sources. In addition to the Himalayan range, two other regions are equally important as Cenozoic sediment sources to the Bengal Basin and the Bengal Fan: the Shillong plateau since the early Miocene and the accretionary complex in the Indo-Burma Ranges developed since late Paleocene time.

#### 4.4. Summary

Exhumation rates as inferred from thermochronological data and coupled studies of thermobarometry and geochronology in the Himalayan orogen are summarized in [Table 8](#). These estimates only consider the uncertainties in the duration of cooling and assume a constant crustal density and geothermal gradient. [Table 8](#) shows that Himalayan exhumation reached two peaks, one at a rate of  $\sim 40$  mm/yr during 55–50 Ma in the western Himalaya and one at a rate of 3–5 mm/yr since 7 Ma in Nepal. In between these extreme events, most of the Himalayan orogen was under slow exhumation and erosion (?), with rates between 0.1 and 1.0 mm/yr. An exception is the North Himalayan gneiss domes, locally displaying an exhumation rate of 6–7 mm/yr. The estimates of the above exhumation rates are quite reliable because they are derived from both temperature–time and pressure–time paths. When placing the areas of

high exhumation rates over the Himalayan tectonic map ([Fig. 2A](#)), high-exhumation-rate regions are all associated with prominent Himalayan structures: UHP with the Indus–Tsangpo suture zone, North Himalayan gneiss domes with low-angle detachment shear zones, and the GHC with the reactivated MCT. These relationships indicate that the mode of deformation rather than climate conditions has played a decisive role in localizing high rates of exhumation in the Himalaya.

## 5. Isotopic compositions and detrital zircon ages of Himalayan and Tibetan units

### 5.1. Tethyan Himalayan Sequence (THS)

Isotopic compositions and detrital zircon ages have been used for the lithologic division of the Himalayan and southern Tibetan units (e.g., [France-Lanord et al., 1993](#); [Najman et al., 2000](#); [Singh and France-Lanord, 2002](#)). For the THS, detrital zircon ages range from 0.5 to 2.6 Ga, with prominent peaks at 0.9–1.1 Ga and 2.6 Ga ([Parrish and Hodges, 1996](#); [DeCelles et al., 2000](#); [Gehrels et al., 2003](#); [Myrow et al., 2003](#)). The existing Nd and Sr isotopic data suggest that Nd model ages of the THS is between 1.6 and 2.0 Ga, the  $\epsilon_{\text{Nd}}(0)$  value between  $-19$  and  $-7$ , and the  $^{87}\text{Sr}/^{86}\text{Sr}$  initial ratio between 0.705 and 0.750 ([Najman et al., 2000](#); [Ahmad et al., 2000](#); [Robinson et al., 2001](#)). When using these results, one should keep in mind that the THS sample size is much smaller than those of the GHC and LHS. There are only six THS samples from NW India in [France-Lanord et al.'s \(1993\)](#) classic analysis and seven THS samples from Nepal in [Robinson et al.'s \(2001\)](#) study. Of the six samples analyzed by [France-Lanord et al. \(1993\)](#), two were from the Indus–Tsangpo suture and another two from the Indus River banks. Because the Indus River drains a significant part of the Karakorum and Lhasa terranes north of the Himalayan orogen ([Fig. 1A](#)) ([Garzanti et al., 2005](#)), samples from the Indus River banks may not be representative for the THS.

### 5.2. Greater Himalayan Crystalline Complex (GHC)

The GHC and THS have similar detrital zircon ages and Nd composition (i.e.,  $\epsilon_{\text{Nd}}(0)$  between

–19 and –7) (Parrish and Hodges, 1996; DeCelles et al., 2000; Robinson et al., 2001). This similarity led Myrow et al. (2003) to suggest that the late Proterozoic–Cambrian parts of the GHC, THS, and LHS are correlative and were once deposited on the same north-facing margin. The existing data suggest that the Sr composition of the GHC and THS are markedly different. The  $^{87}\text{Sr}/^{86}\text{Sr}$  initial ratio is between 0.705 and 0.730 for the THS and between 0.730 and 0.805 for the GHC (France-Lanord et al., 1993; Najman et al., 2000). Because the GHC and THS have similar detrital zircon ages and Nd isotopic composition (Myrow et al., 2003), the difference between the GHC and THS in Sr composition could also be an artifact of the small sample size.

### 5.3. Lesser Himalayan Sequence (LHS)

The detrital zircon ages and isotopic compositions of the LHS vary from place to place. In the south-central Garhwal Himalaya, the lowest LHS is composed of the Munsiri and Ramgarh Groups above the Munsiri and Ramgarh thrusts, respectively. The two units are composed of schist and gneisses in the Kumaun Himalaya of NW India (Valdiya, 1980; Srivastava and Mitra, 1994) and show older Nd model ages (2.0–2.8 Ga) than those for the GHC (1.9–2.2 Ga) (Ahmad et al., 2000). However, the Chandpur Formation of the LHS atop the Munsiri and Ramgarh Groups has Nd and Sr isotopic composition similar to that obtained from the GHC (Ahmad et al., 2000). In the Garhwal Himalaya, the Cambrian strata of the uppermost part of the LHS have detrital zircon ages and Nd isotopic compositions similar to the GHC and THS (Myrow et al., 2003). In Nepal, the Proterozoic part of the LHS contains detrital zircon ages ranging from ~1.6 Ga to ~2.6 Ga with peaks at 1.8 Ga and 1.9 Ga (Parrish and Hodges, 1996; DeCelles et al., 2000). Analysis of Nd composition of major Himalayan units in Nepal indicates that the  $\epsilon_{\text{Nd}}(0)$  value ranging from –26 to –16 for the LHS, from –20 to –6 for the THS, and from –20 to –7 for the GHS (Robinson et al., 2001). These results indicate that the GHS and THS cannot be distinguished on the basis of Nd isotopic composition alone (Myrow et al., 2003).

### 5.4. Southern Tibet (=Lhasa Block)

The southern Lhasa block is dominated by the Cretaceous–early Tertiary Gangdese batholith (also known as the Transhimalayan plutonic belt in southern Tibet; Burg et al., 1983; Allègre et al., 1984; Dewey et al., 1988; Yin and Harrison, 2000). This region has distinctively different Sr and Nd isotopic compositions from those for the main Himalayan lithologic units. Specifically, the  $^{87}\text{Sr}/^{86}\text{Sr}$  initial ratio for the Lhasa block is much lower (<0.715) while the  $\epsilon_{\text{Nd}}(0)$  value is much higher (generally >–8) than the three Himalayan units (e.g., Singh and France-Lanord, 2002).

### 5.5. Foreland sediments

In western Nepal, DeCelles et al. (1998a) obtained U–Pb detrital zircon ages from the Cenozoic foreland basin strata (also see DeCelles et al., 2004). Their detrital zircon ages from the middle Eocene Bhainskati Formation, early or middle Miocene (?) Dumri Formation, and middle Miocene–Pliocene Siwalik Group (Table 5) can be generally matched to the protolith and detrital zircon ages of the GHC, THS, or Cambrian strata of the LHS, all yielding Cambro-Ordovician ages of ~500 Ma. However, the uppermost Cretaceous–Paleogene Amile Formation of Sakai (1983) contains detrital zircon ages of 120 Ma, 1.8 Ga, and 2.4–2.6 Ga, with a noticeable absence of Cambro-Ordovician zircon ages that are present in all other overlying Tertiary units (DeCelles et al., 1998a). DeCelles et al. (1998a) suggest that the detrital zircons of 120 Ma were derived from the underlying Early Cretaceous basalts produced during Early Cretaceous rifting in northeastern India (Sakai, 1983, 1984, 1989; LeFort and Raï, 1999). However, Rb–Sr dating of these volcanic rocks yields an age of  $96.7 \pm 2.8$  Ma (Sakai et al., 1992), which are much younger than the 120-Ma detrital zircon age. It is possible that the detrital zircons of 120 Ma in the Amile Formation were derived from the Rajmahal Trap immediately east of the Rajmahal–Garo Gap some 600 km southwest of western Nepal (Fig. 1A). Cretaceous volcanic rocks there have been dated by the K–Ar method to be 88–128 Ma (Baski et al., 1987).

It is also possible that the 120-Ma zircons in the Amile Formation were derived from the Gangdese

batolith in southern Tibet north of the Indus–Tsangpo suture zone. The Late Jurassic and Early Cretaceous plutons are common along the northern edge of the Lhasa block (e.g., Xu, 1990; Murphy et al., 1997). This region was uplifted during the development of the mid-Cretaceous Coqin thrust belt (Yin et al., 1994; Murphy et al., 1997). This structural high may have shed sediments across the Gangdese batholith and the Indus–Tsangpo suture via rivers that cut across the Gangdese Shan and reached the Gangetic plain during the deposition of the Amile Formation. This speculation implies that the land connection between India and Asia occurred at or prior to the latest Cretaceous and Paleocene. One test of the above hypothesis is to examine the Nd and Sr compositions of the Amile Formation, because the Gangdese batholith has very different Nd and Sr isotopic composition from those of the Himalayan units and the Indian basement (Singh and France-Lanord, 2002).

In the NW Indian foreland basin, Najman et al. (2000) interpret that the Eocene Subathu Formation with an  $\varepsilon_{\text{Nd}}(0)$  value of  $\sim -9$  and the  $^{87}\text{Sr}/^{86}\text{Sr}$  initial ratio of 0.710–0.715 was derived from the THS and the Indus–Tsangpo suture. By contrast, these authors show that the latest Oligocene (?)–early Miocene Dogshai and Kasauli Formations have Nd and Sr compositions ( $\varepsilon_{\text{Nd}}(0) = \sim -12$  to  $-18$ ,  $^{87}\text{Sr}/^{86}\text{Sr} = 0.755$ – $0.775$ ), which are characteristic for the GHC and THS.

### 5.6. Summary

The isotopic compositions and detrital zircon provenances between southern Tibet and the Himalayan units are clearly distinguishable. Specifically, the Nd and Sr isotopic compositions of the Proterozoic LHS are significantly different from those of the GHC and THS. However, the Cambrian strata of the LHS share similar Nd composition and detrital zircon ages to those obtained from the GHS and Cambrian strata of the THS. Nd and Sr isotopic compositions of the Paleocene–Eocene foreland basin strata from NW India suggest that clasts from southern Tibet may have been transported across the Indus–Tsangpo suture to the Himalaya during their deposition. The detrital zircon ages in the Paleocene strata of western Nepal may suggest possible contact between India and Asia by the latest

Cretaceous or early Paleocene. Significant unroofing of the Himalaya may have started in the early Miocene. However, it remains unclear when the THS was completely stripped off and the GHC was first exposed to the surface from the available Nd, Sr, and U–Pb detrital zircon data.

A complication of using Nd and Sr isotopic compositions of the Bengal Fan sediments to infer the unroofing history of the entire Himalaya is that both the eastern and western Himalayan syntaxes may have been long-standing structural highs exposing high-grade Indian basement and its metamorphosed cover by 40 Ma. Their exposure may not be directly related to motion on the MCT during emplacement of the GHC. In the eastern syntaxis region,  $\sim 47$ -Ma K–Ar biotite ages were reported (Zhang et al., 1992) (Fig. 16). K–Ar hornblende ages of 57–31 Ma in the eastern syntaxis and 67–50 Ma from the western syntaxis region are also significantly older than those from the rest of the Himalaya (Zhang et al., 1992; Treloar et al., 1989; Treloar and Rex, 1990; Baig, 1990). As shown by Singh and France-Lanord (2002), most of the sediments transported to the Bengal Basin and the Bengal Fan are derived from the Yalu Tsangpo–Bhramaputra River system that cuts through the eastern Himalayan syntaxis where the GHC is exposed (Burg et al., 1998; Ding et al., 2001; Zeitler et al., 2001). Thus, it is likely that the eastern syntaxis was the dominant source of GHC-like sediments in the Bengal Fan since 17 Ma as detected by France-Lanord et al. (1993) and Galy et al. (1996). However, this isotopic signature does not require that the GHC along the main Himalayan range be exposed by this time.

## 6. Models for the evolution of the Himalayan orogen

Hypotheses for evolution of the Himalayan orogen vary from simple conceptual models to sophisticated numerical simulations based on fully coupled thermo-mechanical–erosional solutions (Fig. 17). As shown in the following discussion, all current models are two-dimensional in nature and were developed mostly to address specific problems across limited segments of the Himalayan orogen.

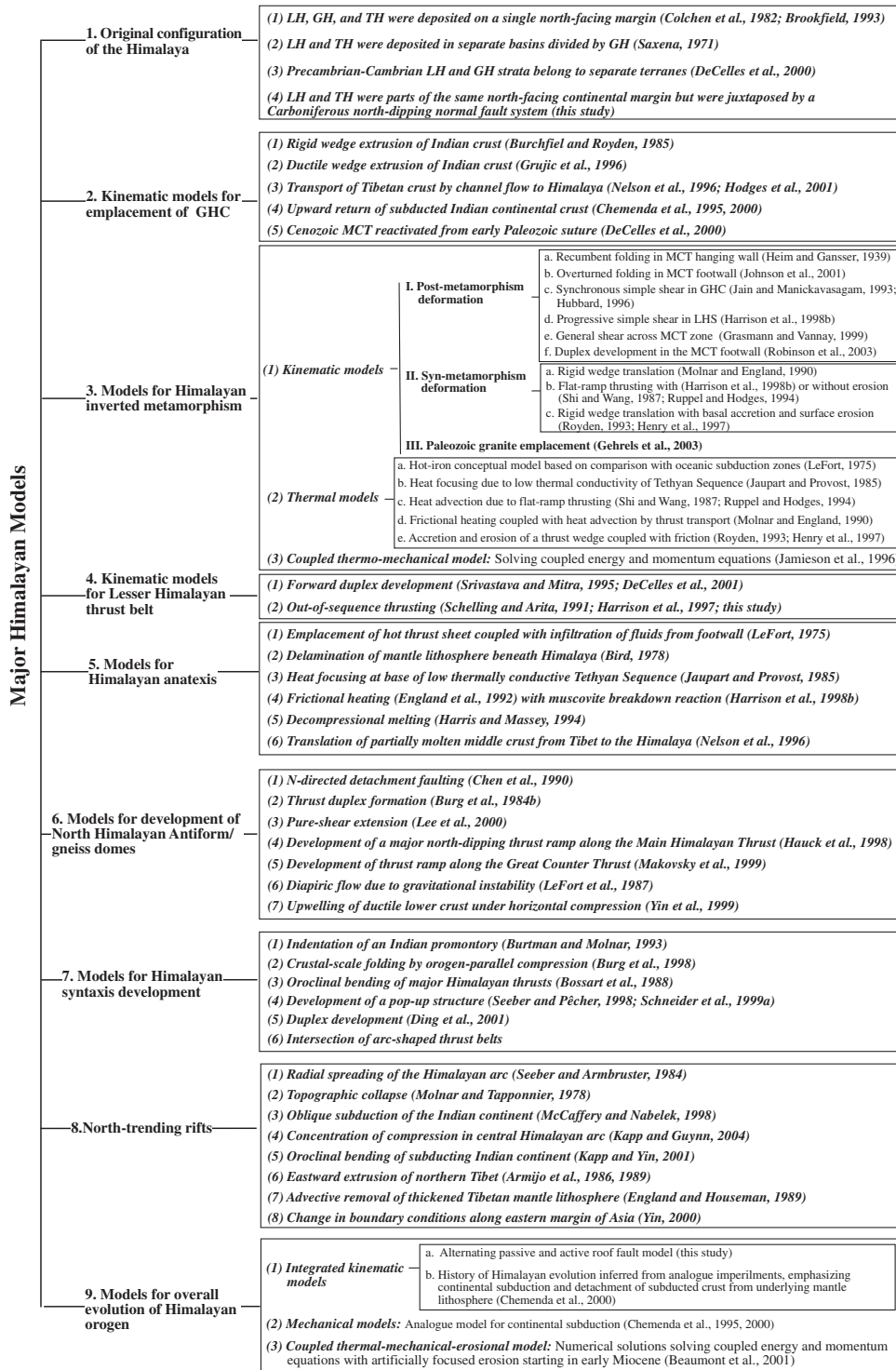


Fig. 17. Summary of major models for the evolution of the Himalayan orogen.

### 6.1. The original configuration of the Himalayan orogen prior to Cenozoic deformation

It is impossible to reconstruct the Cenozoic deformational history of the Himalayan orogen without knowing its initial structural and stratigraphic configurations. The problem is centered on how the main Himalayan lithologic units of the GHC, LHS, and THS were originally arranged in three dimensions prior to the Indo-Asian collision. There are at least four possibilities for the initial Himalayan stratigraphic configuration (Fig. 18).

#### 6.1.1. Single passive continental margin model (Fig. 18A)

Strata of the LHS, GHC, and THS were deposited on the same north-facing continental margin of northern India, each representing different facies from shelf to slope settings. This hypothesis was based on studies in NW India and central Nepal (Frank et al., 1973; Colchen et al., 1982) and was later elaborated by Brookfield (1993) in his regional stratigraphic synthesis of the Himalaya. Because the large magnitude of slip along the MCT and STD and potentially large-magnitude erosion of the MCT hanging wall, the physical connections among these Himalayan units have not been and may never be established with confidence in Nepal and NW India. However, the current knowledge of the Himalayan stratigraphy in the Pakistan Himalaya appears to support the single-margin hypothesis, where a continuous section of the LHS, THS, and GHC equivalent strata are present (Pogue et al., 1999). However, the single-margin model appears at odds with the observations that Paleozoic and Mesozoic strata are rarely present above the Precambrian LHS whereas the strata of the same age are thick and well developed in the THS (Brookfield, 1993). This hypothesis also does not explain why the apparently younger- and higher-grade late Proterozoic–Cambrian GHC thrust over the older but structurally higher Paleoproterozoic LHS along most of the MCT in Nepal (DeCelles et al., 2000).

#### 6.1.2. Separate basin model (Fig. 18B)

The LHS and THS were deposited in two separate but coeval basins divided by the GHC (Saxena, 1971). At least in the NW Indian Himalaya, the results of sedimentological, biostratigraphic, and isotopic anal-

yses of Cambrian strata do not support this hypothesis (Myrow et al., 2003).

#### 6.1.3. Accreted terrane model (Fig. 18C)

Precambrian–Cambrian LHS and GHC strata belong to separate terranes that were assembled together by collision in the Early Ordovician (DeCelles et al., 2000; Gehrels et al., 2002, 2003). This hypothesis has the advantage of explaining the younger-over-older relationship across the MCT, but fails to account the similarities in fauna assemblage and detrital zircon ages in Cambrian strata of both the LHS and THS (Myrow et al., 2003). Building upon DeCelles et al. (2000), Gehrels et al. (2003), further suggest that the THS was shortened by a south-directed imbricate thrust belt; the early Paleozoic crustal thickening event also generated 510–470 Ma granites that intrude the basal part of the THS. This proposal is in contrast to the geochemical results of Miller et al. (2001) who show that Cambro-Ordovician granites in NW India lack the signatures of either arc or collision-related magmatism, but instead have rift-related isotopic characteristics.

#### 6.1.4. Carboniferous-extension model (Fig. 18D)

The main difference between the LHS and THS is the lack of Ordovician to Carboniferous deposits in the LHS. However, the two sections share similar depositional histories after the Permian (Brookfield, 1993). If the LHS did receive sediments during the Ordovician to Carboniferous as in the THS, the thickness of the missing strata may be as much as ~6 km as in the Kashmir and Lahul Himalaya (Fig. 3). This observation has been attributed to either late Carboniferous glacial erosion or rifting (Brookfield, 1993; Vannay and Steck, 1995; Garzanti, 1999). If the rifting model holds, then it is possible that the LHS and the GHC strata were juxtaposed by a Carboniferous north-dipping normal fault system prior to Cenozoic deformation. The fault system places the older LHS strata in the footwall and the younger GHC strata in the hanging wall: the footwall uplift caused removal of the lower Paleozoic strata in the LHS. During the Indo-Asian collision, the MCT may have reactivated this old normal fault and places younger but higher-grade GHC rocks over older but lower-grade LHS strata. Perhaps Pakistan Himalaya

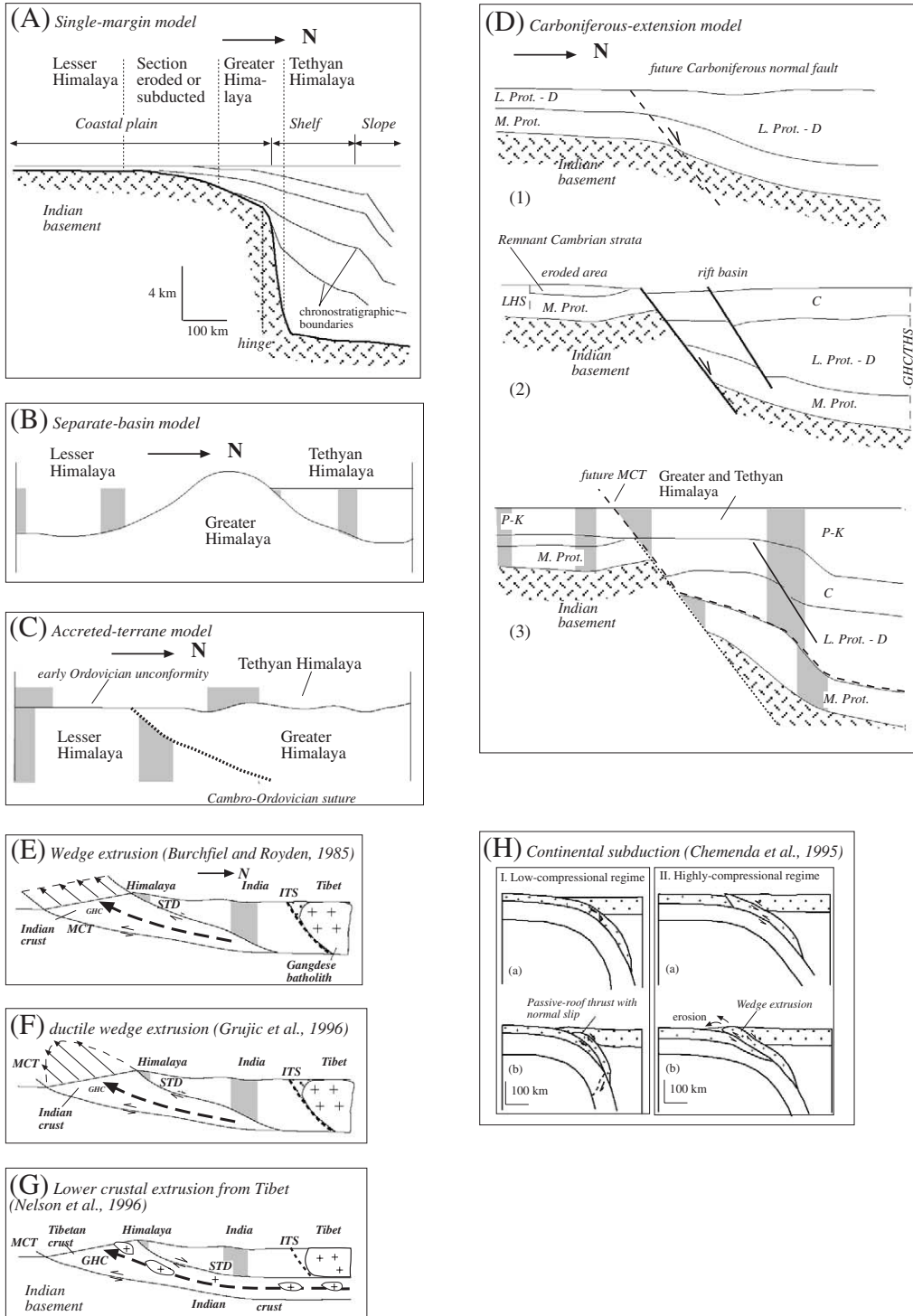


Fig. 18. Selected models for the development of the Himalayan orogen.

Table 9  
Comparison of models for emplacement of GHC

	<b>Wedge Extrusion</b>	<b>Channel Flow</b>	<b>Continental Subduction</b>	<b>Reactivation of MCT from Old Suture</b>
<i>Structural geometry and relationships among major Himalayan structures</i>	1. MCT and STD merge down-dip. 2. Hanging wall and footwall ramps are required for both MCT and STD.	MCT and STD are subparallel and extend beneath Tibet north of Indus-Tsangpo suture	1. For low compression and high slabpull, MCT and STD merge both up-dip and down-dip 2. For high compression and low slabpull, STD and MCT merge down-dip	MCT was preexisting weakness originated from a suture zone
<i>Protolith of GHC</i>	Indian crust	Tibetan crust	Indian crust	An independent terrane between Asia and India
<i>Exhumation history</i>	Exposure of high-grade Indian crust (=GHC) did not occur after activation of MCT and STD	Exposure of high-grade Indian crust (=GHC) did not occur after activation of MCT and STD	Exposure of high-grade Indian crust (=GHC) occurred prior to activation of MCT and STD during first phase upward return of subducted Indian crust	GHC could have exposed as early as Cambro-Ordovician time during Paleozoic thrusting
<i>Timing and style of deformation</i>	Coeval motion on MCT and STD  Rigid wedge: Discrete deformation on MCT and STD  Ductile wedge: Distributed deformation throughout GHC during motion on MCT and STD	Coeval motion on MCT and STD  Distributed deformation throughout GHC during motion on MCT and STD	Coeval motion on MCT and STD  GHC behaves as a relatively coherent block during upward motion via slip along MCT and STD	Early phase of high-grade metamorphism in GHC occurred in Paleozoic during first-phase motion on MCT. It was later superposed by Cenozoic metamorphism during reactivation of MCT movement.
<i>Timing of syn-collisional magmatism in Tibet</i>	No prediction	Magmatism in southern Tibet initiated prior to or within a few m.y. immediately after motion on MCT and STD	Magmatism in southern Tibet initiated synchronously at the start of GHC emplacement and motion on MCT and STD	Early Paleozoic movement on MCT could have been related to widespread Cambro-Ordovician contraction in the Himalaya
<i>Inconsistencies with observations and uncertainties in model testing.</i>	1. MCT and STD also merge updip in western and eastern Himalaya. 2. No STD footwall cutoff has been recognized. 3. It remains uncertain whether STD and MCT merge down-dip. 4. Multiple top-N and top-S shear on STD.	1. Uncertain whether partially melting in southern Tibet is restricted to rift zones only or over entire Tibet. 2. No Gangdese batholith signature of Tibetan crust in GHC and North Himalayan antiform where GHC is exposed.	1. No igneous flare up at 25-20 Ma in southern Tibet when GHC was emplaced along MCT. 2. Lack of records of UHP metamorphism in GHC during motion on MCT in Miocene.	1. Difficult to explain correlative Late Precambrian-Cambrian stratigraphy across MCT in western Himalaya. 2. Lack of early Paleozoic melange complex along MCT. 3. Geochemistry of Cambro-Ordovician granites indicate extensional origin.

would be a good testing ground for this hypothesis where the original contacts between Himalayan stratigraphic sequences are well preserved.

## 6.2. Kinematic models for emplacement of the Greater Himalayan Crystalline Complex

### 6.2.1. Wedge extrusion and channel flow

Understanding the evolution of the Himalayan orogen has been centered on how high-grade metamorphic rocks (mostly GHC) in its core were emplaced from lower crustal levels to their current position. Heim and Gansser (1939) attribute exposure of the GHC to motion on the MCT. The later discovery of the STD (Burg et al., 1984a) has led to the suggestion that the GHC was extruded as a rigid or penetratively deformed ductile wedge within Indian crust (Burchfiel and Royden, 1985; Hodges et al., 1992, 1996; Burchfiel et al., 1992; Grujic et al., 1996; Grasemann and Vannay, 1999; Grasemann et al., 1999; Vannay and Grasemann, 2001) (Fig. 18E and F). This model will be discussed more fully in Section 6.9 below. It has also been proposed that the GHC was transported from partially molten Tibetan crust of Asia to the Himalayan orogen of India via middle crustal flow (Nelson et al., 1996; Hodges et al., 2001; Beaumont et al., 2001, 2004; Jamieson et al., 2004; Grujic et al., 2002) (Fig. 18G), possibly as a result of topographic collapse (e.g., Dewey, 1988).

### 6.2.2. Continental subduction

To investigate the consequence of continental subduction, Chemenda et al. (1995, 2000) performed analogue experiments to simulate the Indo-Asian collision. They present two interesting end-member cases: one under low compressional force with strong down-going slabpull and the other under high compressional force with weak slabpull. In the first case, they simulate a large slice of Indian continental crust to be subducted steeply to a depth >150 km and is later detached from the underlying mantle lithosphere and extruded upward to upper crustal levels (Fig. 18H). The return of the subducted crustal section is accomplished by motion along a south-directed thrust below and a north-directed passive-roof fault with normal slip above. In the second case, wedge extrusion of the deeply subducted continental crust is induced by erosion above the sub-

duction zone (Fig. 18H). Using the experimental results as a guide, Chemenda et al. (2000) speculate that upward return of deeply subducted Indian crust occurred at about 50–45 Ma, while emplacement of the GHC at 25–20 Ma was triggered by breakoff of the subducted Indian continental mantle lithosphere (c.f., Davies and von Blanckenburg, 1995; Ernst and Liou, 1995). Chemenda et al. (2000) further relate the slab breakoff at 25–20 Ma to possibly extensive partial melting in the Tibetan crust. Slightly different from this model, Kohn and Parkinson (2002) envision breakoff of the Indian oceanic slab to have occurred at the start of the Indo-Asian collision, which may have caused widespread Eocene volcanism in southern Tibet (also see Miller et al., 1999; Yin and Harrison, 2000).

### 6.2.3. MCT reactivated from a Paleozoic suture

The Cenozoic MCT may have reactivated from an early Paleozoic suture (DeCelles et al., 2000) and high-grade metamorphism of the GHC may have occurred in part during Cambro-Ordovician time (Gehrels et al., 2003). This proposal is mainly based on U–Pb detrital zircon ages of the GHC found to be younger than the depositional age of the Proterozoic LHS. This model explains why the younger but higher-grade GHC metamorphic rocks are currently juxtaposed over older and lower-grade LHS strata across the MCT in the central Himalayan orogen.

### 6.2.4. Model predictions and comparison

The five kinematic models discussed above (Fig. 18) make specific predictions about the timing of deformation, structural geometry, exhumation history, GHC protolith, and timing of post-collisional magmatism in southern Tibet (Table 9). The major problem with the wedge extrusion model is that the MCT and STD merge in the up-dip direction as indicated by map relationships in the western and eastern Himalaya (Figs. 7 and 11). The major uncertainty with the channel flow model is whether or not the inferred partially molten middle Tibetan crust was restricted to localized regions below the north-trending rifts (Yin, 2000; Yin and Harrison, 2000). This alternative hypothesis is supported by recent seismic surveys in central Tibet that shows no evidence of bright spots outside main Tibetan rifts (Haines et al., 2003). An-

other issue with the channel flow model is that there have been no zircon ages of the Gangdese batholith found in the GHC (DeCelles et al., 2000), which is the dominant type of lithology along the southern margin of the Tibetan plateau (Fig. 2A).

The continental subduction model of Chemenda et al. (2000) requires an igneous flare up in southern Tibet at 25–20 Ma during slab breakoff. However, geologic observations from southern Tibet do not support the occurrence of such dramatic event at the time. Instead, semi-continuous and gradual southward migration of igneous activities from central to southern Tibet has been recorded since the start of the Indo-Asian collision (e.g., Deng, 1998; Miller et al., 1999; Harrison et al., 2000; Ding et al., 2003). Although reactivation of the MCT along a Paleozoic suture zone explains the age relationship across the MCT in Nepal, extrapolation of this interpretation to the western Himalayan orogen is problematic, because the MCT footwall and hanging wall preserve continuous LHS and THS strata and unmetamorphosed sedimentary and igneous rocks of the GHC (Pogue et al., 1999; DiPietro and Pogue, 2004).

### 6.3. Models for Himalayan inverted metamorphism

#### 6.3.1. Kinematic models

Kinematic models for the occurrence of Himalayan inverted metamorphism may be divided into two types: those relating metamorphism to Cenozoic deformation and those ascribing metamorphism to pre-Cenozoic geologic processes. For the first kind, one may divide them further into those emphasizing post-metamorphism deformation and those that do not (Fig. 17). The syn-metamorphism models include rigid-wedge translation along a basal thrust (Molnar and England, 1990), flat-ramp thrusting with or without erosion (Shi and Wang, 1987; Ruppel and Hodges, 1994; Harrison et al., 1998b), and rigid-wedge translation along a basal thrust coupled with basal accretion and surface erosion (Royden, 1993; Henry et al., 1997). The post-metamorphism models include large-scale recumbent folding of isograds either in the MCT hanging wall or footwall (Heim and Gansser, 1939; Gansser, 1964; Searle and Rex, 1989; Johnson et al., 2001), coeval simple-shear deformation across a broad shear zone within the basal MCT hanging wall (Jain and Manickavasagam, 1993; Hubbard, 1996),

progressive younging of simple-shear deformation in the MCT zone (Harrison et al., 1998b), general-shear deformation in the MCT zone and GHC with emphasis on the role of vertical flattening (Grasemann et al., 1999; Grasemann and Vannay, 1999; Law et al., 2004), and duplex development in the MCT footwall (Robinson et al., 2003). The key differences among the major models for inverted metamorphism are summarized in Table 10.

Contrary to the common belief that the Himalayan inverted metamorphism is a Cenozoic phenomenon, Marquer et al. (2000) and Gehrels et al. (2003) show that at least locally garnet-bearing high-grade metamorphism in the Himalaya occurred prior to ~476 Ma. They further suggest that sillimanite-grade metamorphism common in the middle and upper part of the GHC and spatially adjacent to 510–470 Ma granites may be induced by early Paleozoic plutonic emplacement instead of Cenozoic thrusting. This model makes specific predictions about the spatial correlation between early Paleozoic plutons and sillimanite-grade metamorphism in the Himalaya.

#### 6.3.2. Thermal models

Based on comparison with thermal models of oceanic subduction, LeFort (1975) suggests that the Himalayan inverted metamorphism was induced by emplacement of a hot thrust sheet over a cold footwall. This is the well-known “hot-iron” model and the first conceptual model that introduces a testable physical mechanism for Himalayan metamorphism.

The current thermal models may be divided into the following four categories:

- (1) models considering thrust-ramp and fault-bend fold geometry with either syn-thrusting or post-thrusting erosion (Shi and Wang, 1987; Ruppel and Hodges, 1994; Harrison et al., 1998b);
- (2) models considering the role of frictional heating on the MCT (Molnar and England, 1990; England et al., 1992; Royden, 1993; Harrison et al., 1998b);
- (3) models considering advective heat transfer due to basal accretion and surface erosion (Royden, 1993; Henry et al., 1997); and
- (4) models considering contrast in thermal conductivity across the GHC-THS contact (Jaupart and Provost, 1985; Pinet and Jaupart, 1987) (Fig. 17).

Table 10  
Comparison among kinematic models for Himalayan inverted metamorphism

	Thrust geometry	Strain distribution	Timing of deformation
Rigid wedge translation	Wedge-shaped thrust sheet	No internal deformation in hanging wall	Syn-metamorphism
Flat-ramp thrusting	Staircase-shaped thrust sheet	Flexural slip folding in hanging wall as it crosses thrust ramp	Syn-metamorphism
Rigid wedge translation with basal accretion and erosion	Wedge-shaped, constant self-similar geometry despite flux of mass in and out of wedge	No internal deformation in hanging wall	Syn-metamorphism
Recumbent folding	No prediction of thrust geometry	Large strain in MCT hanging wall as measured by fold amplitude and wavelength >10 km	Post-metamorphism
Simultaneous simple shear across MCT zone in GHC	No prediction of thrust geometry	Simple shear strain in lower MCT hanging wall	Post-metamorphism coeval shear motion
Progressive simple shear across MCT zone in LHS	No prediction of thrust geometry	Simple shear strain in upper MCT footwall	Post-metamorphism Shear deformation becomes younger downward
General shear across MCT zone	No prediction of thrust geometry	Combined simple and pure shear strain across MCT zone and its hanging wall	Post-metamorphism
Duplex development	Staircase-shaped thrust sheet	Discrete shear in MCT footwall and flexural-slip as individual horses move across thrust ramps	Post-metamorphism

Perhaps Shi and Wang (1987) are the first to test the simple hot-iron model of LeFort (1975) and show that inverted metamorphism could not be achieved by motion along major thrusts under realistic fault slip rates (also see Ruppel and Hodges, 1994).

The most important difference among the above models is the location of the maximum temperature and pressure condition with respect to the MCT. For the end-member frictional heating model (Molnar and England, 1990), the maximum  $P$ – $T$  condition is recorded along the MCT fault. In contrast, when basal accretion is considered, the maximum  $P$ – $T$  condition would have occurred in the hanging wall of the MCT (Royden, 1993; Huerta et al., 1998) (Fig. 19). However, one should keep in mind that this prediction is an artifact of progressively lowering the basal slip surface as the footwall materials are sequentially added from the MCT footwall to the MCT hanging wall. Thus, the lithologically defined MCT should be spatially close to or at the thermal maximum. The contrast is striking in the predicted  $P$ – $T$  distribution between the recumbent folding model and the thermal models considering frictional heating and accretion/

erosion. The recumbent folding model predicts inversion of both pressure and temperature while the frictional-heating and accretion–erosion models predict only temperature inversion (e.g., Daniel et al., 2003) (Fig. 19).

### 6.3.3. Coupled thermal and mechanical model

The problem with the above thermal models is that deformation in the MCT hanging wall and MCT footwall is prescribed. Thus, the energy equation (i.e., heat-transport equation) is solved without considering rock rheology and force balance. This problem was overcome by the study of Jamieson et al. (1996, 2004) (Fig. 17) who solved the coupled energy and momentum equations and was able to simulate the Himalayan inverted metamorphism with a range of rheological parameters determined by laboratory experiments.

### 6.4. Models for Cenozoic Himalayan anatexis

The occurrence of Cenozoic anatexis is not well understood, but most workers have related its occur-

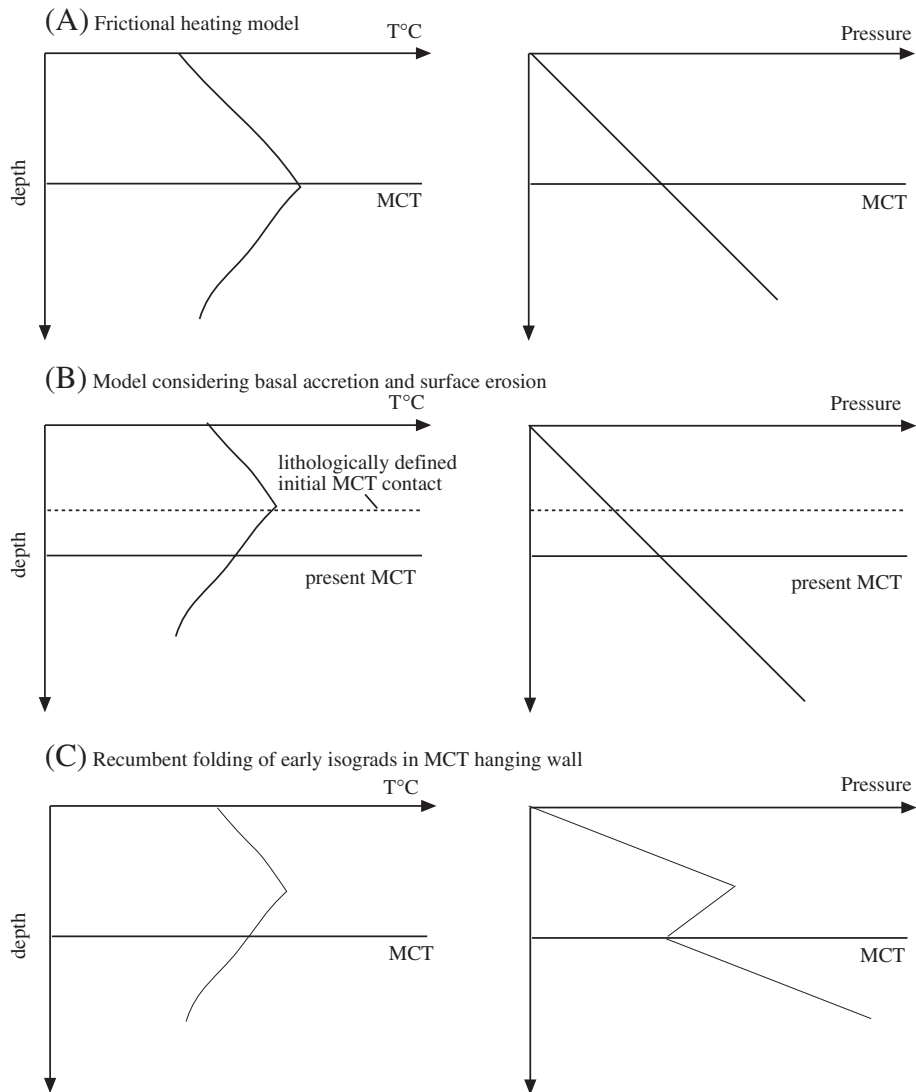


Fig. 19. Distribution of  $P-T$  for various thermal and tectonic models for Himalayan inverted metamorphism.

rence to Himalayan inverted metamorphism (see summary by Harrison et al., 1999). The following models have been proposed:

- (1) emplacement of a hot thrust sheet along the MCT and infiltration of fluids from the MCT footwall (LeFort, 1975);
- (2) delamination of mantle lithosphere beneath the Himalayan orogen (Bird, 1978);
- (3) thermal blanketing effect causing heat focusing at the base of the THS (Jaupart and Provost, 1985; Pinet and Jaupart, 1987);
- (4) frictional heating on the MCT (England et al., 1992) coupled with progressive downward migration of shear zones and muscovite breakdown reaction (Harrison et al., 1998b);
- (5) decompressional melting due to motion on the STD (Harris and Massey, 1994); and

- (6) translation of partially molten middle crust from Tibet to the Himalayan orogen (Nelson et al., 1996).

Strengths and weaknesses of these models were discussed in detail by Harrison et al. (1999).

#### 6.5. Models for development of Lesser Himalayan thrust belt

Since the classic work of Valdiya (1980), the development of the Lesser Himalayan thrust belt has been linked with motion along the MCT. With respect to the age of the MCT, the current models may be divided into those emphasizing forward development of thrusts (DeCelles et al., 2001) and those considering out-of-sequence thrusting (Harrison et al., 1997a, 1998b; Johnson et al., 2001) (Fig. 17). Robinson et al. (2003) discuss in detail the differences of the two models in their predicted thermal and kinematic histories.

#### 6.6. Models for the development of the North Himalayan antiform and gneiss domes

Along the North Himalayan Antiform, the Kangmar dome has received the most attention. Its development has been alternatively related to north-directed detachment faulting (Chen et al., 1990), thrust duplex formation (Burg et al., 1984b; Makovsky et al., 1999), pure-shear extension (Lee et al., 2000), development of a major north-dipping thrust ramp along the Main Himalayan Thrust (Wu et al., 1998; Hauck et al., 1998) or a south-dipping ramp along the Great Counter Thrust (Makovsky et al., 1999), diapiric flow due to gravitational instability (LeFort et al., 1987; LeFort, 1996 and references therein), and upwelling of ductile lower crust under horizontal compression (Yin et al., 1999).

Lee et al. (2000) show that while ductile deformation over the dome has accommodated significant local north–south extension, its cooling history is most compatible with thrusting of colder materials beneath the Kangmar dome between 15 and 10 Ma. This interpretation is broadly consistent with the early work of Maluski et al. (1988) who considered the dome to have cooled between 20 and 13 Ma. This age of dome formation is more consistent with its being related to Miocene motion on the south-

dipping Himalayan backthrust (= Great Counter Thrust) as suggested by Makovsky et al. (1999) rather than to the north-dipping Gyrong–Kangmar thrust as envisioned by Lee et al. (2000). This is because the Gyrong–Kangmar thrust lies in the Eocene–Oligocene Tethyan Himalayan fold-thrust belt (Ratschbacher et al., 1994) and its age is probably Eocene, that is, too old to be related to the middle Miocene dome formation. Another problem of relating the development of the Gyrong–Kangmar thrust to the development of the Kangmar dome as part of the North Himalayan Antiform (NHA) is that this fault is rather limited in its lateral extent in south-central Tibet (e.g., Ratschbacher et al., 1994), whereas the NHA covers the Himalayan orogen between its two syntaxis (Fig. 2A).

Uncertainties on the origin of North Himalayan gneiss domes and the east-trending NHA are largely due to the fact that the deep crustal relationships among the MCT, STD, and GCT are poorly constrained. Results from INDEPTH surveys are inconclusive (Hauck et al., 1998): the STD could either join the MCT downward along the Main Himalayan Thrust or flatten into a ductile shear zone in the middle crust. The first interpretation would support the prediction of the wedge extrusion model of Burchfiel and Royden (1985) while the second would permit channel flow of Tibetan lower crust to the Himalaya (Nelson et al., 1996). It is also possible that the STD links with the coeval Great Counter Thrust via a subhorizontal shear zone in the middle crust beneath the Himalaya (Yin et al., 1994; Lee et al., 2000).

#### 6.7. Models for formation of the Himalayan syntaxes

The following models have been proposed for the development of the Himalayan syntaxes:

- (1) indentation of a promontory on the northern edge of the Indian continent (Burtman and Molnar, 1993);
- (2) crustal scale folding with the maximum compressional direction parallel to the Himalayan orogen (e.g., Burg et al., 1998);
- (3) oroclinal bending of major Himalayan thrusts (Bossart et al., 1988; Treloar et al., 1991; Treloar and Izatt, 1993);

- (4) development of a north-trending pop-up structure (Seeber and Pêcher, 1998; Schneider et al., 1999a);
- (5) duplex development (Ding et al., 2001); and
- (6) intersection of arc-shaped thrust belts (Fig. 17).

Each model appears to apply to the development of specific syntaxes. For example, the pop-up model explains well the pattern of rapid uplift over the Nanga Parbat syntaxis (Zeitler et al., 2001), while the duplex thrust model explains the map relationships of major ductile thrusts within the Namche Barwa syntaxis (Ding et al., 2001).

#### 6.8. Models for development of north-trending rifts

There are two schools of thought with regard to the mode of deformation associated with Neogene north-trending rifting in the Himalayan orogen: those who believe that extension is confined to the upper crust (e.g., Molnar and Lyon-Caen, 1989; Masek et al., 1994) and those who believe that extension involves the entire lithosphere of both Asian and Indian plates (e.g., Yin, 2000). The first model is mainly based on the inference that radially outward thrusting along the Himalayan arc is coupled with east–west extension and the observation that the rift shoulders have short wave-length topography, whereas the second model is based on the fact that the mantle lithosphere beneath the Himalayan orogen records extensional focal mechanisms, the Himalayan rifts are widely spaced requiring the involvement of the underneath mantle lithosphere, and isotopic composition of helium from geothermal springs in the southern Tibetan plateau that are characteristically derived from mantle sources (Hike et al., 2000).

There have been diverse mechanisms proposed for the origin of the north-trending Himalayan rifts. Besides the long tradition of relating radial spreading of the Himalayan arc to east–west Himalayan extension (Seeber and Armbruster, 1984; Klootwijk et al., 1985; Ratschbacher et al., 1994; Seeber and Pêcher, 1998), the following mechanisms have also been considered (Fig. 17): (1) topographic collapse of an overthickened crust (Molnar and Tapponnier, 1978; Dewey, 1988), (2) oblique subduction of the Indian continental lithosphere exerting a shear traction at the base of Tibetan lithosphere (McCaffery and

Nabelek, 1998), (3) concentrated compression on the central part of the Himalayan arc (Kapp and Guynn, 2004), (4) oroclinal bending of the subducting Indian continental lithosphere due to a bending moment induced by transpressional systems along the two shoulders of the north-moving Indian continent (the unbending model of Kapp and Yin, 2001), (5) eastward extrusion of northern Tibet (Armijo et al., 1986, 1989), (6) advective removal of thickened Tibetan mantle lithosphere (England and Houseman, 1989), and (7) a change in boundary conditions along the eastern margin of Asia in the late Miocene to early Pliocene (Yin, 2000).

Figs. 18I and 18J highlight the difference in predicted rift trends in the Himalayan orogen by the radial expansion model and the unbending model (Kapp and Yin, 2001). The first model predicts that rifts should be perpendicular to the trend of the Himalayan orogen everywhere. However, the observed trends of the Himalayan rifts do not fit this prediction. In the western Himalayan orogen, Neogene rifts (e.g., the Tso Moriri rift) trend in the N10–15°W direction and are at an angle of about 30° from the local trend of the Himalayan orogen (Fig. 1A). In the eastern Himalayan orogen, rifts trend at an angle of about 50–70° from the main trend of the Himalayan orogen (Fig. 1A). The trends of the Himalayan rifts are best explained by either the unbending model of Kapp and Yin (2001) or the concentrated compression model of Kapp and Guynn (2004). In the unbending model, the shape of the northern Indian continent has an arc geometry that concaves southwards opposite to curving direction of the Himalayan arc. The arc-shaped geometry of the subducted northern Indian continent is clearly mimicked by the hinge zone of the Himalayan foreland basin (Fig. 1A). Bending of the northern Indian continental margin by shear traction applied on the Chaman and Saigaing faults at its western and eastern ends predicts rifts trending in the northwest direction in the western Himalaya and in the northeast direction in the eastern Himalaya. The model also predicts possible east–west compression in the Himalayan foreland. Perhaps the nearly evenly spaced basement ridges trending at high angles to the Himalayan front may result from buckling under east–west compression during the bending of the northern Indian margin. The Kapp and Guynn model (2004) shows a similar mechanics to the unbending model by using the con-

centrated load on the Himalayan arc to generate bending stress north of the Himalayan front. However, the key difference of their model from the unbending model is that it does not require east–west contraction south of the Himalayan arc.

#### 6.9. Models for the overall evolution of the Himalaya

The existing models that account for the overall evolution of the Himalayan orogen are either based on analogue experiments (Chemenda et al., 2000) or numerical simulations (Beaumont et al., 2001), all in two dimensions (Fig. 17). The Beaumont et al. (2001) model represents a major advance in the Himalayan research in many respects. First, the dynamic model solves the coupled energy and momentum equations simultaneously and considers the role of partial melting and realistic nonlinear rock rheology. Second, the model considers the dynamic interaction between the development of the Himalayan orogen and the formation of the Tibetan plateau. Third, the model considers the possible role of climatic condition and the history and distribution of erosional intensity in controlling the timing and style of deformation and the evolution of thermal structures within the Himalayan–Tibetan orogen. The model has several important predictions and requirements:

- (1) The Tibetan plateau must have reached an elevation of  $>8$  km before the start of southward flow from the Tibetan lower crust to the Himalaya.
- (2) Initiation of the MCT and the STD and vertical extrusion of the GHC were entirely induced by highly localized erosion with high rates (i.e., up to 10 mm/yr) in the southern Himalayan front starting at  $\sim 37$  Ma.
- (3) The MCT hanging wall was eroded as soon as it reached the surface above a thrust ramp.
- (4) The strength of the upper crust in the North Himalaya (= THS) is exceedingly weak, with an angle of internal friction between  $5^\circ$  and  $10^\circ$ .
- (5) The STD as the upper slip surface for southward flow beneath the Himalaya has a unidirectional slip history; that is, top-to-the-south sense of shear was operating throughout its movement history.

- (6) Subduction of Indian continental lithosphere beneath Asia was flat since the initiation of the Indo-Asian collision.

The major problems with this model are as follows:

(1) It does not explain the occurrence of Eocene UHP metamorphism during the early stage of Indo-Asian collision.

(2) There is no geologic evidence for the Tibetan plateau to have reached 8-km elevation and subsequently collapsed to the current height, because the magnitude of Neogene and thus Cenozoic east–west extension over Tibet is rather small (i.e., no more than 10% and most likely in the range of 2–5%, see Taylor et al., 2003).

(3) The assumption that the THS is weak is inconsistent with field observations. The cutoff angles in the Tethyan Himalayan thrust belt, which are the direct measurement of the coefficient of internal friction, are in the range of  $20$ – $30^\circ$  (Ratschbacher et al., 1994; Murphy and Yin, 2003), significantly greater than  $5$ – $10^\circ$  as required by the Beaumont et al. (2001) model.

(4) The predicted MCT geometry with a single ramp below the erosional front is inconsistent with the observed long thrust flat extending towards the Himalayan foreland as expressed by the occurrence of the Lesser Himalayan Crystalline Nappes (Fig. 2A).

(5) The erosion rates assumed in the model appear to be too high (10 mm/yr) over the steep southern Himalayan front from 37 Ma to the present. As shown in Table 8, the denudation rate is mostly below 1 mm/yr for most of the Himalayan history except since  $\sim 7$  Ma in the central Himalaya when the rate reaches to  $\sim 3$ – $5$  mm/yr.

(6) The timing of the abrupt increase in erosional rates in the central Himalaya occurred much later than the initiation age of the MCT, which was already active by 20 Ma (Hubbard and Harrison, 1989). That is, there is no temporal correlation between the underthrusting along the MCT and an increase in erosional rates.

## 7. Discussion

It is surprising that there have been no integrated tectonic models for the overall evolution of the Himalayan orogen and the Himalayan orogenic system

that account for along-strike variation of the Himalayan geology (Fig. 17). One reason is that the geologic studies and model testing are overly focused in the central Himalaya in the past three decades (e.g., LeFort, 1975; Burg and Chen, 1984; Burg et al., 1984a,b, 1987; Colchen et al., 1986; Pêcher, 1989; Chen et al., 1990; Schelling and Arita, 1991; Burchfiel et al., 1992; Schelling, 1992; Hodges et al., 1992, 1994, 1996, 2001; Ratschbacher et al., 1994; Yin et al., 1994, 1999; Makovsky et al., 1996, 1999; DeCelles et al., 1998a,b, 2001, 2002; Hauck et al., 1998; Upreti and LeFort, 1999; Lee et al., 2000; Johnson et al., 2001; Murphy et al., 2002; Murphy and Yin, 2003). As a result, interpretation of Himalayan geology such as the division of the GHC, THS, and LHS has been artificially enforced upon the geology of the western Himalayan orogen despite significant differences between the two regions (e.g., Steck, 2003; cf., DiPietro and Pogue, 2004). The along-strike variation in the Himalayan orogen in fact may provide important clues for its temporal evolution, an approach proven effective in the studies of many other orogenic belts in the world (e.g., Graham et al., 1975; Teng, 1990; Yin and Nie, 1993, 1996).

### 7.1. Geometry and structural relationship among the MCT, STD, and GCT

#### 7.1.1. MCT

Systematic examination of Himalayan geology reveals many first-order features with regard to the geometry and spatial variation of major Himalayan structures. In the western Himalaya of NW India, the MCT cuts up section in the hanging-wall westward across the Mandi Lateral Ramp (Fig. 2A). Due to the presence of the ramp, the MCT hanging-wall rocks change from the high-grade GHC east of the ramp to the low-grade THS west of the ramp. The MCT and the overlying STD are both folded concordantly in the western and eastern Himalaya (Figs. 2A, 7, and 12). The folding event in NW India probably started in the late Miocene and early Pliocene between 10 and 5 Ma, as recorded by the cooling patterns in the Kishtwar and Kullu–Larji–Rampur windows (Fig. 14).

The MCT root zone was reactivated in the late Miocene and Pliocene between 7 and 2 Ma (Harrison et al., 1997a; Catlos et al., 2001, 2002a). The renewed motion on the MCT in its root zone apparently did not

affect the MCT flat extending far south into the Lower Himalaya (Johnson et al., 2001) (see cross-section across the Kathmandu Nappe in Fig. 2E). Instead, the MCT flat may have been passively folded by deformation related to reactivation of the MCT root zone and possibly out-of-sequence thrusts in the Lesser Himalayan thrust belt. These relationships are important in that although the MCT zone can be traced as a regionally continuous structure, different portions of the fault in its transport direction may have different slip histories.

The MCT hanging wall in the eastern Himalayan orogen is dominated by high-grade gneisses and schists (e.g., Liu and Zhong, 1997; Ding et al., 2001; Grujic et al., 2002). In contrast, the MCT hanging wall in the western Himalayan orogen is dominated by low-grade phyllite and unmetamorphosed Proterozoic and Phanerozoic strata (Pogue et al., 1999). The differential denudation in the MCT hanging wall from the east to west along Himalayan strike may have resulted from one or a combination of the following factors:

- (a) an eastward increase in the magnitude of slip along the MCT due to counter-clockwise rotation of India with respect to Asia during Indo-Asian collision (Guillot et al., 1999);
- (b) an eastward change in the dip angle of the subducted Indian continent (Guillot et al., 1999); and
- (c) an eastward increase in the magnitude of exhumation due to regional variation of climatic conditions (e.g., Finlayson et al., 2002).

Cooling of the GHC in the MCT hanging wall below 350 °C appears to have started earlier in the western Himalaya (~29 Ma in Zaskar) than in the central and eastern Himalaya (<~21 Ma) (Figs. 13–16; also see Guillot et al., 1999). If movement along the MCT and STD was responsible for exhumation in the Himalaya, then the initiation of the MCT and STD may have started first in the west and then propagated to the east, possibly in response to diachronous collision between India and Asia. This conclusion is opposite to that reached by DiPietro and Pogue (2004) who consider that the initiation of the MCT was propagating westward from the central Himalaya in the early Miocene to the Pakistan Himalaya in the late Miocene and Pliocene. Clearly more research needs to be done to address this important question.

### 7.1.2. South Tibet Detachment (STD)

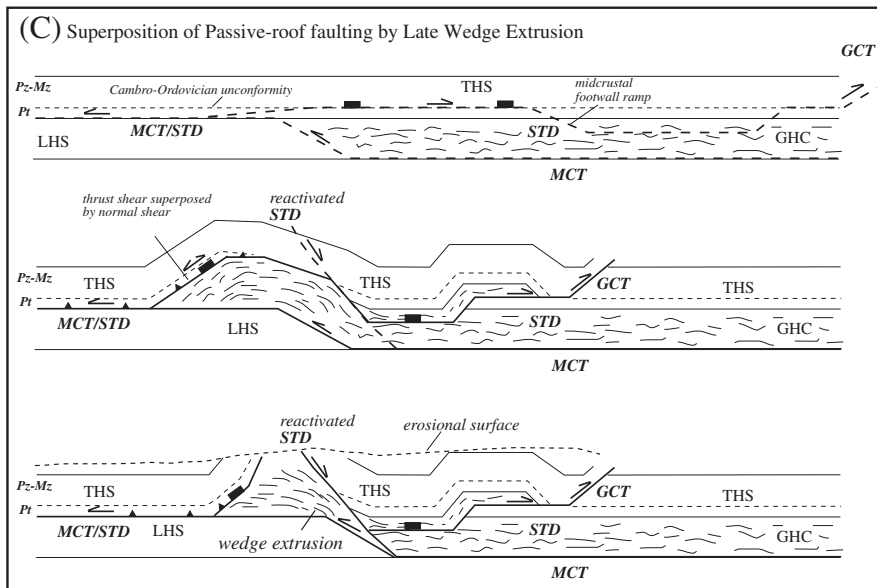
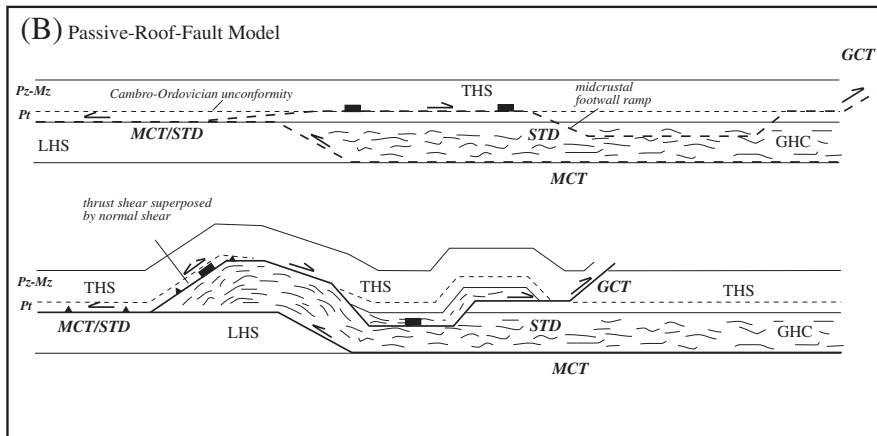
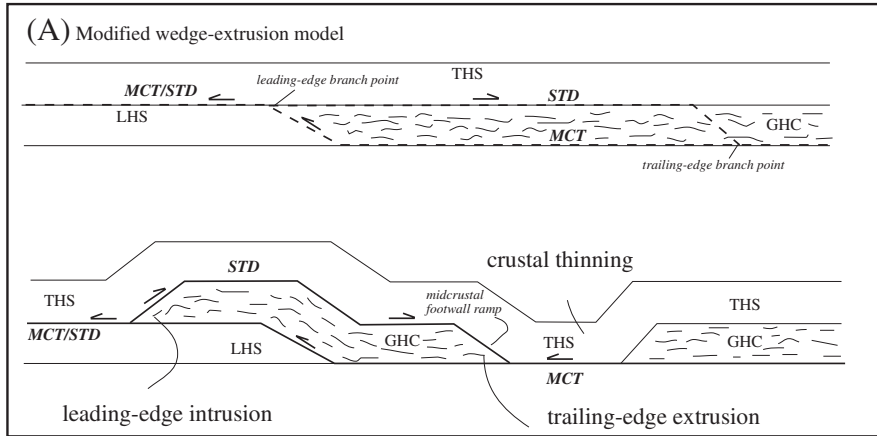
Everywhere exposed, the STD follows approximately the same stratigraphic position below the upper Proterozoic to Cambro-Ordovician strata of the basal THS. The consistent exposure of the fault at the same stratigraphic position over a distance of >60–100 km in the fault transport direction suggests that the exposed segment of the fault over much of the Himalaya is a hanging-wall flat. In most of the Himalaya (Nepal and Bhutan), the metamorphic grade in the upper GHC decreases systematically towards the STD and share a similar metamorphic grade (e.g., typically biotite grade) (e.g., LeFort, 1996; Daniel et al., 2003). This relationship suggests that the STD in these regions is essentially a footwall flat. The only possible footwall ramp for the STD is exposed in the Zaskar region, where the Zaskar shear zone locally truncates metamorphic isograds in its footwall (Fig. 5) (e.g., Herren, 1987; Dèzes et al., 1999; cf. Patel et al., 1993). These isograds may represent paleo-isotherms that were originally sub-horizontal and were subsequently cut by a younger shear zone. Because these isograds were formed at middle and lower crustal levels (i.e., in the sillimanite, staurolite, and garnet grades), the inferred STD ramp must be present at a depth below ~15–20 km. Due to a possible large displacement (>10s km) along the Zaskar shear zone, the corresponding hanging-wall ramp in the lower crust may now lie beneath the Himalaya north of the surface trace of the Zaskar shear zone (Fig. 20B).

Because no footwall cutoffs of the upper crustal rocks across the Tethyan Himalayan strata are present below the STD, the distance between the northernmost fault trace and the STD klippen carrying the Tethyan Himalayan strata may not be used to estimate its total slip. The only exception of such situation appears to occur in Zaskar where the THS may have been metamorphosed and incorporated into the high-grade GHC (Honegger et al., 1982). However, the high-grade THS there could be klippe of the ST that lies structurally above the GHC. The presence of a pure-shear component across the STD zone (Grujic et al., 1996; Grasemann et al., 1999; Law et al., 2004) also makes the slip determination considering only simple-shear deformation an upper bound (e.g., Herren, 1987; Dèzes et al., 1999). Because of these problems, the exact slip along the STD remains unknown.

Geologic relationships in the western and eastern Himalaya suggest that the STD merges and possibly intersects the MCT in the up-dip direction (i.e., to the south) (Figs. 7 and 11). This geometric relationship departs from that for a typical North American Cordillera-style extensional detachment fault (e.g., Lister and Davis, 1989; Wernicke, 1992; Yin and Dunn, 1992) and may imply a different kinematic history for the STD. The difference between the STD and a typical Cordilleran detachment fault system is also indicated by the lack of syn-extensional, supradetachment basins (e.g., Friedmann and Burbank, 1995; Dorsey and Becker, 1995; Forshee and Yin, 1995; Diamond and Ingersoll, 2002; Sozbilir, 2002). For example, along the entire length of the 150-km-long Zaskar shear zone, there is not a single syn-detachment sedimentary basin present (Patel et al., 1993). The sparsely distributed Miocene–Pliocene basins that have been related to the STD in southern Tibet by Burchfiel et al. (1992) and Hodges (2000) are all located in or immediately next to major Neogene north-trending rifts, making it difficult to differentiate whether the sedimentation was related to north-directed STD faulting or younger Neogene east–west extension. This problem may be addressed by detailed sedimentological studies in the near future.

### 7.1.3. Relationship between the STD and MCT

The wedge extrusion model predicts the MCT and STD to diverge upward to the south but intersect with one another at depth to the north (Burchfiel and Royden, 1985). When considering the geologic relationships observed in the Zaskar and Bhutan Himalaya, this model may require revision in that the MCT and STD may also join one another to the south in their up-dip direction. This requires that the GHC be enclosed completely by the MCT and STD. In the context of this structural framework, movement on the MCT and STD would have caused southward extrusion of the GHC at its trailing edge and coeval southward intrusion or wedging along its leading edge (Fig. 20A). This kinematic model is similar to that proposed by Yin (2002) for the emplacement of the Pelona–Orocopia schist during Late Cretaceous–early Tertiary low-angle subduction of the Farallon plate beneath the North American craton. Although the model in Fig. 20A has several similarities to the classic wedge extrusion model of Burchfiel and Roy-



den (1985), it requires significant exhumation of the GHC by eroding off first the THS without the aid of normal faulting along the STD. The revised wedge extrusion model also requires the crust at the trailing edge of the GHC wedge to be thinned due to the presence of a normal fault ramp in the middle crust and thickened at the leading edge of the wedge due to the presence of a thrust ramp (Fig. 20A).

#### 7.1.4. Relationship among the STD, MCT, and GCT

The modified wedge extrusion model (Fig. 20A) assumes that the STD was unrelated to the development of the south-dipping Great Counter Thrust in the North Himalaya. However, the GCT is one of a few Himalayan structures that can be traced along the entire length of the orogen (Fig. 2A). It was active between 25 and 9 Ma (Harrison et al., 2000), coeval with motion along the MCT and STD and the development of the NHA. The fault has a minimum of 38-km slip in SW Tibet (Murphy and Yin, 2003) and possibly >60 km in SW Tibet because the Gangdese batholith may have thrust underneath the Yala Xiangbo gneiss dome (Aikman et al., 2004). The large magnitude of slip along the GCT requires the fault to interact with the Himalayan structures in the middle and lower crust. Because the GCT roots southward, it may be linked with the coeval STD that roots to the north (Yin et al., 1994). That is, movement along the MCT, STD, and GCT would have caused southward wedging of the GHC between the LHS and THS (Fig. 20B). This process is similar to the wedge tectonics or the development of a triangle zone in the southern Canadian foreland fold and thrust belt (Price, 1986). In Fig. 20B, the STD acts as a passive-roof fault (e.g., Banks and Warburton, 1986). Several workers also refer the STD as a passive-roof fault assisting wedge extrusion of the GHC (e.g., J.D. Walker et al., 1999; Searle et al., 1999a; C.B. Walker et al., 2001; Vannay and Grasemann, 2001; Vigneresse and Burg, 2002). However, these authors did not consider the possibility that the STD and MCT may merge with one another to the south in their up-dip direction.

It is also possible that the wedge extrusion and passive-roof faulting occurred as two separate events (Fig. 20C). That is, the STD was initiated as a passive-roof fault and was later reactivated during southward wedge extrusion of the GHC. This model predicts slower cooling during the passive-roof-faulting stage and rapid cooling during wedge extrusion for the GHC.

One potential area to examine the deep crustal relationship among the STD, MCT, and GCT is the eastern Himalayan syntaxis (Zhang et al., 1992; Burg et al., 1998; Zeitler et al., 2001; Ding et al., 2001), where a tilted north–south crustal section of the Himalaya is exposed (e.g., Burg et al., 1998; Burchfiel et al., 2002) (Fig. 12). Because granulite facies of lower crustal rocks are present in the area, one may expect the MCT to merge with the STD in map view towards the syntaxis if the GHC were extruded as a wedge in the fashion of Burchfiel and Royden (1985). The existing geologic maps of the region show that the two faults diverge from one another as they approach the syntaxis: the STD appears to terminate west of the syntaxis and merge with the GCT whereas the MCT lies south of the syntaxis (Fig. 12) (e.g., Ding et al., 2001; Gururajan and Choudhuri, 2003). Although the MCT is bent about 90° around the syntaxis, the absence of the STD east of the eastern Himalayan syntaxis (e.g., Gururajan and Choudhuri, 2003) also suggests that the STD is most likely an upper crustal structure and does not root deeply and merge with the structurally lower MCT. The structural relationships around the eastern syntaxis are consistent with the “ski-jump” model of Yin et al. (1994) in which northward down-slope motion of the north-dipping STD is accommodated by northward up-slope motion on the south-dipping GCT.

#### 7.1.5. Alternation of top-north and top-south shear on the STD

Because the STD and shear zones directly below and above it experienced alternating top-south and

Fig. 20. Three possible models explaining STD and MCT merging with each other in the up-dip directions. (A) Leading edge intrusion model for the emplacement of the Greater Himalayan Crystalline Complex along the STD and MCT. It assumes that the STD joins the MCT both in the up-dip and down-dip directions. (B) Passive-roof-fault model that considers the STD joins with the GCT in its down-dip direction. (C) Early passive-roof faulting along the STD is superposed later by wedge extrusion and out-of-sequence motion in the STD ramp zone.

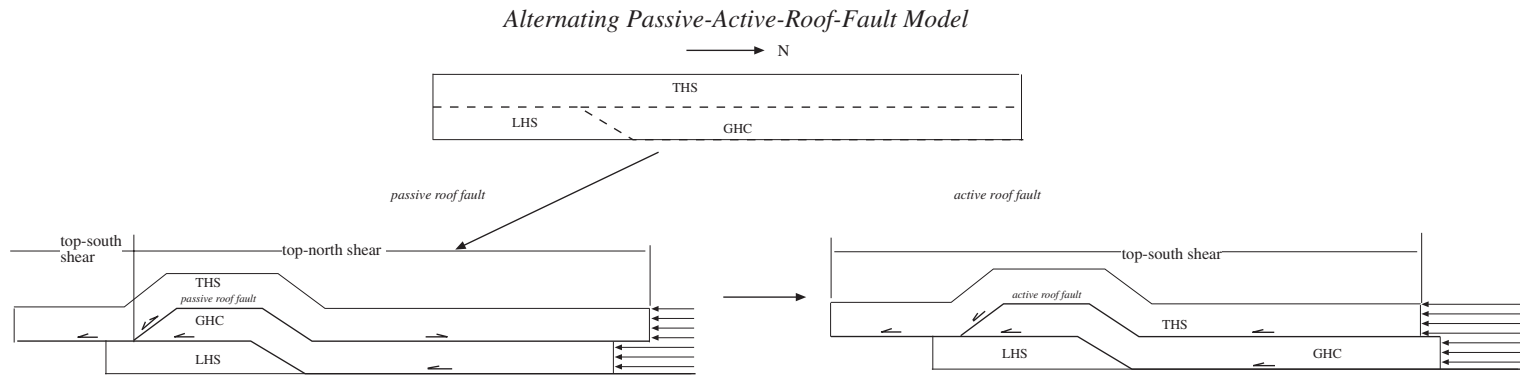


Fig. 21. Passive-versus active-roof-fault models during emplacement of the GHC along the MCT and STD.

top-north sense of shear (Patel et al., 1993; Vannay and Hodges, 1996; Searle, 1999; Wyss et al., 1999), the fault and its related shear zones may have acted as both active and passive-roof structures, depending on the structural positions along the roof fault and the displacement boundary conditions applied on the north end of the MCT-STD-GCT system against the Indus–Tsangpo suture (Fig. 21). For example, the sense of shear along the STD roof fault could change from top-south to top-north as a segment of the STD shear zone moves from the frontal part of the MCT northward across the STD-MCT branch line (Fig. 21). This implies that the deformation history of the STD can be drastically different along its different segments: some parts with only top-north shear, some parts with only top-south shear, and some parts with multiple superposition of top-north and top-south shears.

#### 7.1.6. Relationship between MCT-I and MCT-II

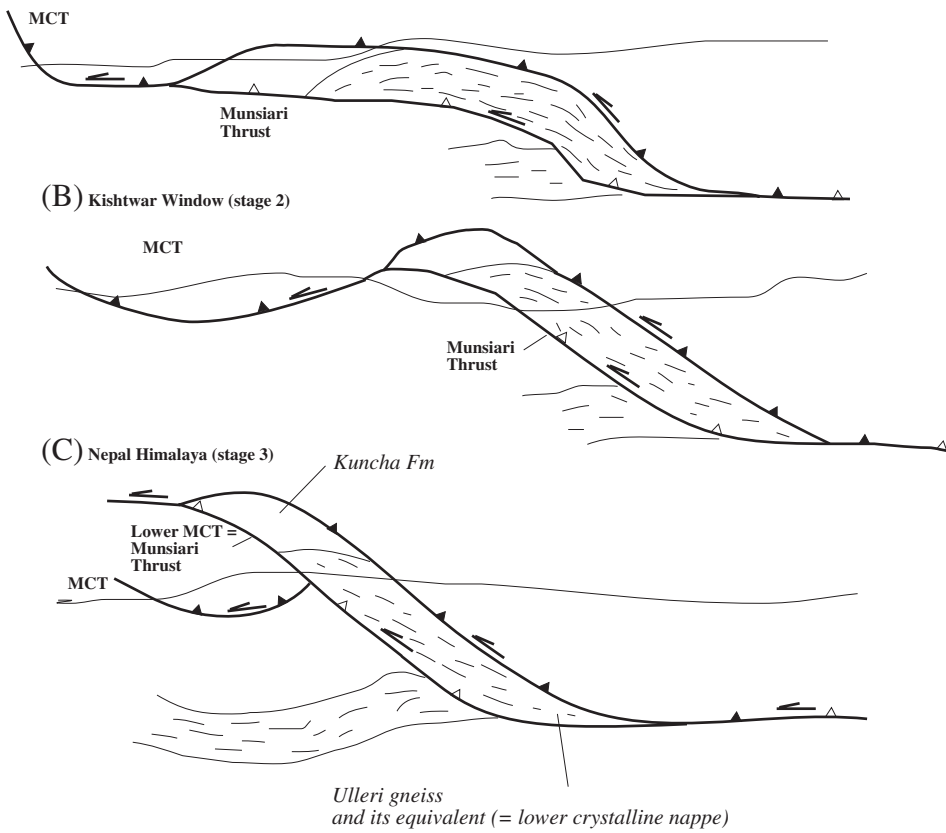
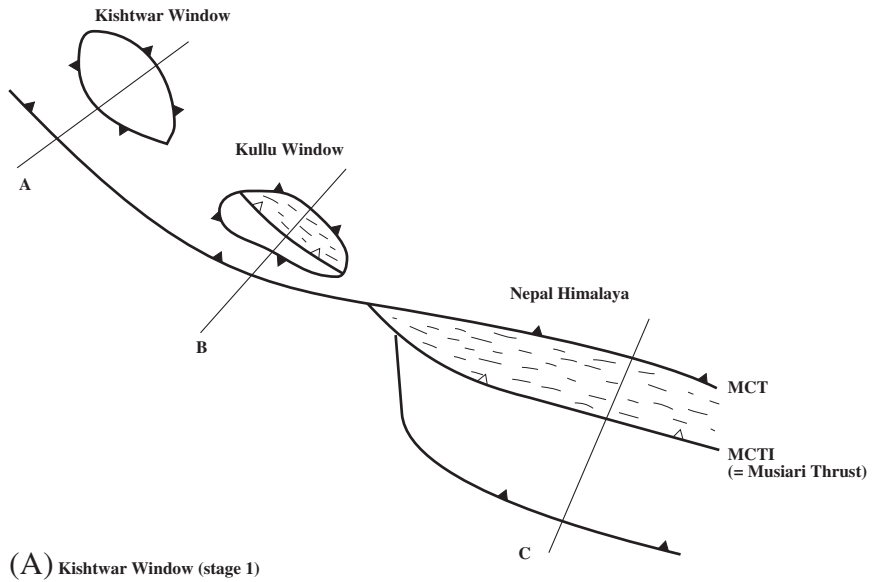
An important problem for the evolution of the MCT zone is how its early–middle Miocene motion was replaced by latest Miocene–Pliocene motion. The lateral variation of geologic relationships between the reactivated young MCT zone below (= the Munsiri thrust) and the older MCT above (= the Vaikrita thrust=MCT-II) in NW India and Nepal provides a critical constraint on this process. As noted above, although the Kishtwar window in the Zaskar Himalaya has experienced recent (<10 Ma) uplift and doming, the base of the GHC does not show muscovite cooling ages younger than ~16 Ma (Fig. 14) (Searle et al., 1999a; Stephenson et al., 2001). This is in contrast to the observed young cooling ages of 5 Ma in the Garhwal and Nepal Himalaya where the latest Miocene–Pliocene reactivation of the MCT zone has been clearly documented. It is likely that doming over the Kishtwar window in the past 10 m.y. was related to the incipient development of a blind thrust (= Munsiri thrust) from below (Fig. 22A), because the timing of doming between 6 and 2 Ma (Kumar et al., 1995) overlaps with the timing of thrusting along the Munsiri thrust (= MCT-I) in NW India (Catlos et al., 2002a,b). In the Garhwal Himalaya, the Munsiri thrust in the Kullu–Larji–Rampur window joins the MCT zone upward (Vannay and Grasemann, 2001; Wiesmayr and Grasemann, 2002), indicating a duplex relationship as

suggested by Robinson et al. (2003) for the latest Miocene–Pliocene reactivation of the MCT zone in Nepal (Fig. 22B). However, the duplex model of Robinson et al. (2003) is difficult to apply for the evolution of the MCT zone in the Nepal Himalaya, because the frontal zone of the MCT as the roof fault of the duplex may have already ceased motion by 14 Ma (Arita et al., 1997; Johnson et al., 2001). This age is much older than the 7–2 Ma reactivation in the MCT root zone. Thus, it is likely that the younger shear zone (i.e., MCT-I of Arita, 1983; the Munsiri thrust of Valdiya, 1980) cuts and offsets the MCT-II above (Fig. 22C), as suggested by Arita et al. (1997) and Johnson et al. (2001) (Fig. 2A). Out-of-sequence thrusts in the LHS offsetting the MCT have also been documented by Schelling and Arita (1991) and Paudel and Arita (2002). This relationship is consistent with younger ages of 7–2 Ma for motion on the MCT root zone in the upper part of the LHS in Nepal (Harrison et al., 1997a).

Because the amplitude of warping for the GHC decreases westward from Zaskar to Kashmir, the slip along the inferred blind Munsiri thrust below the Zaskar structural dome must diminish westward beneath Kashmir before it finally reaches the Nanga Parbat syntaxis. The westward decrease in displacement across the reactivated MCT zone implies that the cross-sections through the Zaskar, Garhwal and Nepal Himalaya in fact may represent a sequential evolution of the Munsiri-MCT-I shear zone from its incipient stage in the west to the final mature development in the east (Fig. 22).

#### 7.2. Tectonic relationship between southern Tibet crust and the Greater Himalaya Crystalline Complex

Although the Himalayan orogen was traditionally viewed to have been built exclusively within the Indian crust (Gansser, 1964), the possible mobility of the Tibetan lower crust due to thermally activated low effective viscosity (e.g., Zhao and Morgan, 1987; Bird, 1991; Royden, 1996; Avouac and Burov, 1996; Shen et al., 2001; Clark and Royden, 2000; Shen et al., 2001) has raised the question of how the Himalayan crust interacted with Tibetan/Asian crust during the Indo-Asian collision. Nelson et al. (1996) and Alsdorf and Nelson (1999) suggest that partial melting in the lower Tibetan crust of the Asian plate was



widespread. In their model, the partially molten Tibetan rocks have been transported continuously via lower crustal channel flow to the Himalayan orogen during the Indo-Asian collision. This in turn may have produced widespread Himalayan leucogranites (e.g., LeFort, 1996; Harrison et al., 1998b; Searle et al., 1999b).

Because the rocks in southern Tibet have been intensely studied in the past three decades (e.g., Allègre et al., 1984; Dewey et al., 1988; Liu, 1988; Yin and Harrison, 2000; Pan et al., 2004), the Nelson et al. (1996) hypothesis can be evaluated by comparing the lithologic compositions in the GHC and southern Tibet. If transportation of Asian middle crust beneath the southern Tibetan plateau to the Himalaya had occurred, then the widespread Cretaceous–early Tertiary Gangdese batholith in southern Tibet and the Ladakh batholith in NW India, as documented by numerous studies (Schärer et al., 1984, 1986; Xu et al., 1985; Xu, 1990; Harris et al., 1988; Harrison et al., 2000), would have been exposed in the GHC (Fig. 2A). Geochronological analyses of the GHC so far in the western and central Nepal have yielded no signal of such rocks in the GHC (Parrish and Hodges, 1996; DeCelles et al., 2000). The absence of Asian crust in the GHC of the Indian plate is also displayed at the eastern and western Himalayan syntaxes. In both places, tilted crustal sections of the whole Himalayan orogen are exposed due to extreme denudation at the core of the syntaxes. However, in both places, the Indian basement and its cover sequences are directly juxtaposed against Mesozoic arc rocks of southern Asia by the Indus–Tsangpo suture (Burg et al., 1998; Ding et al., 2001; Whittington et al., 1999, 2000; Zeitler et al., 2001; Foster et al., 2002; Argles and Edwards, 2002) (Fig. 2A). Because the two Himalayan syntaxes form tectonic windows exposing Indian basement crust and extending >100 km northward into the southern Tibetan blocks (i.e., the Lhasa terrane in the east and the Kohistan–Ladakh plutonic belt in the west), the geologic relationships in the two Himalayan syntaxes support large-scale underthrusting of the Indian continent beneath Asia

(e.g., Powell and Conaghan, 1973b; Ni and Barazangi, 1984; DeCelles et al., 2002) rather than southward transport of the Asian crust to the Himalaya (Nelson et al., 1996).

The absence of Tibetan crust in the Himalaya is also indicated by the contrasting isotopic compositions between the two geologic terranes. As discussed above, the southern Tibetan block is dominated by the Cretaceous–early Tertiary plutons and is characterized by much lower Sr initial ratio and much higher  $\epsilon_{\text{Nd}}(0)$  value than the Himalayan units of the GHC, THS, and LHS. If the Tibetan crust were extruded via lower crustal flow as envisioned by Nelson et al. (1996), then the GHC would show the Sr and Nd isotopic compositions characteristic of southern Tibet, which is not the case (e.g., Singh and France-Lanord, 2002; Myrow et al., 2003).

Examining the geology of the North Himalayan gneiss domes can also test whether or not the lower ductile crust of Tibet was extruded to the Indian plate. For example, the Gurla Mandhata gneiss complex was exhumed by late Miocene detachment faulting, exposing middle crustal rocks (Murphy et al., 2002). Field observations in this gneiss complex have revealed no sign of Gangdese plutonic rocks (Murphy et al., 2002). Similar observations were also made in the Kangmar dome where Indian basement rocks exhumed from middle crustal levels are exposed (i.e., Lee et al., 2000). However, an important exception is noted for the Yala Xiangbo dome in southeast Tibet, where Gangdese batholith may have underthrust beneath the THS along the GCT (Aikman et al., 2004). Because the North Himalayan gneiss domes are located at a similar tectonic position between the STD and GCT, the above interpretation implies that the GCT is the roof fault of all the gneiss domes.

Although wholesale extrusion of Tibetan lower crust to the Himalaya can be ruled out, it remains possible that the subducted Indian continental crust was returned via channel flow from depths as deep as 90–100 km to the middle and upper crustal levels (Steck et al., 1998; Vannay and Grasemann, 2001;

Fig. 22. Schematic cross-sections showing possible relationship between the early Miocene MCT fault and the reactivated late Miocene–Pliocene MCT across the Kishtwar window, Kullu–Larji–Rampur window, and the Nepal Himalaya. The three cross-sections may represent the sequential development of the late Miocene–Pliocene MCT shear zone (= Muniari thrust of Valdiya (1980) and MCTI of Arita (1983)). Initially, the young MCT was developed as a blind thrust. It later extends upward and merges with the older MCT as its roof fault and forms a duplex system. Further motion along the younger MCT cuts and offsets its roof fault, the older MCT.

Grujic et al., 2002). This process has been used to explain the occurrence of UHP eclogite rocks in the western Himalaya (Chemenda et al., 2000; Kohn and Parkinson, 2002). However, a return flow transporting the subducted Indian crust to a shallow crust level is fundamentally different from the physics and the geological processes envisioned by Nelson et al. (1996) and Beaumont et al. (2001). The former is driven by buoyancy of the Indian continental crust (Chemenda et al., 2000) while the latter was caused by the lateral pressure gradient due to differential gravitational potential between Tibet and the Himalaya coupled with strong erosion (Bird, 1991; Royden, 1996; Beaumont et al., 2001; Hodges et al., 2001).

### 7.3. Mechanics of the South Tibet Detachment System

The mechanical origin of low-angle normal faults has been a subject of debate. This is because originating low-angle normal faults is mechanically difficult in the context of Andersonian fault theory (Anderson, 1951) and requires special boundary conditions or mechanical properties of rocks (e.g., Yin, 1990; Westaway, 1999; Colletini and Sibson, 2001). Hypotheses proposed so far range from topographic loading (Spencer and Chase, 1989), basal shearing due to lower crustal flow (Yin, 1989; Melosh, 1990), and plutonic intrusion (Parsons and Thompson, 1993; cf., Yin, 1993).

Burg et al. (1984a) suggest that the initiation of the STD was a result of northward gravitational sliding of the THS along a 15–30° north-dipping lithologic interface. This hypothesis implies that the STD originated from a preexisting mechanical weakness and there should be no matching hanging-wall and footwall cutoffs across the STD. In contrast, Burchfiel and Royden (1985) interpret the formation of the STD as a result of topographic loading by the high-altitude Tibetan plateau, which caused southward extrusion of a wedge-shaped Indian crust between the STD and MCT. The half-space elastic solution of Burchfiel and Royden (1985) also predicts low-angle normal faults dipping southward away from the Tibetan plateau that is opposite to the observed dip direction of the STD. Noting that the ductile lower crust may flow from high- to low-altitude region due to a pressure gradient, Yin (1989) proposes that the coeval develop-

ment of the MCT and STD may have resulted from a horizontal shear traction induced by southward flow of the Himalayan lower crust. Later, Yin (1991) uses the solution of an elastic wedge model to speculate that the STD could be a result of motion on the MCT along which a high pore-fluid pressure was built up during underthrusting of the LHS below the MCT. This may have caused local extension in the top part of the orogenic wedge. This model predicts that the initiation of the STD postdates the MCT. Applying the critical Coulomb wedge model of Dahlen (1984), England and Molnar (1993) explain the occurrence of the STD as a result of an overthickened Himalayan thrust wedge. More recently, Beaumont et al. (2001) propose that the combination of rapid erosion concentrated along the southern Himalayan front and a strong contrast in viscosity between the THS and GHC may lead to the initiation of the STD as a bounding structure of the mid-crustal channel flow.

Because the STD has a >100-km-long hanging wall flat (see cross-sections in Fig. 2), the fault most likely has originated along a gentle-dipping lithologic contact. This observation may help resolve the mechanical problem of the STD, because the preexisting weakness could have a much weaker strength than that of a coherent rock. Therefore, the problem of initiating a low-angle normal fault in the Himalaya may become the problem of how the fault has moved at a low angle, as originally analyzed by Burg et al. (1984a). This latter question could be readily resolved by variable mechanisms such as the presence of high-pore fluid pressure (e.g., Axen, 1992) or a large magnitude of finite extension along a low-angle normal fault (Forsyth, 1992).

### 7.4. Erosion-induced upward heat advection and apparent acceleration of exhumation rates

Although cooling rates provide good proxy to determine the exhumation rates of an orogen, an increase in cooling rates may not indicate an increase in exhumation rates (e.g., George et al., 1995). This is because rapid erosion will cause upward heat advection in the hanging wall of a thrust (e.g., Harrison et al., 1998b) and vertical condensation of

isotherms with time (Fig. 23). Thus, even with the same exhumation rate, the cooling rate could increase simply as a result of upward heat advection due to erosion (Fig. 23). This may be the reason for the observed acceleration of Pliocene cooling rates in many parts of the Himalaya (Figs. 14–16).

### 7.5. Exhumation history of the Himalayan orogen

Exhumation mechanisms, rates, and temporal relationships to tectonic deformation are some of the most fundamental issues in understanding orogenic development (e.g., Hallet et al., 1996; Burbank, 2002). Many workers infer that the GHC has been exposed at the surface by the early Miocene at or before ~21–17 Ma (e.g., France-Lanord et al., 1993; DeCelles et al., 1998b; Najman et al., 2000; White et al., 2001). However, this inference requires a cooling

rate of ~150 °C/Ma in the early Miocene for the GHC, which is about a factor of 10 higher than that actually recorded in the GHC during the same time interval (Figs. 13–16). Although such high cooling rates were locally observed in the western Himalaya (Cerveny et al., 1988, 1989a,b), they are not representative of the whole Himalaya. When the GHC had reached the surface may be best constrained by low-temperature thermochronological data. The available apatite fission track ages suggest that the GHC did not reach Earth's surface until after 10–4 Ma when motion along the STD had completely stopped (Figs. 13–16).

According to the Himalayan cooling history, UHP gneiss terranes in the western Himalayan orogen were exposed at the surface in the Eocene (Figs. 13 and 14). The early exposure of these rocks having similar lithologic composition and isotopic signature to the GHC precludes a simple correlation between the Himalayan foreland sediments and the exposure of the GHC in the MCT hanging wall (cf., Najman et al., 2000). This problem is compounded by the fact that the basal part of the THS also contains abundant Cambro-Ordovician plutons common to both the GHC and THS. Thus, the early Paleozoic detrital zircon ages alone also cannot be used to differentiate clasts derived from the GHC or THS (DeCelles et al., 2000; Myrow et al., 2003).

Despite the widespread early Miocene leucogranites exposed at the top part of the GHC with ages ranging from ~21 to 17 Ma (e.g., Scaillet et al., 1990, 1995; Murphy and Harrison, 1999; Guillot et al., 1999; Searle et al., 1999b; Dèzes et al., 1999), there has been noticeably no record of detrital monazites or zircons of this age range in the Miocene Himalayan foreland basins (DeCelles et al., 1998a; White et al., 2002). This observation could be an artifact of a small sample size of detrital zircons. However, the observation could also imply that the GHC was not exposed to the surface until after the Miocene.

A possible history of the Himalayan erosion and deposition is shown in Fig. 24. The Paleogene Himalayan foreland basin receives sediments mainly from southern Tibet, the Indus–Tsangpo suture zone, and the supracrustal sections of the UHP gneiss terranes in the western Himalaya and possibly the eastern Himalayan syntaxis. In the early Miocene, the foreland basin receives sediments from the Tethyan Himalayan

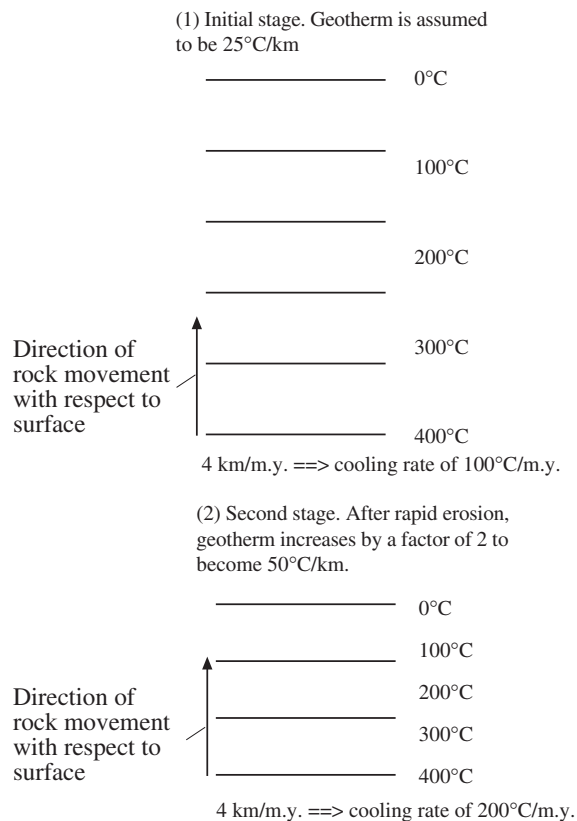


Fig. 23. Hypothetical cases to illustrate the effect of erosion on heat advection and condensation of isotherms.

cover sequence and metamorphic clasts from the UHP gneiss terranes in the western Himalaya. The high-grade GHC along the axis of the Higher Himalaya

was not exposed at the surface until after 11–5 Ma when high-grade metamorphic clasts first appear in the Siwalik Group of the Himalayan foreland basin

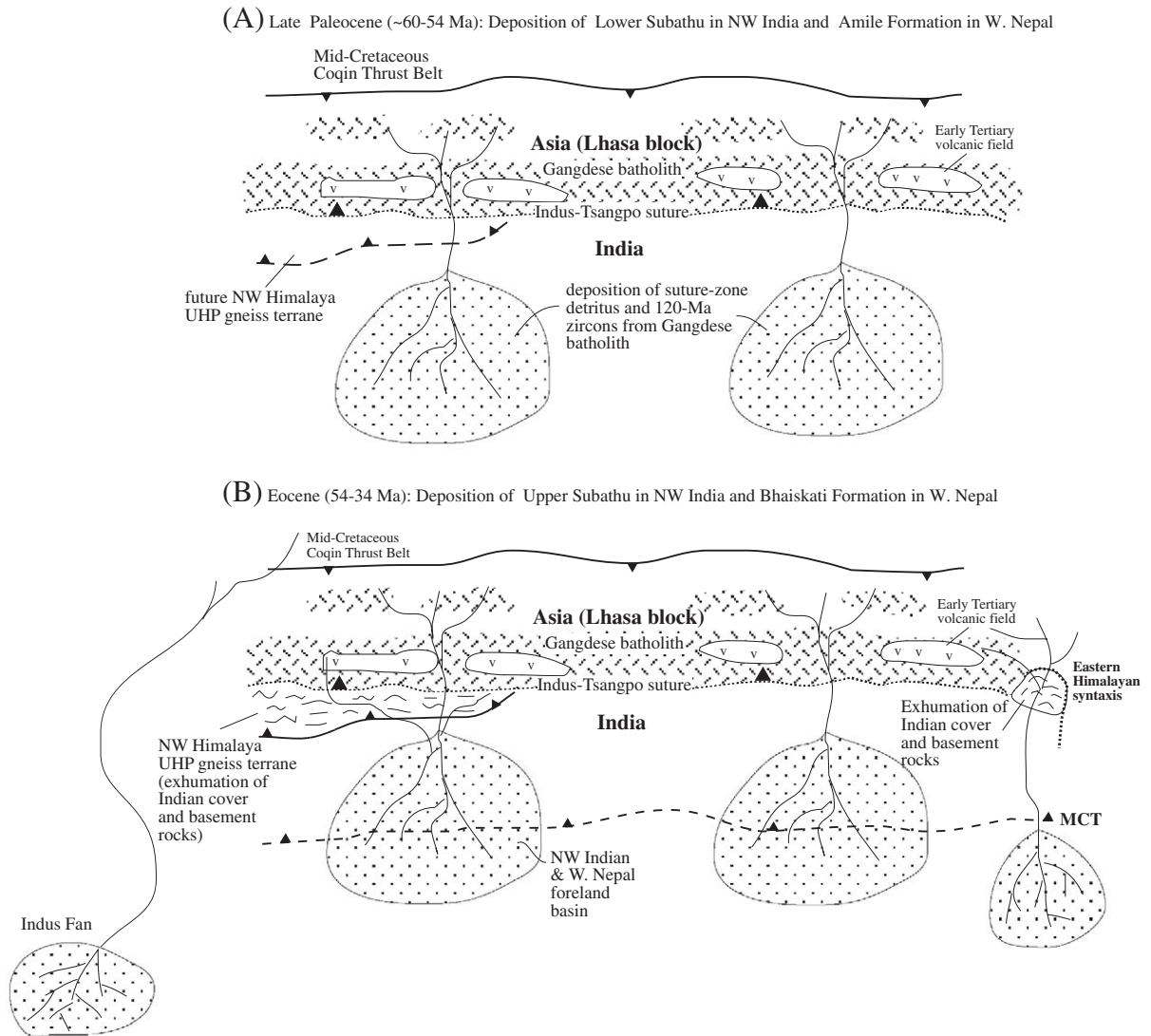
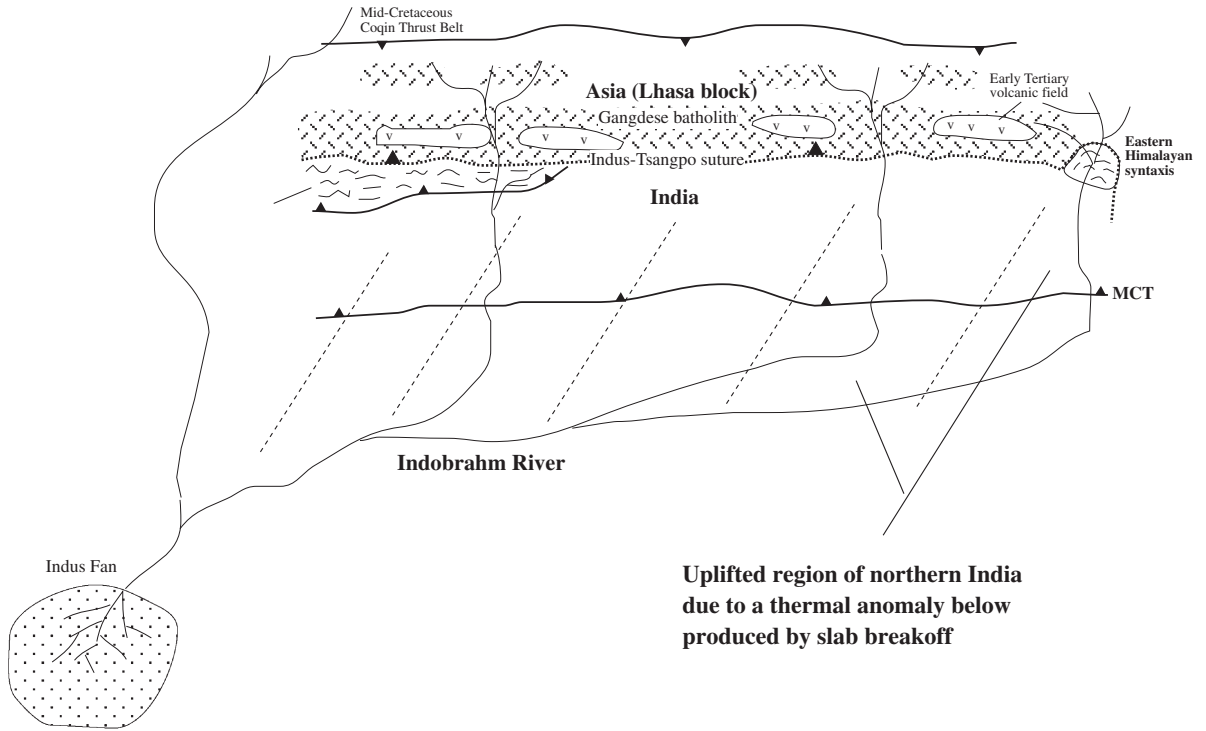


Fig. 24. Possible exhumation history of the Himalaya and depositional history of the Himalayan foreland basin. (A) In the late Paleocene, the Himalayan foreland receives sediments mostly from Mesozoic arcs in southern Tibet and the Indus–Tsangpo suture zone. However, the cover rocks of the Eocene eclogite terranes in northwestern Himalaya and the eastern syntaxis were also significant sources to the foreland basin. (B) In the Eocene, metamorphic clasts of the Himalayan eclogite terrane and the eastern syntaxis may have started being transported to the Himalayan foreland and the Indus and Bengal Fans. (C) In the Oligocene, the Himalayan foreland together with the Himalayan thrust belt was uplifted that leads to the development of the Oligocene unconformity. (D) In the early–middle Miocene, the Tethyan Himalayan strata as the cover sequence of the GHC began to be eroded. However, GHC was not exposed at the surface. Large amount of metamorphic clasts from the Himalayan eclogite terrane and eastern syntaxis and igneous clasts from Cambro-Ordovician granites in the basal part of the Tethyan Himalayan strata were eroded and transported to the Himalayan foreland basin and the Indus and Bengal Fans. (E) In the late Miocene and Pliocene, the GHC was extensively exposed, leading to deposition of large amount of metamorphic clasts in the Siwalik Group.

(C) Oligocene (34-21 Ma): Deposition of Upper Subathu in NW India and Bhaiskati Formation in W. Nepal



(D) Early and middle Miocene (20-12 Ma): Deposition of Dharmasala Group, Dumri Formation, and possibly Lower Siwalik Group

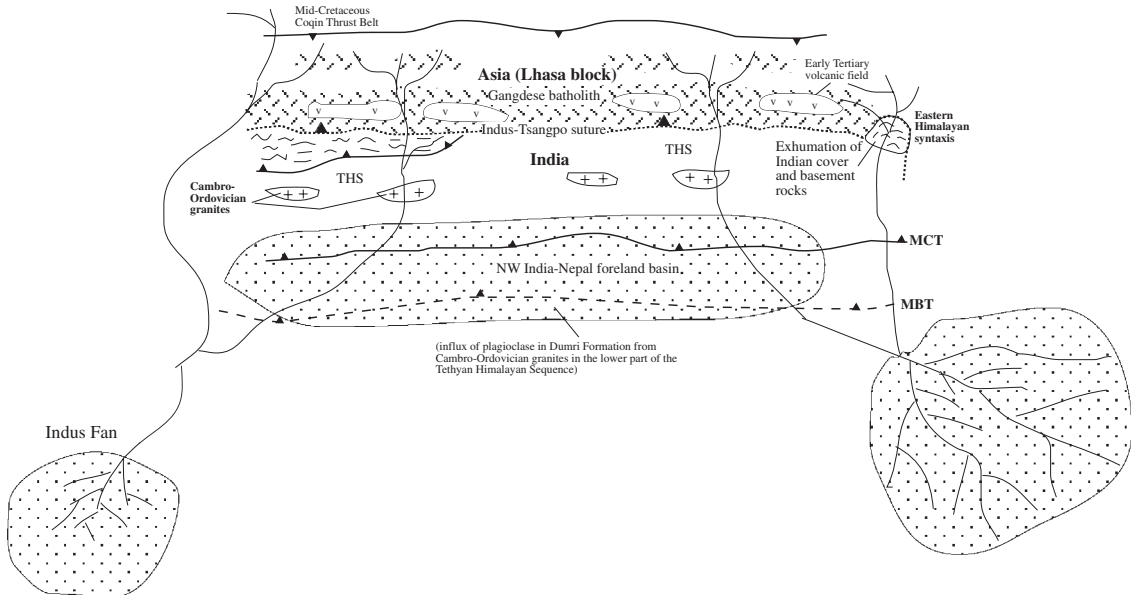


Fig. 24 (continued).

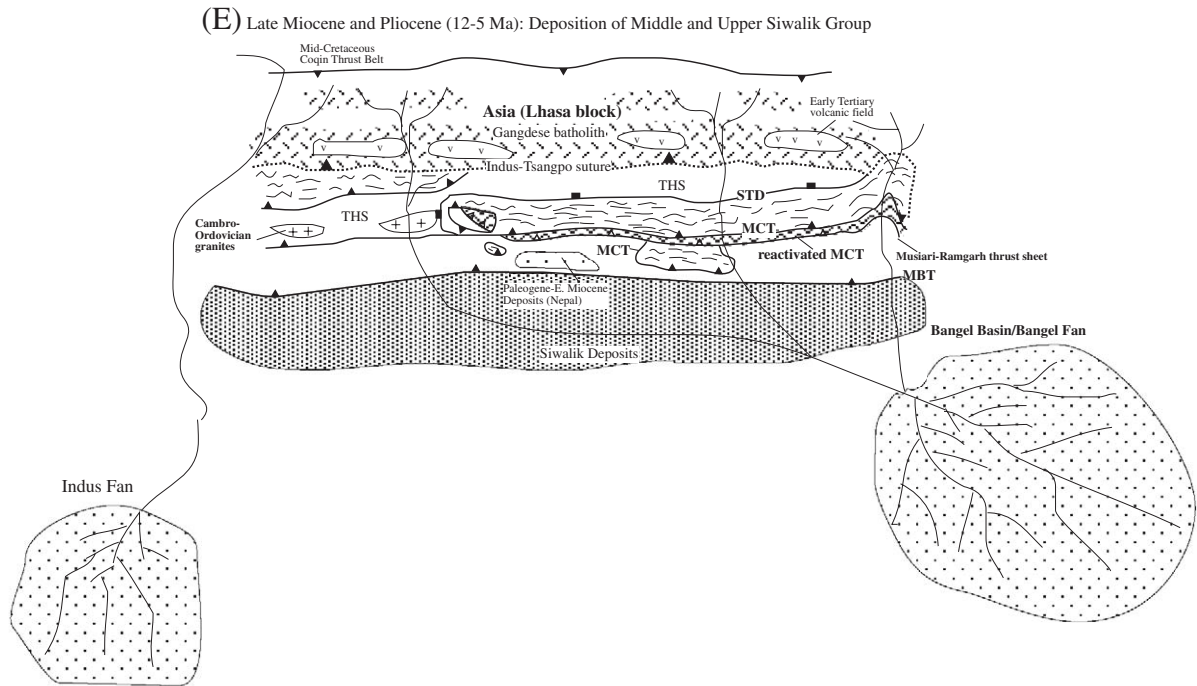


Fig. 24 (continued).

(DeCelles et al., 1998b; Sakai et al., 1999; White et al., 2001).

Although the structural setting of the UHP eclogite terranes remains incompletely understood, it appears that the slab breakoff models of Chemenda et al. (2000) and Kohn and Parkinson (2002) are the most plausible explanation for both their rapid exhumation immediately after the onset of Indo-Asian collision and their tectonic positions directly next to the Indus–Tsangpo suture zone. The lack of UHP terranes in the central and eastern Himalaya may suggest that the northern margin of the Indian continent was irregular prior to Indo-Asian collision, with its western part forming a northward extruding promontory and was subducting to a depth >100 km in the Eocene (e.g., Guillot et al., 1999).

#### 7.6. Origin of the Oligocene unconformity in the Himalayan foreland

An interesting observation made in the Himalayan foreland basin is the lack of latest Eocene and Oligocene sedimentary rocks (Table 5). This unconfor-

mity could be either created by non-deposition or erosion. DeCelles et al. (1998a) suggest that this unconformity represents a surface of non-deposition for 15–20 m.y. between the late Eocene to the end of the Oligocene. They attribute the unconformity to the development of a broad forebulge ~200 km wide in the north–south direction as a result of thrust loading from the Himalayan orogen. Although this model explains the lack of sedimentation immediately south of the Himalaya and continuous deposition in the Bengal Basin and the Kirthar Range farther south in the Oligocene (Table 5), it does not address the question of why no record of a prominent forebulge from the early Miocene after significant crustal shortening along the MCT, MBT, and MFT across the Himalaya (Table 6) (Rao, 1973; Raiverman, 2000). One possibility is that the Miocene–present forebulge is buried beneath the Indo-Gangetic depression. If present, its effect on the modern foreland sedimentation must be limited as no detectable controls by such a regional structural high have been detected by subsurface data from the Indo-Gangetic depression (Rao, 1973; Raiverman, 2000).

There are at least three alternative explanations for the Oligocene development of the Himalayan foreland unconformity:

(1) The absence of the Oligocene deposition occurred during the transition from marine to continental sedimentation. Thus, it is possible that either the sea level drop or uplift of the Indian continent caused the non-deposition in the Oligocene. One possible mechanism is that breakoff of the Indian oceanic slab at the start of the Indo-Asian collision produces a hot thermal anomaly and associated mantle upwelling beneath southern Tibet (Fig. 25A). As the Indian continent traveled northward, its northern margin started to ride over this hot thermal anomaly, causing uplift of the northern Indian continent. Both geologic and geophysical observations from southern Tibet and below the Indian continent support this hypothesis. (A) Widespread latest Paleocene–Eocene Linzizong volcanic rocks in southern Tibet may be the expression of this thermal event, which occurred immediately after the onset of the Indo-Asian collision (Yin and Harrison, 2000). (B) Seismic velocity anomalies may exist beneath India (Van der Voo et al., 1999). It is possible that the relatively high elevation of the Indian Peninsula Highlands is currently supported by this thermal anomaly in a fashion discussed by Zhong and Gurnis (1993).

(2) The Oligocene Himalayan forebulge could have been induced by downward pulling of the Indian oceanic slab rather than by thrust loading from above. The Indian oceanic lithosphere did not detach and fall into the mantle until after the early Miocene (i.e., Chemenda et al., 2000) (Fig. 25B). Continuous subduction of the Indian lithosphere at a relatively high angle in the Oligocene is suggested by the presence of Oligocene granodiorite in the Gangdese batholith in southeast Tibet (~32 Ma, Harrison et al., 2000) and a subduction-induced granite of 26 Ma in the Kohistan arc immediately west of the Nanga Parbat syntaxis (George et al., 1993). After the oceanic slab was detached in the early Miocene, the load that had generated the Oligocene forebulge was removed.

(3) The third explanation (Fig. 25C) is inspired by the geology of the Shillong plateau south of the eastern Himalaya (Fig. 2A). There, the elevation of the plateau exceeds 1500 m, much greater than the ~200-m elevation of a forebulge as predicted by the thrust loading model of Duroy et al. (1989) and DeCelles et al. (1998a). The Shillong plateau is a

pop-up structure initiated since the early Miocene (Alam et al., 2003). The structures bounding the plateau may or may not be linked with the Himalayan thrust system (Billham and England, 2001). It is possible that the Oligocene Himalayan foreland also experienced a phase of mild contraction as expressed by a broad uplift such as the Shillong plateau but at a much larger scale along strike. The motion along the MCT in the early Miocene provides loading to create a Miocene foreland basin (Fig. 25B).

### 7.7. Estimates of Himalayan crustal shortening and its uncertainties

Current estimates of crustal shortening across the Himalayan orogen indicate an eastward increase in the magnitude of shortening. The overall shortening across the westernmost Himalaya in Pakistan is no more than 200 km (DiPietro and Pogue, 2004). However, the minimum amount of crustal shortening across the central Himalayan orogen ranges from >750 km in southwest Tibet and western Nepal to >326 km in eastern Nepal and south-central Tibet (Hauck et al., 1998), and to >570 km in the Arunachal Himalaya (Yin et al., submitted for publication). These estimates are all based on construction of balanced cross-sections, a technique that requires satisfaction of several important assumptions:

- (1) constant thickness of individual lithologic units and flexural-slip folding;
- (2) forward propagation of thrust development;
- (3) no change in rock volume during and after thrusting; and
- (4) the original stratigraphic and structural configuration of the Himalaya prior to Cenozoic thrusting is well understood.

These assumptions are briefly evaluated below in the context of the Himalayan geology. As shown below, the existing shortening estimates in the Himalaya probably represent the minimums.

#### 7.7.1. Constant thickness and flexural-slip folding

The flexural-slip folding mechanism automatically leads to preservation of constant bed thickness (Dahlstrom, 1970; Suppe, 1983). The latter is satisfied for most of the Tethyan Himalayan thrust belt where

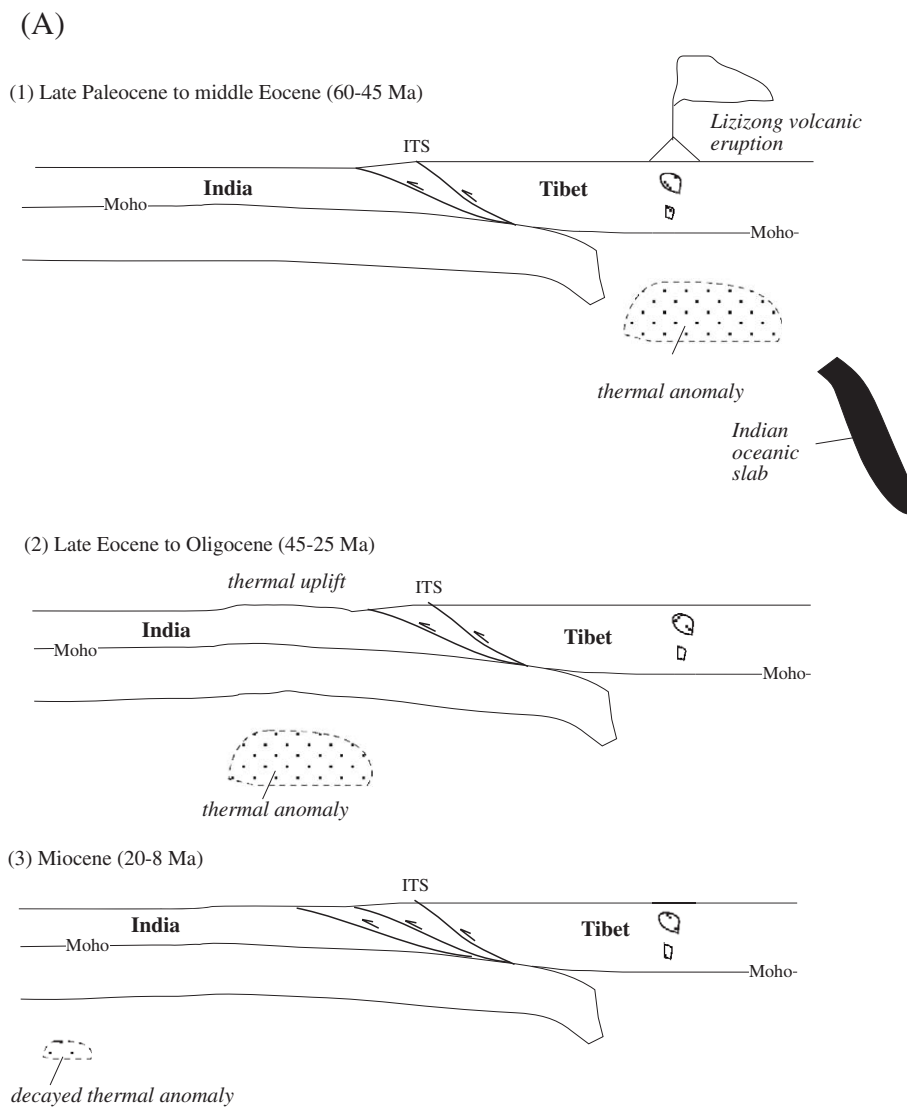
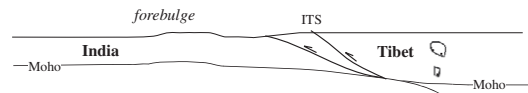


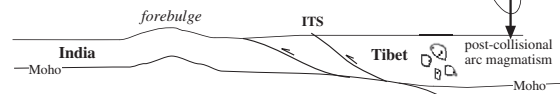
Fig. 25. Three possible mechanisms for generating Oligocene unconformity in the Himalaya foreland. (A) Breakoff of Indian oceanic slab at the start of the Indo-Asian collision in the Eocene may have created a thermal anomaly in southern Tibet. Northward moving Indian continent overrode the thermal anomaly in the Oligocene, causing regional uplift of the Himalayan orogen and its foreland, producing regional unconformity. The thermal anomaly mostly disappeared in the Miocene due to thermal decay. (B) A forebulge is produced a bending moment induced by downward pull of the Indian mantle lithosphere after significant amount of supracrustal materials were scraped off along the Indus–Tsangpo suture (ITS). The magnitude of warping across the bulge increases as more crustal materials of the Indian plate were scraped off and thus a long Indian mantle lithosphere is being subducted, causing thickening in the Tethyan Himalayan fold-thrust belt and the development of unconformity in the Himalayan foreland. (C) The unconformity was produced by horizontal contraction, which causes a broad uplift in the Himalayan foreland south of the present trace of the Main Central Thrust. The MCT was developed within the Oligocene uplift as an out-of-sequence thrust. Motion on the early Miocene MCT induces foreland sedimentation over the Oligocene unconformity. This mode would require angular unconformity between Paleogene and Neogene foreland basin strata.

(B)

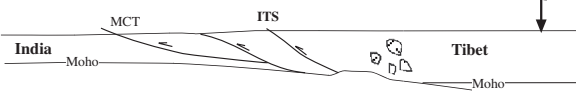
(1) Late Paleocene–Middle Eocene (60–45 Ma)



(2) Late Eocene–Oligocene (45–23 Ma)

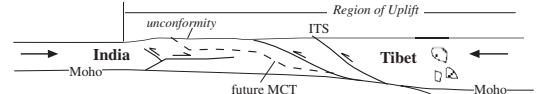


(3) Early Miocene (24–20 Ma)



(C)

(1) Oligocene (32–24 Ma)



(2) Early Miocene (24–20 Ma)

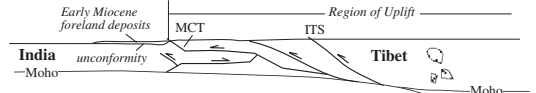


Fig. 25 (continued).

faults and folds exhibit typical thin-skinned thrust geometry (e.g., Ratschbacher et al., 1994; Wiesmayr and Grasemann, 2002; Murphy and Yin, 2003). An important exception is in the eastern Tethyan Himalayan thrust belt where Cenozoic contraction is expressed by isoclinal folds, slaty cleavage that has completely transformed the original bedding, and the occurrence of quartz veins in the folded sequence indicating significant volume loss (Yin et al., 1999).

The constant thickness assumption is probably invalid, but it is difficult to evaluate in the Himalaya. This is obvious for the GHC, because we do not even know its original stratigraphic configuration. Some workers

interpret the Precambrian–Cambrian Haimanta Group in NW India to be the lower-grade equivalent of the GHC (e.g., Fuchs and Linner, 1995; Steck, 2003). If this is correct, the original thickness of the GHC was no more than 2 to 4 km (e.g., Frank et al., 1995; Vannay and Steck, 1995) (Fig. 3). Given that the GHC in most places is greater than 5 km and locally exceeds 10 km (see cross-sections in Fig. 2), it would imply that the GHC has been thickened by a factor of 2 to 5.

Although the GHC may have been significantly thickened via ductile deformation such as isoclinal folding, the spatial distribution and temporal variation of thermochronologic data over the GHC strongly

support its upward transport as a coherent thrust sheet, as discussed above (Figs. 13–16). Burbank et al. (2003) reach a similar conclusion based on a study of much smaller area over a time span of a few million years. Thus, it is possible that the GHC was thickened via ductile deformation when it was on the way down by underthrusting but was behaving as a coherent slab later as it was climbing up the MCT ramp.

If the GHC has been significantly thickened, it raises the question of why it records a strong flattening strain (e.g., Law et al., 2004). One explanation is that the flattening strain recorded in the GHC microstructures only reflects stretching of bedding as the original sedimentary layers were isoclinally folded. That is, the net result of isoclinal folding is to thicken the GHC despite local bedding-parallel stretching. This interpretation indicates that we need to be cautious when using microstructures and finite strain markers to infer the overall evolution of the Himalayan orogen.

The constant thickness assumption may have been violated also when balancing the Lesser Himalayan thrust belt. Slaty units such as the Blaini Formation and Simla Slate of NW India and Kuncha Formation of Nepal (Table 4) preserve widespread isoclinal folds, slaty cleavage that completely transposed the original bedding, and wide occurrence of quartz veins resulting from pressure solution (=negative volume strain) (e.g., Gansser, 1964; Valdiya, 1980; my own observations in NW and NE Indian Himalaya and Nepal Himalaya). Many of the quartz veins in these formations are themselves isoclinally folded and refolded, indicating a protracted history of folding and intra-formational thickening. A possible mechanism for intraformational thickening in the GHC and LHS is schematically shown in Fig. 26. If this mechanism dominated during Himalayan thrusting, area balancing would be a better technique than the line-balancing method for estimating the total crustal shortening across the Himalaya (Laubscher, 1961; also see discussion below).

#### 7.7.2. Forward thrust development

The validity of this assumption has not been critically evaluated for the Tethyan Himalayan thrust belt. However, geologic observations show that out-of-sequence thrusting occurred in the Lesser Himalayan thrust belt (Schelling and Arita, 1991; Harrison

et al., 1997a; Wobus et al., 2003, 2005). The observation that major shallow-dipping thrusts truncate more steeply dipping thrust imbricates below indicates both the line- and area-balancing methods cannot yield accurate estimates of crustal shortening if the offset structures are eroded away as the case in the Lesser Himalayan thrust belt (Fig. 6). However, applying line- and area-balancing methods to regions between the roof and floor thrusts in the Lesser Himalayan duplex system will yield minimum estimates of crustal shortening.

#### 7.7.3. Volume loss

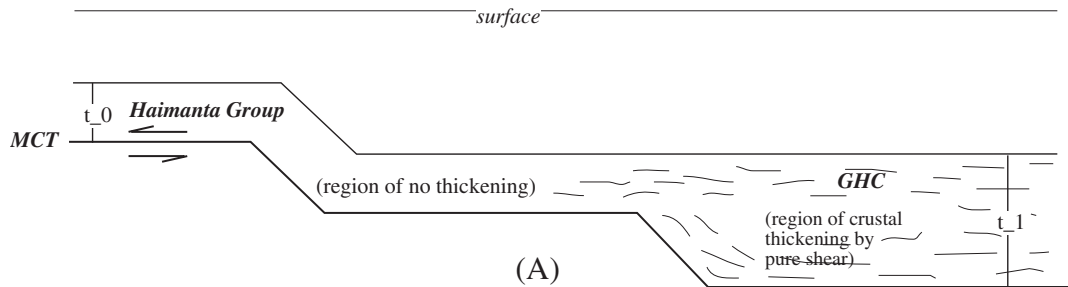
This is a significant problem for cross-section balancing because the development of cleavage due to pressure solution could take up >30–40% negative dilation strata in a slate belt (= volume loss) (e.g., Anastasio et al., 2004 and references therein). For the case of the Lesser Himalaya thrust belt and the eastern Tethyan Himalayan thrust belt where slaty cleavage is well developed, volume loss must be added in the overall estimates of crustal shortening. Neglecting its effect would result in minimum estimates of the total crustal shortening as correctly stated by DeCelles et al. (2001). The processes of Himalayan anatexis certainly contribute to mass transfer among Himalayan units in the Cenozoic (LeFort et al., 1987). However, from the regional map relationship, this effect must be negligible because the total map area occupied by the Cenozoic Himalayan granites is no more than 2–3% of the total Himalayan area (Fig. 2A).

#### 7.7.4. Original configuration of the Himalayan orogen

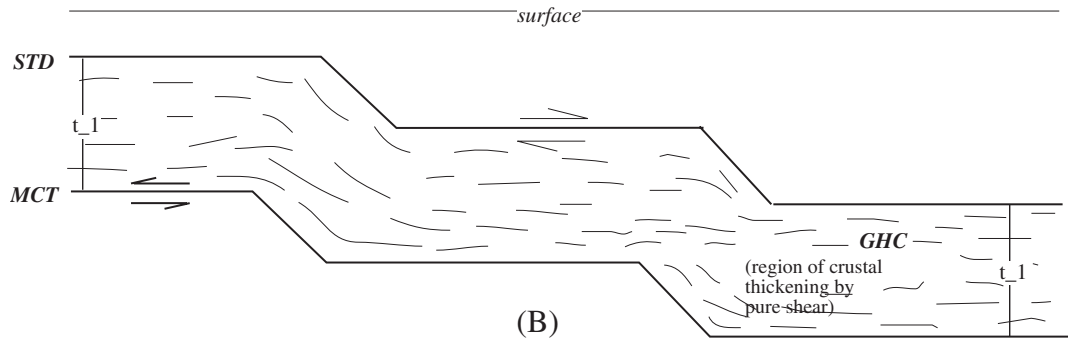
The original stratigraphic configuration of the Himalayan orogen is poorly known due to Cenozoic structural complication. However, current estimates of crustal shortening in the Lesser Himalayan thrust belt (e.g., DeCelles et al., 2001) assuming constant thickness of individual LHS units imply that these units extend for hundreds of kilometers north of their present exposure and maintain the same thickness. This assumption may be valid if these units were deposited in an epicratonal setting where individual units can be continuous for hundreds of kilometers such as in the case for the early Paleozoic strata in North China (e.g., Wang, 1985) and lower Precam-

Possible mechanism for intraformational thickening of GHC.

Stage 1: crustal thickening of the Haimanta Group by pure shear in the middle and lower crust.



Stage 2: Upward translation of thickened and metamorphosed Haimanta Group by translation of a coherent and flexible thrust.



Possible crustal thickening mechanism in shale units of Lesser Himalayan Sequence

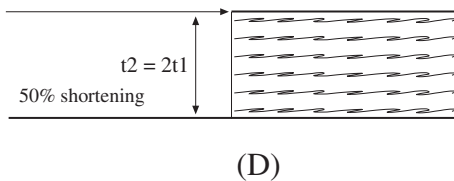
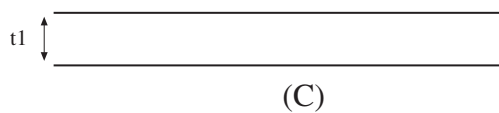


Fig. 26. Possible mechanisms for intra-formational thickening and thrust translations in the GHC and LHS.

brian–Cambrian strata in western North America (Stewart, 1972). These sections are typically less than 2 km thick, in contrast to the estimated thickness of >8 km for the LHS (e.g., Upreti and LeFort, 1999) (Fig. 3). Such a thick section indicates that most of the Proterozoic LHS were deposited in a

continental slope setting where the thickness of individual lithofacies may increase by a factor of 2 or greater from the shelf edge to the base of the slope such as in the cases of the North American Cordillera (e.g., Armstrong, 1968) and the eastern Atlantic margin (e.g., Sheridan, 1976). Line balancing does not

change the result of shortening estimates, but the projected depth to the basal detachment might be too shallow if the variation of thickness for individual stratigraphic units is not accounted for. Using area-balancing techniques, the effect of a linear change in bed thickness may be considered by measuring the taper angle and the structural relief area, as formulated in Fig. 27.

### 7.8. Reversal of the great Himalayan drainage systems in northern India: the Wadia hypothesis

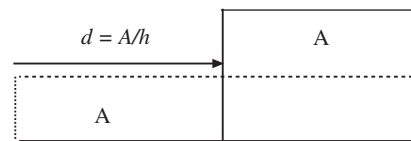
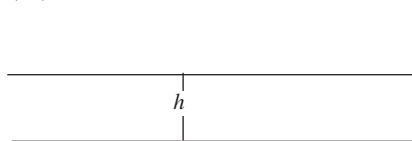
It has been long noted that the current Himalayan drainage system is asymmetric, with the Indus River System covering about one-fifth of the Himalayan range and the rest by the Ganges and Brahmaputra River systems (Fig. 1A). This asymmetric pattern corresponds well with the smaller Indus Fan deposited in the Arabian Sea and the much bigger Bengal Fan in the Bay of Bengal; the Bengal Fan is three times bigger and two times thicker than the Indus Fan (Clift et al., 2001; cf. Curray and Moore, 1971). Wadia (1953) was perhaps the first geologist to explicitly propose that the east–west trending Himalayan drainage system in the foreland reversed the flow direction in the Pliocene after the deposition of

the older part of the Siwalik Group: first flowing to the west across entire northern India parallel to the Himalaya from Assam, to Panjab, and finally to the Arabian Sea and then to the east (p. 55–57, Wadia, 1953). He made this argument based on the following observations and inferences:

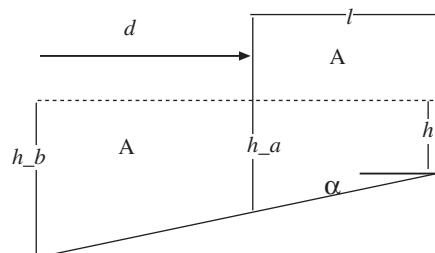
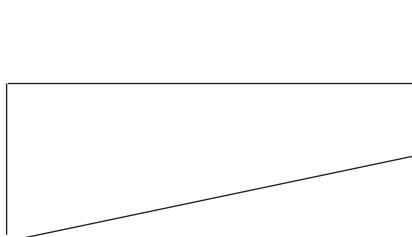
- (1) the Siwalik sedimentary belt widens westward indicating westward retreating of a flood plain system;
- (2) paleocurrent indicators in the Siwalik Group show westward flowing directions; and
- (3) the Cenozoic shallow sea in northern India retreated progressively westward from NE India in the Eocene to western Pakistan in the Miocene (Qayyum et al., 1996).

Wadia (1953) believes that the westward-flowing drainage along the whole northern edge of India existed throughout the deposition of the Siwalik Group from Miocene to Pliocene time and termed the river the Indobrahm River following the usage of Pascoe (1910). In the Pliocene or later, the Ganges River broke through the Rajmahal–Garo Gap and starts to carry the sediments to the Bay of Bengal. If we modify the Wadia hypothesis slightly and assume

(A) Constant bed thickness



(B) Section thickens linearly with a taper angle of  $\alpha$



Displacement  $d$  may be solved from

$$A = [2l \tan(\alpha) + d \tan(\alpha) + 2h]d/2$$

where  $\alpha$ , thickening angle;  $l$ , final length of cross section;  $A$ , structural-relief area

Fig. 27. (A) Area balancing under constant bed thickness. (B) Area balancing when section thickens linearly.

the Rajmahal–Garo Gap was first opened in the early Miocene, we may explain the observation in the Bengal Basin that did not receive Himalayan detritus until after the beginning of the Miocene (Uddin and Lundberg, 1998a,b). Unaware of the Wadia hypothesis, DeCelles et al. (1998a) independently propose that the paleo-Ganges River was first flowing westward in the early Miocene and then changed the flow direction to the west in the middle Miocene (p. 732, DeCelles et al., 1998a).

Two alternative models have also been proposed for the evolution of the Indus and Ganges systems. The first is by Brookfield (1998) who considers the current Himalayan drainage systems to have remained approximately the same configuration since the start of the Indo-Asian collision (see Fig. 23 of Brookfield, 1998). Raynolds (1980, 1981) found that late Pliocene Siwalik strata in the westernmost Potwar Plateau preserve dominantly south-eastward paleocurrent indicators. His conclusion was later expanded to the entire Potwar Plateau by Burbank and Beck (1991) who show this southeastward flow pattern lasted between 10 and 5 Ma in the latest Miocene and early Pliocene and changed to a southward flow pattern since 5 Ma in the late Pliocene. Burbank and Beck (1991) further suggest that the Indus River at this time joined the Ganges River to form a longitudinal drainage flowing eastward. Given the complex structural pattern in the Potwar plateau and the Salt Range, their paleocurrent data may be explained by the interaction between the Indus River and an evolving thrust system. That is, the Indus River may be an eastward flowing river north of the rising Salt Range and joined the southward flowing Jhelum River during deposition of the 10–5 Ma Siwalik sediments. The current straight course of the Indus River across the Indus River syntaxis (Fig. 1A) was later established at 5 Ma due to drainage focusing by the development of the Indus River syntaxis and associated headward erosion. The new course of the Indus River cuts straight to the south across the Salt Range through the Indus River syntaxis and abandoned its older east-flowing course. In this alternative interpretation, the upper reaches of the Indus drainage system had only one trunk prior to 5 Ma and has become two since with the Indus River to the west and the Jhlem River to the east. This

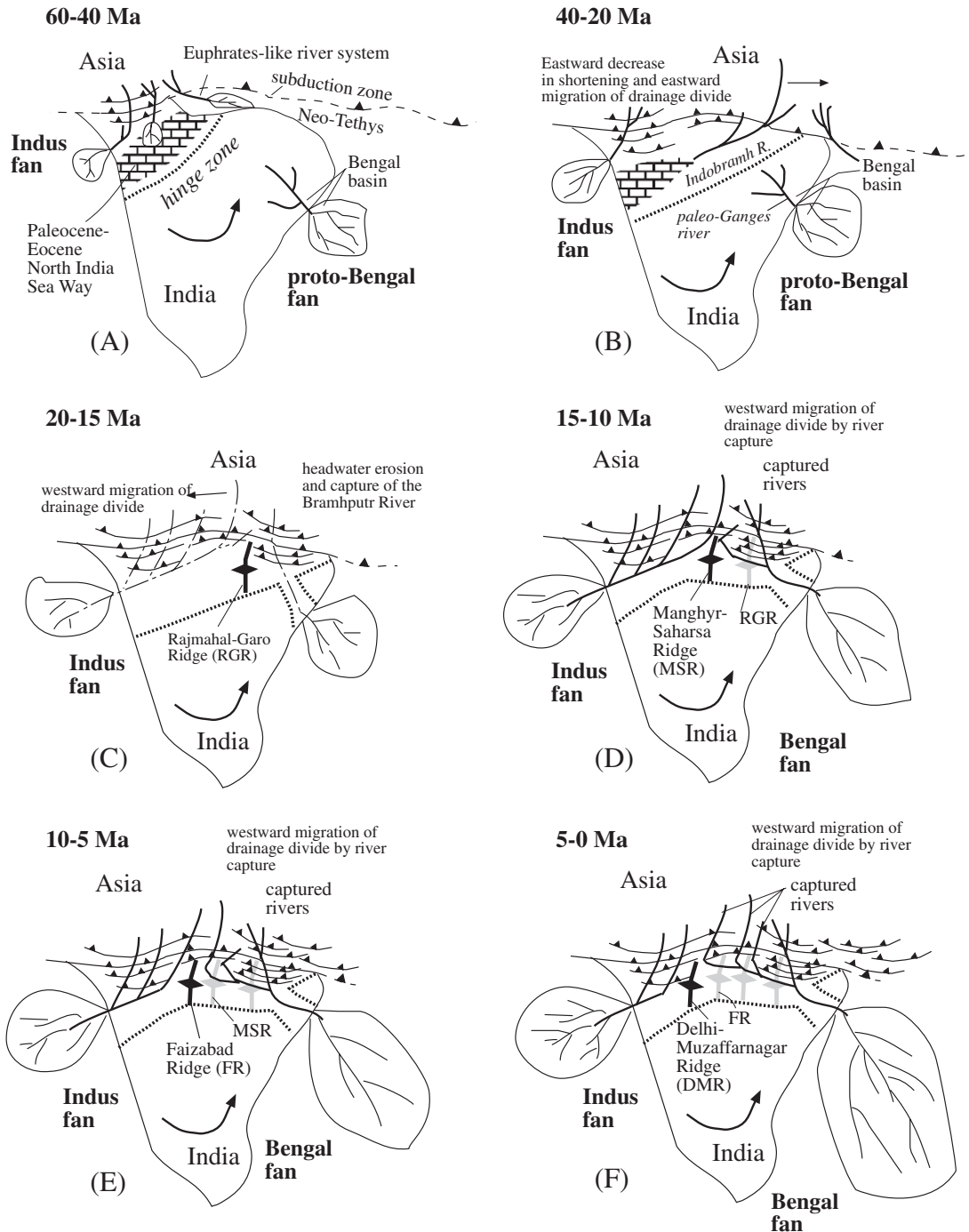
interpretation predicts that there were no east-flowing rivers of Miocene age east of the Jhlem River, consistent with the observation that the early Miocene west-flowing rivers were present in Nepal (DeCelles et al., 1998a).

If the Wadia hypothesis is correct, even in a general sense, with the timing of drainage reversal to be determined, it raises an interesting question of (1) at what time scale this switch was accomplished, and (2) why the northern Indian continent changes tilting direction from sloping to the west first then to the east during the Cenozoic Indo-Asian collision. For the first question, I speculate that the switch in drainage flow direction was progressive and took place on a time scale of > 10 m.y. For the second question, I suggest that this switch may be induced by the competition or combination of the following two factors: (1) eastward younging of diachronous initial contact between India and Asia (e.g., Rowley, 1996; Yin and Harrison, 2000; cf., Ding et al., 2003) and (2) a westward decrease in India–Asia convergence rate over the Cenozoic (e.g., Patriat and Achache, 1984; Dewey et al., 1989; Le Pichon et al., 1992). To account for the Miocene paleocurrent data in the Himalayan foreland basin and the depositional history of the Bengal Basin, I propose a speculative model below that is revised from the proposals of Wadia (1953) and DeCelles et al. (1998a).

Stage A (60–40 Ma) (Fig. 28A). Initial collision between India and Asia occurred at the northwestern corner of the Indian continent. Thrust loading causes northwestward tilting of northern Indian continent and development of a foreland basin hinge zone trending northeast. The major Himalayan drainage systems either flow westward into the Arabian Sea or to the North India Seaway during this time. The Bengal Basin and the proto-Bengal Fan may be developed on the east-central Indian continental margin, receiving sediments exclusively from the Peninsula Highlands of the Indian craton. After completion of the full contact between India and Asia sometime between 50 and 45 Ma, the eastern part of the Indus–Tsangpo suture zone and its neighboring regions starts accumulating crustal shortening at a faster rate than along the western segments of the suture zone. As a result, the tectonic load increases in the east faster than in the west of the Himalaya, causing progressive westward migration of the drainage divide between the Indus and Ganges systems.

Stage B (40–20 Ma) (Fig. 28B). The total magnitude of crustal shortening is still higher in the western than in the eastern Himalaya due to a longer duration

of strain accumulation since the onset of the Indo-Asian collision. As a result, northwestward tilting of Indian continent keeps the Himalayan rivers flowing



westward. They either enter the Arabian Sea or are drained to the North India Seaway during its westward retreat. At the same time, erosion from the Peninsula Highlands continuously sheds sediments to the proto-Bengal Fan. The situation is much like the Euphrates drainage system in Syria and Iraq of Middle East in the Eurasia–Arabian collisional system.

Stage C (20–15 Ma) (Fig. 28C). As the total amount of crustal shortening increases faster in the eastern Himalaya than in the western Himalaya due to a faster convergence rate between India and Asia, the northeastern corner of Indian continent starts to tilt northeastward while the majority of northern India remains tilting northwestward. The opposite tilting direction in the northeast and northwest parts of India creates a drainage divide in the Himalaya. The Rajmahal–Garo ridge trending at a high angle to the Himalayan front may be the first divide formed between the west-flowing and east-flowing river systems in the Himalayan foreland. This hypothesis is based on the observation that the current Indus–Ganges divide is separated by a structural ridge (i.e., Delhi–Mazaffarnagar ridge; Fig. 1A) that trends nearly perpendicular to the Himalayan orogen. This interpretation predicts a systematic westward increase in the amplitude of the drainage divide because the Himalayan thrust load may have increased with time as finite strain has accumulated. Due to headward erosion, the paleo-Ganges River eventually breaks the hinge

zone at the Rajmahal–Garo Gap and starts capturing the Himalayan rivers.

Stage D (15–10 Ma) (Fig. 28D). As the total crustal shortening increases faster in the eastern Himalayan orogen than in the western Himalayan orogen, the Himalayan drainage divide migrates farther to the west. The migration of the divide may not be a continuous process but instead in discrete jumps possibly due to the dynamic instability of the drainage network that has been constantly affected by Himalayan tectonics. This leads to the formation of the Manghyr–Saharsa ridge as the new divide in the west and the abandonment of the Rajmahal–Garo ridge as the old divide in the east.

Stage E (10–5 Ma) (Fig. 28E). As the thrust load increases in the eastern Himalayan orogen and more sediment accumulates in the Bengal Fan, a new drainage divide (the Faizabad ridge) formed farther west. This has forced the Himalayan river system to transport more sediment to the Bengal Fan than to the Indus Fan.

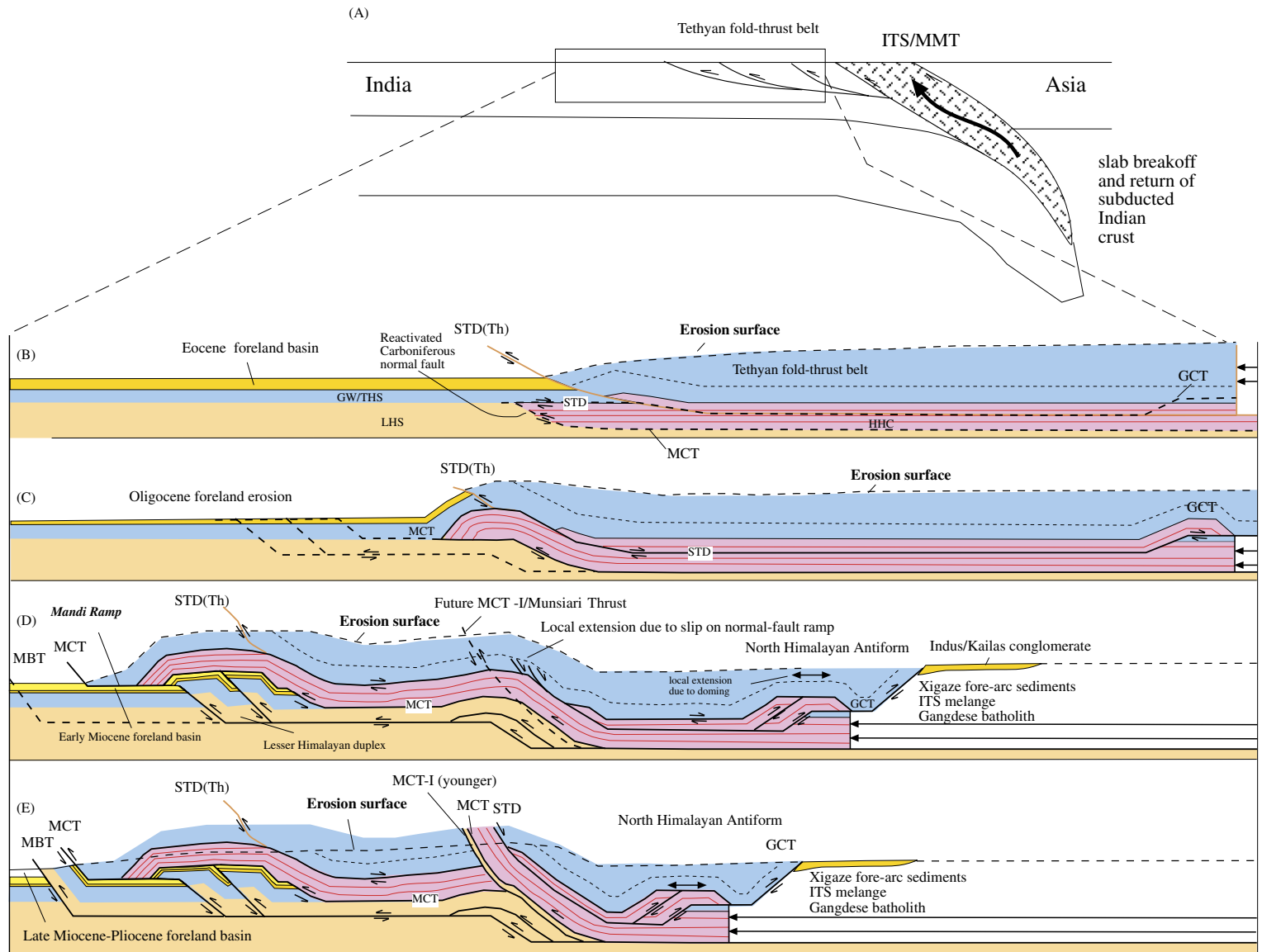
Stage F (5–0 Ma) (Fig. 28F). A similar process occurs as in Stage E, during which a new drainage divide, the Delhi–Muzaffarnagar ridge forms farther west of the old divide.

The above model makes the following testable predictions:

- (1) the Himalayan drainage divide migrates westward in a discrete fashion;
- (2) its amplitude increases westward;

---

Fig. 28. Evolution of the Himalayan drainage systems as a result of diachronous collision and eastward increase in convergence rate between India and Asia. (A) 60–40 Ma. Initial collision between India and Asia occurred at the northwestern corner of the Indian continent. Thrust loading at the northwestern corner of India caused northwestward tilting and development of a hinge zone trending northeast. The major Himalayan drainage systems either flow westward into the Arabian Sea or to the North India Seaway. Meanwhile, the proto-Bengal Fan is developed on the westside of Indian continent receiving sediments only from the Peninsula Highlands. (B) 40–20 Ma. The total magnitude of crustal shortening is still higher in the western than in the eastern Himalayan orogen due to a longer duration of strain accumulation since the onset of the Indo-Asian collision. As a result, northwestward tilting of Indian continent keeps the Himalayan rivers flowing westward. They either enter the Arabian Sea or are drained to the North India Seaway during its westward retreat. At the same time sediments from the Peninsula Highlands continuously provide the sediments to the proto-Bengal Fan. (C) 20–15 Ma. As the total amount of crustal shortening increases faster in the eastern Himalaya than in the western Himalaya due to a faster convergence rate between India and Asia, the northeastern corner of Indian continent starts to tilt northeastward while the majority of northern India remains tilting northwestward. The opposite tilting direction in the northeast and northwest parts of India creates a drainage divide. I suggest that Rajmahal–Garo ridge aligned at a high angle to the Himalayan front is the first divide formed between the west-flowing and east-flowing river systems in the Himalayan foreland. Due to headward erosion, the paleo-Ganges River eventually broke the hinge zone at the Rajmahal–Garo gap and started capturing Himalayan rivers. (D) 15–10 Ma. As the total crustal shortening increases faster in the eastern than in the western Himalayan orogen, the drainage divide farther migrates to the west. The migration of the divide may not be continuous but instead in discrete jumps. This leads to the formation of the Manghyr–Saharsa ridge as the new divide and the abandonment of the old divide in the east. (E) 10–5 Ma. As the thrust loading continues to increase in the eastern Himalayan orogen a new drainage divide (the Faizabad ridge) formed further to the west, making the Himalayan river system transporting more materials to the Bengal Fan than to the Indus Fan. (F) 5–0 Ma. A similar process occurs as in stage (E), during which a new drainage divide, the Delhi–Muzaffarnagar ridge formed.



- (3) the older west-flowing drainages are systematically captured by the younger east-flowing drainages from east to west;
- (4) the Indus Fan was the main repository of the Himalayan sediments in the Paleogene while the Bengal Fan was the main repository of the Himalayan sediments in the Neogene;
- (5) there might be a sudden increase in sedimentary flux in the early Miocene during the Rajmahal–Garo Gap was first broken through; and
- (6) the fluctuation of sedimentary fluxes into the Bengal and Indus Fans may be strongly influenced by the development of the foreland basin hinge zone rather than climate change alone (Burbank et al., 1993).

## 8. Kinematic evolution of the Himalayan orogen

A possible kinematic model for the evolution of the Himalayan orogen is shown in Fig. 29. The main basis of the model is the along-strike variation of the Himalayan geology, which is treated as recording sequential development of the orogen. Thus, the evolutionary cross-sections shown in Fig. 29 can also be viewed as along-strike variation of the Himalayan architecture. That is, Fig. 29B represents structural configuration of the Pakistan Himalaya, Fig. 29C represents the Kashmir Himalaya with the synform between two hanging-wall anticlines as the Kashmir basin, and Fig. 29D represents the Kumaon and Nepal Himalaya with the long and flat MCT hanging wall in front of the younger MCT-I as the Lesser Himalayan Crystalline Nappes.

(A) *Late Paleocene and early Eocene (60–50 Ma)*. Indian continent was subducted beneath Asia to depth of >100 km. A segment of the crust was subsequently returned from a depth at >100 km to a depth 20–15 km in the middle crust. The supracrustal strata above

the UHP gneiss complex were eroded and transported to the Himalayan foreland at this time (Fig. 29A).

(B) *Eocene and early Oligocene (45–24 Ma)*. The Tethyan Himalayan fold-thrust belt was developed as a result of farther continental subduction and crustal thickening of the Indian crust (Ratschbacher et al., 1994; Wiesmayr and Grasemann, 2002), using the STD as its basal thrust (Patel et al., 1993; J.D. Walker et al., 1999, C.B. Walker et al. (2001); Wiesmayr and Grasemann, 2002) (Fig. 29B). This resulted in deposition of Eocene–lower Oligocene strata in the Himalayan foreland basin and prograde metamorphism of the GHC in the northern Indian margin (e.g., DeCelles et al., 1998a; Searle et al., 1999a; Hodges, 2000). Interpreting the STD as originating from a top-south thrust (Patel et al., 1993; Wiesmayr and Grasemann, 2002) is not only consistent with the kinematic analyses that show the STD had experienced early top-south shear (also see Dèzes et al., 1999; Grujic et al., 2002), but also explains the protolith of some high-grade GHC rocks that are apparently younger than the THS (Honegger et al., 1982; J.D. Walker et al., 1999). Note that the upper Paleozoic to Mesozoic Gondwana Sequence (unit GW) in the Lower Himalaya is the epicratonal equivalent of the THS deposited in the shelf-edge and continental slope settings in the Higher and North Himalaya (Stöcklin, 1980; Brookfield, 1993; Frank et al., 1995; Steck et al., 1998).

(C) *Late Oligocene–early Miocene (24–20 Ma)*. Initiation of the MCT may have caused reactivation of the STD as a roof fault to accommodate crustal thickening during emplacement of the GHC over the LHS (Fig. 29C). Because the STD was reactivated from a south-directed thrust, it locally exhibits a north-dipping normal fault ramp in the middle crust that allows the fault to truncate early isograds in its footwall and to cause local extension in its hanging wall. This model specifically explains why the Warwan backthrust and Zanskar shear zone in the Zanskar

Fig. 29. Structural evolution of the Himalaya. (A) Late Paleocene (60–50 Ma): Indian continent was subducted beneath Asia to depth of >100 km. A segment of the crust returned to the middle crust by 50–45 Ma. The supracrustal strata were eroded and transported to the Himalayan foreland. (B) Eocene and Oligocene (45–24 Ma): development of the Tethyan fold-thrust belt and thickening of northern Himalayan crust. STD(th) is the basal thrust for the Tethyan Himalaya fold-thrust belt that was later reactivated as the South Tibet Detachment (STD). The Tethyan Himalayan Sequence includes the terrestrial and marine Carboniferous–Permian strata of the Gondwana Sequence in the Lesser Himalayan zone marked as the GW/THS unit. (C) Late Oligocene–early Miocene (26–20 Ma): Initiation of MCT and reactivation of STD as a normal fault. (D) Early–middle Miocene (20–15 Ma): MCT broke the surface and created the Lesser Himalaya duplex system. MCT2 marks the position of the late Miocene–early Pliocene reactivated break-back thrust in the hanging wall of the original MCT. (E) Late Miocene–early Pliocene (7–4 Ma): The younger reactivated MCT zone carrying part of the Lesser Himalayan Sequence cut and offset the older roof fault MCT.

Himalaya NW India truncate the metamorphic isograds in their common footwall and lower- over higher-grade rocks across the STD (Honegger et al., 1982; Herren, 1987; Searle et al., 1992; Dèzes, 1999; Dèzes et al., 1999).

(D) *Early–middle Miocene (20–15 Ma)*. The MCT broke the surface (Fig. 29D). Northward motion on the STD was accommodated by slip on the south-dipping and north-directed GCT. Movement on the GCT was in turn associated with northward propagation and development of a thrust duplex beneath the North Himalayan Antiform, causing local north–south extension above the ramp and progressively younger cooling ages to the north above the antiform (Lee et al., 2000). I envision that the development of the North Himalayan Antiform is similar to the Ruby Gap duplex of central Australia (Dunlap et al., 1997). There, forward development of a mid-crustal ductile duplex system caused a systematic decrease in cooling age in the thrust transport direction. Although the Tethyan Himalayan strata above the STD and GCT were translated northward relative to the GHC, they are transported southward with respect to the Indian basement beneath the GHC and LHS. Because the GCT has a minimum slip of 38 km in the central Himalaya (Murphy and Yin, 2003) and could be greater than 60 km in the eastern Himalaya, it is also possible that the mélangé complex along the Indus–Tsangpo suture zone, the Xigaze forearc basin, and even portion of the Gangdese batholith were thrust beneath the GCT and now lie below the northern part of the North Himalaya. That is, the model also permits the subduction of the southern Lhasa block beneath the GCT. This required relationship is superficially similar to the prediction of the channel flow model. However, the mechanism of Asian rocks tectonically juxtaposed beneath the THS rocks is fundamentally different in the ski-jump model of Yin et al. (1994) that is shown in Fig. 29D.

(E) *Late Miocene–early Pliocene (7–4 Ma)*. The reactivated lower MCT zone cuts across the upper MCT above (Fig. 29E). Motion on the MBT and development of the Lesser Himalayan duplex system has caused folding of the MCT and STD. Although the STD is shown to be terminated by late Miocene time because it is folded in the western Himalaya, it does not preclude the possibility that the STD has been locally reactivated in the

Pliocene and perhaps even remains active in the Holocene (Hodges et al., 2001; Hurtado et al., 2001). The predicted relationship between the older MCT (= MCT-II = Vaikrita thrust) and the reactivated younger MCT (MCT-I = Munsiri thrust) has been documented by Arita et al. (1997) and Johnson et al. (2001) in Nepal.

## 9. Future tasks in the Himalayan research

Several tasks require urgent attention in the future Himalayan research:

(1) Systematic mapping around the Kishtwar and Kullu–Larji–Rampur windows to determine the structural relationship between the MCT and STD.

(2) A systematic sampling of the Tethyan Himalayan strata for determination their Sr and Nd compositions, particularly in the Pakistan Himalaya and eastern Himalayan orogen. This will help correlate sediments in the Himalayan foreland basin and the Bengal and Indus Fans with their potential source areas.

(3) Investigating the Himalayan foreland strata to detect the first appearance of early–middle Miocene detrital zircons and monazites of the Higher Himalayan leucogranites. These clasts are probably the best indicators for determining when the GHC was first exposed at the surface. As the leucogranites are much more voluminous in the eastern Himalaya such as in Bhutan (e.g., Gansser, 1983) than in the western and central Himalaya, the study of this kind may be best executed in the eastern Himalayan foreland basin.

(4) Investigating the Nd and Sr compositions of the lowest Cretaceous and Paleocene Amile Formation to test whether it was derived from the Indian craton or from the Gangdese batholith of southern Tibet. This has important implications for when India was first collided with Asia.

(5) Detailed field mapping around the eastern Himalayan syntaxis to determine the structural relationship between the GCT and STD. This would help elucidate the deep crustal relationship between the two major Himalayan structures that in turn will help test several first-order tectonics models for the evolution of the Himalaya.

(6) Detailed sedimentologic and structural studies of the scattered Miocene–Pliocene sedimentary basins in the North Himalaya. This will test whether the deposition of these basins were related to the development of Miocene north-directed normal faulting along the STD or younger east–west extension along the Neogene north-trending rifts.

(7) It remains unclear whether the Paleocene Seaway in North India was retreating unidirectionally to the west or bi-directionally to the east and west simultaneously in the Oligocene. This question is important because the initial river flow direction may be correlated with the younging direction of diachronous collision such as in the case of the Arabia–Eurasia collision in the Middle East. In that collisional system, the Euphrates River system flows eastward to the Persian Gulf in the younging direction of initial collision between the two continents. One can certainly assert that if the north-central part of northern India was diamond shaped and first touched the southern margin of Asia as proposed by Treloar and Coward (1991) and Ding et al. (2003), two river systems with one flowing to the east and the other flowing to the west may have developed along the Indus–Tsangpo suture zone. Unraveling depositional settings of the Cenozoic strata along the Indus–Tsangpo suture zone may not only constrain the timing for the onset of Indo-Asian collision, but may also provide insight into how the diachronous collision was actually accomplished.

(8) U–Pb detrital zircon studies are needed for the Cenozoic strata in the Bengal Basin. This will test when the Rajmahal–Garó Gap was first opened, because the basin sediments deposited before its opening would be exclusively derived from the Indian craton, while sediments deposited after its opening should have a significant input from the Himalayan orogen.

(9) It remains unclear whether the variation in the flux of sediments in the Bengal and Indus Fans result from a synchronous regional or global change of climate conditions, a change in the mode and intensity of tectonic activity, the dynamic evolution of the Himalayan drainage system, or a combination of all these processes.

(10) A series of deep crustal reflection profiles should be conducted across the Himalaya from west to east in order to constrain along-strike variation of

structural geometry of the orogen and its three-dimensional evolution.

(11) The role of Carboniferous rifting in northern India in shaping the pre-Cenozoic Himalayan stratigraphic framework needs to be carefully evaluated.

## 10. Conclusions

(1) Geologic thinking on the development of the Himalayan orogen is parallel to research histories of many other prominent problems in geosciences. That is, we “place special emphasis on a selective conjecture, based typically on the initial observation or recognition of a phenomenon, which is thereafter given privileged status over alternate interpretations” (Dickinson, 2003). In the case of the Himalaya, this is reflected in its basic divisions that mix geographic division with structural and stratigraphic divisions. This tradition has limited our ability to decipher the true three-dimensional variation of the Himalayan architecture. To overcome this problem, a new set of Himalayan terminology is proposed that emphasizes independent and objective divisions of Himalayan stratigraphy, structures, and topography.

(2) The major Himalayan stratigraphic units of the Greater Himalayan Crystalline Complex, the Tethyan Himalayan Sequence, and the Lesser Himalayan Sequence were all deposited in a single north-facing continental margin in the Proterozoic and Cambrian–Early Ordovician. However, their current distribution results from an Early Ordovician contractional or extensional orogeny, Carboniferous rifting, and large-scale Cenozoic thrusting. Specifically, a north-dipping Carboniferous normal fault system may have existed between the presently exposed Tethyan and Lesser Himalayan Sequences. Its motion may have led to the removal of Ordovician–Carboniferous strata from most of the Lesser Himalayan Sequence and deposition of a thick Carboniferous section in the Tethyan Himalayan Sequence. The Cenozoic Main Central Thrust may have been reactivated from a Carboniferous north-dipping normal fault, resulting in the juxtaposition of younger and higher-grade metamorphic rocks over older and lower-grade metamorphic rocks across the MCT.

(3) Elevation of the Himalayan orogen increases systematically eastward along strike. In northern Pakistan, the western Himalaya, its highest elevation is generally below 4000 m, with high peaks of >7000 m located exclusively north of the Indus–Tsangpo suture in the Karakorum Mountains, Pamirs, and the Kunlun Shan. In the central and eastern Tibet, the highest peaks are all located south of the Indus–Tsangpo suture in the Himalayan orogen. This change in elevation is associated with progressively narrowing of intermontane basins in the southern Himalayan orogen. The along-strike variation of the Himalayan topography may result from:

- (a) concentration of shortening north of the suture in the western Indo-Asian collision zone and concentration of shortening south of the suture in the central and eastern Himalayan orogen;
  - (b) eastward increase in total shortening; and
  - (c) variation in thrust spacing and depth to the master decollement.
- (4) The first-order Himalayan architecture and the kinematic properties for the Himalayan evolution are characterized by:

- (a) The MCT and STD are subparallel structures; both are folded concordantly and exhibit long flats of over 60–100 km in their north–south transport directions.
- (b) The MCT has a frontal ramp beneath the Higher Himalaya and a major lateral ramp in the western Himalayan orogen.
- (c) Amphibolite facies rocks are exposed above the MCT in the eastern Himalaya whereas low-grade phyllite is exposed above the MCT in the western Himalaya, possibly as a result of an eastward increase in crustal shortening and erosion along the Himalayan orogen.
- (d) Out-of-sequence thrusting dominates the Cenozoic geology of the Lower Himalaya.
- (e) The Miocene MCT and STD merge with one another in their up-dip direction to the south and may interact with the coeval Great Counter Thrust at a middle or lower crustal level beneath the North and Higher Himalaya.

(5) The STD was initiated as a thrust as evidenced by (a) early top-south fabrics, (b) locally preserved

higher-grade over lower-grade relationship (Annapurna of Nepal), and (c) locally preserved older over younger relationship (Zaskar of NW India). It was later reactivated as a top-north shear zone and in places was superposed by the even younger top-south shear. This repeated alternation of top-north and top-south shear might be explained by the alternation of passive-roof and active-roof thrusting during emplacement of the high-grade Greater Himalayan Crystalline Complex.

(6) Although it is well known that the Main Central Thrust, the South Tibet Detachment, and Great Counter Thrust were all active in the Miocene, their initiation ages and potential diachronous development along the Himalayan orogen remain unknown. Using the development of the Shillong plateau as a modern analogue, it is possible that the major faults in the Himalayan orogen were initiated either in its eastern or western ends and then propagated laterally. Much research is needed to test this hypothesis.

(7) Exhumation rates in the Himalayan orogen are strongly dependent on the mode and magnitude of deformation. That is, the location and duration of structural uplifts decide the spatial extent and rates of erosion. Climate conditions do not seem to have exerted a first-order control in the distribution of exhumation rates. Specifically, exhumation rates in the Himalaya reached three peaks:

- (a) during 55–45 Ma at a rate of ~40 mm/yr in small ultra-high pressure metamorphic terranes along the western Indus–Tsangpo suture zone;
- (b) during 12–8 Ma at a rate of 6–7 mm/yr in northern Himalayan gneiss domes; and
- (c) since 7 Ma at a rate of 3–5 mm/yr in the central Himalaya above the reactivated MCT zone.

Excluding these localized high rates of exhumation, most of the Himalayan orogen was exhumed at a rate between 0.1 and 1.0 mm/yr. The clear correlation between high exhumation rates and local structural development suggests that the rate and magnitude of deformation, not the climate condition, have played an important role in deciding where and how fast Himalayan exhumation occurs.

(8) The Nd and Sr isotopic compositions and U–Pb detrital zircon ages between southern Tibet and the

Himalayan units are distinguishable. Although the Nd and Sr isotopic compositions of the Proterozoic LHS are significantly different from those of the GHC and THS, the Cambrian strata of the LHS share similar Nd composition and detrital zircon ages of the GHS and Cambrian THS.

(9) Nd and Sr isotopic compositions of the Paleocene–Eocene foreland basin strata from NW India suggest that clasts from southern Tibet may have been transported across the Indus–Tsangpo suture to the Himalaya during their deposition. The detrital zircon ages from the lower Paleocene strata in western Nepal hint at the possibility that the contact between India and Asia was already established by this time.

(10) From the first appearance of metamorphic minerals in the Siwalik sedimentary rocks, the Greater Himalayan Crystalline Complex excluding those exposed in the two syntaxes and Eocene UHP terranes was not exposed at the surface until after about 11–5 Ma in the Himalaya. This young exposure age is at least 10 m.y. younger than the previously interpreted exposure age of the GHC.

(11) The flow direction of the main Himalayan drainage system in the northern Indian continent may have changed dramatically during the Indo-Asian collision. Specifically, the Indus and Gangdese rivers may have once joined together and flowed westward in Paleogene and possibly early Miocene time. The modern Gangdese River was developed by headward erosion from a river system that drained only the western Indian craton and was not linked with the Himalayan drainage system until the opening of the Rajmahal–Garo Gap in the Miocene.

(12) Eocene slab breakoff of the Indian plate may have created a thermal anomaly beneath the southern Tibet when it was located some 2000 km south of its present position. When north-moving India was overriding this thermal anomaly in the Oligocene immediately after the slab breakoff event, the entire continent was raised above the sea level and caused the development of the widespread Oligocene unconformity in the northern Indian continent. As the thermal anomaly decays with time, thrust loading resumes as the main mechanism of creating accommodation space for sedimentation in the Himalayan foreland basin.

## Acknowledgements

My interests in the Himalayan geology were inspired by interaction and collaboration with Mark Harrison in the past decade at UCLA. Discussions with Bernhard Grasemann and Nigel Hughes led me to the eastern and western Indian Himalaya. Mike Brookfield, J.-P. Burg, Brian Horton, Nigel Hughes, George Gehrels, Kevin Pogue, and Mike Searle read the early drafts of the manuscript and provided many useful suggestions. Special thanks go to Peter DeCelles, Joe DiPietro, Brian Horton, Alex Webb, and Mike Edwards for their careful and critical reviews, which led to numerous revisions and reorganization of the original manuscript. I thank Mike Taylor at University of Kansas for preparing Fig. 1. I would also like to thank Dr. C.S. Dubey at Delhi University, Dr. Ding Lin at the Chinese Academy of Sciences, and Professor Wang Xiao-Feng at the Chinese Academy of Geological Sciences for organizing field trips to the Himalaya. Despite valuable and numerous inputs from the above individuals, the opinion expressed in this paper is mine only and I am responsible for all the mistakes that occur in this article. An Yin's research in the Himalaya has been supported by grants from the US National Science Foundation.

## References

- Acharyya, S.K., 1980. Structural framework and tectonic evolution of the eastern Himalaya. *Himalayan Geology* 10, 412–439.
- Acharyya, S.K., 1994. The Cenozoic foreland basin and tectonics of the eastern sub-Himalaya: problems and prospects. *Himalayan Geology* 15, 3–21.
- Acharyya, S.K., Ray, K.K., 1977. Geology of the Darjeeling–Sikkim Himalaya. Guide to Excursion No. 3, Fourth International Gondwana Symposium (Calcutta). Geological Survey of India, pp. 1–25.
- Ahmad, T., Harris, N., Bickle, M., Chapman, H., Bunbury, J., Prince, C., 2000. Isotopic constraints on the structural relationships between the Lesser Himalayan Series and the High Himalayan Crystalline Series, Garhwal Himalaya. *Geological Society of America Bulletin* 112, 467–477.
- Aikman, A.B., Harrison, T.M., Ding, Lin, 2004. Preliminary results from the Yala Xiangbo leucogranite dome, SE Tibet. *Himalayan Journal of Sciences* 2, 91 (Special issue with extended abstracts presented in the 19th Himalaya–Karakoram–Tibet Workshop, Niseko, Japan).
- Alam, M., Alam, M.M., Curray, J.R., Chowdhury, A.L.R., Gani, M.R., 2003. An overview of the sedimentary geology of the

- Bengal basin in relation to the regional tectonic framework and basin-fill history. *Sedimentary Geology* 155, 179–208.
- Allègre, C.J., et al., 1984. Structure and evolution of the Himalayan–Tibet orogenic belt. *Nature* 307, 17–22.
- Alsldorf, D., Nelson, D., 1999. Tibetan satellite magnetic low: evidence for widespread melt in the Tibetan crust? *Geology* 27, 943–946.
- Amano, K., Taira, A., 1992. 2-Phase uplift of Higher Himalayas since 17 Ma. *Geology* 20, 391–394.
- Anastasio, D.J., Bebout, G.E., Holl, J.E., 2004. Extra-basinal fluid infiltration, mass transfer, and volume strain during folding: insights from the Idaho–Montana thrust belt. *American Journal of Science* 304, 333–369.
- Anderson, E.M., 1951. *The Dynamics of Faulting and Dyke Formation with Applications to Britain*, 2nd edition. Oliver and Boyd, Edinburgh.
- Appel, E., Rosler, W., Corvinus, G., 1991. Magnetostratigraphy of the Miocene–Pleistocene Surai Khola Siwaliks in western Nepal. *Journal of Geophysical Research* 105, 191–198.
- Argles, T.W., Edwards, M.A., 2002. First evidence for high-grade, Himalaya-age synconvergent extension recognized within the western syntaxis—Nanga Parbat Pakistan. *Journal of Structural Geology* 24, 1327–2344.
- Argles, T., Foster, G., Whittington, A., Harris, N., George, M., 2003. Isotope studies reveal a complete Himalayan section in the Nanga Parbat syntaxis. *Geology* 31, 1109–1112.
- Arita, K., 1983. Origin of the inverted metamorphism of the Lower Himalayas Central Nepal. *Tectonophysics* 95, 43–60.
- Arita, K., Ganzawa, Y., 1997. Thrust tectonics and uplift processes of the Nepal Himalaya revealed from fission-track ages. *Journal of Geography* 106, 156–167 (in Japanese with English Abstract).
- Arita, K., Dallmeyer, R.D., Takasu, A., 1997. Tectonothermal evolution of the Lesser Himalaya, Nepal: constraints from Ar/Ar ages from the Kathmandu Nappe. *The Island Arc* 6, 372–385.
- Armijo, R., Tapponnier, P., Mercier, J.L., Han, T.-L., 1986. Quaternary extension in southern Tibet: field observations and tectonic implications. *Journal of Geophysical Research* 91, 13,803–13,872.
- Armijo, R., Tapponnier, P., Han, T., 1989. Late Cenozoic right-lateral strike-slip faulting in southern Tibet. *Journal of Geophysical Research* 94, 2787–2838.
- Armstrong, R.L., 1968. The Cordilleran Miogeosyncline in Nevada and Utah. *Geological and Mineralogical Survey Bulletin*, vol. 78, 58 pp.
- Auden, J.B., 1934. The geology of the krol belt. *Records of Geological Survey of India* 66, 357–454.
- Auden, J.B., 1935. Traverses in the Himalaya. *Records of Geological Survey of India* 69, 123–167.
- Auden, J.B., 1937. The structure of the Himalaya in Garhwal. *Records of Geological Survey of India* 71, 407–433.
- Avouac, J.P., 2003. Mountain building, erosion, and the seismic cycle in the Nepal. *Advances in Geophysics* 46, 1–80.
- Avouac, J.P., Burov, E.B., 1996. Erosion as a driving mechanism of intracontinental mountain growth. *Journal of Geophysical Research* 101, 17747–17769.
- Axen, G.J., 1992. Pore pressure, stress increase, and fault weakening in low-angle normal faulting. *Journal of Geophysical Research* 97, 8979–8991.
- Baig, M.S., 1990. Structure and geochronology of pre-Himalayan and Himalayan orogenic events in the northwest Himalaya, Pakistan, with special reference to the Besham area. PhD thesis, Oregon State University, Corvallis, 300 pp.
- Banks, C.J., Warburton, J., 1986. Passive-roof duplex geometry in the frontal structures of the Kirthar and Sulaiman Mountain Belt Pakistan. *Journal of Structural Geology* 8, 229–237.
- Baski, A.K., Barman, T.R., Paul, D.K., Farrar, E., 1987. Widespread early Cretaceous flood-basalt volcanism in eastern India—Geochemical data from the Rajmahal Bengal Sylhet traps. *Chemical Geology* 63, 133–141.
- Baud, A., Gaetani, M., Garzanti, E., Fois, E., Nicora, A., Tintori, A., 1984. Geological observations in southeastern Zaskar and adjacent Lahul area (northwestern Himalaya). *Eclogae Geologicae Helvetiae* 77, 171–197.
- Beaumont, C., Jamieson, R.A., Nguyen, M.H., Lee, B., 2001. Himalayan tectonics explained by extrusion of a low-viscosity crustal channel coupled to focused surface denudation. *Nature* 414, 738–742.
- Beaumont, C., Jamieson, R.A., Nguyen, M.H., Medvedev, S., 2004. Crustal channel flows: 1. Numerical models with applications to the tectonics of the Himalayan–Tibetan orogen. *Journal of Geophysical Research* 109. doi:10.1029/2003JB002809.
- Bhanot, V.K., Kwartra, S.K., Kansal, A.K., Pandey, B.K., 1978. Rb–Sr whole rock age for Chail Series of northwestern Himalaya. *Journal of the Geological Society of India* 19, 224–225.
- Bhargava, O.N., 1995. The Bhutan Himalaya: a geological account. *Geological Survey of India Special Publication* 39, 245 pp.
- Bilham, R., England, P., 2001. Plateau ‘pop-up’ in the great 1897 Assam earthquake. *Nature* 410, 806–809.
- Bird, P., 1978. Initiation of intracontinental subduction in Himalaya. *Journal of Geophysical Research* 83, 4975–4987.
- Bird, P., 1991. Lateral extrusion of lower crust from under high topography, in the isostatic limit. *Journal of Geophysical Research* 96, 10275–10286.
- Bossart, P., Dietrich, D., Greco, A., Ottiger, R., Ramsay, J.G., 1988. The structure of the Nazara–Kashmir syntaxis, southern Himalayas Pakistan. *Tectonics* 7, 273–297.
- Boyer, S.E., Elliott, D., 1982. Thrust systems. *Bulletin of the American Association of Petroleum Geologists* 66, 1196–1982.
- Brookfield, M.E., 1993. The Himalayan passive margin from Precambrian to Cretaceous. *Sedimentary Geology* 84, 1–35.
- Brookfield, M.E., 1998. The evolution of the great river systems of southern Asia during the Cenozoic India–Asia collision: rivers draining southwards. *Geomorphology* 22, 285–312.
- Brown, R.L., Nazarchuk, J.H., 1993. Annapurna detachment fault in the Greater Himalaya of central Nepal. In: Treloar, P.J., Searle, M.P. (Eds.), *Himalayan Tectonics*. The Geological Society Special Publication, vol. 74, pp. 461–473.
- Brozovic, N., Burbank, D.W., 2000. Dynamic fluvial systems and gravel progradation in the Himalayan foreland. *Geological Society of America Bulletin* 112, 394–412.

- Brun, J.P., Burg, J.P., Chen, G.M., 1985. Strain trajectories above the Main Central Thrust (Himalaya) in southern Tibet. *Nature* 313, 388–390.
- Brunel, M., 1986. Ductile thrusting in the Himalayas: shear sense criteria and stretching lineation. *Tectonics* 5, 247–265.
- Brunel, M., Kienast, J.-R., 1986. Etude petro-structurale des chevauchements ductiles himalayens sur la transversale de l'Everest–Makulu (Nepal oriental). *Canadian Journal of Earth Sciences* 23, 117–1137.
- Brunel, M., Chayé d'Albissin, M.C., Loquin, M., 1984. Détermination d'un âge Cambrien des séris carbonatées à magnésite situées sous le Grand Chevauchement Himalayen (Main Central Thrust–Népal oriental) par la découverte de paléobasidiospores. *Geobios* 17, 595–602.
- Brunel, M., Chayé d'Albissin, M.C., Loquin, M., 1985. The Cambrian age of magnesites from E. Nepal as determined through the discovery of paleobasidiospores. *Journal of the Geological Society of India* 26, 255–260.
- Burbank, D.W., 1992. Causes of recent Himalayan uplift deduced from deposited patterns in the Ganges basin. *Nature* 357, 680–683.
- Burbank, D.W., 2002. Rates of erosion and their implications for exhumation. *Mineralogical Magazine* 66, 25–52.
- Burbank, D.W., Beck, R.A., 1991. Models of aggradation versus progradation in the Himalayan Foreland. *Geologische Rundschau* 80, 623–638.
- Burbank, D.W., Derry, L.A., France-Lanord, C., 1993. Reduced Himalayan sediment production 8 Myr ago despite an intensified Monsoon. *Nature* 364, 48–50.
- Burbank, D.W., Beck, R.A., Mulder, T., 1996. The Himalayan foreland basin. In: Yin, A., Harrison, T.M. (Eds.), *The Tectonics of Asia*. Cambridge University Press, New York, pp. 149–188.
- Burbank, D.W., Blythe, A.E., Putkonen, J., Pratt-Sitaula, B., Gabet, E., Oskin, M., Barros, A., Ojha, T.P., 2003. Decoupling of erosion and precipitation in the Himalayas. *Nature* 426, 652–655.
- Burchfiel, B.C., Royden, L.H., 1985. North–south extension within the convergent Himalayan region. *Geology* 13, 679–682.
- Burchfiel, B.C., Chen, Z., Royden, L.H., Liu, Y., Deng, C., 1991. Extensional development of Gabo valley, southern Tibet. *Tectonophysics* 194, 187–193.
- Burchfiel, B.C., Chen, Z., Hodges, K.V., Liu, Y., Royden, L.H., Deng, C., Xu, J., 1992. The South Tibet Detachment System, Himalayan orogen: Extension contemporaneous with and parallel to shortening in a collisional mountain belt. *Geological Society of America Special Paper* 269, 1–41.
- Burchfiel, B.C., Wang, E., Hodges, K.V., 2002. Possible large scale, Cenozoic, low-angle normal fault in the Namche Barwa area, eastern Himalayan syntaxis. *Abstracts with Programs-Geological Society of America* 34, 84.
- Burg, J.P., Chen, G.M., 1984. Tectonics and structural formation of southern Tibet, China. *Nature* 311, 219–223.
- Burg, J.P., Proust, F., Tapponnier, P., Ming, C.G., 1983. Deformation phases and tectonic evolution of the Lhasa block (southern Tibet China). *Eclogae Geologicae Helvetiae* 76, 643–665.
- Burg, J.P., Brunel, M., Gapais, D., Chen, G.M., Liu, G.H., 1984a. Deformation of leucogranites of the crystalline main central sheet in southern Tibet (China). *Journal of Structural Geology* 6, 535–542.
- Burg, J.P., M.Guiraud, G.M., Chen, Li, G.C., 1984b. Himalayan metamorphism and deformations in the northern Himalayan belt (Southern Tibet China). *Earth and Planetary Science Letters* 69, 391–400.
- Burg, J.P., Leyreloup, A., Girardeau, J., Chen, G.M., 1987. Structure and metamorphism of a tectonically thickened continental crust—the Yalu Tsangpo suture zone (Tibet). *Philosophical Transactions of the Royal Society of London. Series A* 321, 67–86.
- Burg, J.P., Chaudhry, M.N., Ghazanfar, M., Anczkiewicz, R., Spencer, D., 1996. Structural evidence for back sliding of the Kohistan arc in the collisional system of northwest Pakistan. *Geology* 24, 739–742.
- Burg, J.P., Nievergelt, P., Oberli, F., Seward, D., Davy, P., Maurin, J.C., Diao, Z.Z., Meier, M., 1998. The Namche Barwa syntaxis: evidence for exhumation related to compressional crustal folding. *Journal of Asian Earth Sciences* 16, 239–252.
- Burtman, V.S., Molnar, P., 1993. Geological and geophysical evidence for deep subduction of continental crust beneath the Pamir. *Geological Society of America Special Paper* 281, 1–76.
- Butler, R.W.H., Wheeler, J., Treloar, P.J., Jons, C., 2000. Geological structure of the southern part of the Nanga Parbat massif, Pakistan Himalaya, and its tectonic implications. In: Khanm, M.A., Treloar, P.J., Searle, M.P., Jan, M.Q. (Eds.), *Tectonics of the Nanga Parbat Syntaxis and the Western Himalaya*. The Geological Society Special Publication, vol. 170, pp. 123–136.
- Calkin, J.A., Offield, T.W., Abdulah, S.K.M., Tayyab, A.S., 1975. Geology of the southern Himalayan in Hazara, Pakistan, and adjacent areas. *U.S. Geological Survey Professional Paper* 716-C, 29 pp.
- Carosi, R., Lombardo, B., Molli, G., Musumeci, G., Pertusati, P.C., 1998. The South Tibetan detachment system in the Rongbuk valley, Everest region. Deformation features and geological implications. *Journal of Asian Earth Sciences* 16, 299–311.
- Carosi, R., Lombardo, B., Musumeci, G., Pertusati, P.C., 1999. Geology of the Higher Himalayan Crystallines in Khumbu Himal (Eastern Nepal). *Journal of Asian Earth Sciences* 17, 785–803.
- Catlos, E.J., 2000. Geochronologic and thermobarometric constraints on the evolution of the main central thrust, Himalayan orogen, PhD thesis, University of California, Los Angeles, 345 pp.
- Catlos, E.J., Harrison, T.M., Kohn, M.J., Grove, M., Ryerson, F.J., Manning, C.E., Upreti, B.N., 2001. Geochronologic and thermobarometric constraints on the evolution of the Main Central Thrust, central Nepal Himalaya. *Journal of Geophysical Research* 106, 16177–16204.
- Catlos, E.J., Harrison, T.M., Manning, C.E., Grove, M., Rai, S.M., Hubbard, M.S., Upreti, B.N., 2002a. Records of the evolution of the Himalayan orogen from in situ Th–Pb ion microprobe dating of monazite: Eastern Nepal and western Garhwal. *Journal of Asian Earth Sciences* 20, 459–479.
- Catlos, J.E., Harrison, T.M., Dubey, C.S., Edwards, M.A., 2002b. *P–T–t* constraints on the evolution of the Sikkim Himalaya. 17th Himalaya–Karakoram–Tibet Workshop, Gangtok, Sikkim, India, pp. 6–7.

- Catlos, E.J., Dubey, C.S., Harrison, T.M., Edwards, M.A., 2004. Late Miocene movement within the Himalayan Main Central Thrust shear zone, Sikkim, north-east India. *Journal of Metamorphic Geology* 22, 207–226.
- Cervený, P.F., Naeser, N.D., Zeitler, P.K., Naeser, C.W., Johnson, N.M., 1988. History of uplift and relief of the Himalaya during the past 18 million years; evidence from sandstones of the Siwalik Group. In: Kleinspehn, K.L., Paola, C. (Eds.), *New Perspectives in Basin Analysis*. Springer-Verlag, New York, pp. 43–61.
- Cervený, P.F., Johnson, N.M., Tahirkheli, R.A.K., Bonis, N.R., 1989a. Tectonic and geomorphic implications of Siwalik Group heavy minerals, Potwar Plateau, Pakistan. In: Malinconico, L.L., Lillie, R.J. (Eds.), *Tectonics and Geophysics of the Western Himalaya, Special Paper-Geological Society of America*, vol. 232, pp. 129–136.
- Cervený, P.F., Naeser, C.W., Kelemen, P.B., Lieberman, J.E., Zeitler, P.K., 1989b. Zircon fission-track ages from the Gasherbrum Diorite, Karakoram Range, northern Pakistan. *Geology* 17, 1044–1048.
- Chatterji, G.C., Swami Nath, J., 1977. The stratigraphy and structure of the parts of the Simla Himalaya—a synthesis. *Memoir of Geologic Survey of India* 106, 408–490.
- Chaudhry, M.N., Ghazanfar, M., 1990. Position of the Main Central Thrust in the tectonic framework of Western Himalaya. *Tectonophysics* 174, 321–329.
- Chemenda, A.I., Mattauer, M., Malavieille, J., Bokun, A.N., 1995. A mechanism for syn-collisional rock exhumation and associated normal faulting—results from physical modeling. *Earth and Planetary Science Letters* 132, 225–232.
- Chemenda, A.I., Burg, J.P., Mattauer, M., 2000. Evolution model of the Himalaya–Tibet system: geopoem based on new modeling, geological and geophysical data. *Earth and Planetary Science Letters* 174, 397–409.
- Chen, Z., Liu, Y., Hodges, K.V., Burchfiel, B.C., Royden, L.H., Deng, C., 1990. The Kangmar dome—a metamorphic core complex in southern Xizang (Tibet). *Science* 250, 1552–1556.
- Clark, M.K., Royden, L.H., 2000. Topographic ooze: building the eastern margin of Tibet by lower crustal flow. *Geology* 28, 703–706.
- Clark, M.K., Schoenbohm, L.M., Royden, L.H., Whipple, K.X., Burchfiel, B.C., Zhang, X., Tang, W., Wang, E., Chen, L., 2004. Surface uplift, tectonics, and erosion of eastern Tibet from large-scale drainage patterns. *Tectonics* 23, TC1006.
- Clift, P.D., Shimizu, N., Layne, G.D., Blusztajn, J.S., Gaedicke, C., Schluter, H.U., Clark, M.K., Amjad, S., 2001. Development of the Indus Fan and its significance for the erosional history of the Western Himalaya and Karakoram. *Geological Society of America Bulletin* 113, 1039–1051.
- Clift, P., Gaedicke, C., Edwards, R., Lee, J.I., Hildebrand, P., Amjad, S., White, R.S., Schluter, H.U., 2002. The stratigraphic evolution of the Indus Fan and the history of sedimentation in the Arabian Sea. *Marine Geophysical Researches* 23, 223–245.
- Clift, P.D., Lee, J.I., Hildebrand, P., Shimizu, N., Layne, G.D., Blusztajn, J., Blum, J.D., Garzanti, E., Khan, A.A., 2002. Nd and Pb isotope variability in the Indus River System: implications for sediment provenance and crustal heterogeneity in the Western Himalaya. *Earth and Planetary Science Letters* 200, 91–106.
- Colchen, M., Bassoullet, J.P., Mascle, G., 1982. La paléogéographie des orogènes, l'exemple de l'Himalaya. *Memoir Geol. l'Univ. Dijon* 7, 453–471.
- Colchen, M., LeFort, P., Pêcher, A., 1986. *Geological Researches in the Nepal's Himalayan: Annapurna–Manaslu–Ganesh Himal*. Editions du Centre National de la Recherche Scientifique, Paris, France.
- Coleman, M.E., 1996. Orogen-parallel and orogen-perpendicular extension in the central Nepalese Himalayas. *Geological Society of America Bulletin* 298, 553–571.
- Coleman, M.E., 1998. U–Pb constraints on Oligocene–Miocene deformation and anatexis within the central Himalaya, Marsyandi valley, Nepal. *American Journal of Science* 298, 553–571.
- Coleman, M., Hodges, K., 1995. Evidence for Tibetan plateau uplift before 14-Myr ago from a new minimum age for east west extension. *Nature* 374, 49–52.
- Colletini, C., Sibson, R.H., 2001. Normal faults, normal friction? *Geology* 29, 927–930.
- Copeland, P., Harrison, T.M., 1990. Episodic rapid uplift in the Himalaya revealed by  $^{40}\text{Ar}/^{39}\text{Ar}$  analysis of detrital K-feldspar and muscovite, Bengal fan. *Geology* 18, 54–357.
- Copeland, P., Harrison, T.M., Hodges, K.V., Marujól, P., LeFort, P., Pêcher, A., 1991. An early Pliocene thermal disturbance of the Main Central Thrust, central Nepal: implications for Himalayan tectonics. *Journal of Geophysical Research* 96, 8475–8500.
- Copeland, P., LeFort, P., Ray, S.M., Upreti, B.N., 1996. Cooling history of the Kathmandu crystalline nappe: Ar/Ar results. Paper presented at the 11th Himalayan-Karakoram-Tibet Workshop, Flagstaff, Arizona.
- Corfield, R.L., Seale, M.P., 2000. Crustal shortening across the north Indian continental margin, Ladakh, India. In: Khan, M.A., Treloar, P.J., Searle, M.P., Jan, M.Q. (Eds.), *Tectonics of the Nanga Parbat syntaxis and the Western Himalaya*. The Geological Society Special Publication, vol. 170, pp. 395–410.
- Corfield, R.I., Searle, M.P., Green, O.R., 1999. Photang thrust sheet: an accretionary complex structurally below the Spontang ophiolite constraining timing and tectonic environment of ophiolite obduction, Ladakh Himalaya, NW India. *Journal of the Geological Society* 156, 1031–1044.
- Corfield, R.I., Searle, M.P., Pedersen, R.B., 2001. Tectonic setting, origin, and obduction history of the Spontang ophiolite, Ladakh Himalaya, NW India. *Journal of Geology* 109, 715–736.
- Coward, M.P., Butler, R.H.W., 1985. Thrust tectonics and the deep structure of the Pakistan Himalaya. *Geology* 13, 417–420.
- Coward, M.P., Butler, R.H.W., Chambers, A.F., Graham, R.H., Izatt, C.N., Khan, M.A., Knipe, R.J., Prior, D.J., Treloar, P.J., William, M.P., 1988. Folding and imbrication of the Indian crust during Himalayan collision. *Philosophical transactions of the Royal Society of London Series A* 326, 89–116.
- Critelli, S., Garzanti, E., 1994. Provenance of the lower Tertiary Murree redbeds (Hazara–Kashmir syntaxis, Pakistan)

- and the initial rising of the Himalayas. *Sedimentary Geology* 89, 265–284.
- Critelli, S., Ingersoll, R.V., 1994. Sandstone petrology and provenance of the Siwalik Group (northwestern Pakistan and western-southwestern Nepal). *Journal of Sedimentary Research* 64, 815–823.
- Curry, J.R., 1991. Possible greenschist metamorphism at the base of a ~22-km sedimentary section, Bay of Bengal. *Geology* 19, 1097–1100.
- Curry, J.R., Moore, D.G., 1971. Growth of the Bengal deep-sea fan and denudation in the Himalayas. *Geological Society of America Bulletin* 82, 563–572.
- Curry, J.R., Emmel, F.J., Moore, D.G., 2003. The Bengal fan: morphology, geometry, stratigraphy, history and processes. *Marine and Petroleum Geology* 19, 1191–1223.
- Dahlen, F.A., 1984. Non-cohesive critical Coulomb wedges—an exact solution. *Journal of Geophysical Research* 89, 125–133.
- Dahlstrom, C.D.A., 1970. Balanced cross sections. *Canadian Journal of Earth Sciences* 6, 743–757.
- Daniel, C.G., Hollister, L.S., Parrish, R.R., Grujic, D., 2003. Exhumation of the Main Central Thrust from lower crustal depths, Eastern Bhutan Himalaya. *Journal of Metamorphic Geology* 21, 317–334.
- Davies, J.H., von Blanckenburg, F., 1995. Slab breakout: a model of lithosphere detachment and its test in the magmatism and deformation of collisional orogens. *Earth and Planetary Science Letters* 129, 85–102.
- Davidson, C., Grujic, D.E., Hollister, L.S., Schmid, S.M., 1997. Metamorphic reactions related to decompression and synkinematic intrusion of leucogranite, High Himalayan Crystallines, Bhutan. *Journal of Metamorphic Geology* 15, 593–612.
- Debon, F., LeFort, P., Sherpard, S.M.F., Sonet, J., 1986. The 4 plutonic belts of the Transhimalaya and Himalaya—a chemical, mineralogical, isotopic, and chronological synthesis along a Tibet–Nepal section. *Journal of Petrology* 27, 219–250.
- DeCelles, P.G., Gehrels, G.E., Quade, J., Ojha, T.P., 1998a. Eocene–early Miocene foreland basin development and the history of Himalayan thrusting, western and central Nepal. *Tectonics* 17, 741–765.
- DeCelles, P.G., Gehrels, G.E., Quade, J., Ojha, T.P., Kapp, P.A., Upreti, B.N., 1998b. Neogene foreland basin deposits, erosional unroofing, and the kinematic history of the Himalayan fold-thrust belt, western Nepal. *Geological Society of America Bulletin* 110, 2–21.
- DeCelles, P.G., Gehrels, G.E., Quade, J., LaReau, B., Spurlin, M., 2000. Tectonic implications of U–Pb zircon ages of the Himalayan orogenic belt in Nepal. *Science* 288, 497–499.
- DeCelles, P.G., Robinson, D.M., Quade, J., Ojha, T.P., Garzione, C.N., Copeland, P., Upreti, B.N., 2001. Stratigraphy, structure, and tectonic evolution of the Himalayan fold-thrust belt in western Nepal. *Tectonics* 20, 487–509.
- DeCelles, P.G., Robinson, D.M., Zandt, G., 2002. Implications of shortening in the Himalayan fold-thrust belt for uplift of the Tibetan Plateau. *Tectonics* 21 (6), 1062.
- DeCelles, P.G., Gehrels, G.E., Najman, Y., Martin, A.J., Carter, A., Garzanti, E., 2004. Detrital geochronology and geochemistry of Cretaceous–Early Miocene strata of Nepal: implications for timing and diachroneity of initial Himalayan orogenesis. *Earth and Planetary Science Letters* 227, 313–330.
- de Sigoyer, J., Chavagnac, V., Blichert-Toft, J., Villa, I.M., Luais, B., Guillot, S., Cosca, M., Mascle, G., 2000. Dating the Indian continental subduction and collisional thickening in the north-west Himalaya: multichronology of the Tso Moriri eclogites. *Geology* 28, 487–490.
- de Sigoyer, J., Guillot, S., Dick, P., 2004. Exhumation of the ultra-high-pressure Tso Moriri unit in eastern Ladakh (NW Himalaya): A case study. *Tectonics* 23. doi:10.1029/2002TC001492.
- Deng, W., 1998. Cenozoic Intraplate Volcanic Rocks in the Northern Qinghai–Xizang Plateau. Geologic Publishing House, Beijing. (in Chinese with English abstract).
- Dewey, J.F., 1988. Extensional collapse of orogens. *Tectonics* 7, 1123–1139.
- Dewey, J.F., Bird, J.M., 1970. Mountain belts and new global tectonics. *Journal of Geophysical Research* 75, 2625–2685.
- Dewey, J.F., Burke, K., 1973. Tibetan, Variscan and Precambrian basement reactivation: products of continental collision. *Journal of Geology* 81, 683–692.
- Dewey, J.F., Shackleton, R.M., Chang, C., Sun, Y., 1988. The tectonic evolution of the Tibetan Plateau. *Philosophical Transactions of the Royal Society of London. Series A* 327, 379–413.
- Dewey, J.F., Cande, S., Pitman, W.C., 1989. Tectonic evolution of the India–Eurasia collision zone. *Eclogae Geologicae Helveticae* 82, 717–734.
- Dèzes, P.J., 1999. Tectonic and metamorphic evolution of the central Himalayan domain in southeast Zaskar (Kashmir, India). PhD thesis, University of Lausanne, Lausanne, Switzerland, 160 pp.
- Dèzes, P.J., Vannay, J.C., Steck, A., Bussy, F., Cosca, M., 1999. Synorogenic extension: quantitative constraints on the age and displacement of the Zaskar shear zone (northwest Himalaya). *Geological Society of America Bulletin* 111, 364–374.
- Diamond, D.S., Ingersoll, R.V., 2002. Structural and sedimentologic evolution of a Miocene supradetachment basin, Silver Peak range and adjacent areas, west-central Nevada. *International Geology Review* 44, 588–623.
- Dickinson, W.R., 2003. The place and power of myth in geoscience: an associate editor’s perspective. *American Journal of Science* 303, 856–864.
- Ding, L., Zhong, D.L., Yin, A., Kapp, P., Harrison, T.M., 2001. Cenozoic structural and metamorphic evolution of the eastern Himalayan syntaxis (Namche Barwa). *Earth and Planetary Science Letters* 192, 423–438.
- Ding, L., Kapp, P., Zhong, D.L., Deng, W.M., 2003. Cenozoic volcanism in Tibet: evidence for a transition from oceanic to continental subduction. *Journal of Petrology* 44, 1833–1865.
- Ding, L., Kapp, P., Wan, X.Q., 2005. Paleocene–Eocene record of ophiolite obduction and initial India–Asia collision, south central Tibet. *Tectonics* 24, TC3001.
- DiPietro, J.A., Isachsen, C.E., 2001. U–Pb zircon ages from the Indian plate in northwest Pakistan and their significance to Himalayan and pre-Himalayan geologic history. *Tectonics* 20, 510–525.

- DiPietro, J.A., Pogue, K.R., 2004. Tectonostratigraphic subdivisions of the Himalaya: a view from the west. *Tectonics* 23, TC5001. doi:10.1029/2003TC001554.
- DiPietro, J., Pogue, K.R., Hussain, A., Ahmad, I., 1999. Geological map of the Indus syntaxis and surrounding area, northwest Himalaya, Pakistan. In: Macfarlane, A., Sorkhabi, R.B., Quade, J. (Eds.), *Himalaya and Tibet: Mountain Roots to Mountain Tops*. Geological Society of America Special Papers, vol. 328, pp. 159–178.
- DiPietro, J.A., Hussain, A., Ahmad, I., Khan, M.A., 2000. The main mantle thrust in Pakistan: its character and extent. In: Treloar, P.J., Searle, M.P. (Eds.), *Himalayan Tectonics*. The Geological Society Special Publication, vol. 74, pp. 375–393.
- Dogra, N.N., Singh, R.Y., Misra, P.S., 1985. Palyonology of Dharmasala beds, Himachal Pradesh. *Journal of Palaeontological Society of India* 30, 63–77.
- Dorsey, R.J., Becker, U., 1995. Evolution of a large miocene growth-structure in the upper plate of the Whipple detachment fault, northeastern Whipple Mountains, California. *Basin Research* 7, 151–163.
- Draganits, E., 2000. The Muth Formation in the Pin Valley (Spiti, N-India): Depositional Environment and Ichnofauna of a Lower Devonian Barrier Island System. PhD thesis, University of Viena, Viena.
- Duncan, C., Masket, J., Fielding, E., 2003. How steep are the Himalaya? Characteristics and implications along-strike topographic variations. *Geology* 31, 75–78.
- Dunlap, W.J., Hirth, G., Teyssier, C., 1997. Thermomechanical evolution of a ductile duplex. *Tectonics* 16, 983–1000.
- Duroy, Y., Farah, A., Lillie, R.J., 1989. Subsurface densities and lithospheric flexure of the Himalayan foreland in Pakistan. *Special Paper-Geological Society of America* 222, 217–236.
- Edwards, R.M., 1995.  $^{40}\text{Ar}/^{39}\text{Ar}$  geochronology of the Main Central Thrust (MCT) region; evidence for late Miocene to Pliocene disturbances along the MCT, Marsyandi River valley, west-central Nepal Himalaya. *Journal of Nepal Geological Society* 10, 41–46.
- Edwards, M.A., Harrison, T.M., 1997. When did the roof collapse? Late Miocene north–south extension in the High Himalaya revealed by Th–Pb monazite dating of the Khula Kangri granite. *Geology* 25, 543–546.
- Edwards, M.A., Kidd, W.S.F., Li, J.X., Yu, Y.J., Clark, M., 1996. Multi-stage development of the southern Tibet detachment system near Khula Kangri. *New data from Gonto La*. *Tectonophysics* 260, 1–19.
- Edwards, M.A., Pêcher, A., Kidd, W.S.F., Burchfiel, B.C., Royden, L.H., 1999. Southern Tibet detachment system at Khula Kangri, eastern Himalaya: a large-area, shallow detachment stretching into Bhutan? *Journal of Geology* 107, 623–631.
- England, P., Houseman, G., 1989. Extension during continental convergence, with application to the Tibetan Plateau. *Journal of Geophysical Research* 94, 17561–17579.
- England, P., Molnar, P., 1993. Cause and effect among thrust and normal faulting, anatexis melting and exhumation in the Himalaya. In: Treloar, P.J., Searle, P.M. (Eds.), *Himalayan Tectonics*. The Geological Society Special Publication, vol. 74, pp. 401–411.
- England, P., LeFort, P., Molnar, P., Pêcher, A., 1992. Heat sources for Tertiary metamorphism and anatexis in the Annapurna-Manaslu region, central Nepal. *Journal of Geophysical Research* 97, 2107–2128.
- Ernst, G.W., Liou, J.G., 1995. Contrasting plate-tectonic styles of the Qinling–Dabie–Sulu and Franciscan metamorphic belts. *Geology* 23, 353–356.
- Finlayson, D.P., Montgomery, D.R., Hallet, B., 2002. Spatial coincidence of rapid inferred erosion with young metamorphic massifs in the Himalayas. *Geology* 30, 219–222.
- Fontan, D., Schoupe, M., Hunziker, C.J., Martinotti, G., Verkaeren, J., 2000. Metamorphic evolution,  $^{40}\text{Ar}/^{39}\text{Ar}$  chronology and tectonic model for the Neelum valley, Azad Kashmir, NE Pakistan. In: Khan, M.A., Treloar, P.J., Searle, M.P., Jan, M.Q. (Eds.), *Tectonics of the Nanga Parbat Syntaxis and the Western Himalaya*. The Geological Society Special Publication, vol. 170, pp. 431–453.
- Forshee, E.J., Yin, A., 1995. Evolution of monolithological breccia deposits in supradetachment basins, Whipple Mountains, California. *Basin Research* 7, 181–197.
- Forsyth, D.W., 1992. Finite extension and low-angle normal faulting. *Geology* 20, 27–30.
- Foster, G., Kinny, P., Vance, D., Prince, C., Harris, N., 2000. The significance of monazite U–Th–Pb age data in metamorphic assemblages; a combined study of monazite and garnet chronometry. *Earth and Planetary Science Letters* 181, 327–340.
- Foster, G., Vance, D., Argles, T., Harris, N., 2002. The tertiary collision-related thermal history of the NW Himalaya. *Journal of Metamorphic Geology* 20, 827–843.
- France-Lanord, C., Derry, L., Michard, A., 1993. Evolution of the Himalaya since Miocene time: isotopic and sedimentological evidence from the Bengal fan. In: Treloar, P.J., Searle, P.M. (Eds.), *Himalayan Tectonics*. The Geological Society Special Publication, vol. 74, pp. 603–621.
- Frank, W., Hoinkes, G., Miller, C., Purtscheller Richter, W., Thoni, M., 1973. Relations between metamorphism and orogeny in a typical section of the Indian Himalayas. *Tschermaks Mineralogische und Petrographische Mitteilungen* 20, 303–332.
- Frank, W., Grasemann, B., Guntli, P., Miller, C., 1995. Geological map of the Kishwar–Chamba–Kulu region (NW Himalayas India). *Jahrbuch der Geologischen Bundesanstalt* 138, 299–308.
- Friedmann, S.J., Burbank, D.W., 1995. Rift basins and supradetachment basins—intracontinental extensional end-members. *Basin Research* 7, 109–127.
- Fuchs, G., 1975. Contributions to the Geology of the Northwestern Himalayas. *Jahrbuch der Geologischen Bundesanstalt* 32, 1–59 (Wien).
- Fuchs, G., Linner, M., 1995. Geological traverse across the western Himalaya—a contribution to the geology of eastern Ladakh, Lahul, and Chamba. *Jahrbuch der Geologischen Bundesanstalt* 138, 665–685.
- Gaetani, M., Garzanti, E., 1991. Multicyclic history of the northern India continental margin (northwestern Himalaya). *American Association of Petroleum Geologists Bulletin* 75, 1427–1446.

- Galy, A., France-Lanord, C., Derry, L.A., 1996. The late Oligocene–early Miocene Himalayan belt: constraints deduced from isotopic compositions of early Miocene turbidites in the Bengal fan. *Tectonophysics* 260, 109–118.
- Gansser, A., 1964. *The Geology of the Himalayas*. Wiley Interscience, New York, 289 pp.
- Gansser, A., 1983. *Geology of the Bhutan Himalaya*. Birkhäuser Verlag, Boston, 180 pp.
- Gapais, D., Pêcher, A., Gilbert, E., Ballever, M., 1992. Synconvergence spreading of the Higher Himalaya crystalline in Ladakh. *Tectonics* 11, 1045–1056.
- Garzanti, E., 1993. Sedimentary evolution and drowning of a passive margin shelf (Giumal Group; Zaskar Tethys Himalaya, India): palaeoenvironmental changes during final break-up of the Gondwanaland. In: Treloar, P.J., Searle, P.M. (Eds.), *Himalayan Tectonics*. The Geological Society Special Publication, vol. 74, pp. 277–298.
- Garzanti, E., 1999. Stratigraphy and sedimentary history of the Nepal Tethys Himalaya passive margin. *Journal of Asian Earth Sciences* 17, 805–827.
- Garzanti, E., Casnedi, R., Jadoul, F., 1986. Sedimentary evidence of a Cambro-Ordovician orogenic event in the northwestern Himalaya. *Sedimentary Geology* 48, 237–265.
- Garzanti, E., Baud, A., Mascle, G., 1987. Sedimentary record of the northward flight of India and its collision with Eurasia (Ladakh Himalaya India). *Geodynamica Acta* 1, 297–312.
- Garzanti, E., Gorza, M., Martellini, L., Nicora, A., 1994. Transition from diagenesis to metamorphism in the Paleozoic to Mesozoic succession of the Dolpo-Manang Synclinorium and Thakkhola Graben (Nepal Tethys Himalaya). *Eclogae Geologicae Helveticae* 87, 613–632.
- Garzanti, E., Critelli, S., Ingersoll, R.V., 1996. Paleogeographic and paleotectonic evolution of the Himalayan range as reflected by detrital modes of Tertiary sandstones and modern sands (Indus transect, India and Pakistan). *Geological Society of America Bulletin* 86, 273–286.
- Garzanti, E., Vezzoli, G., Ando, S., Paparella, P., Clift, P.D., 2005. Petrology of Indus River sands: a key to interpret erosion history of the Western Himalayan Syntaxis. *Earth and Planetary Science Letters* 229, 287–302.
- Garzanti, E., Dettman, D.L., Quade, J., DeCelles, P.G., Butler, R.F., 2000. High times on the Tibetan Plateau: paleoelevation of the Thakkhola graben, Nepal. *Geology* 28, 339–342.
- Garzanti, E., DeCelles, P.G., Hodkinson, D.G., Ojha, T.P., Upreti, B.N., 2003. East–west extension and Miocene environmental change in the southern Tibetan plateau: Thakkhola graben, central Nepal. *Geological Society of America Bulletin* 115, 3–20.
- Gee, E.R., 1989. Overview of the geology and structure of the Salt Range, with observations on related areas of northern Pakistan. *Special Paper-Geological Society of America* 232, 95–112.
- Gehrels, G.E., DeCelles, P.G., Ojha, T.P., Upreti, B.N., 2002. Initiation of the Himalayan orogen as an early Paleozoic think-skinned thrust belt. *Abstracts with Programs-Geological Society of America* 34, 410.
- Gehrels, G.E., DeCelles, P.G., Martin, A., Ojha, T.P., Pinhasi, G., Upreti, B.N., 2003. Initiation of the Himalayan orogen as an early Paleozoic thin-skinned thrust belt. *GSA Today* 13 (9), 4–9.
- George, M.T., Harris, B.W., Butler, R.W.H., 1993. The tectonic implications of contrasting granite magmatism between Kohistan island arc and the Nanga Parbat–Haramosh Massif, Pakistan Himalaya. In: Treloar, P.J., Searle, P.M. (Eds.), *Himalayan Tectonics*. The Geological Society Special Publication, vol. 74, pp. 173–191.
- George, M., Reddy, S., Harris, N., 1995. Isotopic constraints on the cooling history of the Nanga Parbat–Haramosh Massif and Kohistan arc, western Himalaya. *Tectonics* 14, 237–252.
- Godin, L., Brown, R.L., Hammer, S., Parrish, R., 1999a. Back folds in the core of the Himalayan orogen: an alternative interpretation. *Geology* 27, 151–154.
- Godin, L., Brown, R.L., Hammer, S., 1999b. High strain zone in the hanging wall of the Annapurna detachment, central Nepal Himalaya. In: Macfarlane, A., Sorkhabi, R.B., Quade, J. (Eds.), *Himalaya and Tibet: Mountain Roots to Mountain Tops*, Boulder, Colorado, Geological Society of America Special Papers, vol. 328, pp. 199–210.
- Godin, L., Parrish, R.R., Brown, R.L., Hodges, K.V., 2001. Crustal thickening leading to exhumation of the Himalayan Metamorphic core of central Nepal: insight from U–Pb Geochronology and Ar-40/Ar-39 Thermochronology. *Tectonics* 20, 729–747.
- Godwin-Austen, H.H., 1864. Geological notes on part of the North-Western Himalayas. *Quarterly Journal of Geological Society of London* 20, 383–387.
- Graham, S.A., Dickinson, W.R., Ingersoll, R.V., 1975. Himalayan–Bengal model for flysch dispersal in Appalachian–Ouachita system. *Geological Society of America Bulletin* 86, 273–286.
- Grasemann, B., Vannay, J.C., 1999. Flow controlled inverted metamorphism in shear zones. *Journal of Structural Geology* 21, 450–743.
- Grasemann, B., Fritz, H., Vannay, J.C., 1999. Quantitative kinematic flow analysis from the Main Central Thrust Zone (NW-Himalaya, India): implications for a decelerating strain path and the extrusion of orogenic wedges. *Journal of Structural Geology* 21, 837–853.
- Greco, A., Spencer, D.A., 1993. A section through the Indian plate, Kaghan Valley, NW Himalaya, Pakistan. In: Treloar, P.J., Searle, P.M. (Eds.), *Himalayan Tectonics*. The Geological Society Special Publication, vol. 74, pp. 221–236.
- Greco, A., Martinotti, G., Papritz, K., Ramsay, J.G., Rey, R., 1989. The crystalline rocks of the Kaghan valley (NE-Pakistan). *Eclogae Geologicae Helveticae* 82, 629–653.
- Grujic, D., Casey, M., Davidson, C., Hollister, L.S., Kundig, R., Pavlis, T., Schmid, S., 1996. Ductile extrusion of the Higher Himalayan Crystalline in Bhutan: evidence from quartz microfabrics. *Tectonophysics* 260, 21–43.
- Grujic, D., Hollister, L.S., Parrish, R.R., 2002. Himalayan metamorphic sequence as an orogenic channel: insight from Bhutan. *Earth and Planetary Science Letters* 198, 177–191.
- Guillot, S., Pêcher, A., Rochette, P., LeFort, P., 1993. The emplacement of the Manaslu granite of Central Nepal: field and magnetic susceptibility constraints. In: Treloar, P.J., Searle, P.M. (Eds.), *Himalayan Tectonics*. The Geological Society Special Publication, vol. 74, pp. 413–428.

- Guillot, S., LeFort, P., Pêcher, A., Barman, M.R., Arahamian, J., 1995. Contact-metamorphism and depth of emplacement of the Manaslu granite (Central Nepal)—implications for Himalayan orogenesis. *Tectonophysics* 241, 99–119.
- Guillot, S., de Sigoyer, J., Lardeaux, J.M., Mascle, G., 1997. Eclogitic metasediments from the Tso Morari area (Ladakh, Himalaya): evidence for continental subduction during India–Asia convergence. *Contributions to Mineralogy and Petrology* 128, 197–212.
- Guillot, S., Cosca, M., Allemand, P., LeFort, P., 1999. Contrasting metamorphic and geochronologic evolution along the Himalayan belt. In: Macfarlane, A., Sorkhabi, R.B., Quade, J. (Eds.), *Himalaya and Tibet: Mountain Roots to Mountain Tops*. Geological Society of America Special Papers, vol. 328, pp. 117–128.
- Gururajan, N.S., Choudhuri, B.K., 2003. Geology and tectonic history of the Lhith Valley, eastern Arunachal Pradesh, India. *Journal of Asian Earth Sciences* 21, 341–731.
- Guzman-Speziale, M., Ni, J.F., 1996. Seismicity and active tectonics of the Western Sunda Arc. In: Yin, A., Harrison, T.M. (Eds.), *The Tectonics of Asia*. Cambridge University Press, New York, pp. 63–84.
- Haines, S.S., Klemperer, S.L., Brown, L., Jingru, G.R., Mechie, J., Meissner, R., Ross, A., Zhao, W.J., 2003. INDEPTH III seismic data: from surface observations to deep crustal processes in Tibet. *Tectonics* 22 (Art. No. 1001).
- Hallet, B., Molnar, P., 2001. Distorted drainage basins as markers of crustal strain east of the Himalaya. *Journal of Geophysical Research* 106, 13697–13709.
- Hallet, B., Hunter, L., Bogen, J., 1996. Rates of erosion and sediment evacuation by glaciers: a review of field data and their implications. *Global and Planetary Change* 12, 213–235.
- Harris, N., Massey, J., 1994. Decompression and anatexis of Himalayan metapelites. *Tectonics* 13, 1537–1546.
- Harris, N.B.W., Xu, R., Lewis, C.L., Hawkeworth, C.J., Zhang, Y., 1988. Isotope geochemistry of the 1985 Tibet Geotraverse, Lhasa to Golmud. *Philosophical Transactions of the Royal Society of London. Series A* 327, 263–285.
- Harris, N.B.W., Caddick, M., Kosler, J., Goswami, S., Vance, D., Tindle, A.G., 2004. The pressure–temperature–time path of migmatites from the Sikkim Himalaya. *Journal of Metamorphic Geology* 22, 249–264.
- Harrison, T.M., Copeland, P., Kidd, W.S.F., Yin, A., 1992. Raising Tibet. *Science* 255, 1663–1670.
- Harrison, T.M., Copeland, P., Halls, S.A., Quade, J., Burner, S., Ojha, T.P., Kidd, W.S.F., 1993. Isotopic preservation of Himalayan Tibetan uplift, denudation, and climatic histories of two molasse deposits. *Journal of Geology* 101, 157–175.
- Harrison, T.M., Copeland, P., Kidd, W.S.F., Lovera, O.M., 1995. Activation of the Nyainqentanghla shear zone: implications for uplift of the southern Tibetan Plateau. *Tectonics* 14, 658–676.
- Harrison, T.M., Ryerson, F.J., LeFort, P., Yin, A., Lovera, O.M., Catlos, E.J., 1997a. A Late Miocene–Pliocene origin for the Central Himalayan inverted metamorphism. *Earth Planetary Science Letters* 146, E1–E8.
- Harrison, T.M., Lovera, O.M., Grove, M., 1997b. New insights into the origin of two contrasting Himalayan granite belts. *Geology* 25, 899–902.
- Harrison, T.M., Yin, A., Ryerson, F.J., 1998a. Orographic evolution of the Himalaya and Tibetan plateau. In: Crowley, T. (Ed.), *Boundary Conditions for Climate Changes*. Oxford University Press, New York, pp. 38–72.
- Harrison, T.M., Grove, M., Lovera, O.M., Catlos, E.J., 1998b. A model for the origin of Himalayan anatexis and inverted metamorphism. *Journal of Geophysical Research* 103, 27017–27032.
- Harrison, T.M., Grove, M., Lovera, O.M., Catlos, E.J., D’Andrea, J., 1999. The origin of Himalayan anatexis and inverted metamorphism: models and constraints. *Journal of Asian Earth Sciences* 17, 755–772.
- Harrison, T.M., Yin, A., Grove, M., Lovera, O.M., Ryerson, F.J., Zhou, X.H., 2000. The Zedong window: a record of superposed tertiary convergence in southeastern Tibet. *Journal of Geophysical Research* 105, 19211–19230.
- Hauck, M.L., Nelson, K.D., Brown, L.D., Zhao, W.J., Ross, A.R., 1998. Crustal structure of the Himalayan orogen at similar to 90 degrees east longitude from Project INDEPTH deep reflection profiles. *Tectonics* 17, 481–500.
- Hayden, H.H., 1913. Relationship of the Himalayas to the Indo-Gangetic Plains and the Indian Peninsula. *Records of Geological Survey of India* 43, 138–167.
- Heim, A., Gansser, A., 1939. Central Himalaya Geological Observations of Swiss, pp. 1–246.
- Henry, P., Le Pichon, X., Goffè, B., 1997. Kinematic, thermal, and petrological model of the Himalayas: constraints related to metamorphism within the underthrust Indian crust and topographic elevation. *Tectonophysics* 273, 31–56.
- Herren, E., 1987. Zaskar shear zone: northeast–southwest extension within the Higher Himalaya. *Geology* 15, 409–413.
- Hike, L., Lamb, S., Hilton, D.R., Poreda, R.J., 2000. Southern limit of mantle-derived geothermal helium emissions in Tibet: implications for lithospheric structure. *Earth and Planetary Science Letters* 180, 297–308 (AUG 15).
- Hodges, K.V., 2000. Tectonics of the Himalaya and southern Tibet from two perspectives. *Geological Society America Bulletin* 112, 324–350.
- Hodges, K.V., Silverber, D.S., 1988. Thermal evolution of the Greater Himalaya, Garhwal, India. *Tectonics* 7, 583–600.
- Hodges, K.V., Parrish, R.R., Housh, T.B., Lux, D.R., Burchfiel, B.C., Royden, L.H., Chen, Z., 1992. Simultaneous Miocene extension and shortening in the Himalayan orogen. *Science* 258, 1446–1470.
- Hodges, K.V., Hames, W.E., Olszewski, W.J., Burchfiel, B.C., Royden, L.H., Chen, Z., 1994. Thermobarometric and <sup>40</sup>Ar/<sup>39</sup>Ar geochronologic constraints on Eohimalayan metamorphism in the Dinggy area, southern Tibet. *Contributions to Mineralogy Petrology* 117, 151–163.
- Hodges, K.V., Parrish, R.R., Searle, M.P., 1996. Tectonic evolution of the central Annapurna Range, Nepalese Himalayas. *Tectonics* 15, 1264–1291.
- Hodges, K.V., Hurtado, J.M., Whipple, K.X., 2001. Southward extrusion of Tibetan crust and its effect on Himalayan tectonics. *Tectonics* 20, 799–809.
- Honegger, K., Dietrich, V., Frank, W., Gansser, A., Thöni, M., Trommsdorff, V., 1982. Magmatism and metamorphism in the

- Ladakh Himalayas (the Indus–Tsangpo suture zone). *Earth and Planetary Science Letters* 60, 253–292.
- Hooker, J.D., 1854. *Himalayan Journals* 2 (London).
- Hubbard, M.S., 1989. Thermobarometric constraints on the thermal history of the Main Central thrust zone and Tibetan slab, eastern Himalaya. *Journal of Metamorphic Geology* 7, 19–30.
- Hubbard, M.S., 1996. Ductile shear as a cause of inverted metamorphism: example from the Nepal Himalaya. *Journal of Geology* 104, 493–499.
- Hubbard, M.S., Harrison, T.M., 1989.  $^{40}\text{Ar}/^{39}\text{Ar}$  age constraints on deformation and metamorphism in the MCT Zone and Tibetan Slab, eastern Nepal Himalaya. *Tectonics* 8, 865–880.
- Hubbard, M.S., Spencer, D.A., West, D.P., 1995. Tectonic exhumation of the Nanga–Parbat massif, northern Pakistan. *Earth and Planetary Science Letters* 133, 213–225.
- Huerta, A.D., Royden, L.H., Hodges, K.V., 1998. The thermal structure of collisional orogens as a response to accretion, erosion, and radiogenic heating. *Journal of Geophysical Research* 103, 15287–15302.
- Hughes, N.C., Droser, M.L., 1992. Trace fossils from the Phe formation (Lower Cambrian), Zaskar Valley, northwestern India. *Memoirs Queensland Museum* 32, 139–144.
- Hughes, N.C., Jell, P.A., 1999. Biostratigraphy and biogeography of Himalayan Cambrian trilobites. In: Macfarlane, A., Sorkhabi, R.B., Quade, J. (Eds.), *Himalaya and Tibet: mountain roots to mountain tops*. Geological Society of America Special Papers, vol. 328, pp. 109–116.
- Hughes, N.C., Shanchi, Peng, Huilin, Luo, 2002. *Kunmingaspis* (Trilobita) putatively from the Yunling Collage, and the Cambrian faunal history of the eastern Himalayan syntaxial region. *Journal of Paleontology* 76, 709–717.
- Hurtado, J.M., Hodges, K.V., Whipple, K.X., 2001. Neotectonics of the Thakkhola graben and implications for recent activity on the South Tibetan fault system in the central Nepal Himalaya. *Geological Society of America Bulletin* 113, 222–240.
- Huyghe, P., Galy, A., Mugnier, J.L., France-Lanord, C., 2001. Propagation of the thrust system and erosion in the Lesser Himalaya: geochemical and sedimentological evidence. *Geology* 29, 1007–1010.
- Ingersoll, R.V., Suczek, C.A., 1979. Petrology and provenance of Neogene sand from Nicobar and Bengal fans, DSDP sites 211 and 218. *Journal of Sedimentary Petrology* 49, 1217–1228.
- Jacobs, J., Thomas, R.J., 2004. Himalayan-type indenter-escape tectonics model for the southern part of the late Neoproterozoic-early Paleozoic East African–Antarctic. *Geology* 32, 721–724.
- Jager, E., Bhandari, A.K., Bhanot, V.B., 1971. Rb–Sr age determination of biotites and whole rock samples from the Mandi and Chor granite (H. P.), India. *Eclogae Geologicae Helvetiae* 64, 523–527.
- Jain, A.K., Manickavasagam, R.M., 1993. Inverted metamorphism in the intracontinental ductile shear zone during Himalayan collision tectonics. *Geology* 21, 407–410.
- Jain, A.K., Thakur, V.C., Tandon, S.K., 1974. Stratigraphy and structure of the Siang district, Arunachal (NEFA) Himalaya. *Himalayan Geology* 4, 28–60.
- Jain, A.K., Manickavasagam, R.M., Singh, S., 1999. Collision tectonics in the NW Himalaya: deformation, metamorphism, emplacement of leucogranite along Beas-Parbati Valleys, Himachal Pradesh. *Gondwana Research Group Memoir* 6, 3–37.
- Jain, A.K., Kumar, D., Singh, S., Kumar, A., Lal, N., 2000. Timing, quantification and tectonic modeling of Pliocene–Quaternary movements in the NW Himalaya: evidence from fission-track dating. *Earth and Planetary Science Letters* 179, 437–451.
- Jamieson, R.A., Beaumont, C., Hamilton, J., Fullsack, P., 1996. Tectonic assembly of inverted metamorphic sequences. *Geology* 24, 839–842.
- Jamieson, R.A., Beaumont, C., Medvedev, S., Nguyen, M.H., 2004. Crustal channel flows: 2. Numerical models with implications for metamorphism in the Himalayan–Tibetan orogen. *Journal of Geophysical Research* 109. doi:10.1029/2003JB002811.
- Jaupart, C., Provost, A., 1985. Heat focusing, granite genesis and inverted metamorphic gradient in continental collision zones. *Earth and Planetary Science Letters* 73, 385–397.
- Johnson, M.R.W., 1994. Culmination and domal uplift in the Himalaya. *Tectonophysics* 239, 139–147.
- Johnson, M.R.W., 2002. Shortening budgets and the role of continental subduction during the India–Asia collision. *Earth-Science Reviews* 59, 101–123.
- Johnson, S.Y., Alam, A.M.N., 1991. Sedimentation and tectonics of the Sylhet trough, Bangladesh. *Geological Society of America Bulletin* 103, 1513–1527.
- Johnson, M.R.W., Rogers, G., 1997. Rb–Sr ages of micas from the Kathmandu complex, Central Nepalese Himalaya: implications for the evolution of the Main Central Thrust. *Journal of the Geological Society* 154, 863–869.
- Johnson, M.R.W., Oliver, G.J.H., Parrish, R.R., Johnson, S.P., 2001. Synthrusting metamorphism, cooling, and erosion of the Himalayan Kathmandu Complex, Nepal. *Tectonics* 20, 394–415.
- Jouanne, F., Mugnier, J.L., Pandey, M.R., Gamond, J.F., LeFort, P., Serrurier, L., Vigny, C., Avouac, J.P., and the Idylhim members, 1999. Oblique convergence in the Himalayas of western Nepal deduced from preliminary results of GPS measurements. *Geophysical Research Letters* 26, 1933–1936.
- Kapp, P., Guynn, J.H., 2004. Indian punch rifts Tibet. *Geology* 32, 993–996.
- Kapp, P.A., Yin, A., 2001. Unbending of the lithosphere as a mechanism for active rifting in Tibet: insight from elastic modeling. *EOS Transaction, American Geophysical Union* 82 (47) (Fall Meeting Supplementals, T11E-0893).
- Klootwijk, C.T., Conaghan, P.J., Powell, C.M., 1985. The Himalayan arc: large-scale continental subduction, oroclinal bending, and back-arc spreading. *Earth and Planetary Science Letters* 75, 316–319.
- Kohn, M.J., Parkinson, C.D., 2002. Petrologic case for Eocene slab breakoff during the Indo-Asian collision. *Geology* 30, 591–594.
- Kumar, G., 1997. *Geology of Arunachal Pradesh*. Geological Society of India, Bangalore, 217 pp.
- Kumar, A., Lal, N., Jain, A.K., Sorkhabi, R.B., 1995. Late Cenozoic–Quaternary thermo-tectonic history of Higher Himalaya n Crystalline (HC) in Kishtwar–Padar–Zaskar region, NW Himalayan: evidence from fission ages. *Journal of geological Society of India* 45, 375–391.

- Kumar, S., Wesnousky, S.G., Rockwell, T.K., Ragona, D., Thakur, V.C., Seitz, G.G., 2001. Earthquake recurrence and rupture dynamics of Himalayan frontal thrust, India. *Science* 294, 2328–2331.
- Kündig, R., 1989. Domal structures and high-grade metamorphism in the Higher Himalayan Crystalline, Zaskar region, northwest Himalaya, India. *Journal of Metamorphic Geology* 7, 43–55.
- Lahiri, A., 1941. Geology of Buxa Duras. *Quarterly Journal of Geological Society of London* 13, 1–62.
- Lal, N., Mehta, Y.P., Kumar, D., Kumar, A., Jain, A.K., 1999. Cooling and exhumation history of the Mandi granite and adjoining tectonic units, Himachal Pradesh, and estimation of closure temperature from external surface of zircon. In: Jain, A.K., Manickavasagam, R.M. (Eds.), *Geodynamics of the NW Himalaya*. Gondwana Research Group Memoir, vol. 6, pp. 207–216.
- Larson, K.M., Burgmann, R., Bilham, R., Freymueller, J.T., 1999. Kinematics of the India–Eurasia collision zone from GPS. *Journal of Geophysical Research* 104, 1077–1093.
- La Touche, T.D., 1883. Notes on the geology of the Aka Hills, Assam. *Records of Geological Survey of India* 18, 121–124.
- Laubscher, J.P., 1961. Ein Fernschubhypothese der Jurafaltung. *Eclogae Geologicae Helveticae* 54, 221–282.
- Lavé, J., Avouac, J.P., 2000. Active folding of fluvial terraces across the Siwaliks Hills, Himalayas of central Nepal. *Journal of Geophysical Research* 105, 5735–5770.
- Law, R.D., Searle, M.P., Simpson, R.L., 2004. Strain, deformation temperatures and vorticity of flow at the top of the Greater Himalayan slab, Everest massif, Tibet. *Journal of the Geological Society of London* 161, 305–320.
- Lee, J., Hacker, B.R., Dinklage, W.S., Wang, Y., Gans, P., Calvert, A., Wan, J.L., Chen, W.J., Blythe, A.E., McClelland, W., 2000. Evolution of the Kangmar Dome, southern Tibet: structural, petrologic, and thermochronologic constraints. *Tectonics* 19, 872–895.
- Leech, M.L., Singh, S., Jain, A.K., Klemperer, S.L., Manickavasagam, R.M., 2005. The onset of India–Asia continental collision: Early, steep subduction required by the timing of UHP metamorphism in the western Himalaya. *Earth and Planetary Science Letters* 234, 83–97.
- LeFort, P., 1975. Himalayas—collided range—present knowledge of continental arc. *American Journal of Science* A275, 1–44.
- Lefort, P., 1996. Evolution of the Himalaya. In: Yin, A., Harrison, T.M. (Eds.), *The Tectonics of Asia*. Cambridge University Press, New York, pp. 95–106.
- LeFort, P., Rai, S.M., 1999. Pre-Tertiary felsic magmatism of the Nepal Himalaya: recycling of continental crust. *Journal of Asian Earth Sciences* 17, 607–628.
- LeFort, P., Vuney, M., Deniel, C., France-Lanoed, C., 1987. Crustal generation of the Himalayan leucogranites. *Tectonophysics* 134, 39–57.
- Lemmonier, C.G., Marquis, F., Perrier Avouac, J.P., Chitrakar, G., Kafle, B., Sapkota, S., Gautam, U., Tiwari, D., 1999. Electrical structure of the Himalaya of central Nepal: high conductivity around the mid-crustal ramp along the MHT. *Geophysical Research Letters* 26, 3261–3264.
- Le Pichon, X., Fournier, J., Jolivet, L., 1992. Kinematics, topography, shortening, and extrusion in the India–Eurasia collision. *Tectonics* 11, 1085–1098.
- Lister, G.S., Davis, G.A., 1989. The origin of metamorphic core complexes and detachment faults formed during Tertiary continental extension in the northern Colorado River region, USA. *Journal of Structural Geology* 11, 65–94.
- Liu, Z.Q., 1988. Geologic map of the Qinghai–Xizang Plateau and its neighboring regions (scale at 1:1,500,000). Chengdu Institute of Geology and Mineral Resources, Geologic Publishing House, Beijing.
- Liu, G., Einsele, G., 1994. Sedimentary history of the Tethyan basin in the Tibetan Himalayas. *Geologische Rundschau* 82, 32–61.
- Liu, G., Einsele, G., 1999. Jurassic sedimentary facies and paleogeography of the former Indian passive margin in southern Tibet. In: Macfarlane, A., Sorkhabi, R.B., Quade, J. (Eds.), *Himalaya and Tibet: Mountain Roots to Mountain Tops*. Geological Society of America Special Papers, vol. 328, pp. 75–108.
- Liu, Y.D., Zhong, D.L., 1997. Petrology of high-pressure granulites from the eastern Himalayan syntaxis. *Journal of Metamorphic Petrology* 15, 451–466.
- Lombardo, B., Rolfo, F., 2000. Two contrasting eclogite types in the Himalayas: implications for the Himalayan orogeny. *Journal of Geodynamics* 30, 37–60.
- Lombardo, B., Pertusati, P., Borghi, S., 1993. Geology and tectonomagmatic evolution of the eastern Himalaya along the Chomolungma–Makalu transect. In: Treloar, P.J., Searle, M.P. (Eds.), *Himalayan Tectonics*. The Geological Society Special Publication, vol. 74, pp. 341–355.
- Lombardo, B., Rolfo, F., Campagnoni, R., 2000. Glaucofanite and barosite eclogites from the Upper Kaghan nappe: implications for the metamorphic history of the NW Himalaya.
- Lyon-Caen, H., Molnar, P., 1985. Gravity anomalies, flexure of the Indian plate, and the structure, support and evolution of the Himalaya and the Ganga Basin. *Tectonics* 4, 513–538.
- Macfarlane, A.M., 1992. A structural analysis of the Main Central thrust zone, Langtang National Park, central Nepal Himalaya. *Geological Society of America Bulletin* 104, 1389–1402.
- Macfarlane, A.M., 1993. Chronology of tectonic events in the crystalline core of the Himalaya, Langtang National Park, central Nepal. *Tectonics* 12, 1004–1025.
- Macfarlane, A.M., 1995. An evaluation of the inverted metamorphic gradient at Langtang National Park. *Journal of Metamorphic Petrology* 13, 595–612.
- Makovsky, Y., Klemperer, S.L., Huang, L., Lu, D., Project INDEPTH Team, 1996. Structural elements of the southern Tethyan Himalaya crust from wide-angle seismic data. *Tectonics* 15, 997–1005.
- Makovsky, Y., Klemperer, S.L., Ratschbacher, L., Alsdorf, D., 1999. Midcrustal reflector on INDEPTH wide-angle profiles: an ophiolitic slab beneath the India–Asia suture in southern Tibet? *Tectonics* 18, 793–808.
- Mallet, F.R., 1875. On the geology and mineral resources of the Darjiling district and the Western Duars. *Memoir of Geological Survey of India* 11, 1–50.
- Maluski, H., Matte, P., Brunel, M., Xiao, X.S., 1988. Argon-39–Argon-40 dating of metamorphic and plutonic events in the

- north and High Himalaya belts (southern Tibet–China). *Tectonics* 7, 299–326.
- Marquer, D., Chawla, H.S., Challandes, N., 2000. Pre-alpine high-grade metamorphism in High Himalaya crystalline sequences: Evidence from Lower Palaeozoic Kinnaur Kailas granite and surrounding rocks in the Sutlej Valley (Himachal Pradesh, India). *Eclogae Geologicae Helvetiae* 93, 207–220.
- Masek, J.G., Isacks, B.L., Fielding, E.J., Browaeys, J., 1994. Rift flank uplift in Tibet: evidence for a viscous lower crust. *Tectonics* 13, 659–667.
- McCaffery, R., Nabelek, J., 1998. Role of oblique convergence in the active deformation of the Himalayas and southern Tibet plateau. *Geology* 26, 691–694.
- McClelland, W.C., Gilotti, J.A., 2003. Late-stage extensional exhumation of high-pressure granulites in the Greenland Caledonides. *Geology* 31, 259–262.
- McDougall, I., Harrison, T.M., 1999. *Geochronology and Thermochronology by the  $^{40}\text{Ar}/^{39}\text{Ar}$  Method*. Oxford University Press, New York, 267 pp.
- Means, W.D., 1990. One dimensional kinematics of stretching faults. *Journal of Structural Geology* 12, 267–272.
- Mehta, P.K., 1977. Geochronology of the Kulu–Mandi belt: its implications for the Himalayan tectonogenesis. *Geologisches Rundschau* 6, 156–188.
- Meigs, A.J., Burbank, D.W., Beck, R.A., 1995. Middle–late Miocene (>10 Ma) formation of the Main Boundary Thrust in the western Himalaya. *Geology* 23, 423–426.
- Melosh, H.J., 1990. Mechanical basis for low-angle normal faulting in the Basin and Range province. *Nature* 343, 331–335.
- Metcalfe, R.P., 1993. Pressure, temperature and time constraints on metamorphism across the Main Central Thrust zone and High Himalayan slab in the Garhwal Himalaya. In: Treloar, P.J., Searle, M.P. (Eds.), *Himalayan Tectonics*. The Geological Society Special Publication, vol. 74, pp. 485–509.
- Miller, C., Schuster, R., Klotzli, U., Frank, W., Purtscheller, F., 1999. Post-collisional potassic and ultrapotassic magmatism in SW Tibet: geochemical and Sr–Nd–O isotopic constraints for mantle source characteristics and magma genesis. *Journal of Petrology* 40, 1399–1424.
- Miller, C., Klotzli, U., Frank, W., Thoni, M., Grasemann, B., 2000. Proterozoic crustal evolution in the NW Himalaya (India) as recorded by circa 1.80 Ga mafic and 1.84 Ga granitic magmatism. *Precambrian Research* 103 (3–4), 191–206 (OCT 1).
- Miller, C., Thoni, M., Frank, W., Grasemann, B., Klotzli, U., Guntli, P., Draganits, E., 2001. The early Paleozoic magmatic event in the northwest Himalaya, India: source, tectonic setting and age of emplacement. *Geological Magazine* 138, 237–251.
- Mishra, D.C., Laxman, G., Arora, K., 2004. Large-wavelength gravity anomalies over the Indian continent: indicators of lithospheric flexure and uplift and subsidence of Indian Peninsular Shield related to isostasy. *Current Science* 86, 861–867.
- Mohan, A., Windley, B.F., Searle, M.P., 1989. Geothermometry and development of the inverted metamorphism in Dajeeling–Sikkim region in eastern Nepal. *Journal of Metamorphic Geology* 7, 95–110.
- Molnar, P., 1988. A review of geophysical constraints on the deep structure of the Tibetan plateau, the Himalaya and the Karakoram, and their implications. *Philosophical Transactions of the Royal Society of London. Series A* 326, 33–88.
- Molnar, P., England, P., 1990. Temperatures, heat flux, and frictional stress near major thrust faults. *Journal of Geophysical Research* 95, 4833–4856.
- Molnar, P., Lyon-Caen, H., 1989. Fault plane solutions of earthquakes and active tectonics of the Tibetan plateau and its margins. *Geophysical Journal International* 99, 123–153.
- Molnar, P., Tapponnier, P., 1978. Active tectonics of Tibet. *Journal of Geophysical Research* 83, 5361–5375.
- Molnar, P., England, P., Martinod, J., 1993. Mantle dynamics, the uplift of the Tibetan Plateau, and the Indian monsoon. *Review of Geophysics* 31, 357–396.
- Morley, C.K., 1988. Out-of-sequence thrusts. *Tectonics* 7, 539–561.
- Mukherjee, B.K., Sachan, H.K., Ogasawara, Y., Muko, A., Yoshioka, N., 2003. Carbonate-bearing UHPM rocks from the Tso-Morari region, Ladakh, India: petrological implications. *International Geology Review* 45, 49–69.
- Murphy, M.A., Harrison, T.M., 1999. Relationship between leucogranites and the Qomolangma detachment in the Rongbuk Valley, south Tibet. *Geology* 27, 831–834.
- Murphy, M.A., Yin, A., 2003. Structural evolution and sequence of thrusting in the Tethyan fold-thrust belt and Indus-Yalu suture zone, southwest Tibet. *Geological Society of America Bulletin* 115, 21–34.
- Murphy, M.A., Yin, A., Harrison, T.M., Durr, S.B., Chen, Z., Ryerson, F.J., Kidd, W.S.F., Wang, X., Zhou, X., 1997. Significant crustal shortening in south-central Tibet prior to the Indo-Asian collision. *Geology* 25, 719–722.
- Murphy, M.A., Yin, A., Kapp, P., Harrison, T.M., Manning, C.E., Ryerson, F.J., Ding, L., Guo, J.H., 2002. Structural evolution of the Gurla Mandhata detachment system, southwest Tibet: implications for the eastward extent of the Karakoram fault system. *Geological Society of America Bulletin* 114, 428–447.
- Myrow, P.M., Hughes, N.C., Paulsen, T.S., Williams, I.S., Parcha, S.D., Thompson, K.R., Bowering, S.A., Peng, S.C., Ahluwalia, A.D., 2003. Integrated tectonostratigraphic analysis of the Himalaya and implications for its tectonic reconstruction. *Earth and Planetary Science Letters* 212, 433–443.
- Nabelek, P.I., Liu, M., Sirbescu, M.L., 2001. Thermo-rheological, shear heating model for leucogranite generation, metamorphism, and deformation during the Proterozoic Trans-Hudson orogeny, Black Hills, South Dakota. *Tectonophysics* 342, 371–388.
- Najman, Y., Garzanti, E., 2000. Reconstructing early Himalayan tectonic evolution and paleogeography from Tertiary foreland basin sedimentary rocks, northern India. *Geological Society of America Bulletin* 112, 435–449.
- Najman, Y., Clift, P., Johnson, M.R.W., Roberson, A.H.F., 1993. Early stages of foreland basin evolution in the Lesser Himalaya, N India. In: Treloar, P.J., Searle, M.P. (Eds.), *Himalayan Tectonics*. The Geological Society Special Publication, vol. 74, pp. 541–558.
- Najman, Y.M.R., Pringle, M.S., Johnson, M.R.W., Robertson, A.H.F., Wijbrans, J.R., 1997. Laser Ar-40/Ar-39 dating of single

- detrital muscovite grains from early foreland-basin sedimentary deposits in India: implications for early Himalayan evolution. *Geology* 25, 535–538.
- Najman, Y., Bickle, M., Chapman, H., 2000. Early Himalayan exhumation: isotopic constraints from the Indian foreland basin. *Terra Nova* 12, 28–34.
- Najman, Y., Pringle, M., Godin, L., Oliver, G., 2001. Dating of the oldest continental sediments from the Himalayan foreland basin. *Nature* 410, 194–197.
- Najman, Y., Pringle, M., Godin, L., Oliver, G., 2002. A reinterpretation of the Balakot formation: implications for the tectonics of the NW Himalaya, Pakistan. *Tectonics* 21 (Art. No. 1045).
- Najman, Y., Garzanti, E., Pringle, M., Bickle, M., Stix, J., Khan, I., 2003. Early–middle Miocene paleodrainage and tectonics in the Pakistan Himalaya. *Geological Society of America Bulletin* 115, 1265–1277.
- Nakata, T., 1989. Active faults of the Himalaya of India and Nepal. *Special Paper-Geological Society of America* 232, 243–264.
- Nelson, K.D., et al., 1996. Partially molten middle crust beneath Southern Tibet: synthesis of project INDEPTH results. *Science* 274, 1684–1696.
- Neumayer, J., Wisemayr, G., Janda, C., Grasemann, B., 2004. Eohimalayan fold and thrust belt in the NW-Himalaya (Lingti-Pin Valleys): shortening and depth to detachment calculation. *Austrian Journal of Earth Sciences* 95/96, 28–36.
- Neogi, S., Dasgupta, S., Fukuoka, M., 1998. High  $P$ – $T$  polymetamorphism, dehydration, melting, and generation of migmatites and granites in the Higher Himalayan Crystalline Complexes, Sikkim, India. *Journal of Petrology* 39, 61–99.
- Ni, J., Barazangi, M., 1984. Seismotectonics of the Himalayan collision zone: geometry of the underthrusting Indian plate beneath the Himalaya. *Journal of Geophysical Research* 89, 1147–1163.
- Nie, S.Y., Yin, A., Rowley, D., Jin, Y.G., 1994. Exhumation of the Dabie-Shan ultrahigh-pressure rocks and accumulation of the Songpan–Ganzi flysch sequence, central China. *Geology* 22, 999–1002.
- Norlander, B.H., Whitney, D.L., Teyssier, C., Vanderhaeghe, O., 2002. Partial melting and decompression of the Thor-Odin dome, Shuswap metamorphic core complex, Canadian Cordillera. *Lithos* 61, 103–125.
- O'Brien, P.J., Zotov, N., Law, R., Khan, M.A., Jan, M.Q., 2001. Coesite in Himalayan eclogite and implications for models of India–Asia collision. *Geology* 29, 435–438.
- Ojha, T.P., Butler, R.F., Quade, J., DeCelles, P.G., Richards, D., Upreti, B.N., 2000. Magnetic polarity stratigraphy of the Neogene Siwalik Group at Khutia Khola, far western Nepal. *Geological Society of America Bulletin* 112, 424–434.
- Pan, G., Ding, J., Yao, D., Wang, L., 2004. Geological map of Qinghai-Xiang (Tibet) plateau and adjacent areas (1 : 1,500,000). Chengdu Institute of Geology and Mineral Resources, China Geological Survey, Chengdu Cartographic Publishing House, Chengdu, China.
- Pandey, M.R., Tandukar, R.P., Avouac, J.-P., Vergne, J., Héritier, T., 1999. Seismotectonics of Nepal Himalayas from a local seismic network. *Journal of Asian Earth Sciences* 17, 703–712.
- Pandy, A.K., Viridi, N.S., 2003. Microstructural and fluid inclusion constraints on the evolution of Jakhri thrust zone in the Satluj valley of NW Himalaya. *Current Science* 84, 1355–1364.
- Papritz, K.9, Rey, R., 1989. Evidence for the occurrence of Permian Panjal Trap basalts in the Lesser and Higher Himalayas of the western syntaxis area, NE Pakistan. *Eclogae Geologicae Helvetiae* 82, 602–627.
- Parrish, R.R., Hodges, K.V., 1996. Isotopic constraints on the age and provenance of the Lesser and Greater Himalayan Sequences, Nepalese Himalaya. *Geological Society of America Bulletin* 108, 904–911.
- Parsons, T., Thompson, G.A., 1993. Does magmatism influence low-angle normal faulting? *Geology* 21, 247–250.
- Pascoe, E.H., 1910. Oil-fields of India, Records of Geological Survey of India 38, part 4.
- Patel, R.C., Singh, S., Asokan, A., Manickavasagam, R.M., Jain, A.K., 1993. Extensional tectonics in the Himalayan orogen, Zaskar, NW India. In: Treloar, P.J., Searle, M.P. (Eds), *Himalayan Tectonics*. The Geological Society Special Publication 74, 265–276. 445–459.
- Patriat, P., Achache, J., 1984. India–Eurasia collision chronology has implications for crustal shortening and driving mechanism of plates. *Nature* 311, 615–621.
- Paudel, L.P., Arita, K., 2002. Locating the Main Central Thrust in central Nepal using lithologic, microstructural and metamorphic criteria. *Journal of Nepal Geological Society* 26, 29–42.
- Pêcher, A., 1989. The metamorphism in the central Himalaya. *Journal of Metamorphic Geology* 7, 31–41.
- Pêcher, A., 1991. The contact between the Higher Himalaya crystallines and the Tibetan sedimentary series: miocene large scale dextral shearing. *Tectonics* 10, 587–598.
- Pêcher, A., Le Fort, P., 1986. The metamorphism in central Himalaya: its relations with the thrust tectonic. *Sciences de la Terre, Mémoire* 47, 285–309.
- Pêcher, A., Scaillet, B., 1989. La structure du Haut-Himalaya au Garhwal (Indes). *Eclogae Geologicae Helvetiae* 82, 655–668.
- Pilgrim, G.E., 1906. Notes on the geology of a portion of Bhutan. *Records of Geological Survey of India* 34, 22–30.
- Pinet, C., Jaupart, C., 1987. A thermal model for the distribution in space and time of the Himalayan granites. *Earth and Planetary Science Letters* 84, 87–99.
- Pognante, U., Spencer, D.A., 1991. First report of eclogites from the Himalayan belt, Kaghan valley (northern Pakistan). *European Journal of Mineralogy* 3, 613–618.
- Pognante, U., Castelli, D., Benna, P., Genovese, G., Oberli, F., Meier, M., Tonarino, S., 1990. The crystalline units of the High Himalayas in the Lahul–Zaskar region (northwestern India): metamorphic–tectonic history and geochronology of the collided and imbricated Indian plate. *Geological Magazine* 127, 101–116.
- Pogue, K.R., Wardlaw, B.R., Harris, A.G., Hussain, A., 1992. Paleozoic stratigraphy of the Peshawar basin, Pakistan: correlations and implications. *Geological Society of America Bulletin* 104, 915–927.
- Pogue, K.R., Hylland, M.D., Yeats, R.S., Khattak, W.U., Hussain, A., 1999. Stratigraphic and structural framework of Himalayan

- foothills, northern Pakistan. In: Macfarlane, A., Sorkhabi, R.B., Quade, J. (Eds.), *Himalaya and Tibet: Mountain Roots to Mountain Tops*. Geological Society of America Special Papers, vol. 328, pp. 257–274.
- Powell, Mc.A., Conaghan, P.J., 1973a. Plate tectonics and the Himalayas. *Earth and Planetary Science Letters* 20, 1–12.
- Powell, Mc.A., Conaghan, P.J., 1973b. Polyphase deformation in Phanerozoic rocks of the central Himalayan gneiss, northwest India. *Journal of Geology* 81, 127–143.
- Powers, P.M., Lillie, R.J., Yeats, R.S., 1998. Structure and shortening of the Kangra and Debra Dun reentrants, sub-Himalaya, India. *Geological Society of America Bulletin* 110, 1010–1027.
- Price, R.A., 1986. The southeastern Canadian Cordilleran thrust faulting, tectonic wedge, and delamination of the lithosphere. *Journal of Structural Geology* 8, 239–254.
- Qayyum, M., Niemi, A.R., Lawrence, R.D., 1996. Newly discovered Paleogene deltaic sequence in the Katawaz basin, Pakistan and its tectonic implications. *Geology* 24, 835–838.
- Qu, G., Zhang, J., 1994. Oblique thrust systems in the Altay orogen, China. *Journal of Southeast Asian Earth Sciences* 9, 277–287.
- Quidelleur, X., Grove, M., Lovera, O.M., Harrison, T.M., Yin, A., Ryerson, F.J., 1997. The thermal evolution and slip history of the Renbu Zedong Thrust, southeastern Tibet. *Journal of Geophysical Research* 102, 2659–2679.
- Rahman, M.J.J., Faupl, P., 2003. Ar-40/Ar-39 multigrain dating of detrital white mica of sandstone of the Surma Group in the Sylhet Trough, Bengal Basin, Bangladesh. *Sedimentary Geology* 155, 383–392.
- Rai, S.M., Guillot, S., LeFort, P., Upreti, B.N., 1998. Pressure-temperature evolution in the Kathmandu and Gosainkund regions, Central Nepal. *Journal of Asian Earth Sciences* 16, 283–298.
- Raiverman, V., 2000. Foreland Sedimentation in Himalayan Tectonic Regime: a relook at the orogenic processes. Bishen Singh Mahendra Pal Singh, Dehra Dun, India, 378 pp.
- Ramstein, G., Fluteau, F., Besse, J., Joussaume, S., 1997. Effect of orogeny, plate motion and land sea distribution on Eurasian climate change over the past 30 million years. *Nature* 386, 788–795.
- Rao, M.B.R., 1973. The subsurface geology of the Indo-Gangetic plains. *Journal of the Geological Society of India* 14, 217–242.
- Ratschbacher, L., Frisch, W., Chen, C.S., Pan, G.T., 1992. Deformation and motion along the southern margin of the Lhasa block (Tibet) prior to and during the India–Asian collision. *Journal of Geodynamics* 16, 21–54.
- Ratschbacher, L., Frisch, W., Liu, G., Chen, C., 1994. Distributed deformation in southern and western Tibet during and after the India–Asia collision. *Journal of Geophysical Research* 99, 19817–19945.
- Raynolds, R.G.H., 1980. The Pliocene-Pleistocene structural and stratigraphic evolution of the eastern Potwar Plateau, Pakistan. PhD thesis, Dartmouth College, Hanover, New Hampshire, 256 pp.
- Raynolds, R.G.H., 1981. Did the ancestral Indus flow into the Ganges drainage. *Geological Bulletin of University of Peshawar* 14, 141–150.
- Reuber, I., 1986. Geometry of accretion and oceanic thrusting of the Spongtang Ophiolite, Ladakh-Himalaya. *Nature* 321, 396–592.
- Ricou, L.-E., 1994. Tethys reconstructed: plates, continental fragments and their boundaries since 260 Ma from central America to South-eastern Asia. *Geodynamica Acta* 7, 169–218.
- Robinson, D.M., DeCelles, P.G., Patchett, P.J., Garzzone, C.N., 2001. The kinematic evolution of the Nepalese Himalaya interpreted from Nd isotopes. *Earth and Planetary Science Letters* 192, 507–521.
- Robinson, D.M., DeCelles, P.G., Garzzone, C.N., Pearson, O.N., Harrison, T.M., Catlos, E.J., 2003. Kinematic model for the Main Central Thrust in Nepal. *Geology* 31, 359–362.
- Robyr, M., Vannay, J.C., Epard, J.L., Steck, A., 2002. Thrusting, extension, and doming during the polyphase tectono-metamorphic evolution of the High Himalayan Crystalline Zone in NW India. *Journal of Asian Earth Sciences* 21, 221–239.
- Rowley, D.B., 1996. Age of collision between India and Asia: a review of the stratigraphic data. *Earth Planetary Science Letters* 145, 1–13.
- Royden, L.H., 1993. The steady-state thermal structure of eroding orogenic belts and accretionary prisms. *Journal of Geophysical Research* 98, 4487–4507.
- Royden, L.H., 1996. Coupling and decoupling of crust and mantle in convergent orogens: implications for strain partitioning in the crust. *Journal Geophysics Research* 101, 17679–17705.
- Royden, L.H., Burchfiel, B.C., King, R.W., Wang, E., Chen, Z., Shen, F., Liu, Y., 1997. Surface deformation and lower crustal flow in eastern Tibet. *Science* 276, 788–790.
- Ruppel, C., Hodges, K.V., 1994. Pressure–temperature–time paths from 2-dimensional thermal models—prograde, retrograde, and inverted metamorphism. *Tectonics* 13, 17–44.
- Sakai, H., 1983. Geology of the Tansen Group of the Lesser Himalaya in Nepal. *Memoir of Faculty of Sciences Kyushu University Series D XXV*, 27–74.
- Sakai, H., 1984. Stratigraphy of Tansen area in the Nepal Lesser Himalayas. *Journal of Nepal Geological Society* 4, 41–52.
- Sakai, H., 1989. Rifting of the Gandwanaland and uplifting of the Himalayas recorded in Mesozoic and Tertiary fluvial sediments in the Nepal Himalayas. In: Taira, A., Masuda, F. (Eds.), *Sedimentary Facies in the Active Plate Margin*. Terra Scientific Publications Company, Tokyo, pp. 723–732.
- Sakai, H., Hamamoto, R., Arita, K., 1992. Radiometric ages of alkaline volcanic rocks from the upper Gondwana of the Lesser Himalayas, west central Nepal, and their tectonic significance. *Bulletin of the Department of Geology, Tribhuvan University, Katmandu* 2, 65–74.
- Sakai, H., Takigami, Y., Nakamura, Y., Nomura, H., 1999. Inverted metamorphism in the Pre-Siwalik foreland basin sediments beneath the crystalline nappe, western Nepal Himalaya. *Journal of Asian Earth Sciences* 17, 727–739.
- Sangode, S.J., Kumar, R., Ghosh, S.K., 1996. Magnetic polarity stratigraphy of the Siwalik sequence of Haripur area (H.P.), NW Himalaya. *Journal of the Geological Society of India* 47, 683–704.
- Saxena, M.N., 1971. The crystalline axis of the Himalaya, Indian shield and continental drift. *Tectonophysics* 12, 433–447.

- Scaillet, B., France-Lanord, C., LeFort, P., 1990. Badrinath–Gangotri plutons (Garhwal, India)—petrological and geochemical evidence for fractionation processes in a High Himalayan leucogranite. *Journal of Volcanology and Geothermal Research* 44, 163–188.
- Scaillet, B., Pêcher, A., Rochette, P., Champenois, M., 1995. The Gangotri granite (Garhwal Himalaya)—Laccolithic emplacement in an extending collisional belt. *Journal of Geophysical Research* 100, 585–607.
- Schärer, U., Xu, R.H., Allègre, C.J., 1984. U–Pb geochronology of Gangdese (Transhimalaya) plutonism in the Lhasa–Xigaze region, Tibet. *Earth and Planetary Science Letters* 69, 311–320.
- Schärer, U., Xu, R.H., Allègre, C.J., 1986. U–(Th)–Pb systematic and ages of Himalayan leucogranites, south Tibet. *Earth and Planetary Science Letters* 77, 35–48.
- Schelling, D., 1992. The tectonostratigraphy and structure of the eastern Nepal Himalaya. *Tectonics* 11, 925–943.
- Schelling, D., 1999. Frontal structural geometries and detachment tectonic of the northeastern Karachi arc, southern Kirthar Range, Pakistan. In: Macfarlane, A., Sorkhabi, R.B., Quade, J. (Eds.), *Himalaya and Tibet: Mountain Roots to Mountain Tops*. Geological Society of America Special Papers, vol. 328, pp. 287–302.
- Schelling, D., Arita, K., 1991. Thrust tectonics, crustal shortening, and the structure of the far-eastern Nepal, Himalaya. *Tectonics* 10, 851–862.
- Schneider, C., Masch, L., 1993. The metamorphism of the Tibetan series from the Manang area, Marsyandi valley, central Nepal. In: Treloar, P.J., Searle, M.P. (Eds.), *Himalayan Tectonics*. Geological Society Special Publication, vol. 74, pp. 357–374.
- Schlup, M., Carter, A., Cosca, M., Steck, A., 2003. Exhumation history of eastern Ladakh revealed by Ar-40/Ar-39 and fission-track ages: the Indus River–Tso Moriri transect, NW Himalaya. *Journal of the Geological Society* 160, 385–399.
- Schneider, D.A., Edwards, M.A., Zeitler, P.K., 1999a. Mazemo Pass pluton and Jutial pluton, Pakistan Himalaya: age and implications for entrapment mechanism of two granites in the Himalaya. *Contributions to Mineralogy and Petrology* 136, 273–284.
- Schneider, D.A., Edwards, M.A., Zeitler, P.K., Coath, C.D., 1999b. Mazemo Pass Pluton and Jutial Pluton, Pakistan Himalaya: age and implications for entrapment mechanisms of two granites in the Himalaya. *Contributions to Mineralogy and Petrology* 136, 273–284.
- Schneider, D.A., Edwards, M.A., Kidd, W.S.F., Zeitler, P.K., Coath, C.D., 1999. Early Miocene anatexis identified in the western syntaxis, Pakistan Himalaya. *Earth and Planetary Science* 167, 121–129.
- Searle, M.P., 1986. Structural evolution and sequence of thrusting in the High Himalayan, Tibetan Tethyan and Indus suture zones of Zaskar and Ladakh, western Himalaya. *Journal of Structural Geology* 8, 923–936.
- Searle, M.P., 1999. Extensional and compressional faults in the Everest–Lhotse massif, Khumbu Himalaya, Nepal. *Journal of the Geological Society, London* 156, 227–240.
- Searle, M.P., Godin, L., 2003. The South Tibetan Detachment system and the Manaslu leucogranite: a structural re-interpretation and restoration of the Annapurna–Manaslu Himalaya, Nepal. *Journal of Geology* 111, 505–523.
- Searle, M.P., Rex, A.J., 1989. Thermal model for the Zaskar Himalaya. *Journal of Metamorphic Petrology* 7, 127–134.
- Searle, M.P., Rex, A.J., Tirrul, R., Rex, D.C., Barnicoat, A., Windley, B.F., 1989. Metamorphic, magmatic, and tectonic evolution of the central Karakoram in the Biafo–Baltoro–Hushe regions of northern Pakistan. In: Malinconico, L.L., Lillie, R.J. (Eds.), *Tectonics of the Western Himalaya*. Special Paper–Geological Society of America, vol. 232, pp. 47–73.
- Searle, M.P., Waters, D.J., Rex, A.J., Wilson, R.N., 1992. Pressure, temperature, and time constraints on Himalayan metamorphism from eastern Kashmir and western Zaskar. *Journal of the Geological Society, London* 149, 753–773.
- Searle, M.P., Parrish, R.R., Hodges, K.V., Hurford, A., Ayers, M.W., Whitehouse, M.J., 1997. Shisha Pangma leucogranite, South Tibetan Himalaya: field relations, geochemistry, age, origin and emplacement. *Journal of Geology* 105, 295–317.
- Searle, M.P., Waters, D.J., Dransfield, M.W., Stephenson, B.J., Walker, C.B., Walker, J.D., Rex, D.C., 1999a. Thermal and mechanical models for the structural and metamorphic evolution of the Zaskar. *High Himalaya*. In: MacNiocail, C., Ryan, P.D. (Eds.), *Continental Tectonics*. Special Publication–Geological Society of London, vol. 164, pp. 139–156.
- Searle, M.P., Nobles, S.R., Hurford, A.J., Rex, D.C., 1999b. Age of crustal melting, emplacement and exhumation history of the Shivering leucogranite, Garhwal Himalaya. *Geological Magazine* 136, 513–525.
- Searle, M.P., Simpson, R.L., Law, R.D., Parrish, R.R., Waters, D.J., 2003. The structural geometry, metamorphic and magmatic evolution of the Everest massif, High Himalaya of Nepal–South Tibet. *Journal of the Geological Society, London* 160, 345–366.
- Seeber, L., Armbruster, J.G., 1984. Some elements of continental subduction along the Himalayan front. *Tectonophysics* 105, 263–278.
- Seeber, L., Pêcher, A., 1998. Strain partitioning along the Himalayan arc and the Nanga Parbat antiform. *Geology* 26, 791–794.
- Sengör, A.M.C., 1984. The Cimmeride orogenic system of the tectonics of Eurasia. *Special Paper–Geological Society of America* 195, 82 pp.
- Sengör, A.M.C., Natal'in, B.A., 1996. Paleotectonics of Asia: fragments of a synthesis. In: Yin, A., Harrison, T.M. (Eds.), *The Tectonics of Asia*. Cambridge University Press, New York, pp. 486–640.
- Sharma, V.P., 1977. *Geology of the Kulu–Rampur belt, Himachal Pradesh*. Geological Survey of India Memoir 106, 235–407.
- Shen, F., Royden, L.H., Burchfiel, B.C., 2001. Large-scale crustal deformation of the Tibetan Plateau. *Journal of Geophysical Research* 106, 6793–6816.
- Sheridan, R.E., 1976. Sedimentary basins of the Atlantic margin of North America. *Tectonophysics* 36, 113–132.
- Shi, Y., Wang, C.-Y., 1987. Two-dimensional modeling of the  $P$ – $T$  paths of regional metamorphism in simple overthrust terrains. *Geology* 15, 1048–1051.
- Simpson, R.L., Parrish, R.R., Searle, M.P., Waters, D.J., 2000. Two episodes of monazite crystallization during metamorphism and

- crustal melting in the Everest region of the Nepalese Himalaya. *Geology* 28, 403–406.
- Singh, S., Chowdhary, P.K., 1990. An outline of the geological framework of the Arunachal Himalaya. *Journal of Himalayan Geology* 1, 189–197.
- Singh, S.K., France-Lanord, C., 2002. Tracing the distribution of erosion in the Brahmaputra watershed from isotopic compositions of stream sediments. *Earth and Planetary Science Letters* 202, 645–662.
- Singh, S., Jain, A.K., 1995. Deformational and strain patterns of the Jutogh Nappe along the Sutlej Valley in Jeori-Wangtu region, Himachal Pradesh, India. *Himalayan Geology* 16, 41–55.
- Singh, S., Barley, M.E., Brown, S.J., Jain, A.K., Manickavasagam, R.M., 2002. SHRIMP U–Pb in zircon geochronology of the Chor granitoid: evidence for Neoproterozoic magmatism in the Lesser Himalayan granite belt of NW India. *Precambrian Research* 118, 285–292.
- Smith, H.A., Chamberlain, P.C., Zeitler, P.K., 1992. Documentation of Neogene regional metamorphism in the Himalayas of Pakistan using U–Pb in monazite. *Earth and Planetary Science Letters* 113, 93–106.
- Smith, H.A., Chamberlain, C.P., Zeitler, P.K., 1994. Timing and duration of Himalayan metamorphism within the Indian plate, Northwest Himalaya, Pakistan. *Journal of Geology* 102, 493–508.
- Sorkhabi, R.B., Macfarlane, A., 1999. Himalaya and Tibet: mountain root to mountain top. In: Macfarlane, A., Sorkhabi, R.B., Quade, J. (Eds.), *Himalaya and Tibet: Mountain roots to Mountain Tops*, Boulder, Colorado, Special Paper–Geological Society of America, vol. 328, pp. 1–7.
- Sorkhabi, R.B., Stump, E., Foland, K.A., Jain, A.K., 1996. Fission-track and  $^{40}\text{Ar}/^{39}\text{Ar}$  evidence for episodic denudation of the Gangotri granites in the Garhwal Higher Himalaya, India. *Tectonophysics* 260, 187–199.
- Sorkhabi, R.B., Stump, E., Foland, K., Jain, A.K., 1997. Tectonic and cooling history of the Garhwal Higher Himalaya (Bhagirathi Valley): constraints from thermochronological data. *Gondwana Research Group Memoir* 6, 217–235.
- Sorkhabi, R.B., Stump, E., Foland, K., Jain, A.K., 1999. Tectonic and cooling history of the Garhwal Higher Himalaya (Bhagirathi Valley): constraints from thermochronological data. In: Jain, A.K., Manickavasagam, R.M. (Eds.), *Geodynamics of the NW Himalaya*. *Gondwana Research Group Memoir*, vol. 6, pp. 217–235.
- Sozbilir, H., 2002. Geometry and origin of folding in the Neogene sediments of the Gediz Graben, western Anatolia, Turkey. *Geodinamica Acta* 15, 277–288.
- Spencer, J.E., 1984. Role of tectonic denudation in warping and uplift of low-angle normal faults. *Geology* 12, 95–98.
- Spencer, J.E., Chase, C.G., 1989. Role of crustal flexure in initiation of low-angle normal faults and implications for structural evolution of the Basin and Range province. *Journal of Geophysical Research* 94, 1765–1775.
- Spring, L., Crespo-Blanc, A., 1992. Nappe tectonics, extension, and metamorphic evolution in the Indian Tethys Himalaya (Higher Himalaya, SE Zaskar and NW Lahul). *Tectonics* 11, 978–989.
- Srikantia, S.V., 1977. Sedimentary cycles in the Himalaya and their significance in the orogenic evolution of the mountain belt—international colloquium. *C.N.R.S. (Paris)* 268, 395–408.
- Srikantia, S.V., 1981. The lithostratigraphy, sedimentation, and structure of Proterozoic–Phanerozoic formations of Spiti basin in the Higher Himalaya of Himachal Pradesh, India. In: Shina, A.K. (Ed.), *Contemporary Geoscientific Research in Himalaya*, vol. 1. Singh, Dehra Dun, India, pp. 41–48.
- Srivastava, P., Mitra, G., 1994. Thrust geometries and deep structure of the outer and Lesser Himalaya, Jumoan and Garhwal (India): implications for evolution of the Himalayan fold and thrust belt. *Tectonics* 13, 89–109.
- Srivastava, P., Mitra, G., 1996. Deformation mechanisms and inverted thermal profiles in the North Almora Thrust mylonite zone, Kumaon Lesser Himalaya, India. *Journal of Structural Geology* 18, 27–39.
- Stäubli, A., 1989. Polyphase metamorphism and the development of the Main Central Thrust. *Journal of Metamorphic Geology* 7, 73–93.
- Steck, A., 2003. Geology of the NW Indian Himalaya. *Eclogae Geologicae Helveticae* 96, 147–213.
- Steck, A., Spring, L., Vannay, J.-C., Masson, H., Bucher, H., Stutz, E., Marchant, R., Tietche, J.-C., 1993. The tectonic evolution of the Northwestern Himalaya in eastern Ladakh and Lahul, India. In: Treloar, P.J., Searle, M.P. (Eds.), *Himalayan Tectonics*. Geological Society Special Publication, vol. 74, pp. 265–276.
- Steck, A., Epard, J.L., Vannay, J.C., Hunziker, J., Girard, M., Morard, A., Robyr, M., 1998. Geological transect across the Tso Moriri and Spiti areas: the nappe structures of the Tethys Himalaya. *Eclogae Geologicae Helveticae* 91, 103–122.
- Steck, A., Epard, J.L., Robyr, M., 1999. The NE-directed Shikar Beh Nappe: a major structure of the Higher Himalaya. *Eclogae Geologicae Helveticae* 92, 239–250.
- Stephenson, B.J., Waters, D.J., Searle, M.P., 2000. Inverted metamorphism and the Main Central Thrust: field relations and thermobarometric constraints from the Kishtwar Window, NW Indian Himalaya. *Journal of Metamorphic Geology* 18, 571–590.
- Stephenson, B.J., Searle, M.P., Waters, D.J., Rex, D.C., 2001. Structure of the Main Central Thrust zone and extrusion of the high Himalayan deep crustal wedge, Kishtwar–Zaskar Himalaya. *Journal of the Geological Society* 158, 637–652.
- Stewart, J.H., 1972. Initial deposits in the cordilleran geosyncline: evidence of a late precambrian (<850 m.y.) continental separation. *Geological Society of America Bulletin* 83, 1345–1360.
- Stöcklin, J., 1980. Geology of Nepal and its regional frame. *Journal of the Geological Society* 137, 1–34.
- Stüwe, K., Foster, D., 2001. Ar-40/Ar-39, pressure, temperature and fission-track constraints on the age and nature of metamorphism around the Main Central Thrust in the eastern Bhutan Himalaya. *Journal of Asian Earth Sciences* 19, 85–95.
- Suppe, J., 1983. Geometry and kinematics of fault-bend folding. *American Journal of Science* 283, 648–721.
- Swapp, S.M., Hollister, L.S., 1991. Inverted metamorphism within the Tibetan slab of Bhutan—evidence for a tectonically transported heat source. *Canadian Mineralogist* 29, 1019–1041.

- Takagi, H., Arita, K., Sawaguchi, T., Kobayashi, K., Awaji, D., 2003. Kinematic history of the Main Central Thrust zone in the Langtang area, Nepal. *Tectonophysics* 366, 151–163.
- Tapponnier, P., Xu, Z.Q., Roger, F., Meyer, B., Arnaud, N., Wittlinger, G., Yang, J.S., 2001. Geology-oblique stepwise rise and growth of the Tibet plateau. *Science* 294, 1671–1677.
- Taylor, M.H., Yin, A., Ryerson, F.J., Kapp, P., Ding, L., 2003. Conjugate strike-slip faulting along the Bangong–Nujiang suture zone accommodates coeval east–west extension and north–south shortening in the interior of the Tibetan Plateau. *Tectonics* 22. doi:10.1029/2002TC001361.
- Teng, L.S., 1990. Geotectonic evolution of late Cenozoic arc-continent collision in Taiwan. *Tectonophysics* 183, 57–76.
- Thakur, V.C., 1992. *Geology of Western Himalaya*. Pergamon Press, New York, 363 pp.
- Thakur, V.C., 1998. Structure of the Chamba nappe and position of the Main Central Thrust in Kashmir Himalaya. *Journal of Asian Earth Sciences* 16, 269–282.
- Thakur, V.C., 2004. Active tectonics of Himalayan frontal thrust and seismic hazard to Ganga Plain. *Current Science in India* 86, 1554–1560.
- Thakur, V.C., Jain, A.K., 1974. Tectonics of eastern region. *Current Science in India* 43, 783–785.
- Thakur, V.C., Rawat, B.S., 1992. *Geological Map of Western Himalaya, 1:1,000,000*. Wadia Institute of Himalayan Geology, Dehra Dun, India.
- Tiwari, B.N., Misra, P.S., Kumar, M., Kulshrestha, S.K., 1991. Microfaunal remains from the upper Dhamsala formation, Dhamsala, Kangra Valley, H.P. *Journal of Palaeontological Society of India* 36, 31–41.
- Tonarini, S., Villa, I., Oberli, F., Meier, M., Spencer, D.A., Pogranante, U., Ramsay, J.G., 1993. Eocene age of eclogite metamorphism in the Pakistan Himalaya: implications for India–Eurasia collision. *Terra Nova* 5.
- Treloar, P.J., Coward, M.P., 1991. Indian Plate motion and shape: constraints on the geometry of the Himalayan orogen. *Tectonophysics* 191, 189–198.
- Treloar, P.J., Izatt, C.N., 1993. Tectonics of the Himalayan collision between the Indian plate and the Afghan Block: a synthesis. In: Treloar, P.J., Searle, M.P. (Eds.), *Himalayan Tectonics*. Geological Society Special Publication, vol. 74, pp. 69–87.
- Treloar, P.J., Rex, D.C., 1990. Cooling, uplift and exhumation rates in the crystalline thrust stack of the North Indian Plate, west of the Nanga Parbat syntaxis. *Tectonophysics* 180, 323–349.
- Treloar, P.J., Rex, D.C., Guise, P.G., Coward, M.P., Searle, M.P., Windley, B.F., Petterson, M.G., Jan, M.Q., Luff, I.W., 1989. K–Ar and Ar–Ar geochronology of the Himalayan collision in NW Pakistan: constraints on the timing of suturing, deformation, metamorphism and uplift. *Tectonics* 8, 881–909.
- Treloar, P.J., Potts, G.J., Wheeler, J., Rex, D.C., 1991. Structural evolution and asymmetric uplift of the Nanga Parbat syntaxis, Pakistan Himalaya. *Geologische Rundschau* 80, 411–428.
- Treloar, P.J., Rex, D.C., Guise, P.G., Wheeler, J., Hurford, A.J., Carter, A., 2000. Geochronological constraints on the evolution of the Nanga Parbat syntaxis, Pakistan Himalaya. In: Khan, M.A., Treloar, P.J., Searle, M.P., Jan, M.Q. (Eds.), *Tectonics of the Nanga Parbat syntaxis and the Western Himalaya*. The Geological Society Special Publication, vol. 170, pp. 137–162.
- Treloar, P.J., O’Brien, P.J., Parrish, R.R., Khan, M.A., 2003. Exhumation of early Tertiary, coesite-bearing eclogites from the Pakistan Himalaya. *Journal of The Geological Society* 160, 367–376.
- Trevidi, J.R., Gopalan, K., Valdiya, K.S., 1984. Rb–Sr ages of granitic rocks within the Lesser Himalayan Nappes, Kumaun. *Journal of Geological Society of India* 25, 641–654.
- Uddin, A., Lundberg, N., 1998a. Unroofing history of the eastern Himalaya and the Indo-Burman Ranges: heavy-mineral study of Cenozoic sediments from the Bengal Basin, Bangladesh. *Journal of Sedimentary Research* 68, 465–472.
- Uddin, A., Lundberg, N., 1998b. Cenozoic history of the Himalayan–Bengal system: sand composition in the Bengal basin, Bangladesh. *Geological Society of America Bulletin* 110, 497–511.
- Upreti, B.N., 1996. Stratigraphy of the western Nepal Lesser Himalaya: a synthesis. *Journal of Nepal Geological Society* 13, 11–28.
- Upreti, B.N., 1999. An overview of the stratigraphy and tectonics of the Nepal Himalaya. *Journal of Asian Earth Sciences* 17, 577–606.
- Upreti, B.N., LeFort, P., 1999. Lesser Himalayan crystalline nappes of Nepal: problems of their origin. *Special Paper—Geological Society of America*, vol. 328, 225–238.
- Valdiya, K.S., 1978. Extension and analogues of the Chail Nappe in Kumaun Himalaya. *Indian Journal of Earth Sciences* 5, 1–10.
- Valdiya, K.S., 1979. An outline of the structural setup of the Kumaun Himalaya. *Journal of Geological Society of India* 20, 145–157.
- Valdiya, K.S., 1980. *Geology of the Kumaon Lesser Himalaya*. Wadia Institute of Himalaya, Dehra Dun, India, 291 pp.
- Valdiya, K.S., 1981. tectonics of the central sector of the Himalaya. In: Gupta, H.K., Delany, F.M. (Eds.), *Zagros, Hindu Kush, Himalaya: Dynamic Evolution*. American Geophysical Union Geodynamics Series, vol. 3, pp. 87–110.
- Valdiya, K.S., 1988. Tectonics and evolution of the central sector of the Himalaya. *Philosophical Transactions of the Royal Society of London. Series A* 326, 151–174.
- Valdiya, K.S., 1989. Trans-Himaladri intracrustal fault and basement upwards south of the Indus–Tsangpo suture zone. In: Malinconico Jr., L.L., Lillie, R.J. (Eds.), *Tectonics of the Western Himalaya*. Special Paper–Geological Society of America, vol. 232, pp. 153–168.
- Vance, D., Harris, N., 1999. Timing of prograde metamorphism in the Zaskar Himalaya. *Geology* 27, 395–398.
- Van der Voo, R., Spakman, W., Bijwaard, H., 1999. Tethyan subducted slabs under India. *Earth and Planetary Science Letters* 171, 7–20.
- Vannay, J.C., Grasemann, B., 1998. Inverted metamorphism in the High Himalaya of Himachal Pradesh (NW India): phase equilibria versus thermobarometry. *Schweizerische Mineralogische und Petrographische Mitteilungen* 78, 107–132.
- Vannay, J.C., Grasemann, B., 2001. Himalayan inverted metamorphism and syn-convergence extension as a consequence of a general shear extrusion. *Geological Magazine* 138, 253–376.

- Vannay, J.C., Hodges, K.V., 1996. Tectonometamorphic evolution of the Himalayan metamorphic core between the Annapurna and Dhaulagiri, central Nepal. *Journal of Metamorphic Geology* 14, 635–656.
- Vannay, J.C., Steck, A., 1995. Tectonic evolution of the High Himalaya in Upper Lahul (NW Himalaya, India). *Tectonics* 14, 253–263.
- Vannay, J.C., Sharp, Z.D., Grasemann, B., 1999. Himalayan inverted metamorphism constrained by oxygen isotope thermometry. *Contributions to Mineralogy and Petrology* 137, 90–101.
- Vannay, J.C., Grasemann, B., Rahn, M., Frank, W., Carter, A., Baudraz, V., Cosca, M., 2004. Miocene to Holocene exhumation of metamorphic crustal wedges in the NW Himalaya: Evidence for tectonic extrusion coupled to fluvial erosion. *Tectonics* 23, TC1014.
- Verma, P.K., Tandon, S.K., 1976. Geological observations in parts of Kameng district, Arunachal Pradesh (NEFA). *Himalayan Geology* 6, 259–286.
- Vigneresse, J.-P., Burg, J.P., 2002. The paradoxical aspect of the Himalayan granites. In: Singh, S. (Ed.), *Granitoids of the Himalayan Collisional Belt*. *Journal of Virtual Explorer*, vol. 9, pp. 1–13.
- Wadia, D.N., 1931. The syntaxis of the northwest Himalaya: its rocks, tectonics and orogeny. *Records of Geological Survey of India* 65, 189–220.
- Wadia, D.N., 1934. The Cambrian–Trias sequences of northwest Kashmir (parts of the Mazaffarabad and Baramula District). *Records of Geological Survey of India* 68, 121–146.
- Wadia, D.N., 1953. *Geology of India*, third edition. MacMillan and Co. Limited, London. 553 pp.
- Walker, J.D., Martin, M.W., Bowring, S.A., Searle, M.P., Waters, D.J., Hodges, K.V., 1999. Metamorphism, melting, and extension: age constraints from the High Himalayan slab of south-east Zaskar and northwest Lahaul. *Journal of Geology* 107, 473–495.
- Walker, C.B., Searle, M.P., Waters, D.J., 2001. An integrated tectonothermal model for the evolution of the High Himalaya in western Zaskar with constraints from thermobarometry and metamorphic modeling. *Tectonics* 20, 810–833.
- Wang, H.Z., 1985. *Atlas of the Palaeogeography of China*. Cartographic Publishing House, Beijing (in Chinese and English).
- Wang, E., Zhou, Y., Chen, Z., Burchfiel, B.C., Ji, J., 2001. Geologic and geomorphic origins of the east Himalayan gap. *Chinese Journal of Geology* 36, 122–128 (in Chinese with English abstract).
- Wernicke, B., 1992. Cenozoic extensional tectonics of the U.S. Cordillera. In: Burchfiel, B.C., Lipman, P.W., Zoback, M.L. (Eds.), *The Geology of North America G-3*. Geological Society of America, Boulder, Colorado, pp. 553–581.
- Westaway, R., 1999. The mechanical feasibility of low-angle normal faulting. *Tectonophysics* 308, 407–443.
- White, N.M., Parrish, R.R., Bickle, M.J., Najman, Y.M.R., Burbank, D., Maithani, A., 2001. Metamorphism and exhumation of the NW Himalaya constrained by U–Th–Pb analyses of detrital monazite grains from early foreland basin sediments. *Journal of the Geological Society* 158, 625–635.
- White, N.M., Pringle, M., Garzanti, E., Bickle, M., Najman, Y., Chapman, H., Friend, P., 2002. Constraints on the exhumation and erosion of the High Himalayan Slab, NW India, from foreland basin deposits. *Earth and Planetary Science Letters* 195, 29–44.
- Whittington, A., Foster, G., Harris, N., Vance, D., Ayres, M., 1999. Lithostratigraphic correlations in the western Himalaya—an isotopic approach. *Geology* 27, 585–588.
- Whittington, A., Harris, N.B.W., Ayres, M.W., Foster, G., 2000. Tracing the origin of the western Himalaya: an isotopic comparison of the Nanga Parbat massif and Zaskar Himalaya. In: Khan, M.A., Treloar, P.J., Searle, M.P., Jan, M.Q. (Eds.), *Tectonics of the Nanga Parbat syntaxis and the Western Himalaya*. The Geological Society Special Publication, vol. 170, pp. 201–218.
- Wiesmayr, G., Grasemann, B., 2002. Eohimalayan fold and thrust belt: implications for the geodynamic evolution of the NW-Himalaya (India). *Tectonics* 2, 1058.
- Windley, B.F., 1983. Metamorphism and tectonics of the Himalaya. *Geological Society of London Journal* 140, 849–865.
- Winslow, D.M., Chamberlain, C.P., Zeitler, P.K., 1995. Metamorphism and melting of the lithosphere due to rapid denudation, Pakistan Himalaya. *Journal of Geology* 103, 395–408.
- Winslow, D.M., Chamberlain, C.P., Zeitler, P.K., Williams, I.S., 1996. Geochronological constraints on syntaxial development in the Nanga Parbat region, Pakistan. *Tectonics* 15, 1292–1308.
- Wobus, C.W., Hodges, K.V., Whipple, K.X., 2003. Has focused denudation sustained active thrusting at the Himalayan topographic front? *Geology* 31, 861–864.
- Wobus, C., Heimsath, A., Whipple, K., Hodges, K., 2005. Active out-of-sequence thrust faulting in the central Nepalese Himalaya. *Nature* 434, 1008–1011.
- Wu, C., Nelson, K.D., Wortman, G., Samson, S., Yue, Y., Li, J., Kidd, W.S.F., Edward, M.A., 1998. Yadong cross structure and South Tibetan Detachment in the east central Himalaya (89–90 E). *Tectonics* 17, 28–45.
- Wyss, M., 2000. Metamorphic evolution of the northern Himachal Himalaya: phase equilibria constraints and thermobarometry. *Schweizerische Mineralogische Mineralogische und Petrographische Mitteilungen* 80, 317–334.
- Wyss, M., Hermann, J., Steck, A., 1999. Structural and metamorphic evolution of the northern Himachal Himalayas, NW India–(Spiti–eastern Lahul–Parvati valley traverse). *Eclogae Geologicae Helveticae* 92, 3–44.
- Xizang BGMR (Xizang Bureau of Geology and Mineral Resources), 1993. *Regional Geology of the Xizang Autonomous Region*. Geological Publishing House, Beijing.
- Xu, R.H., 1990. Age and geochemistry of granites and metamorphic rocks in south-central Xizang (Tibet). In: *Igneous and Metamorphic Rocks of the Tibetan Plateau*. Chinese Academy of Geological Sciences. Science Press, pp. 287–302.
- Xu, R.H., Schärer, U., Allègre, C.J., 1985. Magmatism and metamorphism in the Lhasa block (Tibet): a geochronological study. *Journal of Geology* 93, 41–57.
- Yang, X., Xie, G., Li, Z., 1992. Mylonite–migmatite lithogenic series—an important tectono-dynamic rock forming process. *Geotectonica et Metallogenia* 16, 151–159.

- Yeats, R.S., 1987. Timing of structural events in the Himalaya foothills of northwest Pakistan. *Geological Society of America Bulletin* 99, 161–176.
- Yeats, R.S., Lawrence, R.D., 1984. Tectonics of the Himalayan thrust belt in northern Pakistan. In: Haq, B.U., Milliman, J.D. (Eds.), *Marine Geology and Oceanography of Arabian Sea and Coastal Pakistan*. Van Nostrand, Reinhold, New York, pp. 177–198.
- Yeats, R., Lillie, S., 1991. Contemporary tectonics of the Himalayan frontal fault system: folds, blind thrusts and 1905 Kangra earthquake. *Journal of Structural Geology* 13, 215–225.
- Yin, A., 1989. Origin of regionally, rooted low-angle normal faults—a mechanical model and its tectonic implications. *Tectonics* 8, 469–482.
- Yin, A., 1990. Reply to “comment on origin of regional, rooted low-angle normal faults: a mechanical model and its tectonic implications”. *Tectonics* 9, 547–548.
- Yin, A., 1991. Mechanics of wedge-shaped fault blocks: 1. An elastic solution for compressional wedges. *Journal of Geophysical Research* 98, 14245–14256.
- Yin, A., 1993. Does magmatism influence low-angle normal faulting-comment. *Geology* 21, 956.
- Yin, A., 2000. Mode of Cenozoic eastwest Extension in Tibet suggests a common origin of rifts in Asia during Indo-Asian collision. *Journal of Geophysical Research* 105, 21745–21759.
- Yin, A., 2002. A passive-roof thrust model for the emplacement of the Orocopia-Pelona Schist in Southern California. *Geology* 30, 183–186.
- Yin, A., 2004. Gneiss domes and gneiss dome systems. In: Whitney, D.L., Teyssier, C., Siddoway, C.S. (Eds.), *Gneiss Domes and Orogeny*, Geological Society of America Special Paper, vol. 380, pp. 1–14. 7466: Beijing, 185 pp.
- Yin, A., Dunn, J.F., 1992. Structural and stratigraphic development of the Whipple–Chemehuevi detachment fault system, southeastern California: implications for the geometrical evolution of domal and basinal low-angle normal faults. *Geological Society of America Bulletin* 104, 659–674.
- Yin, A., Harrison, T.M., 2000. Geologic evolution of the Himalayan–Tibetan orogen. *Annual Review of Earth and Planetary Sciences* 28, 211–280.
- Yin, A., Nie, S., 1993. An indentation model for North and South China collision and the development of the Tanlu and Honam fault systems, eastern Asia. *Tectonics* 12, 801–813.
- Yin, A., Nie, S., 1996. A Phanerozoic palinspastic reconstruction of China and its neighboring regions. In: Yin, A., Harrison, T.M. (Eds.), *The Tectonics of Asia*. Cambridge University Press, New York, pp. 442–485.
- Yin, A., Harrison, T.M., Ryerson, F.J., Chen, W., Kidd, W.S.F., Copeland, P., 1994. Tertiary structural evolution of the Gangdese thrust system, southeastern Tibet. *Journal of Geophysical Research* 99, 18175–18201.
- Yin, A., Harrison, T.M., Murphy, M.A., Grove, M., Nie, S., Ryerson, F.J., Feng, W.X., Le, C.Z., 1999. Tertiary deformation history of southeastern and southwestern Tibet during the Indo-Asian collision. *Geological Society of America Bulletin* 111, 1644–1664.
- Yin, A., Rumelhart, P.E., Butler, R., Cowgill, E., Harrison, T.M., Foster, D.A., Ingersoll, R.V., Zhang, Q., Zhou, X.Q., Wang, X.F., Hanson, A., Raza, A., 2002. Tectonic history of the Altyn Tagh fault system in northern Tibet inferred from Cenozoic sedimentation. *Geological Society of America Bulletin* 114, 1257–1295.
- Yin, A., Harrison, T.M., Dubey, C.S., Sharma, B.K., Webb, A., 2003. The Kumharsain shear zone in the Garhwal Himalaya, a segment of the folded South Tibet Detachment south of the Greater Himalayan Crystallines? Abstracts with Programs–Geological Society of America 34 (7), 30.
- Yin, A., Dubey, C.S., Kelty, T.K., Gehrels, G.E., Chou, C.Y., Grove, M., Lovera, M. submitted for publication. Structural Architecture of the Eastern Himalaya and its Implications for Asymmetric Development of the Himalayan Origin. *Geology*.
- Zeitler, P.K., 1985. Cooling history of the NW Himalaya. *Tectonics* 4, 127–135.
- Zeitler, P.K., Chamberlain, C.P., 1991. Petrogenic and tectonic significance of young leucogranites from the northwestern Himalaya, Pakistan. *Tectonics* 10, 729–741.
- Zeitler, P.K., Sutter, J.F., Williams, I.S., Zartman, R., Tahir-kelli, R.A.K., 1989. Geochronology and temperature history of the Nanga Parbat–Haramosh massif, Pakistan. In: Maliniconico, L.L., Lillie, R.J. (Eds.), *Tectonics of the Western Himalaya*. Special Paper–Geological Society of America, vol. 232, pp. 1–22.
- Zeitler, et al., 2001. Crustal reworking at Nanga Parbat, Pakistan: metamorphic consequences of thermal–mechanical coupling facilitated by erosion. *Tectonics* 20, 712–728.
- Zhang, J., Guo, L. submitted for publication. Yalashangbo dome: a metamorphic core complex and the exposure of Southern Tibetan Detachment System in northern Himalaya. *Tectonophysics*.
- Zhang, Z.G., Liu, Y.H., Wang, T.W., Yang, H.X., Xu, B.C., 1992. *Geology of the Namche Bawar Region*. Chinese Science Press, Beijing. 185 pp.
- Zhao, W., Morgan, W.J., 1987. Injection of Indian crust into Tibetan lower crust: a two-dimensional finite element model study. *Tectonics* 6, 489–504.
- Zhao, W., Nelson, K.D., and the Project INDEPTH Team, 1993. Deep seismic reflection evidence for continental underthrusting beneath southern Tibet. *Nature* 366, 557–559.
- Zhu, B., Kidd, W.S.F., Rowley, D.B., Currie, B.S., Shafique, N., 2005. Age of initiation of the India–Asia collision in the east-central Himalaya. *Journal of Geology* 113, 265–285.
- Ziabrev, S.V., Aitchison, J.C., Abrajevitch, A.V., Badengzhu., Davis, A.M., Luo, H., 2004. Bainang Terrane, Yarlung-Tsangpo suture, southern Tibet (Xizang, China): a record of intra-Neotethyan subduction–accretion processes preserved on the roof of the world. *Journal of the Geological* 161, 523–538.
- Zhong, S.J., Gurnis, M., 1993. Dynamic feedback between a continent-like raft and thermal convection. *Journal of Geophysical Research* 98, 12219–12232.

An Yin obtained his B.S. degree in Geomechanics in 1982 from Beijing University, China. He received a PhD degree in 1988 in structural geology from University of Southern California. He has been teaching at University of California, Los Angeles (UCLA) since 1987. His research have focused on the kinematics and mechanics of low-angle normal faults and thrust systems in the North American Cordillera, tectonic reconstruction of the Qinling-Dabie-Imjingang orogenic system in east Asia, accretionary tectonics of the Altai orogen in central Asia, and the evolution of the Himalayan–Tibetan orogen.